Niloufar Sadat Ghavami Masouleh

Advances in Process Integration Studies for Novel Biorefinery Concepts and Biofuel Production for Sustainability Transformation

Åbo Akademi University

Advances in Process Integration Studies for Novel Biorefinery Concepts and Biofuel Production for Sustainability Transformation

Niloufar Sadat Ghavami Masouleh

Energy Technology
Faculty of Science and Engineering
Åbo Akademi University

Åbo, Finland 2024

Supervisor

Associate Professor Cataldo De Blasio
Laboratory of Energy Technology
Faculty of Science and Engineering
Åbo Akademi University

Co-Supervisor

Dr. Karhan Özdenkci
Laboratory of Energy Technology
Faculty of Science and Engineering
Åbo Akademi University

Pre-examiner and opponent

Assistant Professor Mauro Prestipino
Department of Engineering
University of Messina, Italy.

Pre-examiner
Professor Vladimir Strezov
School of Natural Sciences
Centre for Energy and Natural Resources Innovation and Transformation (CENRIT)
Macquarie University, Australia

ISBN 978-952-12-4373-8 (printed)
ISBN 978-952-12-4374-5 (digital)
Painosalama; Turku, Finland 2024

To my Mom,

For your unwavering love and endless support, this thesis is dedicated to you. Your belief in me has been my guiding light. Thank you for being my inspiration and constant source of strength.

With love,

Nilu

Acknowledgements

I extend my deepest gratitude to those who have played an instrumental role in the realization of this thesis. First and foremost, my sincere appreciation goes to my supervisor Prof. Cataldo De Blasio and co-supervisor Dr. Karhan Özdenkçi whose guidance and expertise have been invaluable throughout this research journey. Their constructive feedback and unwavering support have shaped the trajectory of this work.

Furthermore, I would like to acknowledge my colleagues at the Laboratory of Energy Technology and Professor Margareta Biörklund-Sänkiaho for the constructive conversations and support.

I am indebted to my family for their boundless encouragement, understanding, and patience. Their unwavering belief in my abilities provided the emotional foundation necessary for navigating the challenges inherent in such a substantial undertaking.

A heartfelt thanks to my friends and colleagues who offered valuable insights and engaged in stimulating discussions, enriching the depth and breadth of my research.

Lastly, I express my gratitude to Högskolestiftelsen, Aktia, Kaute, and Tekniikan foundations whose support made this research possible.

Abstract

This research work started in 2020 and the place of research has been the Laboratory of Energy Technology at the Faculty of Science and Engineering of Åbo Akademi University.

In the context of circular bioeconomy, the process integration refers to inserting a valorization process into the existing waste-generating sectors. Especially, the wastes related to population growth and human activities are challenging to process due to being high-volume, dilute streams. Hydrothermal processes are suitable for this kind of waste streams. There is a research gap as these waste wet biomass feedstocks are not effectively processed, thus highlighting the need for an innovative solution in this area.

The main goal of this research project is to contribute to sustainability transformation to the circular economy. This contribution is achieved through comprehensive research on the most economically and technologically viable processes for biorefineries.

The objective of this research is to develop biorefinery integration concepts enhancing the energy and resource recovery from the waste streams, thus achieving circularity in the waste-generating sectors. Especially, high-volume, dilute aqueous wastes introduce challenges regarding recovery. This kind of wastes can be processed most effectively through hydrothermal processes: using water as the reaction media and not requiring energy-demanding drying or evaporation step. The case studies in this research included the integration of hydrothermal processes with biogas plants.

The biorefinery concepts should be developed following the desired products or recovery needs and the biomass waste. Furthermore, the operational aspects can be addressed through novel biorefinery concepts combining the hydrothermal processes effectively. The investigation on the operational aspects of supercritical water gasification and hydrothermal liquefaction highlighted the safety issues, long-term operational issues, and an operational aspect affecting the economic performance. The main solution is proposed as selecting the conditions to minimize these issues. Meanwhile, this research proposed new process integration concepts to address the operational aspects and to improve the economic performance as well as improving the mineral and nutrient recovery. One of the proposed processes is hydrothermal

carbonization of digestate followed by supercritical water gasification of the aqueous effluent, integrated with biogas plants. The other is hydrothermal liquefaction of sewage sludge, hydrothermal carbonization of digestate and supercritical water gasification of the aqueous effluents.

The research proposed here is well in line with the strategic research profile in Technologies for a Sustainable Future at FNT, ÅAU. This research contributes to the Sustainable Development Goals proposed by the United Nations and in particular it contributes to the SDG-7. Affordable and Clean Energy; SDG-12: Responsible Consumption and Production and SDG-13: Climate Action.

Sammanfattning

Detta forskningsarbete startade 2020 och forskningsplats har varit Laboratoriet för energiteknik vid Åbo Akademis naturvetenskapliga fakultet.
I samband med cirkulär bioekonomi avser processintegration att infoga en valoriseringsprocess i de befintliga avfallsgenererande sektorerna. Särskilt avfallet relaterat till befolkningstillväxt och mänskliga aktiviteter är utmanande att bearbeta på grund av att det innebär stora volymer, utspädda strömmar. Hydrotermiska processer är lämpliga för denna typ av avfallsströmmar. Det finns en forskningslucka eftersom dessa våta biomassaråvaror inte behandlas effektivt, vilket visar på behovet av en innovativ lösning på detta område.
Huvudmålet med detta forskningsprojekt är att bidra till hållbarhetsomvandling till den cirkulära ekonomin. Detta bidrag uppnås genom omfattande forskning om de mest ekonomiskt och tekniskt genomförbara processerna för bioraffinaderier.
Målet med denna forskning är att utveckla koncept för bioraffinaderiintegrering som förbättrar energi- och resursåtervinningen från avfallsströmmarna och på så sätt uppnå cirkularitet i de avfallsgenererande sektorerna. Stora volymer, utspädda vattenhaltiga avfall innebär speciellt utmaningar när det gäller återvinning. Denna typ av avfall kan bearbetas mest effektivt genom hydrotermiska processer: med vatten som reaktionsmedium och kräver inte energikrävande torkning eller förångningssteg. Fallstudierna i denna forskning inkluderade integrationen av hydrotermiska processer med biogasanläggningar.
Bioraffinaderikoncepten bör utvecklas efter önskade produkter eller återvinningsbehov och biomassaavfallet. Dessutom kan de operativa aspekterna hanteras genom nya bioraffinaderikoncept som kombinerar de hydrotermiska processerna effektivt. Undersökningen om de operativa aspekterna av superkritisk vattenförgasning och hydrotermisk kondensering lyfte fram säkerhetsfrågorna, långsiktiga operativa frågor och en operativ aspekt som påverkar det ekonomiska resultatet. Den huvudsakliga lösningen föreslås vara att välja förutsättningar för att minimera dessa problem. Samtidigt föreslog denna forskning nya processintegrationskoncept för att ta

itu med de operativa aspekterna och för att förbättra den ekonomiska prestandan samt förbättra återvinningen av mineraler och näringsämnen. En av de föreslagna processerna är hydrotermisk förkolning av rötrest följt av superkritisk vattenförgasning av det vattenhaltiga avloppsvattnet, integrerat med biogasanläggningar. Den andra är hydrotermisk kondensering av avloppsslam, hydrotermisk förkolning av rötgas och superkritisk vattenförgasning av de vattenhaltiga avloppsvattnet.
Den forskning som föreslås här ligger väl i linje med den strategiska forskningsprofilen inom Technologies for a Sustainable Future vid FNT, ÅAU. Denna forskning bidrar till de hållbara utvecklingsmål som föreslagits av FN och i synnerhet bidrar den till SDG-7. Prisvärd och ren energi; SDG-12: Responsible Consumption and Production och SDG-13: Climate Action.

Contents

List of figures

List of tables

List of publications

This doctoral dissertation consists of a summary of the following publications, which referred to the text by their numerals.

I. N. Ghavami, K. Özdenkçi, G. Salierno, M. Björklund-Sänkiaho, and C. De Blasio, 'Analysis of operational issues in hydrothermal liquefaction and supercritical water gasification processes: a review', Biomass Conversion and Biorefinery, Volume 13, pages 12367–12394, December 2021, doi: 10.1007/s13399-021-02176-4.

II. G. Salierno, F. Marinelli, B. Likozar, N. Ghavami, and C. De Blasio, 'Supercritical Water Gasification of glycerol: Continuous reactor kinetics and transport phenomena modeling', International Journal of Heat and Mass Transfer, Volume 183, Part C, February 2022, 122200, https://doi: 10.1016/j.ijheatmasstransfer.2021.122200

III. N. Ghavami, K. Özdenkçi, S. Chianese, D. Musmarra, and C. De Blasio, 'Process simulation of hydrothermal carbonization of digestate from energetic perspectives in Aspen Plus', Energy Conversion and Management, vol. 270, page 116215, October 2022, doi: 10.1016/j.enconman.2022.116215.

IV. N. Ghavami, K. Özdenkçi, and C. De Blasio, 'Process simulation of co-HTC of sewage sludge and food waste digestates and supercritical water gasification of aqueous effluent integrated with biogas plants', Energy, vol. 291, page 130221, March 2024, doi: 10.1016/j.energy.2023.130221.

V. N. Ghavami, K. Özdenkçi, S. Chianese, D. Musmarra, and C. De Blasio, 'Novel biorefinery ideas for conversion of biomass to biofuel', Computer Aided Chemical Engineering, vol. 52, A. C. Kokossis, M. C. Georgiadis, and E. Pistikopoulos, Eds., in 33 European Symposium on Computer Aided Process Engineering, vol. 52, Elsevier, 2023, pages 1963–1968. doi: 10.1016/B978-0-443-15274-0.50312-7.

Authors' contribution

Paper I: Analysis of operational issues in hydrothermal liquefaction and supercritical water gasification processes: a review

Niloufar Ghavami: Writing – review & editing, Writing – original draft, Validation, Investigation, Data curation, Conceptualization. Karhan Özdenkçi: Writing – review & editing, Writing – original draft, Validation, Supervision, Investigation, Formal analysis, Data curation, Conceptualization. Cataldo De Blasio: Project administration, Supervision, Funding acquisition, Writing – review & editing.

Paper II: Supercritical Water Gasification of glycerol: Continuous reactor kinetics and transport phenomena modeling

Gabriel Salierno: Formal analysis, Writing –original draft, Conceptualization, Methodology. Fabrizio Marinelli: Formal analysis, Data curation, Investigation. Blaž Likozar: Writing –review & editing, Visualization. Niloufar Ghavami: Writing –original draft. Cataldo De Blasio: Data curation, Writing –review & editing, Funding acquisition, Supervision, Project administration, Resources.

Paper III: Process simulation of hydrothermal carbonization of digestate from energetic perspectives in Aspen Plus

Niloufar Ghavami: Writing – original draft, Writing – review & editing, Conceptualization, Methodology, Software, Investigation. Karhan Özdenkçi: Writing – original draft, Writing – review & editing, Conceptualization, Methodology, Software. Simeone Chianese: Writing – review & editing, Visualization. Dino Musmarra: Supervision, Funding acquisition. Cataldo De Blasio: Project administration, Supervision, Funding acquisition, Writing – review & editing.

Paper IV: Process simulation of co-HTC of sewage sludge and food waste digestates and supercritical water gasification of aqueous effluent integrated with biogas plants

Niloufar Ghavami: Writing – review & editing, Writing – original draft, Validation, Software, Methodology, Investigation, Data curation,

Conceptualization. Karhan Özdenkçi: Writing – review & editing, Writing – original draft, Validation, Supervision, Software, Methodology,

Investigation, Formal analysis, Data curation, Conceptualization. Cataldo De Blasio: Project administration, Supervision, Funding acquisition, Writing – review & editing.

Paper V: Novel biorefinery ideas for conversion of biomass to biofuel

Niloufar Ghavami: Writing – original draft, Writing – review & editing, Conceptualization, Methodology, Software, Investigation. Karhan Özdenkçi: Writing – original draft, Writing – review & editing, Conceptualization, Methodology, Software. Simeone Chianese: Writing – review & editing, Visualization. Dino Musmarra: Supervision, Funding acquisition. Cataldo De Blasio: Project administration, Supervision, Funding acquisition, Writing – review & editing.

List of abbreviations

Agricultural residue	AGR
Anaerobic digestion	AD
Biochemical methane potential	BMP
Chemical oxygen demand	COD
Combined heat and power	CHP
Circular economy	CE
Food waste digestate	FWD
Greenhouse gas	GHG
Higher heating value	HHV
Hydrothermal carbonization	HTC
Hydrothermal gasification/ supercritical water gasification	HTG/SCWG
Hydrothermal liquefaction	HTL
Kraft black liquor	KBL
Residence time	RT
Severity factor	SF
Sewage sludge digestate	SSD
Supercritical water	SCW
Synergistic coefficient	SC
Synergistic effect	SE
Sustainable development goals	SDGs

1. Introduction

The United Nations defines sustainable development as 'the development that meets the needs of the present without compromising the ability of future generations to meet their own needs.'[1,2] Sustainable development and sustainability have never been a critical global concern as in recent years. Sustainability relies on three pivotal pillars: environment, economy, and society. Consequently, sustainable development goals (SDGs) are designed by the United Nations to mitigate the overreliance on fossil fuels, environmental preservation, and socioeconomic development.

Human activities coupled with current energy technologies put the environment and the future of human civilization in danger. The human activities affecting the nature include processes like extracting and processing raw materials and fossil fuels, energy production, agricultural and industrial activities as well as transportation. Renewable energies and novel energy technologies can mitigate adverse consequences such as greenhouse gas (GHG) emissions. Renewable energies are considered roughly emission-free energy resources including solar, hydro, wind, and biomass. However, it is crucial to note that these sources also have some effects, and their negative impact is different from one technology to another. For instance, geothermal power plants emit lower GHG compare to traditional power plants; however, the CO_2 emission needed to be evaluated case by case since some plants emit almost 14 times higher than solar and wind power plants [3,4]. Therefore, three main changes need to be considered to achieve sustainable development in the energy sector: substitution of fossil fuels, emission reduction, and energy efficiency enhancement.

Assessment of renewable energy development in the European Union [5] indicates that the energy transition in Europe has a fast pace. According to recent statistics, renewable energies provided 29% of the worldwide electricity generation in 2020, a substantial increase from 18% recorded in 2009 [6]. The EU electricity production derived from renewables demonstrated noticeable growth from 21.18% in 2013 to 38.16% in 2018 [7]. However, there is more capacity for renewable energy production in the future.

Furthermore, renewable energies have an important role in decarbonization of energy production, thus reducing carbon dioxide in the environment.

Decarbonization of the energy system is essential to reduce the emission and also meet the emission target outlined in the Paris Agreement [8]; a target regarding the substantive contribution of renewable energy resources.

Aligned with the research profile of Technologies for a Sustainable Future, Åbo Akademi University and the Faculty of Science and Engineering strive to develop pioneer innovative methods and technical solutions that support and promote the transition toward sustainable production and energy supply within the framework circular economy concept. Finland is one of the countries with the highest renewable energy resources. In a noteworthy achievement, Finland achieved the top position in the UN Sustainable Development Goals (SDGs) for the first time in 2021, and again in 2022. [9]. Finland reaffirmed its leadership in the annual global ranking of sustainable development. This underscores Finland's steadfast commitment to sustainability. Therefore, the most significant endeavor is needed to sustain, reduce climate change, and improve more sustainable consumption and production patterns.

The current linear economic model operates on the take-make-dispose principle (Figure 1-1). In this model, significant amounts of pollutants and waste are generated, and a product is treated as waste after utilization. This approach leads to environmental problems and endangers human well-being [1].

Figure 1-1. Linear (non-cyclic) economic model

In contrast, the circular economy (CE) represents a paradigm shift, focusing on the efficient utilization of resources, increasing materials' lifecycle, recycling, and decreasing the negative impact on the environment (Figure 1-2). In a CE framework, the lifespan of resources and materials increases, i.e. the materials are active in the economy as long as possible. There is no exclusive definition for CE but according to Kirchherr et al. [10], CE is "an economic system that replaces the 'end-of-life' concept with reducing, alternatively reusing, recycling and recovering materials in production/distribution and consumption processes". In fact, CE is an essential element and pivotal component for moving towards sustainable development and a sustainable future.

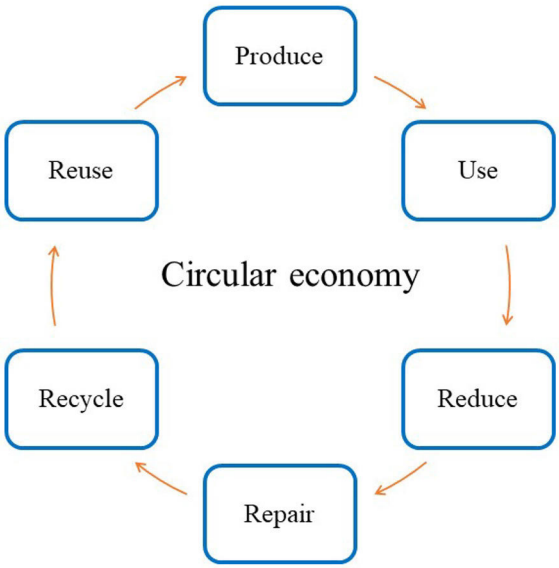

Figure 1-2. Circular economy concept

The key principles of the CE are the 3Rs; reduce, reuse, and recycle which are the bases for waste management processes [11]. This approach not only decreases waste disposal in landfills but also mitigates the environment extraction, by increasing the material life cycle. In other words, effective waste management and minimizing waste are the key for moving towards the CE.

Bio-based products have a central role and can provide several advantages in the circular economy or more accurately circular bioeconomy. The circular bioeconomy concept represents flawless integration of bioeconomy and circular economy principles in which bio-based resources are the primary raw material. This paradigm provides an efficient system for by-products and waste materials to transform into value-added products such as biofuels, biochemical, and biomaterials [12]. In this system, the biorefinery concept emerges as a pioneering concept and can be defined as an integration of different processes capable of producing biofuels and electricity from biomass [13]. Biorefinery is the foundation for accomplishing the SDGs and the transition to the bioeconomy. Biorefineries use a variety of bio-based raw materials and generate minimum waste. These features reduce strain on the environment and are important elements in the circular bioeconomy. Research and investigation on biorefinery

ideas also provide a holistic view for decision-makers, resulting in economic, social, and environmental advantages.

Biomass is considered any organic matter used to produce energy, which comes from a living organism by photosynthesis or from animals. It is formed by the interaction between air, carbon dioxide, water, sunlight and soil with plants and animals [14]. Biomass materials are divided into two main groups: wood and non-wood. The classification of different types of biomass is depicted in Figure 1-3 [15]. Both biomass categories come from forestry, agricultural, and urban wastes. Woody biomass constitutes trees, root leaves, and bark and their major components are lignin and carbohydrate. This form of biomass is converted to electricity and heat by combustion or other conversion processes. Herbaceous biomass is a non-woody part of the plant that remains after the growing season, including seeds crops, grains, or by-products of food processing. Aquatic biomass encompasses emerging plants, macroalgae, and microalgae, regarded as a resource for third-generation biofuels. It is noteworthy that animal and human waste were used as fertilizers traditionally; however, it is currently not possible to use these wastes directly due to pollution and environmental regulations. Therefore, further processes are needed to convert these waste products into valuable chemicals.

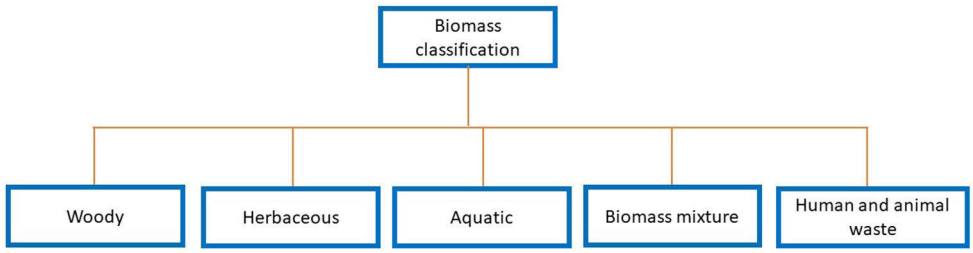

Figure 1-3. Biomass classification

The main components of woody biomass are cellulose, hemicelluloses and lignin while non-wood biomass contains a diverse array of components such as lipids, proteins, extractives, starches, sugars, hydrocarbons, water-soluble substances. In addition, biomass also contain ash, a small amount of alkali, alkaline, and traces of heavy metals [16]. Biomass waste resources are the center of this work, representing renewable energy sources with zero carbon emissions, positioning

as the fourth energy source globally. The solar energy saved in biomass can be recovered by combustion or via fuel production processes effectively.

1.1. Biomass conversion technologies

Waste biomass feedstock is converted to value-added biochemicals and biofuels via diverse methodologies including thermochemical, biochemical, and physicochemical technologies [17,18]. Several factors affect selection of the conversion method such as type, characteristics, the quantity of the feedstock, the final form of product, desired type of energy, adherence to environmental policies, and economic conditions.

Thermochemical conversion encompasses four main processes: combustion, pyrolysis, liquefaction (hydrothermal), and gasification (Figure 1-4) which employ chemical processes and heat to achieve primary products [19]. The biochemical conversion method includes two main processes employing microorganisms to convert biomass into liquid or gaseous fuels: anaerobic digestion (AD) producing biogas, and fermentation for ethanol production. The physicochemical method can be applied as a mechanical pretreatment including pulping, extraction, or hammer mill to separate lignin [20].

Thermochemical conversion methods have higher efficiencies and lower reaction times compared to alternative approaches. Moreover, the non-biodegradable organic compounds, such as lignin, are decomposed via thermochemical methods [21].

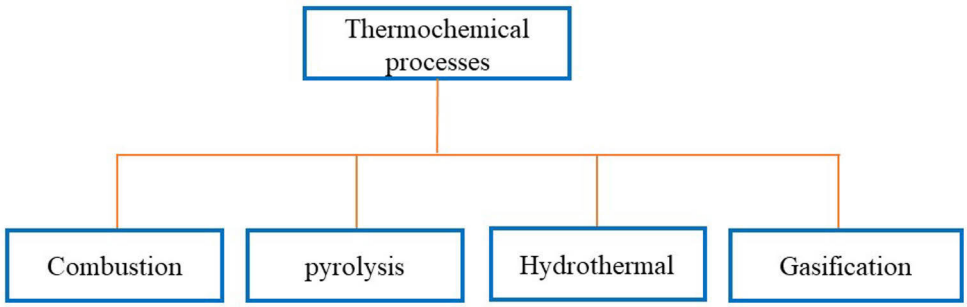

Figure 1-4. Thermochemical conversion methods

Thermochemical conversion methods can also be classified as thermal and hydrothermal processes. Hydrothermal processes are suitable technologies for

converting wet biomass feedstock to biofuels; these processes include hydrothermal carbonization (HTC), hydrothermal liquefaction, (HTL), and hydrothermal gasification or supercritical water gasification (HTG/SCWG). The superiority of these processes is due to omitting the costly drying pretreatment since these technologies handle biomass slurries with 10-30% of solids [22]. As an example, almost 60% of the total cost results from the required energy for the dewatering of sludge before thermal processes [23]. Hydrothermal processes require external energy to heat up the feedstock up to the reaction temperature, after a heat exchange with the reactor outlet. This energy requirement can be covered through combustion of small part of the product or from the excess heat of the integrated process (if any), compromising the district heat or combined heat and power (CHP) production depending on the reaction temperature. Despite this energy requirement, hydrothermal processes are more energy efficient than thermal processes because of higher product quality and occurring at lower temperatures [24,25].

The treatment of wet biomass feedstock can be in subcritical or supercritical water; therefore, hydrothermal processes can be divided into three processes based on the process condition and severity. HTC process occurs in subcritical conditions at 180-280^{o}C temperature and under autogenous pressure, the main product is hydrochar similar to low-rank coal. HTL occurs at intermediate temperatures (280-375 ^{o}C) and results in biocrude oil production. HTG/SCWG occurs at temperatures higher than 375 ^{o}C and the final product is syngas. Figure 1-5 briefly illustrates the main product of each process and the product applications.

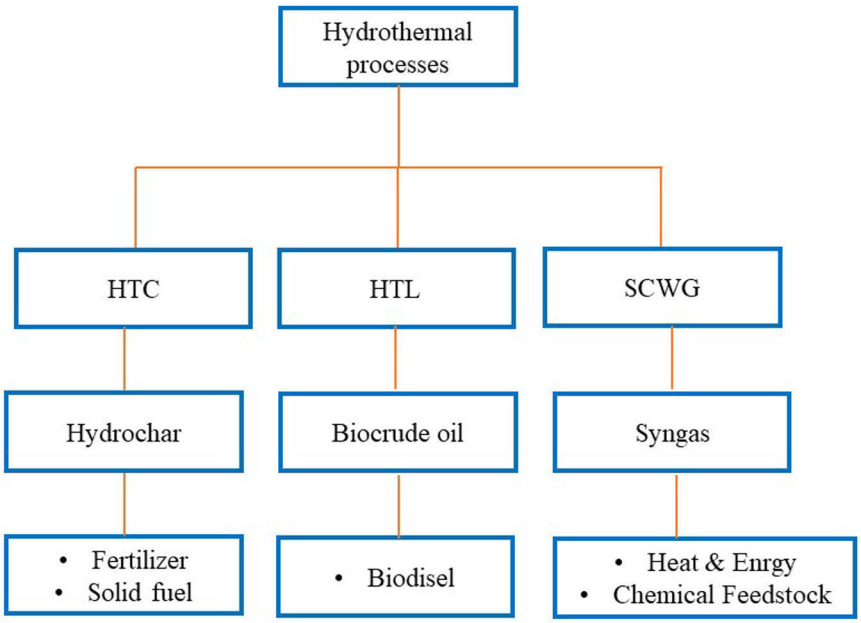

Figure 1-5. Hydrothermal processes and their applications

Hydrothermal methods are the most promising conversion routes for biofuel production; however, some operational issues prevent the industrialization of the mentioned processes, e.g. corrosion, char formation in HTL and SCWG, reactor plugging in SCWG due to solid deposition, and catalyst deactivation [24,26–28]. Meanwhile, the studies on hydrothermal processes briefly discuss the operational issues while investigating the impacts of conditions through experiments or simulations and feasibility assessments. Similarly, the review articles usually mention the operational aspects briefly while investigating the feedstock types, reaction mechanisms, catalysts, and the impacts of reaction conditions. Therefore, there is a need for the study and investigation of these processes: deeper investigations of the operational issues and the solutions addressing these issues.

1.2. Process integration for circular bioeconomy

Biomass feedstock can be categorized into first and second generations. First-generation biomass includes edible feedstock (e.g., sugarcane and food crops) that conflict with food production as well as requiring land and water usage, thus

introducing issues regarding environmental sustainability. On the other hand, second-generation biomass includes waste biomass material. Unlike the first generation, waste biomass is a more sustainable resource that contributes to a circular bioeconomy. It not only minimizes competition with food resources but also addresses the problems related to pollution and landfilling of wastes.

In the context of circular bioeconomy, the process integration refers to inserting a valorization process into the existing waste-generating sectors, i.e., utilizing the waste stream as a feedstock for further chemical production or energy recovery. Especially, the wastes related to population growth and human activities are challenging to process due to being high-volume, dilute streams, e.g., digestate streams of biogas plants. Hydrothermal processes are suitable for this kind of waste streams.

There is a research gap as these waste wet biomass feedstocks are not effectively processed, thus highlighting the need for an innovative solution in this area. Furthermore, effective processing methodologies have great importance in the regional context. For instance, Stormossen in Vaasa and Gasum in Turku provide a compelling case study. These companies' biogas plants process waste biomass including sewage sludge, agricultural crop, manure, and food waste in different digesters. The integration of hydrothermal processes offers multiple advantages to these biogas plants. The regional investigations of such integrations not only address local waste challenges but also serves as a practical model for broader adoption in similar contexts internationally, contributing to sustainable practices and a circular bioeconomy.

Another aspect of process integration is constructing the optimum process concept for valorizing the waste streams: addressing weaknesses of an individual process, selecting the optimum reaction conditions, and combining the process options to maximize productivity and minimize operational issues. Hence, the efficiency of processes is synergistically enhanced. Integration of processes can create a robust system to mitigate challenges and optimize resource recovery while producing energy and multiple products.

2. Objectives

The main goal of this research project is to contribute to sustainability transformation to the circular economy. This thesis strives to expand the knowledge in the field of sustainability by addressing crucial aspects related to biorefineries. This contribution is achieved through comprehensive research on the most economically and technologically viable processes for biorefineries. As mentioned earlier, biorefineries represent integrated processes that use bio-based raw materials, minimize waste generation, and produce diverse products. This concept reduces strain on the environment, and it is a fundamental element in the circular economy. This research aims at addressing the challenges of chemical and energy recovery on aqueous waste streams. Therefore, the scope is to investigate hydrothermal conversion technologies including SCWG, HTL, and HTC to develop innovative biorefinery concepts.

The objective of this research is to develop novel biorefinery concepts to reach a sustainable, circular bioeconomy.

The research questions include:

- Determine the target products based on the feedstock and recovery needs
- Develop process concepts benefitting the strengths of conversion technology while addressing the weaknesses of each
- Selection of optimum reaction conditions from both the productivity and techno-economic viewpoints

Figure 2-1 illustrates the connections of articles regarding the need for circularity in biomass sectors and the objective of this dissertation. Paper I investigated the operational issues of SCWG and HTL and their possible solutions. There were only a few studies investigating the operational issues as the main scope despite the impacts on techno-economic performance. From the operational viewpoint, Paper I demonstrated the need for novel process concepts empowering the strengths of each hydrothermal conversion and addressing the weaknesses.

Paper II investigated the impacts of reaction conditions in SCWG of glycerol through experiments in a tubular reactor. This paper illustrated the necessity of process configuration enhancing the heat and mass transfer. In addition, this paper also determined the various sets of conditions can result in similar hydrogen productivities. Therefore, the reaction conditions should be selected also considering the techno-economic aspects.

Paper III and Paper IV simulated the HTC process integrated with biogas plants, referring to the need for biogas plants to valorize digestate wastes. Paper III introduced a methodology to select optimum conditions, utilization of experimental results for obtaining the simulation data, and process simulation of HTC of agricultural residue digestate. Paper IV simulated co-HTC of food waste and sewage sludge digestates by selecting the optimum conditions and utilizing the experimental results as introduced in Paper III. Paper IV also simulated co-HTC of digestates followed by SCWG of aqueous effluent to increase the recovery.

Paper V proposed a novel biorefinery concept for biogas plants in case of capacity increase. In the case of a biogas plant processing sewage sludge; the integration concept is HTC of digestate, HTL of extra sewage sludge, and SCWG of the aqueous effluents of HTC and HTL. This concept is a multi-product process with optimum conversion of wastes and addressing the operational issues.

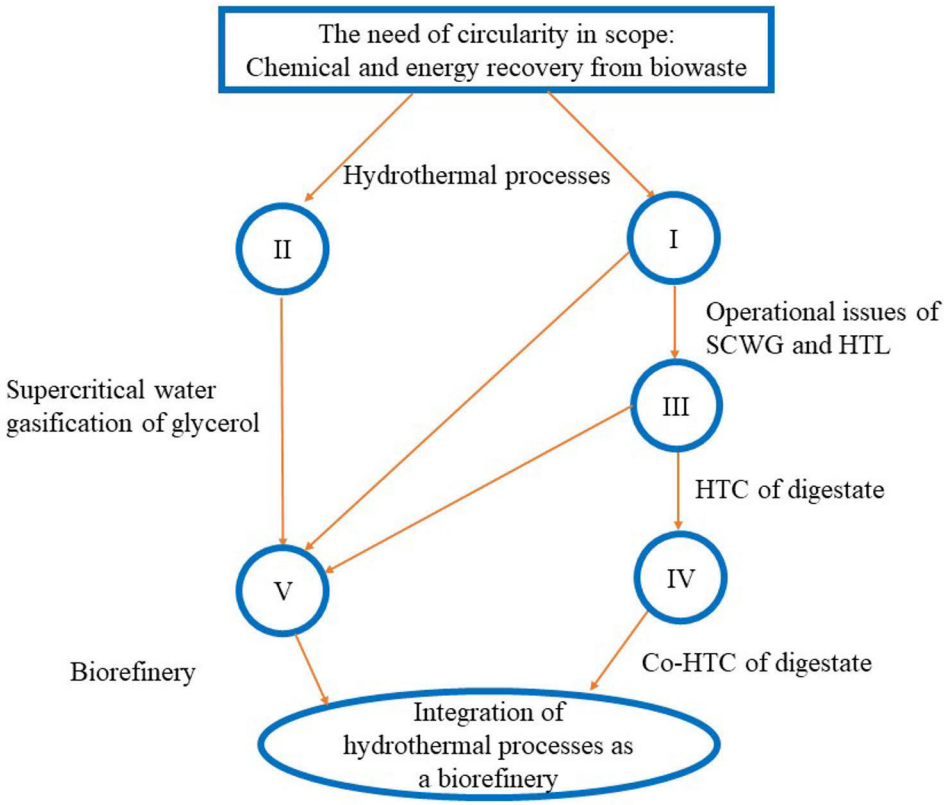

Figure 2-1. Objectives of the thesis and the roles of articles

In summary, this doctoral dissertation significantly contributes to the field by advancing the understanding of hydrothermal conversion technologies, proposing innovative biorefinery concepts, and emphasizing the importance of operational considerations in achieving a sustainable, circular bioeconomy. In addition, this dissertation investigates the process simulation and economic aspects by using experimental data: prioritizing the usage of characterization data, thermodynamic models, and selection of optimum conditions from the economic viewpoint. The systematic exploration of diverse aspects and the integration of findings across multiple papers underscore the comprehensive and impactful nature of this research endeavor.

3. Theory

This section explains the process chemistry of the thermochemical conversion methods in detail. Hydrothermal processes occur in excess water at high pressure and temperature, and water acts as a reaction medium and reactant. Therefore, it is important to study the properties of water as the reaction medium in subcritical and supercritical conditions. On the contrary, operational cost increases in these conditions due to high temperature and pressure. After illustrating the water properties, this section introduces each hydrothermal process and thermodynamic models used in process simulations.

3.1. Water properties and processes chemistry

Water thermo-physical characteristics undergo significant changes in different conditions. In normal conditions, water acts as a polar solvent and dissolves most inorganic salts. However, organic compounds and gases are insoluble or slightly soluble. High polarity of water is attributed to hydrogen bonds that are dissociated in high temperatures and pressures. The critical point of water is 374 ^{o}C and 22.1 MPa. Water phase diagram is depicted in Figure 3-1 [29].

At subcritical and supercritical conditions, water characteristics change significantly including dielectric constant, density, viscosity, ion product, thermal conductivity, dissolution performance, and diffusion coefficient. The dielectric constant shows the liquid polarity and can be defined as absolute permittivity of a substance to the absolute permittivity of free space. Water dielectric constant is around 78.4 at ambient condition that is poorly miscible with gases and hydrocarbons; however, it is a proper solvent for polar materials. The ion product (K_w) of water can be explained as the production of the two concentrations of acid $H3O^+$ and basic OH^- ions dissociated from water (with the unit of $(mol/L)^2$). It significantly changes around water critical point and the amount of H^+ and OH^- ions increases which is favoring hydrolysis reaction [30,31]. Supercritical water (SCW) has low viscosity, a low dielectric constant, and a reduced amount of hydrogen bonds. [20,32].

Table 3-1 provides a comparative analysis of water characteristics in normal and supercritical conditions [31].

Therefore, water-dissolving ability changes in supercritical conditions, and both organic and inorganic matters are soluble and convert water to an ideal reaction medium with low mass transfer resistance. However, it is noteworthy that the solubility of salt decreased in supercritical conditions which resulted in corrosion and plugging problems. Moreover, operational challenges increase due to the high temperature and pressure.

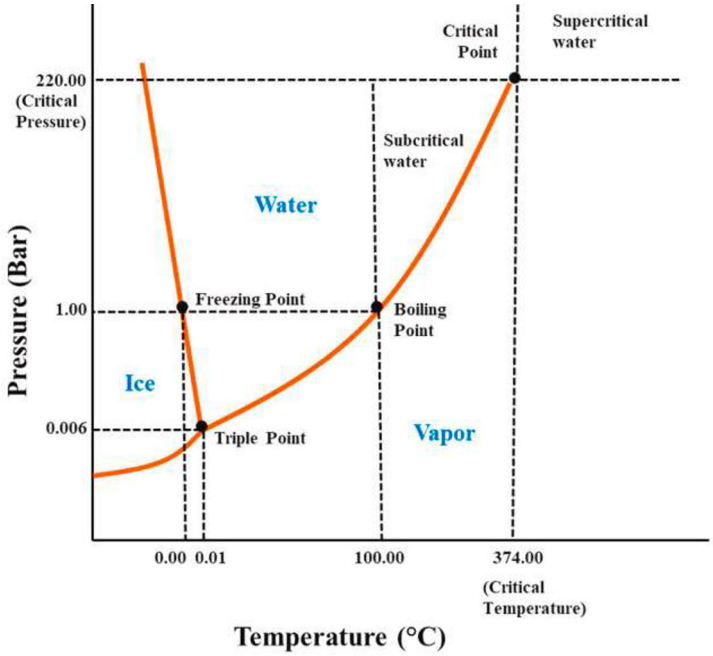

Figure 3-1. water phase diagram [29]

Equation *3-1* explains the water diffusion coefficient (D) which is the Stokes–Einstein relationship, where k is the Boltzmann constant (1.3806503.10−23 J/K), T is absolute temperature (K), η is dynamic viscosity of solvent, and r radius of molecule assumed as spherical (m) [31]. Low viscosity in subcritical and supercritical conditions results in higher molecular mobility and diffusion coefficient.

$$D = \frac{k.T}{6\pi\eta r} \qquad \textit{Equation 3-1}$$

Table 3-1. Water characteristics at different conditions

Water properties	Normal	Subcritical	Supercritical
T (^{o}C)	25	350	450
P (MPa)	0.1	25	25
Density (Kg/m^{3})	997.45	625.45	108.98
Dielectric constant (-)	78.5	14.87	1.75
Ionic product (mol/L)^{2}	14	11.55	18.14

Table *3-1* listed some water properties in normal (25 ^{o}C), subcritical (Tc<374°C), and supercritical (Tc>374°C) conditions. The density and dielectric constant decrease with the temperature and in contrast, ion production increases. It clearly shows that supercritical water acts as a non-polar organic solvent and a perfect reaction medium in hydrothermal gasification. Figure 3-2, Figure 3-3, and Figure 3-4 depict density values, the dielectric constant, and the specific heat of water in various temperatures and pressures [33].

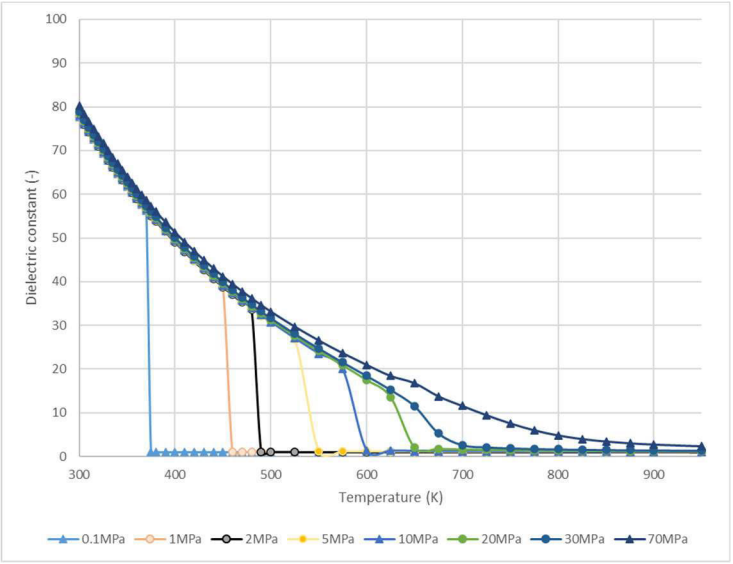

Figure 3-2. The dielectric constant of water as a function of temperature at different pressures

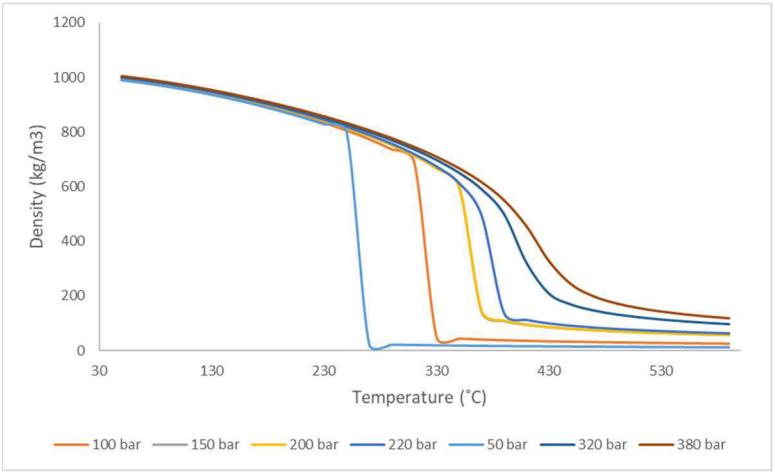

Figure 3-3. Density values for water as a function of temperature at different pressures

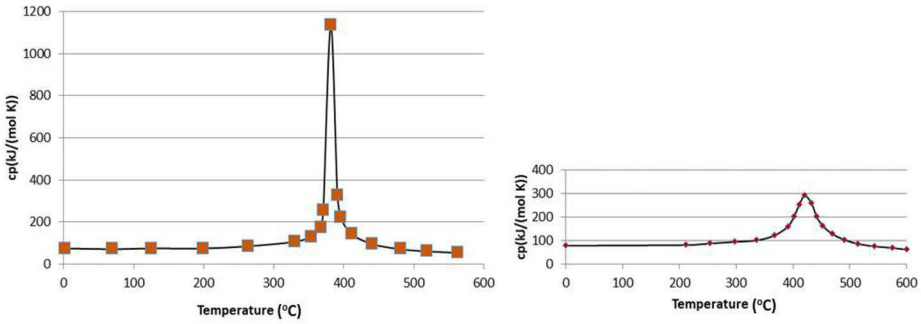

Figure 3-4. Variation of the specific heat at constant pressure for water. Left: 24 MPa, Right: 36 MPa.

3.2. Hydrothermal processes

Hydrothermal processes include hydrothermal carbonization, hydrothermal liquefaction, and supercritical water gasification that are conducted at high pressure and temperature in which water acts as a reaction medium.

3.2.1. Hydrothermal carbonization

Hydrothermal carbonization simulates the natural coalification process of the biomass feedstock under relatively moderate conditions compared to

hydrothermal liquefaction and supercritical methods. It is also known as a wet torrefaction that can destroy the pathogenic bacteria in the biomass feedstock without the disadvantages of dry torrefaction [34]. The reaction condition is under moderate pressures (2- 10 MPa) and temperatures (120- 250 ^{o}C), and the reaction period is 15 min- 4 hours. Process residence time and temperature are influential parameters in the HTC process. Higher temperatures can increase aromatization and polymerization reactions while the residence time controls the extent of carbonization. The HTC process results in the production of hydrochar (solid product), process water (liquid product), and a minor amount of gas product. Hydrochar, a versatile product, can be used as a biofuel, absorbent, or fertilizer [35,36].

The overall HTC process mechanism consists of chemical hydrolysis, dehydration, decarboxylation, condensation, and polymerization reactions for converting organic waste to hydrochar [37,38]. However, the mechanism is influenced by the feedstock type and composition of lignocellulosic and protein-containing organic waste [39]. For a visual representation, Figure 3-5 depicts the HTC mechanism and the resulting products of different steps of the process. In the hydrolysis stage, water is in the sub-critical region, functioning as a non-polar solvent and reacts as a catalyst in the reactions. The presence of water in this condition facilitates hydrolysis at low temperatures by reducing the activation energy levels for bond cleavage. At high temperature and pressure, the degree of ionization is high causing water to dissociate into basic and acidic ions (hydroxide ions (OH^-) and hydronium ions (H_3O^+)) that have both basic and acidic characteristics. According to Kannan et al. [38], biomass coalification is accelerated in subcritical conditions, emphasizing the influential role of water in promoting the hydrolysis stage of the process.

Following the hydrolysis process, the biomass feedstock undergoes decarboxylation and dehydration processes to eliminate water and carbon dioxide. In this stage, the pH decreases due to the production of organic acids including lactic, acetic, levulinic, propionic, and formic acids [40]. Hydronium ions are the catalysts for this stage resulting from the acid production. Intermediates formed in the hydrolysis step undergo decarboxylation and dehydration that leads to a reduction in oxygen-to-carbon (O/C) and hydrogen-to-carbon (H/C) ratios, and the formation of H_2O and CO_2 [38]. In the next step, the intermediates undergo condensation and polymerization processes accompanied by Maillard reaction.

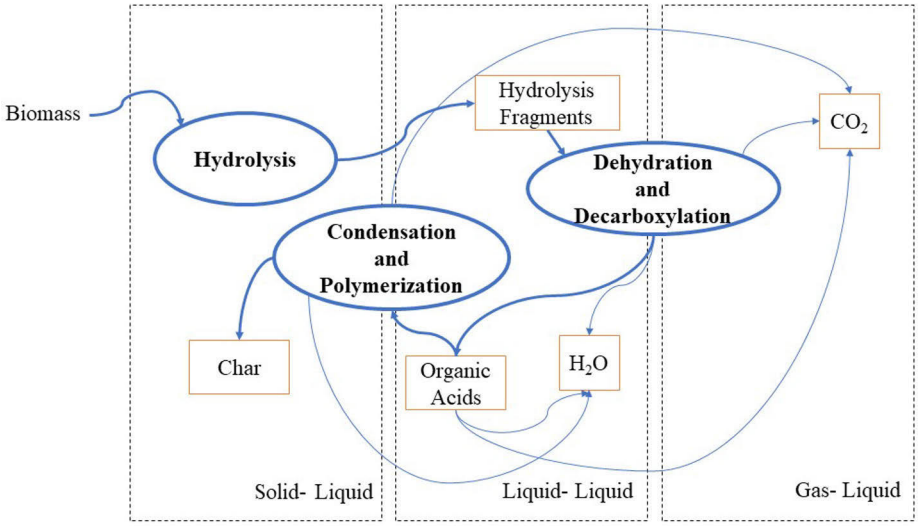

Figure 3-5. HTC mechanism and products (adapted from [38])

Lignocellulosic biomass is composed of cellulose, hemicellulose, and lignin. In the HTC process, the first affected component is hemicellulose, a branched short-chain polymer. Hemicellulose starts to hydrolyze at a temperature of 180 °C and breaks down into monosaccharide units (fructose, glucose, galactose, etc.) and polysaccharides. Cellulose is a linear polymer connected by a single thread and hydrolyzes at temperatures higher than those required for hemicellulose. Contrary, only a small amount of lignin dissolves at higher temperatures due to its complex and highly branched polymer structure. The remaining undissolved part participates in a solid-solid reaction and transforms into hydrochar [39].

There are two separate pathways in the HTC process of non-lignocellulosic and protein-base biomass for hydrochar formation. The conversion process of polysaccharides is the same as hemicellulose while the pathway is quite complicated for the proteins. Initially, the proteins undergo depolymerization, resulting in polypeptides and oligomers such as tetramers, trimers, and dimers. The reaction between the linear polypeptide and cyclic polypeptide is reversible and by enhancing the reaction condition, both convert into amino acids. Amino acids are involved in two main routes: 1) decarboxylation, producing amines and CO_2, and 2) deamination yielding organic acids and NH_4^+. The Maillard reaction occurs also between amino acids and reducing sugars. Lipids

decompose into glycerol and fatty acids gradually during the HTC process. As the process proceeds, fatty acids undergo hydrolysis, dehydration and decarboxylation processes which result in the formation of the hydrochar.

The HTC process is influenced by different parameters including temperature, residence time, feedstock composition, pressure, and the presence of a catalyst. Since HTC is an exothermic process, temperature has a significant role in the HTC process, directly affecting the hydrochar yield. At low temperatures, macromolecular compounds undergo hydrolysis, leading to intermediates production. As the temperature increases, the polymerization of small molecules accelerates. On the other hand, only a small fraction of organic matter undergoes hydrolysis at low temperatures, remaining in the solid phase. As the temperature increases, the solid production (hydrochar yield) decreases while the liquid and gas products increase. Moreover, the carbon content of hydrochar increases with temperature while oxygen and hydrogen contents decrease. This shift upgrades the fuel properties of the hydrochar. In addition, the hydrochar yield decreases significantly with temperature when operating at temperatures lower than 250 ^{o}C while the yield decreases slowly with temperature at 250 to 280 ^{o}C [39,41].

Residence time stands out as another important factor in the HTC process that influences product distribution, spanning a range from 15 minutes to 4 hours. Longer residence time increases higher heating value and reduces hydrochar yield. In addition, the residence time is directly related to the reactor size, i.e., equipment cost. Increasing residence time by more than 1 hour will increase the cost and energy for the HTC process without significantly improving the hydrochar properties.

Severity factor (SF) emerges as a valuable factor showing the combined impact of residence time and temperature on the final products. It can be expressed by

$$R_0 = t \cdot exp\left(\frac{T-100}{14.75}\right) \qquad \textit{Equation 3-2}$$

R_0 is the severity factor, T is HTC temperature (^{o}C), and t is residence time (minute). At high temperatures, higher reaction activity leads to the transition of water-soluble components into aqueous and gaseous phases, facilitating the transfer of organic matter. This transformative process occurs during

dehydration and decarboxylation reactions. As the temperature increases, a decrease is observed in –OH (hydroxyl) functional and O-containing groups.

The quantity of water is also an important factor in the HTC process, influencing both product distribution and higher heating value (HHV). The high amount of water accelerates the HTC reactions, particularly hydrolysis and decarboxylation. Contrary, an insufficient amount of water results in overheating of the reactor [42]. According to the literature, HHV reduces in case of a high amount of water in sludge feedstock which is due to a lack of solid load in the feedstock. Moreover, technical aspects are required to consider for the optimum water and feedstock ratio.

The HTC process is generally carried out at autogenous pressure and few investigations are available for the effect of pressure. Some investigations studied pressure modifications such as raising the pressure by injecting N_2, which showed a positive effect on dewatering performance (resulting in low moisture cakes). However, this adjustment had a negative effect on HHV [43]. According to some studies, an increase in pressure does not affect the HTC process [44,45].

The synergistic effect (SE) in HTC is linked to a series of reaction mechanisms, occurring during the process, particularly, when two different feedstocks are mixed. The SE can result in enhancing hydrochar properties as a fuel, energy yield, hydrochar yield, and carbon content. The SE is defined by the synergistic coefficient (SC), which is the comparison between the co-HTC experimental values and calculated values from the individual HTC results, as shown in Equation 3-3.

$$SC = \frac{Experimental\ value - Calculate\ \ value}{Calculated\ value} \times 100\% \qquad \textit{Equation 3-3}$$

3.2.2. Hydrothermal liquefaction

Hydrothermal liquefaction is another thermochemical conversion method that is carried on temperatures (200-450 ^{o}C) and pressure (4-35 MPa). In this process, water acts as a solvent, catalyst, and reactant in subcritical regions due to the changes in water properties such as viscosity and dielectric constant. Moreover, other organic solvents can be used in the HTL process as a co-solvent

such as glycerol, methanol, acetone, and ethylene glycol, or a mixture of an organic solvent and water. The biomass feedstock undergoes many reactions including hydrolysis, dehydration, decarbonylation, decarboxylation, denitrogenating, oxygenation/deoxygenation, dehydrogenation, esterification, alkylation/dealkylation, cracking, re-polymerization, and condensation [46]. The extensive number of reactions highlights the diversity of valuable products in the HTL process and the complex series of chemical transformations.

HTL process yields a variety of products, including biochar, biocrude, aqueous phase, and gaseous product. Biochar, the solid product, is considered an undesirable product resulting from the repolymerization of unsaturated compounds, i.e. low hydrogen content. Bio-crude oil is the main product in the HTL process with high viscosity. This product is rich in carbon and hydrogen with low moisture and oxygen content. The chemical compounds in bio-crude oil include aldehydes, aromatics, alcohols, ketones, and carboxylic acids [47]. The diverse composition of bio-crude requires refining and upgrading, incurring additional costs. Biocrude oil quantity depends on the types of biomass feedstock, operating conditions, and catalysts employed.

The aqueous phase contains water-soluble by-products from the dehydration step. The main compounds in the aqueous phase are formic acid, acetic acid, phenol, glycolic acid, methanol, lactone, and ethanol [48]. The gaseous product is a mixture of carbon monoxide (CO), carbon dioxide (CO_2), methane, alkenes, and alkanes, with low generation of NO_x and SO_x [49].

In the HTL process, cellulose decomposes into monosaccharides and oligosaccharides. Elevated temperatures prompt the conversion of monosaccharides into furan derivatives and aldehydes. The main products in the liquefaction of cellulose are fructose, glucose, erythrose, 5-hydroxymethylfurfural (5-HMF), levoglucosan, glyceraldehyde, ethanol aldehyde, acetone aldehyde, dihydroxyacetone, and some oligosaccharides. During the process, the breaking of hydrogen bonds in cellulose (inter- and intramolecular) occurs in reaction with water, and glucose monomers are formed. The main reactions that the glucose undergoes include 1) glucose isomerization to fructose, 2) glucose dehydration to 1, 6-anhydroglucose, and 3) glucose decomposition to ketones and aldehydes.

Hemicellulose is composed of monomers like glucose, galactose, mannose, xylose, and arabinose, etc. It hydrolyzed faster compared to cellulose, which is attributed to the less rigid crystalline structure. Hemicellulose undergoes the hydrolysis process into two main types of monosaccharides: hexose and pentose and then to 5-HMF. The reaction pathways involve 1) cleavage of sugar to alcohols and organic acids, 2) oxidation, dehydration, and isomerization, 3) oxidation, deoxygenation, and formation of macromolecular fragments from sugars, and 4) a small amount of condensation and esterification between lignin and hemicellulose.

In rapid hydrolysis, glucose and other saccharides are formed and further degraded into different oxygenated hydrocarbons such as lactic acid, formic acid, hydroxymethyl furfural (HMF), and levulinic acid. Lignin is also hydrolyzed during the liquefaction process in which the C–C bond and ether bond are cleaved and alkylation, demethoxylation, and condensation reactions happen. However, aromatic rings remain relatively stable during the HTL reactions, particularly the biphenyl-type compounds [50,51].

Lignin has a different and complex structure compared to cellulose and hemicellulose, consisting of three basic unites guaiacyl (G), syringyl (S), and p-hydroxyphenyl (H). During HTL of lignin, oligomers, monomers, and dimers are formed, catalyzing the conversion of lignin into aromatic chemicals. The degradation includes hydrolysis, breakage of carbon-carbon bonds, ether, alkylation of groups on the benzene ring, and degradation of methoxy on the benzene ring. Due to the complexity of lignin, some studies use phenolic model compounds. It is concluded that the aromatic ring is almost unaffected and the ether bond was broken easily in hydrothermal conditions [52].

Non-lignocellulosic feedstock contains proteins, lipids, and carbohydrate molecules. During the HTL process, these constituents are distributed in the liquid, solid, and gas. Lipid molecules are converted to biocrude oil due to having large molecule size, mainly hydrolyzed to produce long-chain fatty acids and glycerol. Carbohydrates and proteins are also hydrolyzed to sugars and amino acids. An increase in the temperature results in a series of reactions including dehydration, decarboxylation, deamination, etc. to produce ketones, furfural, aromatic hydrocarbons, alkenes, and alkanes. Maillard reaction is one of the important pathways for nitrogenous compound production in which amino acids react with carbonyl groups of reducing sugars [53].

The reaction pathways and products are predominantly affected by the feedstock type and reaction conditions. According to the literature, lignocellulosic biomass with a higher cellulose and hemicellulose concentration has a higher biocrude oil yield and conversion rate [54]. Both residence time and temperature affect the HTL product properties and yields.

Temperature is the main parameter that affects the calorific value and elemental composition of biocrude oil. The biocrude yield increases gradually with rising the reaction temperature up to 300 ^{o}C while the yield decreases with temperature when it exceeds 300 ^{o}C [55,56]. In the subcritical region, hydrolysis and dehydration are dominant, and increasing the temperature leads to the decomposition of lignocellulose components into small molecules, thus increasing the biocrude oil yield. By increasing the temperature, large molecules of biocrude oil polymerize into coke or decompose into a gas product. In conclusion, below the critical temperature, decomposition reactions govern the HTL process and above the critical temperature, repolymerization reactions are dominant.

Pressure is another parameter in the HTL process. In the subcritical region, elevated pressure increases water density, resulting in a single phase. This facilitates easier penetration into the lignocellulose and improves the interaction of hydrolysis ions. However, after reaching the supercritical condition, the effect of the pressure is negligible on the biocrude oil yield. To sum up, pressure effect is limited in the HTL process. Therefore, low pressure is preferred to save cost and energy [57,58].

Residence time is another influential factor affecting biocrude oil yield and composition of products. Biocrude oil yield rises with the increase of the residence time; however, short residence time leads to a decomposition reaction. Long residence times intensify condensation reactions, cracking of biocrude oil, and producing intermediate products to form gas or re-polymerize to produce coke, consequently, decreasing biocrude oil yield.

3.2.3. Hydrothermal gasification/Supercritical water gasification

Another hydrothermal conversion method is supercritical water gasification which converts biomass feedstock into a hydrogen-rich gas product. SCWG is a

prominent technology that has been known as a pollution-free method in recent years [59]. It is often conducted at a temperature of 375-700 °C and pressure of 22.1 MPa with or without using various heterogeneous/homogenous catalysts. Similar to the other hydrothermal methods, the process performance and product characteristics are affected by the feedstock composition, temperature, pressure and residence time [60].

The key advantage of the process is the utilization of supercritical water, characterized by a significant reduction in dielectric constant and viscosity. Water acts as an organic solvent, enhancing the miscibility of gases and organics, creating a single-phase environment in the reactor.

The overall reaction in SCWG can be described by Equation 3-4 in which x and y represent the molar ratios of H/C and O/C, respectively. The overall reaction is endothermic and includes several steps and intermediates as shown in Equation 3-5 to Equation 3-9.

$$CH_xO_y + (2 - y)\, H_2O \rightarrow CO_2 + (2 - y + \frac{x}{2})\, H_2 \qquad \textit{Equation 3-4}$$

- Steam reforming reaction: Produces carbon monoxide and hydrogen

$$CH_xO_y + (1 - y)\, H_2O \rightarrow CO + (1 - y + \frac{x}{2})\, H_2 \qquad \textit{Equation 3-5}$$

- Water Gas Shift reaction: The reaction is reversible and influenced by the temperature and presence of alkaline catalysts

$$CO + H_2O \leftrightarrow CO_2 + H_2 \qquad \textit{Equation 3-6}$$

- Methanation reaction of CO

$$CO + 3H_2 \rightarrow CH_4 + H_2O \qquad \textit{Equation 3-7}$$

- Methanation reaction of CO_2

$$CO_2 + 3H_2 \rightarrow CH_4 + H_2O \qquad \textit{Equation 3-8}$$

- Hydrogenation reaction

$$CO + 2H_2 \rightarrow CH_4 + 0.5\, O_2 \qquad \textit{Equation 3-9}$$

It is worth mentioning that hydrogenation and methanation reactions occur in longer residence time and the presence of catalysts.

Temperature is an important factor in hydrogen generation during the SCWG process. The steam reforming reaction is favored by higher temperatures due to its endothermic nature. Contrarily, the water-gas-shift reaction is exothermic and an increase in temperature accelerates the reverse reaction leading to higher consumption of hydrogen. According to the literature [31], hydrogen production increases up to an optimum temperature and decreases at higher temperatures.

Feedstock concentration is an economic factor influencing the equipment size as well as affecting the product composition. A high biomass concentration leads to a decrease in CO amount, i.e. suppressing the water-gas-shift reaction and reduces hydrogen production. Conversely, a low amount of water can also cause fouling and clogging problems due to salt precipitation and the high cost of pumping the feedstock.

Residence time is a key parameter in SCWG. In a short residence time, both hydrogen and carbon production show the same trend. The production increases up to its maximum and further increases showing no significant impact. Therefore, a combination of high temperature and short residence time is favorable for hydrogen production [61].

Pressure has a considerable effect on the water properties that cause an elevation in ionic compounds and the dielectric constant at subcritical region. Thus, it favors hydrolysis reaction due to improving generation of H^+ and OH^-. In addition, high pressure is desirable in CO and CO_2 methanation and water-gas-shift reactions although it decreases the decomposition reaction rate of biomass. However, based on studies, an increase in pressure has a low impact on the product gas composition in SCWG process [62].

The main pathways in SCWG of biomass include hydrolysis, pyrolysis, synthetic, steam-reforming, and dehydrogenation reactions; however, the pathways may vary due to the type of the feedstock. In the case of protein-base feedstock, proteins undergo hydrolysis to form amino acids, which then decompose into carboxylic acids and smaller molecules, and finally to acetic acid and formic acid. Organic acids convert into hydrogen, carbon dioxide, and carbon monoxide [63].

3.3. Thermodynamic models

Thermodynamic models represent the relations among thermodynamic, kinetic, and transport properties concerning conditions (pressure and temperature) and molecular interactions. An appropriate thermodynamic model is required for modeling a process simulation and to achieve reliable results. These models are classified as ideal models, activity coefficient models, and equation of state models. The ideal models are relatively simpler because of ignoring the molecular interactions. On the other hand, these models are accurate only in case of negligible or quite low molecular interactions. This requires low pressure and temperature resulting in low system density and slow movements of molecules. Meanwhile, the elevated temperature and system density require non-ideal models also representing the molecular interactions as in the systems of this research. Non-ideal liquid-liquid mixtures are modeled by using activity coefficient models while the non-ideal equation of state models represents the relations among pressure, temperature, and molar density of a system. For instance, the models below (Equations 3-10 to 3-13) are the most used ones for real systems and the ones used in our simulations.

Van der Waal's equation

$$\left[P_{obs} + a\left(\frac{n}{V}\right)^2\right](V - nb) = nRT \qquad \textit{Equation 3-10}$$

Redlich-Kwong equation of state

$$p = \frac{RT}{v_m - b} - \frac{a}{\sqrt{T}v_m(v_m + b)} \qquad \textit{Equation 3-11}$$

$$a = \frac{0.42748R^2T_c^{2.5}}{p_c}; b = \frac{0.086 \quad c}{p_c}$$

Soave-Redlich-Kwong equation of state

$$p = \frac{RT}{v_m - b} - \frac{a}{v_m(v_m + b)} \qquad \textit{Equation 3-12}$$

Where:

$$a = \frac{0.42748R^2T_c^2}{p_c}\alpha; b = \frac{0.08664 \quad c}{p_c};$$

$$\alpha = [1 + (1 - T_r^{0.5})(0.48508 + 1.55171\omega - 0.15613\omega^2)]^2;$$

$$\omega = -1 - log_{10}\left(\frac{p^{sat}}{P_c}\right)_{T/T_c=0.7};$$

Peng-Robinson equation of state

$$p = \frac{RT}{v_m - b} - \frac{a}{v_m^2 + 2bv_m - b^2} \qquad \textit{Equation 3-13}$$

Where

$$a = \frac{0.45724R^2T_c^2}{p_c}\alpha; b = \frac{0.07780RT_c}{p_c};\ \alpha = [1 + (1 - T_r^{0.5})(0.37464 + 1.54226\omega - 0.26992\omega^2)]^2$$

Selecting a proper thermodynamic model is crucial for the reliability of process simulation results. Due to numerous models being formulated, it is useful to utilize a selection guide classifying these models based on the system conditions. Figure 3-6 shows a scheme for thermodynamic model selection [64].

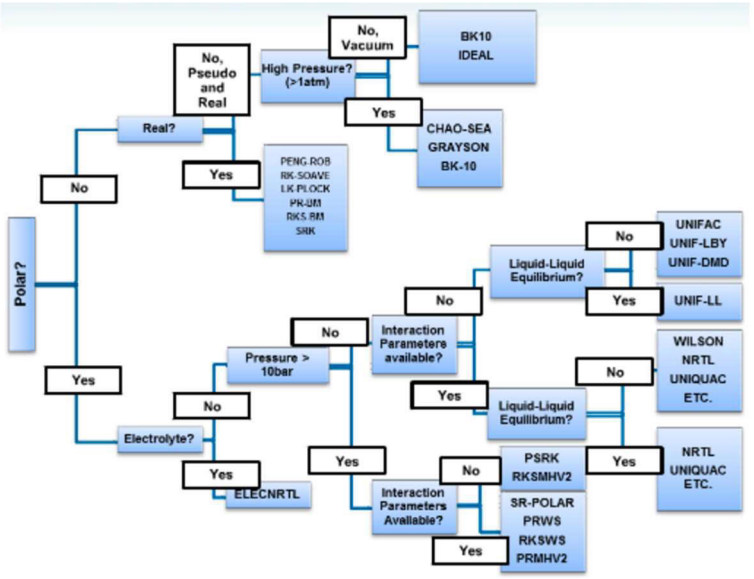

Figure 3-6. Thermodynamic property method guide adapted from [64]

4. Materials and Methods

The initial phase of this research project (Paper I) is based on the literature review to investigate the bottlenecks, constraints, and operational problems in biomass to biofuel conversion technologies that hinder the industrialization process. For Paper II, SCWG of glycerol was performed through a laboratory-scale continuous tubular flow reactor at the Process and Systems Engineering Laboratory at the Åbo Akademi University (Turku, Finland). Then, Paper III and Paper IV involved the simulations of the HTC process and HTC followed by SCWG of aqueous effluent. Similarly, Paper V was also a simulation study of a proposed biorefinery concept.

4.1. Supercritical water gasification of glycerol

The experimental setup is illustrated in Figure 4-1 The experiments were conducted in two different reactors with the same shape: stainless steel (SS-316) and Inconel-625. The total inner volume of the reactors is 83 ml, and their length is 0.51 m. The piping and fittings have an internal diameter of 3 mm and an outside diameter of 6 mm with a working pressure of up to 420 bar. The pressure is measured with an electronic manometer and controlled through a back-pressure valve. The feedstock is pressurized by introducing nitrogen gas from the top of the feed cylinder. Temperature is measured at three different points (inlet, center, and outlet) through thermocouples placed at the outer wall of the reactor. Temperature is controlled to maintain 610 °C at the central thermocouple (T2).

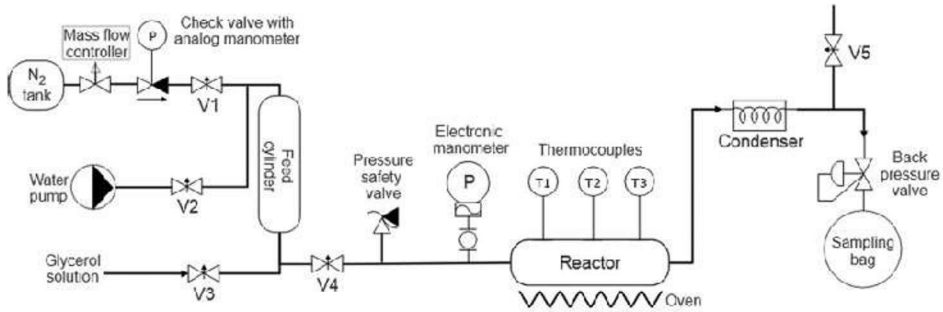

Figure 4-1. The experimental setup for SCWG of glycerol

The experiments were conducted at varying flow rates and glycerol concentrations. Nine runs were conducted with the combinations of 125, 250, and 375 mL/min flow rates, and 2.5, 5, and 10 % glycerol concentration by weight. Each run included the start-up and reaction stages. The reactor was fed with distilled water and heated at the rate of 140 °C/h during the start-up stage. After reaching the reaction temperature and pressure, the glycerol solution was fed into the reactor. The gas samples were collected through sampling bags. The sampling durations were also recorded to obtain gas flow rates. The gas compositions were analyzed with a gas chromatographer.

4.2. Process simulations of HTC and co-HTC processes

Digestate (waste of AD process in biogas plants) was selected as the feedstock for the HTC and co-HTC processes, considering the need for biogas plants to recover energy and key fertilizer elements. Paper III and Paper IV involved the selection of optimum conditions, utilizing the experimental results for obtaining the simulation inputs, constructing process simulations, and evaluating hydrochar production and energy requirements through simulation results.

Paper III investigated the integration of the HTC process with a biogas plant as shown in Figure 4-2. The study compared the experimental HTC results from the literature regarding various digestates (e.g., derived from food waste, sewage sludge, cow manure, and agricultural residue) and reaction conditions (temperature, solid load, and residence time). Among the listed HTC results, one feedstock and set of conditions are selected for the process simulation regarding the HTC integration. The optimum feedstock and conditions were selected based on the energetic yield defined as the energy content of hydrochar per mass of the total reactor inlet (MJ/kg reactor inlet). The integrated HTC process had a capacity of processing 300 kg/h dry digestate.

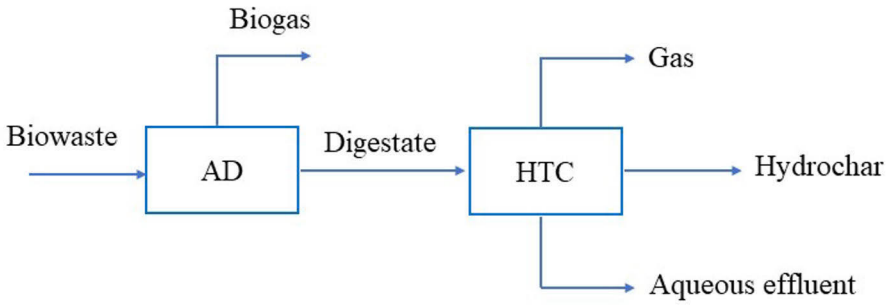

Figure 4-2. Block diagram of integrated HTC process with a biogas plant

After selecting the optimum feedstock and conditions, the experimental results were processed to determine the reactor yields (based on non-inert inlet) and to identify the non-conventional compounds as the inputs to the simulation model. Paper III determined the need to prioritize the experimental data as well. The simulation inputs were determined by using the data with the order of total mass balance using the yields to define the flow rates, identifying the digestate and hydrochar using the characterization data, assumed gas composition, and elemental balances around the reactor to define the elemental contents of aqueous effluent, and using BMP (biochemical methane potential) and COD (chemical oxygen demand) data to identify the water amount and dissolved organics.

The simulation model was constructed to represent the integrated HTC process, including the heat integration and product separation. The process simulation involves pressurizing the digestate feedstock, the heat exchange between the reactor downstream and feed stream, heating the feed further to reach the reaction temperature, the HTC reactor, separation of the solid product, and thermal drying to decrease the moisture content of hydrochar. The HTC reactor was inserted as a RYIELD block operating at a constant temperature (an isothermal reactor); thus, outlet yields are input and lead to heat release from the exothermic conversion. After an expansion unit, dewatering the reactor downstream was simulated based on the experimental filtration results presented by Aragon-Briceno et al. (2022) [65]: reducing the water content of hydrochar to 50 % with the energy requirement of 79.09 MJ/kg dry solid, and recovering 85 % of the dry solid in the hydrochar slurry. Afterwards, the water content of hydrochar was reduced to 20 % by thermal drying to avoid molding

in case the product is transported or stored before further usage. The heat requirement of drying was assumed as 3.82 MJ/kg water evaporated [66]; therefore, the drying section was simulated with the corresponding amount of excess air. The thermodynamic method is also a critical aspect of simulation models. Paper III simulated the HTC process with different methods to achieve more accurate data, including SRK, PSRK, NRTL, and 'IDEAL' methods.

Paper IV investigated the integration of the co-HTC process with a biogas plant processing sewage sludge and food waste in parallel, generating 300 kg/h sewage sludge digestate (SSD) and 300 kg/h food waste digestate (FWD) on a dry basis. Figure 4-3 shows the integration scheme. The study simulated the co-HTC of sewage sludge digestate (SSD) and food waste digestate (FWD) with different mixing ratios to investigate the synergetic impact and to represent a possible capacity increase: SSD:FWD ratios of 1:1 (300 kg/h SSD and 300 kg/h FWD), 1:3 (300 kg/h SSD and 900 kg/h FWD) and 3:1 (900 kg/h SSD and 300 kg/h FWD). The optimum conditions are selected based on the energetic yields of co-HTC data. In addition, the aqueous effluent of the co-HTC process (process water) was conducted to the SCWG process for the mixing ratio of 1:1, to investigate the energy recovery from the dissolved organics.

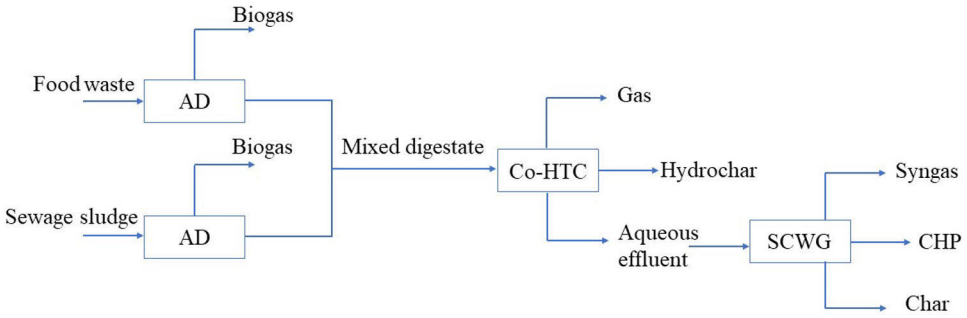

Figure 4-3. The block diagram of co-HTC process followed by SCWG

The simulation model was constructed similarly to the model in Paper III: the same unit operations and assumptions of dewatering and thermal drying. Meanwhile, due to the lack of experimental results on the co-HTC of SSD and FWD, the co-HTC data were generated by combining the individual HTC results in the literature, as mass-weighted averages to identify the mixed digestate, dissolved organics, the hydrochar product, and yields. For the 1:1 mixing ratio, the simulation continues with the SCWG of the process water. The process water

stream was conducted to the flash separation to remove the gases, pressurized to 250 bars, heat exchange with the reactor outlet, external heat to reach SCWG temperature, and then to SCWG reactor. The SCWG reactor was simulated first with a yield reactor to decompose non-conventional components into elemental components. After separating the ash in the solid separator, the remaining components are conducted to the SCWG reactor represented by a RGIBBS block, determining the outlet by minimizing Gibbs free energy. The reactor was simulated as an adiabatic reactor at 600 °C, i.e., the sum of heat duties in RYIELD and RGIBBS were zero. The reactor inlet was heated to more than 600 °C to conduct the endothermic gasification. After cooling down via heat exchange with the process water, the SCWG outlet stream is expanded and conducted to the flash separator to separate syngas and aqueous phase. The thermodynamic method was PSRK in this simulation model, except for SCWG reactor units conducted with the IDEAL method.

4.3. The hydrothermal biorefinery concept

Paper V proposes a biorefinery integration concept for a biogas plant processing sewage sludge in case of a capacity increase. Figure 4-4 illustrates the integration concept. The digestate stream (300 kg/h dry solid) goes through the HTC process, sewage sludge (190 kg/h dry solid) goes through the HTL process, and the aqueous effluents go through SCWG. The experimental data were taken from Parmar and Ross (2019) [67] and Rahman et al. (2021) [68] for the HTC of SSD and HTL of sewage sludge, respectively. Table 4-1 shows the characterization and product yield data. The HTC process of sewage sludge digestate is at 200 ^{o}C and autogenous pressure with 30% solid load. The HTL process is simulated under the condition of 350 ^{o}C and autogenous pressure with 19% solid load. The aqueous phase from HTL and HTC is gasified in 600 ^{o}C and 250 bar conditions.

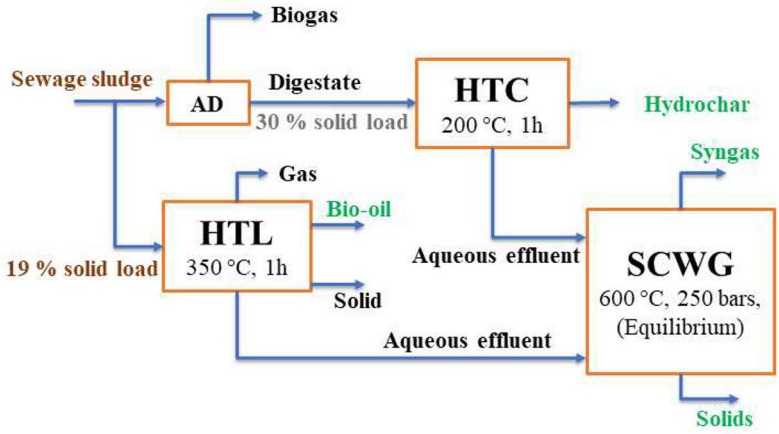

Figure 4-4. The block diagram of the biorefinery concept

Table 4-1. Analysis of feedstocks and products [67,68]

Sample	HHV (MJ/kg)	C	H	N	S	O	Ash	Yield
SS	14.1	33.1	5.5	5	0.7	25.9	29.8	-
SS digestate	14.9	28.7	3.1	3.4	1.5	16.4	46.9	-
Biocrude	28.3	53.3	6.01	3.9	1.1	29.9	4.7	37.1
Hydrochar	15.4	34.5	4.3	2.9	1.2	12.8	44.3	78

The simulation model was constructed after determining the simulation inputs. The HTC and SCWG sections were constructed in a similar way to Paper IV. The HTL section was also constructed as a pump to pressurize the sewage sludge, heat exchange with the reactor outlet, and external heat to reach the HTL temperature and separation stages.

5. Results and discussion

This research combines the operational aspects with the selection of optimum conditions and process simulations to develop circular biorefinery concepts. The research started with a comprehensive review on operational issues in hydrothermal processes specifically SCWG and HTL processes. It continued with an experimental study of SCWG of glycerol. In the next step, HTC and co-HTC of waste biomass feedstock are simulated and investigated. The final research topic is the integration of mentioned processes as a biorefinery to achieve sustainable development goals and a circular economy.

5.1. Operational issues of SCWG and HTL (Paper I)

Paper I reviewed operational issues as obstacles to the industrialization of SCWG and HTL technologies. The covered issues include:

- Process safety with respect to the operating conditions
- Corrosion
- Pumpability of feedstock
- High investment and operating costs
- Plugging due to solid deposition
- Catalyst sintering and deactivation

The primary challenge is to ensure process safety due to high pressure and temperature, causing thermal and mechanical stress on the reactor. This challenge can be addressed by proper selections of reactor material and outer diameter-to-thickness ratio with respect to the operational pressure and the tensile strength of materials at the operating temperature. For example, the maximum outer diameter-to-thickness ratio can be around 12mm in a steel reactor at 250 bars, as determined with the correlation derived by Oh et al. (2020) [69]. Inconel 625 reactor has a higher tensile strength: 565 MPa versus 714-1103 MPa [70]. However, regardless of material, SCWG requires very thick reactors due to high pressure. Consequently, the reactor thickness causes the external heating to be impractical in industrial scales. In addition, the selection of material is influenced by thermal stability as well. Stainless steel 316L can

operate up to 650 °C regarding a long-term implementation while Inconel can remain stable at over 1000 °C. Nevertheless, stainless steel can be modified to operate at up to 1150 °C by adjusting the ferric and chromium contents [71].

As another safety aspect, solid deposition arises from char formation and precipitation of inorganic salts. Solid deposition is a major problem, especially in the SCWG process. Meanwhile, HTL has less risk of plugging due to solid deposition, and control is possible with a pressure letdown valve [72]. Moreover, solid deposition is the main issue, also causing the increased risks of other operational issues. The solid deposition issue induces under-deposit corrosion, catalyst deactivation through fouling, dealloying in the case of the presence of sulfide and mechanical stress on the reactor due to pressure gradient. Various methods are employed to address these concerns, including diverse reactor configurations to prevent plugging and optimization of process conditions to mitigate other potential problems. Table 5-1 is adapted from Paper I and listed some studies about SCWG and the related results for each study. Figure 5-1 depicts an operational issue due to salt formation. The figure is adapted from a research experiment on SCWG of black liquor conducted by De Blasio et al. [73]. Efficiently addressing this issue requires specialized reactor configurations capable of simultaneous solid separation during the reactions while providing a surface area of the catalytic wall in an economically feasible way, besides optimum conditions to minimize the char formation. Therefore, Paper I proposed a vertical reactor configuration with multiple, coil-shaped riser tubes as shown in Figure 5-2. Since the external heating is impractical due to reactor thickness, the biomass feed and SCW can be fed separately and mixed in the reactor. This leads to a faster transition to the reaction temperature, and a vertical vessel reactor can have higher mechanical stability than tubular reactors. The riser tubes enable the solid separation by collecting the syngas while the solid outlet precipitates to the bottom. The multiple, coil-shaped configuration increases the surface area as well. Therefore, the reactor material can include a stainless-steel vessel as a cheaper material and Inconel riser tubes as a catalytic material.

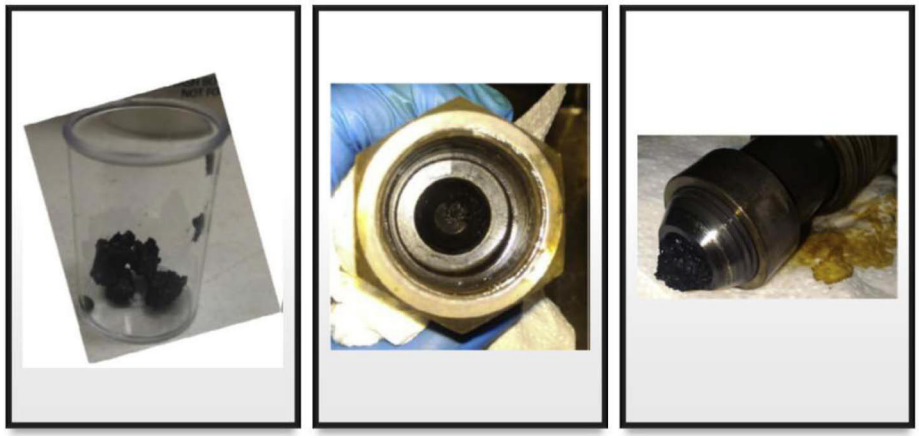

Figure 5-1. Operational problem due to formation of salt [73]

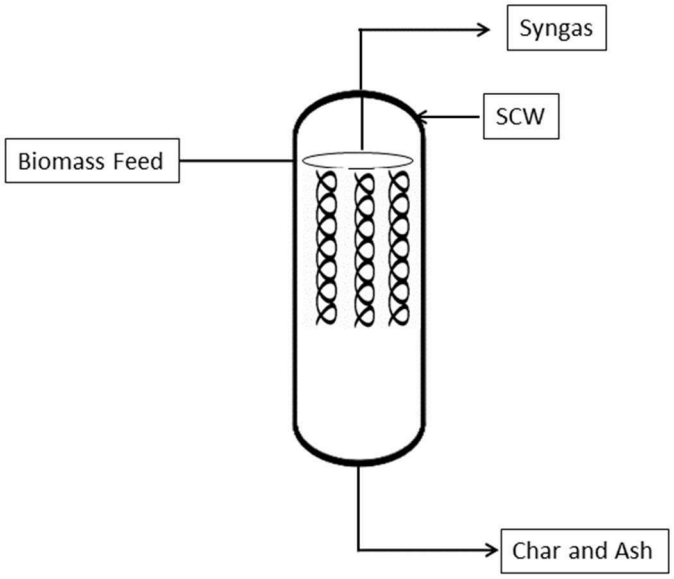

Figure 5-2. The reactor configuration proposed in Paper I

Table 5-1. Literature studies on SCWG (adapted from Paper I)

Ref.	Research question	Feedstock	Results/Findings
[60]	Performance and interaction of biomass in SCW and technical challenges	Biomass model compounds Binary or multi-component systems	Understanding the interactions within multicomponent systems
[74]	Recent development in the SCWG process	The components of biomass (carbohydrates, lignin, ash, proteins, and lipids) and real biomass	Risk analysis/Catching salts and salt separation to avoid reactor plugging/Integration of SCWG in a biorefinery
[75]	Degradation routs of biomass model compounds	Biomass model compounds such as cellulose and lignin	Changes reactor configurations to overcome plugging/Separation of corrosive ingredients
[28]	Research on catalytic SCWG and physicochemical properties of water in sub and supercritical conditions	Glucose, Glycerol, Lignin, Phenol, Lignin and 4-propyl phenol, Methanol, Glycerol, glucose and wood, and Cellulose	Catalysts increase hydrogen selectivity and conversion rate/More research about stable and efficient catalysts was suggested
[76]	Summarized catalytic hydrothermal gasification findings in the last two decades	Lignocellulosic biomass from different sources, sewage sludge, chicken manure, food wastes, algae, and fermentation residue	Sulfur and inorganics in biomass deactivate catalysts/Moderate temperatures and long residence time increased tar/High heating rates reduce char/Capillary quartz reactors are cheap and safe in high pressures

[77]	Reviewed economic costs, life cycle assessment (LCA), energy and exergy efficiencies, and thermodynamic equilibrium in SCWG	Sewage sludge, algal biomass, and black liquor	The yield of H_2 and CO_2 increased with temperature and decreased with concentration and oxygen addition/Major exergy destruction is in the reactor, heat exchanger, and preheater/Hydrogen production costs are lower in the SCWG
[78]	Reviewed the role of water in converting biomass feedstock to syngas	Petrochemical waste, mixed plastics, food waste, sewage sludge, used tires, animal manure, industrial effluents, and municipal solid waste	High pressure and temperature increase corrosion/Heterogeneous and homogeneous catalysts are effective, deactivation, sintering, and recovery are still challenges/Biorefinery concept to reduce the costs

Corrosion is a long-term issue affecting the operation. Corrosion is attributed to alkali salts, char formation, and corrosive inorganics such as sulfur, chloride, or nitrate. HTL process involves electrochemical corrosion due to high density and polarity of water while SCWG process involves chemical corrosion due to salt deposition. This issue can be managed through proper selection of corrosion-resistant material, ensuring optimal conditions to minimize char formation, and pre-neutralization of the feedstock or mixing the feedstock with other non-corrosive alternatives. The main corrosion-resistant materials are stainless steel, nickel alloys, titanium, tantalum, noble metals and ceramics. The economic aspects and catalytic impacts direct the selection of reactor materials to stainless steel and nickel alloys (e.g., Inconel and Hastelloy). The corrosion resistances of these materials are also temperature-dependent. Stainless steel has higher corrosion resistance at HTL conditions and lower cost. Meanwhile, Inconel has higher corrosion resistance and catalytic impact at SCWG conditions.

Catalyst deactivation is another long-term operational issue decreasing product yields. The catalysts are deactivated through chemical degradation, sintering at high temperatures, and the deposition of unreactive species on the catalyst

surface. The phenomena causing catalyst deactivation can be minimized through diverse catalyst preparation methods, enhanced dispersion, and adding a trace amount of transition metals to alkali metal catalysts and bimetallic catalysts. A trace of amount of transition metals or a bimetallic catalyst reduce the solid deposition by promoting the gasification reactions and suppressing the repolymerization, thus increasing the gas yields as well. The diverse methods of catalyst preparation and enhanced dispersion address the chemical degradation and sintering issues, respectively.

Additionally, the solid concentration of reactor inlet is constrained by pumpability limits at high pressure. The pumpability limit depends on the biomass constituents and pressure: 45 % at 130 bars and 10-18 % at 206-320 bars for lignocellulosic biomass, 22 % at 220-300 bars for sewage sludge, and 15 % for woody biomass [79]. Operating at higher concentrations than the pumpability limit causes clogging problems in high-pressure pumps. This issue introduces a constraint to the applicable concentration range when investigating the optimum conditions. The reactor inlet concentration directly influences the equipment size and energy requirements to process the defined amount of dry solid. For instance, Paper I compiled the studies on SCWG of black liquor in terms of energy yield (energy content of syngas) on a dry-ash-free basis and based on of a non-inert reactor inlet, as shown in Table 5-2. Despite improving the dry-ash-free yields, the dilute inlets result in low yields based on reactor inlet, i.e., requiring much larger equipment. In other words, the feedstock concentration influences the equipment size more dominantly than improving the dry-based or dry-based yields.

Table 5-2. Various results on SCWG of Kraft black liquor (KBL) (RT: residence time)

Reactor feed	P (MPa)	T (°C)	Reactor material	RT (s)	Hydrogen yield (mol/kg non-inert) Energy yield (kJ/kg non-inert)	Hydrogen yield (mol/kg organics) Energy yield (kJ/kg organics)	Ref.
KBL 4.25 wt%	25	750	Inconel 625	300	0.646 458	24.92 17644	[26]
KBL 4.25 wt%	25	750	Inconel 625	133	0.440 315	16.93 12162	[26]
KBL 4.25 wt%	25	750	Stainless steel	133	0.370 310	14.27 11963	[26]
KBL 12.3 wt%	25	700	Inconel 625	77	1.238 912	14.43 10627	[80]
KBL 12.3 wt%	25	700	Stainless steel	77	1.232 793	14.36 9240	[80]
KBL 12.3 wt%	25	600	Inconel 625	91	1.478 750	17.22 8736	[80]
KBL 0.81 wt%	23.3	700	Inconel 625	25	0.162 75	33.62 15521	[81]
KBL 1.62 wt%	23.4	700	Inconel 625	25	0.195 81	20.10 16786	[81]

5.2. Supercritical water gasification of glycerol (Paper II)

Paper II investigated supercritical water gasification of glycerol carried out in laboratory-scale tubular reactors made of industrially relevant materials, such as Stainless Steel 316 and Inconel-625. The design of the experiment analysis determined that glycerol molar flow rate is the inlet affecting the productivity of gases, rather than residence time and glycerol content separately. Figure 5-3

shows the gas productivity results versus glycerol inlet flow rate for both reactors. Stainless steel resulted in higher hydrogen productivity (Figure 5-3, A) than Inconel, implying the catalytic impact towards the hydrogenation of C2 intermediates. Meanwhile, the productivity of methane (Figure 5-3, D) and ethylene (Figure 5-3, E) were higher in the Inconel-625 reactor, indicating a catalytic impact towards cracking and the hydrogenation of the acetaldehyde intermediate. The high nickel content of Inconel 625 resulted in the enhancement of hydrocarbon production to the detriment of the hydrogen yield. In any case, considering the significant amount of produced C2 hydrocarbons, the acetaldehyde intermediate appears to be rather active towards hydrogenation regardless of the wall material. Another plausible explanation of the observed productivity of methane could be the accumulation of acetaldehyde that could decompose into methane and carbon monoxide. The interpretation of the ethane production, shown in Figure 5-3, F, appears to be less straightforward, and ethane is a minor product. The production of carbon monoxide (Figure 5-3, B) and carbon dioxide (Figure 5-3, C) were quite similar for both reactor materials, thus implying that there is no catalytic effect of Inconel-625 over water gas shift or methanation reactions. To sum up, the productivity of each gas is approximately linear with glycerol molar flow rates. However, in the case of H_2, CO, and CO_2, the linear tendency breaks around 0.2 mol/min, adopting a lower slope when the residence time of the substrate decreases.

From the techno-economic viewpoint, the selected molar flow rate of glycerol can be conducted through various combinations of residence time and inlet glycerol concentration. Since equipment size and energy requirement decrease with inlet concentration, selecting a high concentration will favor the economic performance as also mentioned in Paper I.

Another aspect is the heat transfer to the reaction mixture. Besides being impractical on an industrial scale, the external heating resulted in temperature gradient and subcritical water conditions in a large part of the reactor as determined in Paper II through kinetic modeling. Therefore, the reactor configuration in Figure 5-2 can address the heat transfer limitation as well.

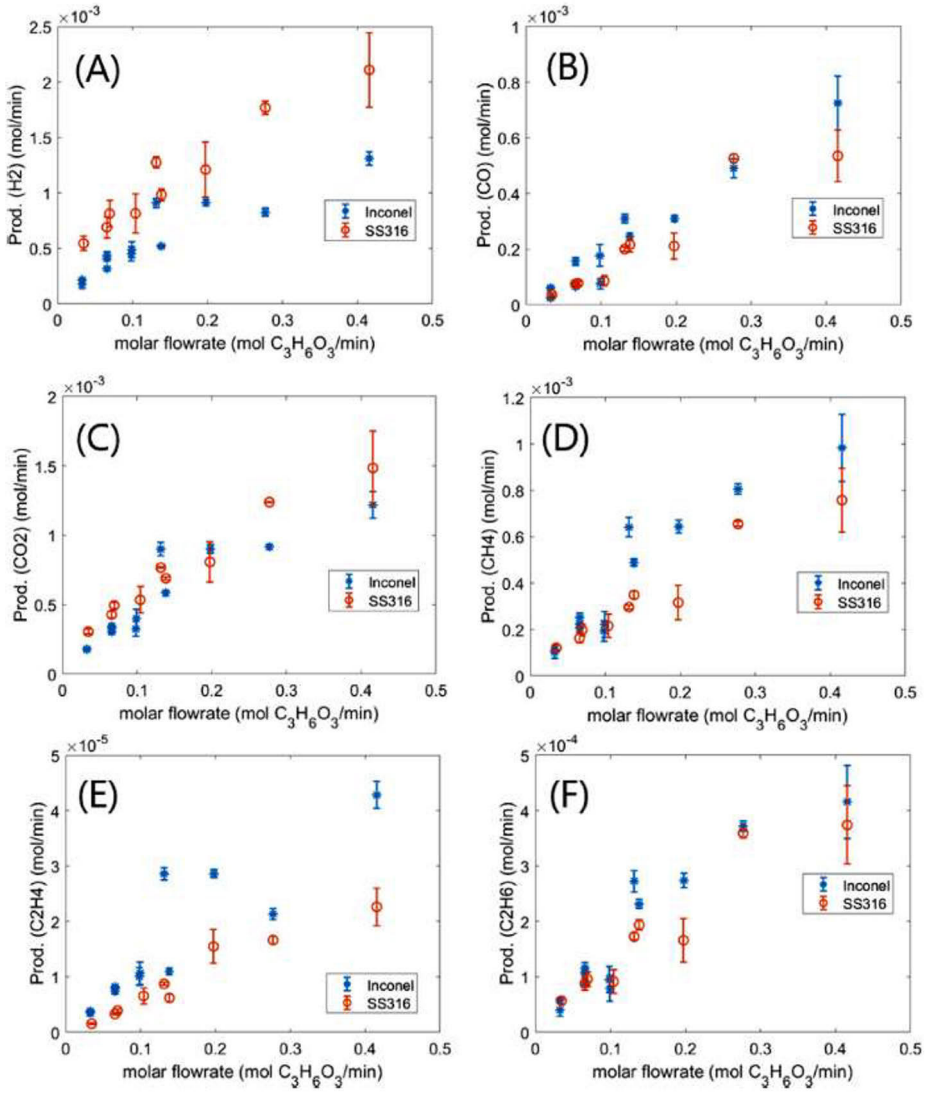

Figure 5-3. Molar production as a function of the glycerol molar inflow rate

5.3. HTC of digestates (Paper III and IV)

Papers III and IV investigated HTC and co-HTC of waste biomass feedstock, specifically digestate from anaerobic digestion. Paper III delves into the simulation aspects of the HTC process of the digestate, aiming to estimate the optimum condition and establish mass and energy balances. Paper IV research

is in continuation of paper III, studying co-HTC of two different waste biomass feedstocks including food waste and sewage sludge digestates.

Paper III had the scope of selecting optimum HTC conditions concerning feedstock and reaction conditions, utilizing the experimental results for determining simulation inputs, and process simulation to obtain mass and energy balances. The optimum conditions were selected based on energetic yield defined as the energy content in hydrochar per reactor inlet. The energetic yield is an important factor from the techno-economic viewpoint, implying the relative equipment sizes and the optimum compromise of the opposite impact of temperature on hydrochar yield and heating value. Table 5-3 shows some of the compiled HTC results and calculated energetic yields [67]. Among the investigated data for various digestates, the optimum feedstock and conditions were selected as agricultural residue at 200 °C and the residence time of 1 hour with 30 % solid load based on the energetic yields, resulted in the energetic yield of 5.02 MJ/kg reactor inlet.

Table 5-3. The hydrochar properties and process performances for HTC of digestates (complete list in Paper III)

Feedstock digestate	*HTC conditions*			*Hydrochar*				*Process performance*	
	T_{HTC} (°C)	t_{res} (h)	Solid load (%)	C (%)	H (%)	O (%)	HHV (MJ/kg)	Yield (% dry basis)	Energetic yield (MJ/kg reactor inlet)
AGR	200	1	10	52.0	6.9	23.1	21.6	60.0	1.30
			20	50.8	6.0	24.4	20.7	67.8	2.81
			30	51.2	6.1	22.8	20.9	80.1	5.02
	250		10	57.3	6.3	11.5	24.0	47.2	1.13
			20	57.1	6.6	12.0	24.2	51.1	2.47
			30	56.7	5.8	12.7	23.3	49.4	3.45
MSW	200	1	10	22.6	1.6	11.7	15.5	85.0	1.32
			20	21.4	1.6	13.9	15.6	87.1	2.72
			30	24.0	1.8	12.2	15.4	85.7	3.96
	250		10	23.0	1.6	9.7	15.6	82.0	1.28
			20	21.7	1.6	7.9	15.6	84.1	2.62
			30	23.4	1.7	7.8	15.5	83.5	3.88
SS	200	1	10	34.0	4.2	13.0	15.0	72.6	1.09
			20	34.0	4.2	14.0	15.1	76.1	2.30
			30	35.2	4.4	12.7	15.4	78.0	3.60
	250		10	34.4	4.0	9.2	15.2	65.6	1.00
			20	34.7	4.1	10.6	15.3	67.9	2.08
			30	36.4	4.3	9.0	15.7	69.5	3.27

After selecting the optimum feedstock and conditions for simulation, the experimental data were utilized to identify the non-conventional compounds and to determine flow rates. The first step is to determine the flow rates of hydrochar, process water, and gas by using the yield data. Afterwards, it is important to prioritize the data based on characterization reliability. The ultimate and proximate analysis on solid samples are typically conducted after drying at low temperatures avoiding further decomposition. However, CHNS analysis on process water can cause high uncertainty due to losses of light organic compounds during sample drying. Therefore, the first step was to identify the feedstock and hydrochar. The gas composition was assumed as 90 % CO_2, 6 % CO, 3 % CH_4, and 1 % H_2 by volume based on the selected

temperature [82,83]. The elemental contents of dissolved organics can then be identified through elemental balances, except hydrogen and oxygen. The hydrogen and oxygen contents in dissolved organics were identified through the experimental BMP and COD data. Then, water in reactor outlet can also be determined accordingly. The accuracy of mass balance can be increased with more data on process water and gas composition. The mass balance accuracy influences the simulation model as well since the reactor outlet is defined based on the experimental results. Table 5-4 and

Table 5-5 show the non-conventional compounds and yields as the simulation inputs. The digestate, dissolved organics, and hydrochar were represented in dry-ash-free form, and ash was introduced as another compound. Figure 5-5 illustrates mass balance results of HTC of agricultural residue digestate.

Table 5-4. Non-conventional compounds in the simulation model

NC components	Ultimate analysis (wt%)					Proximate analysis(wt%)			
	C	H	N	S	O	Ash	FC	VM	HHV (MJ/kg)
Digestate	52.5	6.07	3.81	0.36	37.3	-	16.4	83.6	21.19
Hydrochar	61.2	7.29	4.18	0.12	27.2	-	20.3	79.7	24.97
Ash	-	-	-	-	-	100	-	-	-
Organics	17.6	9.57	3.0	1.7	68.1	-	-	100	Default value

Table 5-5. The calculated yields as defined in the simulation

Component	Yield (kg/kg non-inert)
Hydrochar	0.2113
Water	0.7390
Organics	0.04122
CO_2	0.008289
H_2	0.000004186
CH_4	0.0001005
CO	0.0003516

The HTC process was simulated to obtain the mass and energy balances. The simulation process is depicted in Figure 5-4. The HTC simulation in Paper III includes only the HTC section but not the SCWG section, and the stream "PWATER" is the outlet as the aqueous effluent. The mass balance results are shown in Table 5-5. The energy balances were obtained by simulating the

process with SRK, PSRK, NRTL, and IDEAL methods to compare the impact of the thermodynamic method. Nevertheless, these methods resulted in similar results with minor differences in the duties of heat exchangers. The PSRK method was selected to evaluate the energy requirements.

Table *5-6* shows the energy requirements. The energy balance shows that heat released in the reactor can cover the majority of the requirement of air heating, as a further heat integration concept. Due to the importance of the heat of reaction in heat integration, the heat duty of the reactor was determined based on the simulation result. The heat duty of the HTC reactor was -122 kW, corresponding to -1.46 MJ/kg dry solid and -1.74 MJ/kg dry-ash-free solid inlet as the heat of reaction. The heat of reaction was also verified by comparing the data reported in the literature for model compounds and similar biomass feedstocks. For instance, the heat of reaction was measured as -1.07 MJ/kg dry-ash-free cellulose and -0.76 MJ/kg dry-ash-free wood at 240 °C with 10-h residence time [84]. The heat of reaction varies with temperature and residence time as well. The heat of reaction varied between -0.59 and -1.33 MJ/kg cellulose at 180-240°C with a 3-h residence time [85]. Similarly, the heat of reaction was measured as -2.53 and -3.47 MJ/kg dry wood at 180 °C with 2.5-h and 5.83-h (350 min) residence times [86]. To sum up, the obtained heat of reaction is consistent with the literature values despite the need for more precise verification.

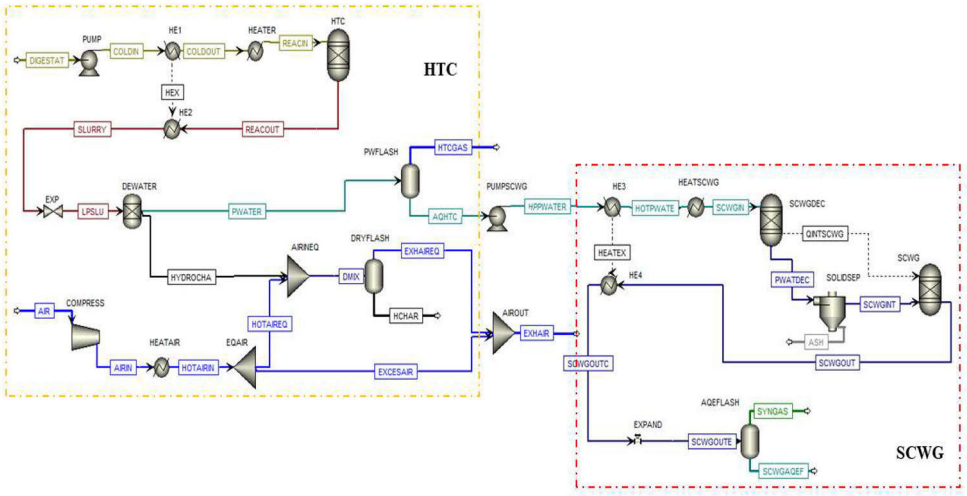

Figure 5-4. HTC and co-HTC process simulation models

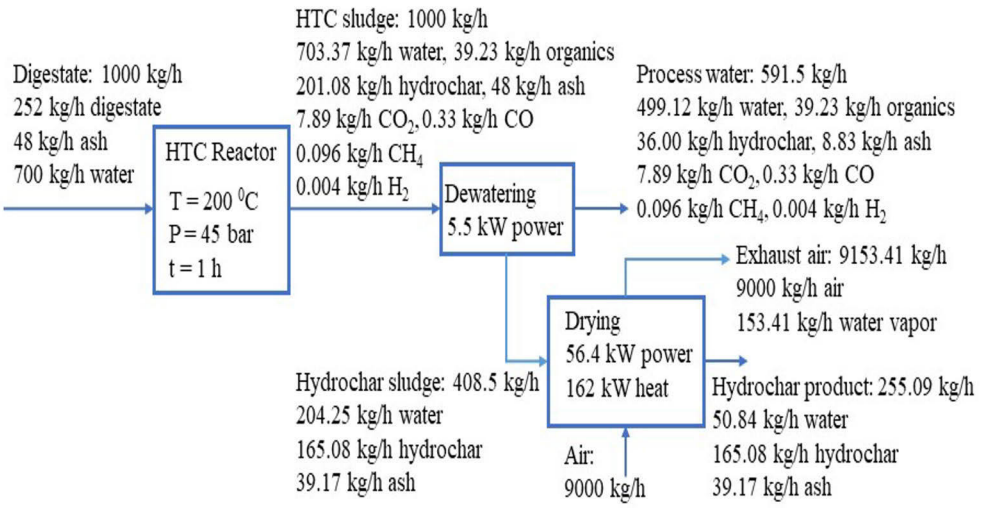

Figure 5-5. The mass balance results of HTC of agricultural residue digestate

Table 5-6. Heat and power requirements of HTC of agricultural residue digestate.

Electricity requirement	
PUMP	1.75 kW
COMPRESS	56.4 kW
DEWATER	5.5 kW
Total electricity consumption	**63.65 kW**
Heat requirement	
HEATER	21 kW
HEATAIR	162 kW
HTC	-122 kW
Net heat consumption	**61 kW**

Paper IV investigated integrating the co-HTC process with SCWG for nutrient recovery and energy production. The aqueous effluent from the HTC section is conducted to the SCWG section. The optimum co-HTC conditions were selected based on the energetic yields, comparing relative equipment sizes besides the hydrochar product. Due to the lack of experimental co-HTC on sewage sludge digestate (SSD) and food waste digestate (FWD), the co-HTC data was generated using the individual HTC data of each digestate, mass-weighted averages with

respect to mixing ratios. Table *5-7* shows the digestate characterizations of various HTC studies, and Table 5-8 shows the energetic yields concerning the conditions and mixing ratios. The selected conditions are 200 °C, 30 % solid load, and 1-h residence time for the mixing ratios in scope: resulting in the energetic yields of 3.58-3.59 MJ/kg reactor inlet.

Table 5-7. Analysis of the selected digestate samples (dry basis)

Digestate	HHV (MJ/kg)	C (%)	H (%)	N (%)	S (%)	O (%)	Ash (%)	Ref.
SSD1	14.9	28.9	3.2	3.4	1.5	16.1	46.9	[87]
SSD2	14.4	33.3	4.6	4	1.2	20.3	36.7	[88]
SSD4	11.5	30.3	4.2	3.5	2.3	18.8	40.9	[89]
SSD7	14.3	29.6	4.3	4.4	1.6	20.1	40.1	[90]
FWD1	14.9	29.5	3.0	2.0	0.3	21.3	43.9	[87]
FWD3	19.7	46.0	6.5	2.7	0.3	36.6	8.0	[91]
FWD4	13.4	34.3	4	1.9	0.2	23.8	35.8	[92]

Table 5-8. The co-HTC results and the energetic yields for the SSD:FWD ratios of 1:1, 1:3 and 3:1, respectively

	Conditions			Hydrochar		Process performance
	T (°C)	Solid load (%)	t_{res} (h)	Yield (% dry)	HHV (MJ/kg)	Energetic yield (MJ/kg reactor inlet)
SSD1: FWD1	200	10	1	76.1 - 77.8 - 74.3	14.89 - 14.85 - 14.94	1.13 - 1.15 - 1.11
		20		78.5 - 79.7 - 77.3	15.10 - 15.10 - 15.10	2.37 - 2.41 - 2.33
		30		78.9 - 79.4 - 78.5	14.99 - 15.02 - 15.27	**3.59 - 3.58 - 3.59**
	250	10		68.4 - 69.7 - 67.0	15.15 - 14.89 - 15.09	1.02 - 1.04 - 1.01
		20		69.7 - 70.5 - 68.8	15.09 - 15.00 - 15.20	2.10 - 2.12 - 2.09
		30		71.6 - 72.3 - 70.6	15.34 - 15.17 - 15.52	3.29 - 3.31 - 3.28
SSD7: FWD1	150	20	1	89.8 - 89.4 - 90.2	15.10 - 15.05 - 15.15	2.71 - 2.69 - 2.73
	200			79.0 - 79.9 - 78.0	15.15 - 15.12 - 15.17	2.39 - 2.42 - 2.37
	250			71.0 - 71.1 - 70.7	15.05 - 14.97 - 15.12	2.13 - 2.13 - 2.14
SSD1: FWD3	200	10	1	57.9 - 50.6 - 65.3	18.77 - 21.48 - 16.67	1.09 - 1.09 - 1.09
SSD2: FWD3	250	10	0.5	54.8 - 44.6 - 64.9	19.42 - 22.47 - 17.33	1.06 - 1.00 - 1.12
SSD4: FWD4	210	15	2	83.8 - 81.5 - 86.0	11.64 - 11.76 - 11.52	1.46 - 1.44- 1.48
	230			75.2 - 74.0 - 76.5	11.94 - 12.16 - 11.71	1.35 - 1.35 - 1.34
	250			69.9 - 68.9 - 71.0	12.44 - 12.57 - 12.32	1.31 1.30 1.31

The co-HTC process involves synergetic impact due to the interactions among different feedstock, thus causing deviation between experimental co-HTC results and calculated results using individual HTC results. Therefore, it is

important to investigate SC to evaluate the reliability of selecting the conditions based on calculated co-HTC data. Due to the lack of experimental co-HTC data on SSD and FWD, the preliminary evaluation can be conducted by determining the synergetic impact for co-HTC of SS and FW as the origin of the digestates. Since this study selects the optimum conditions based on the energetic yield, the SC on the energetic yield indicates the role of SE in the optimum conditions. Therefore, Figure 5-6 shows the SCs on the energetic yields for the experimental results of co-HTC of SS and FW presented by Zheng et al. (2019) [93]. The SC decreases with temperature in all mixing ratios and is close to zero at the selected co-HTC temperature. This investigation determines that the SE has no major impact on selecting of the optimum conditions despite the need of verification. Therefore, future co-HTC experiments can involve some ranges of conditions around the selected optimum (e.g. 180-220 °C, 20-30 % solid load, and 0.5-1.5 hours residence time) rather than numerous experiments to cover wide ranges.

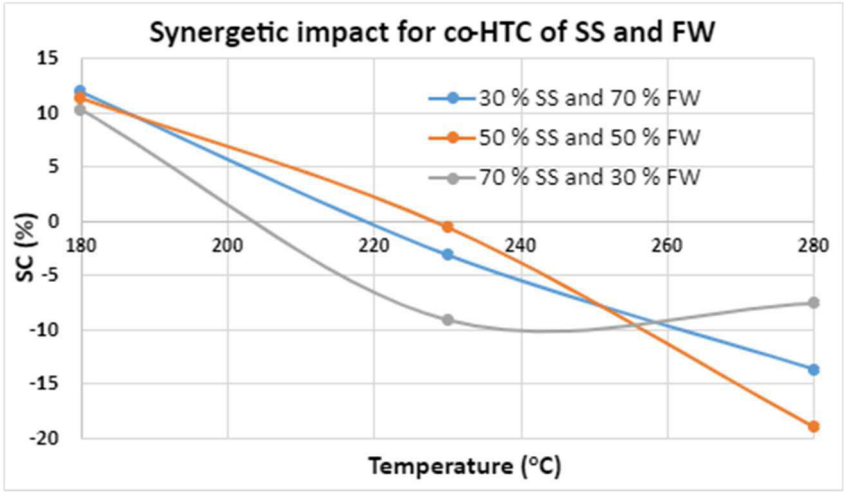

Figure 5-6. Synergetic impact for SS and FW

After selecting the optimum conditions, the experimental data were utilized to determine the flow rates and to identify the non-conventional components. The mass balances were conducted in the same way as Paper III for the mass-weighted averages of individual HTC data. Table 5-9 shows the dry-ash-free digestate and hydrochar, and Table 5-10 shows the dissolved organics as the non-conventional compounds.

Table *5-11* shows the calculated reaction yields introduced to the simulation model.

Table 5-9. Feedstock and hydrochar properties (daf)

Material		C (%)	H (%)	O (%)	N (%)	S (%)	HHV(MJ/kg)
1:1	Digestate	53.48	5.68	34.25	4.94	1.65	27.29
	Hydrochar	62.73	7.14	24.67	4.13	1.34	29.31
1:3	Digestate	53.03	5.51	36.13	4.24	1.08	26.92
	Hydrochar	63.28	6.83	25.43	3.56	0.89	30.27
3:1	Digestate	53.95	5.85	32.31	5.67	2.23	27.67
	Hydrochar	62.21	7.42	23.94	4.68	1.75	28.40

Table 5-10. The elemental analysis and heating values of organics

SSD:FWD ratio	***Dissolved organics (dry-ash-free)***					
	C (%)	H (%)	O (%)	N (%)	S (%)	HHV (MJ/kg)
1:1	24.84	2.61	58.03	10.76	3.76	4.29
1:3	28.61	2.96	57.35	8.79	2.29	6.70
3:1	19.86	2.15	58.92	13.37	5.70	1.10

Table 5-11. Calculated yields in kg/kg non-inert

Component	***SSD:FWD ratio***		
	1:1	1:3	3:1
Hydrochar	0.140	0.136	0.145
Water	0.809	0.809	0.808
Organics	0.033	0.038	0.029
CO_2	0.017	0.016	0.017
H_2	8.479E-06	8.291E-06	8.668E-06
CH_4	0.0002	0.0002	0.0002
CO	0.0007	0.0007	0.0007

After selecting the optimum conditions and determining the simulation inputs, the co-HTC process was simulated as shown in Figure 5-4. All the mixing ratios were simulated without the SCWG section, i.e. the "PWATER" stream was an outlet as the aqueous effluent. In addition, the mixing ratio of 1:1 was simulated with the SCWG section to investigate energy production from dissolved organics as well as enabling further recovery of minerals and nutrients. Table 5-12 shows the inlet and outlet streams in all the mixing ratios. Paper IV showed the extended version of this table including some intermediate streams as well. The results indicated that SSD causes slightly more gas formation while FWD

promotes the dissolved organics in the co-HTC conversion. In addition, water also participates into the reactions: a small amount was consumed in the SSD:FWD ratios of 1:1 and 3:1 while being generated in small amount in the ratio of 1:3. Furthermore, the majority of ash was recovered in the hydrochar product, thus encouraging the use of hydrochar as a fertilizer. The K, P, and N recoveries on hydrochar were observed to be higher than 60 %.

Table 5-12. Mass flows of the co-HTC process in kg/h: stream names as in Figure 5-4

Stream	Component	***SSD:FWD ratio***		
		1:1	1:3	3:1
DIGESTAT	Digestate	327.6	664.2	646.2
	Ash	272.4	535.8	553.8
	Water	1400	2800	2800
PWATER	Water	999.43	2000.44	1997.27
	Ash	45.35	57.86	123.54
	Hydrochar	72.34	145.94	143.20
	Organics	57.30	130.44	98.76
	Gases	30.60	60.00	62.40
AIR	Air	17550	35450	34760
EXHAIR	Air	17550	35450	34760
	Water	298.43	603.7	591.02
HCHAR	Water	99.09	198.96	196.41
	Ash	227.05	477.94	430.26
	Hydrochar	170.41	324.72	357.14
SYNGAS	Water	51.06		
	CO_2	143.40		
	CO	2.14		
	CH_4	26.27		
	H_2	6.63		
	N_2	8.85		
	H_2S	3.31		
	NH_3	0.17		
SCWGAQEF	Water	885.79		
	NH_3	0.19		
	H_2S	0.01		
	Gases	0.153		

The energy balances were obtained from the simulation results. Table 5-13 and

Table *5-14* present the energy requirements of the co-HTC process for all the mixing ratios and of the SCWG section for the 1:1 mixing ratio, respectively. The energy requirements in the co-HTC section are proportional to flow rates with only minor deviations regarding the mixing ratio, except for the reactor. The exothermicity of co-HTC conversion increased with the FWD ratio. Conducting SCWG of process water led to the supply of energy required in the whole process. The net heating value of the syngas is 9.03 MJ/kg. The CHP production from syngas covers most of the power consumption and provides extra heat of 455 kW.

The study also provides useful information for preliminary assessment of the proposed integration and directing the co-HTC experiments towards the promising ranges of conditions, despite the uncertainties in the methodology. Two main uncertainty factors are the heat of reaction in the co-HTC conversion and the SE of mixing feedstocks. The heat of reaction were obtained from the simulation results as -2.56, -2.12, and -2.90 MJ/kg dry-solid and -4.69, -3.83, -5.39 MJ/kg dry-ash-free-solid for 1:1, 1:3, and 3:1 SSD and FWD ratios, respectively. These values are consistent with the literature values for HTC of similar feedstocks and model compounds, e.g., for FW (-1.19 MJ/$kg_{dry\text{-}solid}$), SS (-2.62 MJ/$kg_{dry\text{-}solid}$), organic waste (-7.30 MJ/$kg_{dry\text{-}solid}$), and glucose (-1.06 MJ/$kg_{dry\text{-}solid}$) [94–96]. Similarly, this study investigated the synergetic coefficient (SC) on the energetic yields for co-HTC of SS and FW as the feedstocks with similar constituents, due to lack of data on co-HTC of SSD and FWD.

Table 5-13. Co-HTC energy requirements

	SSD-FWD ratio		
	1:1	1:3	3:1
Electricity requirement (kW)			
PUMP	3.5	7	7
COMPRESS	110.0	222.3	217.9
DEWATER	11.4	22.1	23.2
Total	124.9	251.4	248.1
Heat requirement (kW)			
HAETER	40.45	80.8	80.9
HEATAIR	316.26	638.8	626.4
Co-HTC	-427.2	-706.8	-967.1
Total	-70.49	12.8	-259.8

Table 5-14. SCWG energy balance

Electricity requirement (kW)		Heat requirement (kW)	
HTC Section	124.9	HTC Section	-70.49
PUMPSCWG	31.5	-	
0.25×HEATSCWG	11	0.75×HEATSCWG	33
Electricity outcome (kW)		Heat outcome (kW)	
0.25×SYNGAS	151.68	0.75×SYNGAS	455.06

5.4. Biorefinery concept of hydrothermal processes (Paper V)

Compiling the knowledge on hydrothermal processes, Paper V proposed a novel biorefinery idea and simulated for the conversion of waste biomass to biofuels. The proposed process was integrated to a biogas plant processing sewage sludge and increasing the capacity. The simulated biorefinery is depicted in Figure 5-7: HTC of digestate, HTL of extra sewage sludge, and SCWG of the aqueous effluents. Table 5-15 reports the dry basis elemental composition and the heating values (HHV) of the feedstocks and products based on the reported experimental results [67,68]. The HTC of SSD (300kg/h dry solid) was conducted at 200 °C and autogenous pressure with 30% solid load. The HTC section resulted in 239 kg/h hydrochar product with 18 % moisture and 43 % ash (the "HYDROCHAR" stream). The HTL of sewage sludge (190 kg/h dry solid) were conducted at 350 °C and autogenous pressure with 19% solid load. This section resulted in 52.2 kg/h biocrude with 4.7 % ash content (the "BIOCRUDE" stream) and 49.5 kg/h char with 57 % ash (the "HTLSOLID" stream). The aqueous effluents from HTL and HTC were mixed and gasified in 600 °C and 250 bar conditions. SCWG section produced 173 kg/h syngas having the gross heating value of 12.8 MJ/kg (the "SYNGAS" stream).

Table 5-15. Dry basis elementary composition of feedstocks and products [67,68]

Sample	HHV (MJ/kg)	C	H	N	S	O	Ash	Yield
SS	14.1	33.1	5.5	5	0.7	25.9	29.8	-
SS digestate	14.9	28.7	3.1	3.4	1.5	16.4	46.9	-
Biocrude	28.3	53.3	6.01	3.9	1.1	29.9	4.7	37.1
Hydrochar	15.4	34.5	4.3	2.9	1.2	12.8	44.3	78

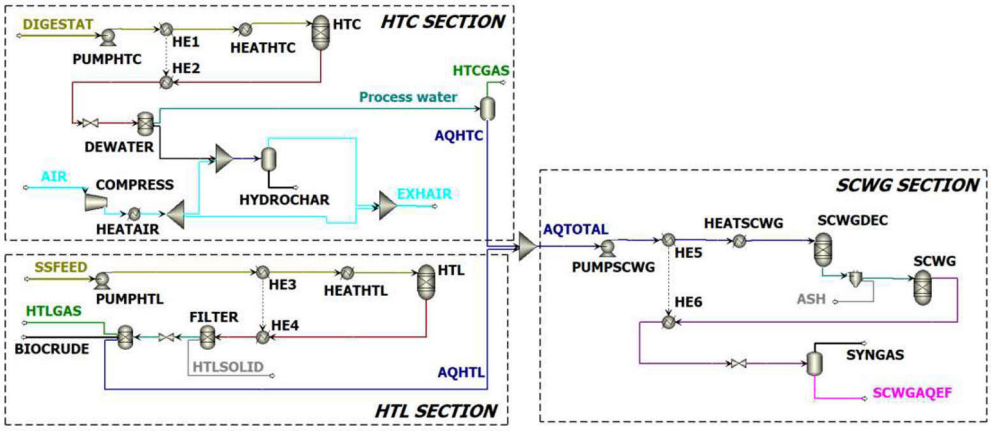

Figure 5-7. Process simulation of the proposed biorefinery

Table 5-16 reports the power and heat requirement for the proposed biorefinery as well as energy obtained from HTL solid and syngas. Since the SCWG inlet is at a high temperature, it is compromising the combined heat and power (CHP) production. Therefore, the duty of the "HEATSCWG" unit was considered as 25 % electricity and 75 % heat requirement. Similarly, the CHP obtained from the combustion of syngas and HTL solid was also assumed as 25 % electricity and 75 % heat. The proposed biorefinery required 482.8 kW of total heat and power while producing 765.1 kW of total energy. The biocrude oil can also be used as a fuel in the process or be upgraded to a transportation fuel. Meanwhile, the hydrochar can be used as a fertilizer, benefiting from the nutrients and minerals. In addition, the remaining fertilizer elements can be recovered from the SCWG process as the solid outlet.

Table 5-16. Power and heat requirement for the biorefinery

Electricity requirement (kW)		Heat requirement (kW)	
PUMPHTC	1.7	HEATHTC	16.1
PUMPHTL	7.8	HEATHTL	50.2
PUMPSCWG	15.1	HEATAIR	162.1
COMPRESS	56.4	DEWATER	5.9
0.25 x HEATSCWG	41.9	0.75 x HEATSCWG	125.6
Total	122.9	Total	359.9
Electricity outcome (kW)		Heat outcome (kW)	
Syngas	152.8	Syngas	458.3
HTL solid	38.5	HTL solid	115.5
Total	191.3	Total	573.8

The proposed biorefinery process applies to biogas plants with various feedstocks. Hydrothermal processes are suitable for converting the wet biomass. In addition, the nutrients and minerals can be recovered on the solid downstream regarding the usage as a fertilizer. The proposed process has high potential in terms of feasibility since the combination improves economic performance and overcomes the operational issues of each conversion method. SCWG of aqueous effluents produces syngas sufficient for net CHP production and addresses the discharge issue of HTL and HTC sections.

6. Conclusion/ Future perspectives

As the global population continues to increase which is coupled with urbanization, new concerns and challenges have come to the forefront. Among emerging challenges, the significant issues are energy demand, the need for an effective waste management system, and the critical aspect of nutrient recovery. The energy demand increases with population while the environmental impacts of fossil sources necessitate a shift towards innovative and eco-friendly renewable alternatives. Simultaneously, waste management is becoming a serious concern due to the increasing amount of waste. From another perspective, finite nutrient and mineral resources pose a significant challenge, especially considering their indispensable role in agriculture and as essential food supplements. However, energy supply, waste management, and nutrient recovery emerge as interconnected concepts demanding novel solutions regarding the circular bioeconomy concept. In other words, this research aims at not only producing biofuel but also enhancing the nutrient recovery, which turns the traditional waste streams into valuable resources.

The objective of this research is to develop biorefinery integration concepts enhancing the energy and resource recovery from the waste streams, thus achieving circularity in the waste-generating sectors. Especially, high-volume, dilute aqueous wastes introduce challenges regarding recovery. These streams are usually discharged or used for low-value purposes. The dilute, aqueous wastes can be processed most effectively through hydrothermal processes: using water as the reaction media and not requiring energy-demanding drying or evaporation step. The case studies in this research included the integration of hydrothermal processes with biogas plants. Biogas plants have a digestate waste stream of which the current utilization (composting) requires too long time and area. Instead, a hydrothermal biorefinery concept can recover minerals and nutrients while producing biofuels as well.

This research promotes a paradigm shift in energy production, resource recovery, and waste management by integrating hydrothermal processes. Conducting a comprehensive investigation on supercritical water gasification and hydrothermal liquefaction, this research highlighted the safety issues (solid deposition causing reactor plugging, thermal and mechanical stress due to high temperature and pressure), long-term operational issues (catalyst deactivation

and corrosion), and an operational aspect affecting the economic performance (pumpability limit of feedstock). Currently, the main solution is proposed as selecting the conditions to minimize these issues. Meanwhile, this research proposed addressing the weaknesses of each hydrothermal process through novel biorefinery concepts. On this regard, the operational issues of supercritical water gasification and hydrothermal liquefaction directed the process development towards the hydrothermal carbonization process occurring at moderate conditions.

The proposed process integration concepts involve hydrothermal carbonization of digestate integrated with biogas plants. The simulation results of this research indicated that HTC is a promising process to integrate with biogas plants. The hydrochar product recovers the majority of nutrients and minerals regarding the product used as a fertilizer. HTC leads to lower investment costs and more moderate operation because of lower temperature and pressure. Alternatively, the integrated process can involve HTC of digestate and SCWG of aqueous effluent. This concept enhances the recovery of minerals and nutrients in the solid products, i.e., more efficient transfer to far distances. Furthermore, using the syngas for CHP production enables surplus energy generation. This research ultimately proposed a novel, multiproduct biorefinery concept for a biogas plant increasing its capacity: HTC of digestate and HTL of extra sewage sludge followed by SCWG of the aqueous effluents. From the operational viewpoint, SCWG of aqueous effluent leads to more effective operation than SCWG of the waste streams. Processing dissolved organics in more dilute streams leads to less char formation, hence reduced risk of reactor plugging and less corrosion, compared to processing large and partly unhydrolyzed molecules.

As crucial steps prior to constructing process simulations, this research proposes new methodologies for the selection of optimum conditions and utilizing the experimental data to determine the simulation inputs. The experimental data on product yields are usually reported on a dry or dry-ash-free basis with respect to reaction conditions. Meanwhile, from the economic viewpoint, the optimum conditions should be determined by compiling the impacts of conditions on the relative equipment size as well as the product yield and quality. Therefore, this research proposed energetic yield as a critical metric for selecting the conditions of hydrothermal conversions, defined as the energy content of product per total mass of reactor inlet (MJ/kg reactor inlet). This metric offers a more comprehensive approach to optimizing conditions,

considering both energy content and process efficiency. After selecting the reaction conditions, the simulation models require reactor yields per unit mass of non-inert inlet and identification of non-conventional components. These inputs are determined by utilizing the experimental data on the yields and characterization of samples. However, it is important to prioritize the usage of characterization data to overcome the potential mismatches in the data. This research utilizes the characterization data starting from the most reliable ones: hydrochar, gas and liquid yields, hydrochar analysis to identify the elemental composition, assumed gas composition, elemental balances to determine the C, N, S in the dissolved organics, and using BMP and COD data to determine the oxygen and hydrogen content in dissolved organics and produced or consumed water amount.

Process simulations at the optimum conditions will enable the techno-economical evaluation of the investigated integration concept and narrow down the verification experiments on a specific feedstock around the selected optimum conditions. For instance, the co-HTC of SSD and FWD was simulated by using the individual HTC data of each digestate due to the absence of experimental co-HTC data. Since the synergetic impact is expected to be quite low between the wastes having similar constituents, it is possible to conduct a preliminary assessment with the generated co-HTC data despite the need for verification experiments. Nevertheless, the co-HTC experiments can be conducted at some ranges around the optimum conditions, rather than numerous experiments covering wide ranges.

In conclusion, the biorefinery acts as a central hub for combined heat and power production (CHP) production, waste biomass management, and nutrient recovery. The biorefinery process integration represents a sustainable and holistic solution for waste management and biomass utilization. The biorefinery concepts should be developed following the desired products or recovery needs and the biomass waste. Furthermore, the operational aspects can be addressed through novel biorefinery concepts combining the hydrothermal processes effectively. The future developments of the proposed biorefinery concepts can continue with:

1) Optimization and Verification Experiments

The proposed biorefinery needs further verification and optimization through experiments. Integration of co-HTC process and SCWG is capable of multiproduct biorefinery and requires more assessment and feasibility studies. The experiments validate the simulation results and fine-tune the processes for real-world application and commercialization.

2) Techno-economic Analysis

A comprehensive techno-economic study is required to be conducted for the evaluation of the proposed biorefinery specifically, from a financial perspective. Assessing the effect of the process condition on equipment size, product yield, and product quality provides holistic insights into the economic feasibility and scaling up the processes.

3) Collaboration and Knowledge Transfer

Collaboration between academia, industry stakeholders, and policymakers is essential to accelerate the scale-up and commercialization process. More importantly, conferences, workshops, and collaborative projects can be encouraged to fill the gap between research and implementation.

4) Policy Advocacy for Circular Bioeconomy

The successful implementation and commercialization of an innovative biorefinery relies on support from policymakers. Advocacy for policies promoting the circular bioeconomy, incentivizing sustainable waste management practices, and fostering the development of eco-friendly technologies will play a pivotal role in driving these advancements from the laboratory to the market.

7. References

[1] Solarte-Toro JC, Cardona Alzate CA. Biorefineries as the base for accomplishing the sustainable development goals (SDGs) and the transition to bioeconomy: Technical aspects, challenges and perspectives. Bioresource Technology 2021;340:125626. https://doi.org/10.1016/j.biortech.2021.125626.

[2] Zeng Y, Maxwell S, Runting RK, Venter O, Watson JEM, Carrasco LR. Environmental destruction not avoided with the Sustainable Development Goals. Nat Sustain 2020;3:795–8. https://doi.org/10.1038/s41893-020-0555-0.

[3] Khan I. Chapter 4 - Sustainability assessment of energy systems: Indicators, methods, and applications. In: Ren J, editor. Methods in Sustainability Science, Elsevier; 2021, p. 47–70. https://doi.org/10.1016/B978-0-12-823987-2.00016-7.

[4] Bonafin J, Bonzanini A. Chapter 3 - CO2 emissions from geothermal power plants and state-of-the-art technical solutions for CO2 reinjection. In: Colpan CO, Ezan MA, Kizilkan O, editors. Thermodynamic Analysis and Optimization of Geothermal Power Plants, Elsevier; 2021, p. 43–52. https://doi.org/10.1016/B978-0-12-821037-6.00012-3.

[5] Brodny J, Tutak M, Bindzár P. Assessing the Level of Renewable Energy Development in the European Union Member States. A 10-Year Perspective. Energies 2021;14:3765. https://doi.org/10.3390/en14133765.

[6] Al-Shetwi AQ. Sustainable development of renewable energy integrated power sector: Trends, environmental impacts, and recent challenges. Science of The Total Environment 2022;822:153645. https://doi.org/10.1016/j.scitotenv.2022.153645.

[7] Farghali M, Osman AI, Chen Z, Abdelhaleem A, Ihara I, Mohamed IMA, et al. Social, environmental, and economic consequences of integrating renewable energies in the electricity sector: a review. Environ Chem Lett 2023;21:1381–418. https://doi.org/10.1007/s10311-023-01587-1.

[8] OECD. World Energy Outlook 2018. Paris: Organisation for Economic Co-operation and Development; 2018.

[9] Finland ranks first in international sustainable development comparison. Valtioneuvosto n.d. https://valtioneuvosto.fi/en/-/10616/finland-ranks-first-in-international-sustainable-development-comparison (accessed March 2, 2023).

[10] Kirchherr J, Reike D, Hekkert M. Conceptualizing the circular economy: An analysis of 114 definitions n.d. https://doi.org/10.1016/j.resconrec.2017.09.005.

[11] Neves SA, Marques AC. Drivers and barriers in the transition from a linear economy to a circular economy. Journal of Cleaner Production 2022;341:130865. https://doi.org/10.1016/j.jclepro.2022.130865.

[12] Kumar Awasthi M, Yan B, Sar T, Gómez-García R, Ren L, Sharma P, et al. Organic waste recycling for carbon smart circular bioeconomy and sustainable development: A review.

Bioresource Technology 2022;360:127620. https://doi.org/10.1016/j.biortech.2022.127620.

[13] Mussatto SI, Bikaki N. Chapter 25 - Technoeconomic Considerations for Biomass Fractionation in a Biorefinery Context. In: Mussatto SI, editor. Biomass Fractionation Technologies for a Lignocellulosic Feedstock Based Biorefinery, Amsterdam: Elsevier; 2016, p. 587–610. https://doi.org/10.1016/B978-0-12-802323-5.00025-6.

[14] Basu P, Kaushal P. Chapter 4 - Biomass characteristics. In: Basu P, Kaushal P, editors. Biomass Gasification, Pyrolysis, and Torrefaction (Fourth Edition), Academic Press; 2024, p. 63–105. https://doi.org/10.1016/B978-0-443-13784-6.00009-3.

[15] Patel G, Banerjee S. 18 - Synthesis and applications of biomass-derived carbonaceous materials. In: Dhoble SJ, Nande A, Kalyani NT, Tiwari A, Arof AK, editors. Functional Materials from Carbon, Inorganic, and Organic Sources, Woodhead Publishing; 2023, p. 559–78. https://doi.org/10.1016/B978-0-323-85788-8.00009-4.

[16] Jawaid M, Paridah MT, Saba N. 1 - Introduction to biomass and its composites. In: Jawaid M, Md Tahir P, Saba N, editors. Lignocellulosic Fibre and Biomass-Based Composite Materials, Woodhead Publishing; 2017, p. 1–11. https://doi.org/10.1016/B978-0-08-100959-8.00001-9.

[17] Adams P, Bridgwater T, Lea-Langton A, Ross A, Watson I. Chapter 8 - Biomass Conversion Technologies. In: Thornley P, Adams P, editors. Greenhouse Gas Balances of Bioenergy Systems, Academic Press; 2018, p. 107–39. https://doi.org/10.1016/B978-0-08-101036-5.00008-2.

[18] Darmawan A, Aziz M. Chapter 2 - Process and products of biomass conversion technology. In: Darmawan A, Aziz M, editors. Innovative Energy Conversion from Biomass Waste, Elsevier; 2022, p. 25–60. https://doi.org/10.1016/B978-0-323-85477-1.00004-X.

[19] Jeguirim M, Khiari B. Chapter 10 - Thermochemical conversion. In: Jeguirim M, Khiari B, Jellali S, editors. Palm Trees and Fruits Residues, Academic Press; 2023, p. 391–437. https://doi.org/10.1016/B978-0-12-823934-6.00012-5.

[20] Meenakshisundaram S, Fayeulle A, Leonard E, Ceballos C, Pauss A. Fiber degradation and carbohydrate production by combined biological and chemical/physicochemical pretreatment methods of lignocellulosic biomass – A review. Bioresource Technology 2021;331:125053. https://doi.org/10.1016/j.biortech.2021.125053.

[21] Siwal SS, Sheoran K, Saini AK, Vo D-VN, Wang Q, Thakur VK. Advanced thermochemical conversion technologies used for energy generation: Advancement and prospects. Fuel 2022;321:124107. https://doi.org/10.1016/j.fuel.2022.124107.

[22] Biller P, Ross AB. 17 - Production of biofuels via hydrothermal conversion. In: Luque R, Lin CSK, Wilson K, Clark J, editors. Handbook of Biofuels Production (Second Edition), Woodhead Publishing; 2016, p. 509–47. https://doi.org/10.1016/B978-0-08-100455-5.00017-5.

[23] Gaur RZ, Khoury O, Zohar M, Poverenov E, Darzi R, Laor Y, et al. Hydrothermal carbonization of sewage sludge coupled with anaerobic digestion: Integrated approach for sludge management and energy recycling. Energy Conversion and Management 2020;224:113353. https://doi.org/10.1016/j.enconman.2020.113353.

[24] Tekin K, Karagöz S, Bektaş S. A review of hydrothermal biomass processing. Renewable and Sustainable Energy Reviews 2014;40:673–87. https://doi.org/10.1016/j.rser.2014.07.216.

[25] Naqvi M, Yan J, Dahlquist E. Black liquor gasification integrated in pulp and paper mills: A critical review. Bioresource Technology 2010;101:8001–15. https://doi.org/10.1016/j.biortech.2010.05.013.

[26] Özdenkçi K, Prestipino M, Björklund-Sänkiaho M, Galvagno A, De Blasio C. Alternative energy valorization routes of black liquor by stepwise supercritical water gasification: Effect of process parameters on hydrogen yield and energy efficiency. Renewable and Sustainable Energy Reviews 2020;134:110146. https://doi.org/10.1016/j.rser.2020.110146.

[27] Özdenkçi K, De Blasio C, Muddassar HR, Melin K, Oinas P, Koskinen J, et al. A novel biorefinery integration concept for lignocellulosic biomass. Energy Conversion and Management 2017;149:974–87. https://doi.org/10.1016/j.enconman.2017.04.034.

[28] Guo Y, Wang SZ, Xu DH, Gong YM, Ma HH, Tang XY. Review of catalytic supercritical water gasification for hydrogen production from biomass. Renewable and Sustainable Energy Reviews 2010;14:334–43. https://doi.org/10.1016/j.rser.2009.08.012.

[29] Sarker TR, Pattnaik F, Nanda S, Dalai AK, Meda V, Naik S. Hydrothermal pretreatment technologies for lignocellulosic biomass: A review of steam explosion and subcritical water hydrolysis. Chemosphere 2021;284:131372. https://doi.org/10.1016/j.chemosphere.2021.131372.

[30] Machmudah S, Wahyudiono, Kanda H, Goto M. Chapter 3 - Hydrolysis of Biopolymers in Near-Critical and Subcritical Water. In: Dominguez González H, González Muñoz MJ, editors. Water Extraction of Bioactive Compounds, Elsevier; 2017, p. 69–107. https://doi.org/10.1016/B978-0-12-809380-1.00003-6.

[31] Houcinat I, Outili N, García-Jarana B, Sánchez-Oneto J, Portela JR, Meniai A-H. Chapter 6 - Hydrogen production by supercritical water gasification: a review. In: Jeguirim M, editor. Renewable Energy Production and Distribution, vol. 1, Academic Press; 2022, p. 189–225. https://doi.org/10.1016/B978-0-323-91892-3.00010-8.

[32] Wei N, Xu D, Hao B, Guo S, Guo Y, Wang S. Chemical reactions of organic compounds in supercritical water gasification and oxidation. Water Research 2021;190:116634. https://doi.org/10.1016/j.watres.2020.116634.

[33] Blasio CD. Fundamentals of Biofuels Engineering and Technology. Springer International Publishing; 2019. https://doi.org/10.1007/978-3-030-11599-9.

[34] Zhuang X, Liu J, Zhang Q, Wang C, Zhan H, Ma L. A review on the utilization of industrial biowaste via hydrothermal carbonization. Renewable and Sustainable Energy Reviews 2022;154:111877. https://doi.org/10.1016/j.rser.2021.111877.

[35] Kannan S, Raghavan V. Chapter 8 - Hydrothermal carbonization of nonlignocellulosic wastes using enzyme pretreatment. In: Kuddus M, Ramteke P, editors. Value-Addition in Agri-food Industry Waste Through Enzyme Technology, Academic Press; 2023, p. 123–36. https://doi.org/10.1016/B978-0-323-89928-4.00001-8.

[36] Atallah E, Zeaiter J, Ahmad MN, Kwapinska M, Leahy JJ, Kwapinski W. The effect of temperature, residence time, and water-sludge ratio on hydrothermal carbonization of DAF dairy sludge. Journal of Environmental Chemical Engineering 2020;8:103599. https://doi.org/10.1016/j.jece.2019.103599.

[37] Sharma HB, Dubey BK. Binderless fuel pellets from hydrothermal carbonization of municipal yard waste: Effect of severity factor on the hydrochar pellets properties. Journal of Cleaner Production 2020;277:124295. https://doi.org/10.1016/j.jclepro.2020.124295.

[38] Pauline AL, Joseph K. Hydrothermal carbonization of organic wastes to carbonaceous solid fuel – A review of mechanisms and process parameters. Fuel 2020;279:118472. https://doi.org/10.1016/j.fuel.2020.118472.

[39] Wang Q, Wu S, Cui D, Zhou H, Wu D, Pan S, et al. Co-hydrothermal carbonization of organic solid wastes to hydrochar as potential fuel: A review. Science of The Total Environment 2022;850:158034. https://doi.org/10.1016/j.scitotenv.2022.158034.

[40] Inada M, Enomoto N, Hojo J, Hayashi K. Structural analysis and capacitive properties of carbon spheres prepared by hydrothermal carbonization. Advanced Powder Technology 2017;28:884–9. https://doi.org/10.1016/j.apt.2016.12.014.

[41] Nizamuddin S, Baloch HA, Griffin GJ, Mubarak NM, Bhutto AW, Abro R, et al. An overview of effect of process parameters on hydrothermal carbonization of biomass. Renewable and Sustainable Energy Reviews 2017;73:1289–99. https://doi.org/10.1016/j.rser.2016.12.122.

[42] Czerwińska K, Śliz M, Wilk M. Hydrothermal carbonization process: Fundamentals, main parameter characteristics and possible applications including an effective method of SARS-CoV-2 mitigation in sewage sludge. A review. Renewable and Sustainable Energy Reviews 2022;154:111873. https://doi.org/10.1016/j.rser.2021.111873.

[43] Yan M, He L, Prabowo B, Fang Z, Lin J, Xu Z, et al. Effect of pressure and atmosphere during hydrothermal treatment on the properties of sewage sludge-derived solid fuel. J Mater Cycles Waste Manag 2018;20:1594–604. https://doi.org/10.1007/s10163-018-0723-8.

[44] Güleç F, Riesco LMG, Williams O, Kostas ET, Samson A, Lester E. Hydrothermal conversion of different lignocellulosic biomass feedstocks – Effect of the process conditions on hydrochar structures. Fuel 2021;302:121166. https://doi.org/10.1016/j.fuel.2021.121166.

[45] Minaret J, Dutta A. Comparison of liquid and vapor hydrothermal carbonization of corn husk for the use as a solid fuel. Bioresource Technology 2016;200:804–11. https://doi.org/10.1016/j.biortech.2015.11.010.

[46] Nallasivam J, Prashanth PF, Vinu R. Chapter 4 - Hydrothermal liquefaction of biomass for the generation of value-added products. In: Varjani S, Pandey A, Taherzadeh MJ, Ngo HH, Tyagi RD, editors. Biomass, Biofuels, Biochemicals, Elsevier; 2022, p. 65–107. https://doi.org/10.1016/B978-0-323-88511-9.00018-5.

[47] Beims RF, Hu Y, Shui H, Xu C (Charles). Hydrothermal liquefaction of biomass to fuels and value-added chemicals: Products applications and challenges to develop large-scale operations. Biomass and Bioenergy 2020;135:105510. https://doi.org/10.1016/j.biombioe.2020.105510.

[48] Panisko E, Wietsma T, Lemmon T, Albrecht K, Howe D. Characterization of the aqueous fractions from hydrotreatment and hydrothermal liquefaction of lignocellulosic feedstocks. Biomass and Bioenergy 2015;74:162–71. https://doi.org/10.1016/j.biombioe.2015.01.011.

[49] Gundupalli MP, Gundupalli SP, Somavarapu Thomas AS, Jayakumar M, Bhattacharyya D, Gurunathan B. Chapter 4 - Hydrothermal liquefaction of lignocellulosic biomass for production of biooil and by-products: current state of the art and challenges. In: Gurunathan B, Sahadevan R, Zakaria ZA, editors. Biofuels and Bioenergy, Elsevier; 2022, p. 61–84. https://doi.org/10.1016/B978-0-323-85269-2.00001-0.

[50] Singh R, Prakash A, Balagurumurthy B, Bhaskar T. Chapter 10 - Hydrothermal Liquefaction of Biomass. In: Pandey A, Bhaskar T, Stöcker M, Sukumaran RK, editors. Recent Advances in Thermo-Chemical Conversion of Biomass, Boston: Elsevier; 2015, p. 269–91. https://doi.org/10.1016/B978-0-444-63289-0.00010-7.

[51] Barbier J, Charon N, Dupassieux N, Loppinet-Serani A, Mahé L, Ponthus J, et al. Hydrothermal conversion of lignin compounds. A detailed study of fragmentation and condensation reaction pathways. Biomass and Bioenergy 2012;46:479–91. https://doi.org/10.1016/j.biombioe.2012.07.011.

[52] Xu Y-H, Li M-F. Hydrothermal liquefaction of lignocellulose for value-added products: Mechanism, parameter and production application. Bioresource Technology 2021;342:126035. https://doi.org/10.1016/j.biortech.2021.126035.

[53] Shahbeik H, Kazemi Shariat Panahi H, Dehhaghi M, Guillemin GJ, Fallahi A, Hosseinzadeh-Bandbafha H, et al. Biomass to biofuels using hydrothermal liquefaction: A comprehensive review. Renewable and Sustainable Energy Reviews 2024;189:113976. https://doi.org/10.1016/j.rser.2023.113976.

[54] Xue Y, Chen H, Zhao W, Yang C, Ma P, Han S. A review on the operating conditions of producing bio-oil from hydrothermal liquefaction of biomass. International Journal of Energy Research 2016;40:865–77. https://doi.org/10.1002/er.3473.

[55] Wu X-F, Zhang J-J, Huang Y-H, Li M-F, Bian J, Peng F. Comparative investigation on bio-oil production from eucalyptus via liquefaction in subcritical water and supercritical ethanol. Industrial Crops and Products 2019;140:111695. https://doi.org/10.1016/j.indcrop.2019.111695.

[56] Zhang S, Zhou S, Yang X, Xi W, Zheng K, Chu C, et al. Effect of operating parameters on hydrothermal liquefaction of corn straw and its life cycle assessment. Environ Sci Pollut Res 2020;27:6362–74. https://doi.org/10.1007/s11356-019-07267-4.

[57] Mathanker A, Das S, Pudasainee D, Khan M, Kumar A, Gupta R. A Review of Hydrothermal Liquefaction of Biomass for Biofuels Production with a Special Focus on the Effect of Process Parameters, Co-Solvents, and Extraction Solvents. Energies 2021;14:4916. https://doi.org/10.3390/en14164916.

[58] Ni J, Qian L, Wang Y, Zhang B, Gu H, Hu Y, et al. A review on fast hydrothermal liquefaction of biomass. Fuel 2022;327:125135. https://doi.org/10.1016/j.fuel.2022.125135.

[59] Ren C, Guo S, Wang Y, Liu S, Du M, Chen Y, et al. Thermodynamic analysis and optimization of auto-thermal supercritical water gasification polygeneration system of pig manure.

Chemical Engineering Journal 2022;427:131938. https://doi.org/10.1016/j.cej.2021.131938.

[60] Hu Y, Gong M, Xing X, Wang H, Zeng Y, Xu CC. Supercritical water gasification of biomass model compounds: A review. Renewable and Sustainable Energy Reviews 2020;118:109529. https://doi.org/10.1016/j.rser.2019.109529.

[61] Jin H, Chen Y, Ge Z, Liu S, Ren C, Guo L. Hydrogen production by Zhundong coal gasification in supercritical water. International Journal of Hydrogen Energy 2015;40:16096–103. https://doi.org/10.1016/j.ijhydene.2015.09.003.

[62] Hantoko D, Su H, Yan M, Kanchanatip E, Susanto H, Wang G, et al. Thermodynamic study on the integrated supercritical water gasification with reforming process for hydrogen production: Effects of operating parameters. International Journal of Hydrogen Energy 2018;43:17620–32. https://doi.org/10.1016/j.ijhydene.2018.07.198.

[63] Khorasani R, Khodaparasti MS, Tavakoli O. Hydrogen production from dairy wastewater using catalytic supercritical water gasification: Mechanism and reaction pathway. International Journal of Hydrogen Energy 2021;46:22368–84. https://doi.org/10.1016/j.ijhydene.2021.04.089.

[64] AL-MALAH KIM. ASPEN PLUS® Chemical Engineering Applications n.d.

[65] Aragon-Briceño C, Pożarlik A, Bramer E, Brem G, Wang S, Wen Y, et al. Integration of hydrothermal carbonization treatment for water and energy recovery from organic fraction of municipal solid waste digestate. Renewable Energy 2022;184:577–91. https://doi.org/10.1016/j.renene.2021.11.106.

[66] Zhao P, Shen Y, Ge S, Yoshikawa K. Energy recycling from sewage sludge by producing solid biofuel with hydrothermal carbonization. Energy Conversion and Management 2014;78:815–21. https://doi.org/10.1016/j.enconman.2013.11.026.

[67] Parmar KR, Ross AB. Integration of Hydrothermal Carbonisation with Anaerobic Digestion; Opportunities for Valorisation of Digestate. Energies 2019;12:1586. https://doi.org/10.3390/en12091586.

[68] Rahman T, Jahromi H, Roy P, Adhikari S, Hassani E, Oh T-S. Hydrothermal liquefaction of municipal sewage sludge: Effect of red mud catalyst in ethylene and inert ambiences. Energy Conversion and Management 2021;245:114615. https://doi.org/10.1016/j.enconman.2021.114615.

[69] Oh DH, Race J, Oterkus S, Chang E. A new methodology for the prediction of burst pressure for API 5L X grade flawless pipelines. Ocean Engineering 2020;212:107602. https://doi.org/10.1016/j.oceaneng.2020.107602.

[70] Steel M. Inconel vs Stainless Steel: Which is Stronger? n.d. https://www.marlinwire.com/blog/inconel-vs-stainless-steel-which-is-stronger (accessed November 3, 2021).

[71] Kosmač A. Stainless steels at high temperatures. Brussels: Euro Inox; 2012.

[72] Lee A, Lewis D, Kalaitzidis T, Ashman P. Technical issues in the large-scale hydrothermal liquefaction of microalgal biomass to biocrude. Current Opinion in Biotechnology 2016;38:85–9. https://doi.org/10.1016/j.copbio.2016.01.004.

[73] De Blasio C, De Gisi S, Molino A, Simonetti M, Santarelli M, Björklund-Sänkiaho M. Concerning operational aspects in supercritical water gasification of kraft black liquor. Renewable Energy 2019;130:891–901. https://doi.org/10.1016/j.renene.2018.07.004.

[74] Rodriguez Correa C, Kruse A. Supercritical water gasification of biomass for hydrogen production – Review. The Journal of Supercritical Fluids 2018;133:573–90. https://doi.org/10.1016/j.supflu.2017.09.019.

[75] Reddy SN, Nanda S, Dalai AK, Kozinski JA. Supercritical water gasification of biomass for hydrogen production. International Journal of Hydrogen Energy 2014;39:6912–26. https://doi.org/10.1016/j.ijhydene.2014.02.125.

[76] Azadi P, Farnood R. Review of heterogeneous catalysts for sub- and supercritical water gasification of biomass and wastes. International Journal of Hydrogen Energy 2011;36:9529–41. https://doi.org/10.1016/j.ijhydene.2011.05.081.

[77] Chen J, Liang J, Xu Z, E J. Assessment of supercritical water gasification process for combustible gas production from thermodynamic, environmental and techno-economic perspectives: A review. Energy Conversion and Management 2020;226:113497. https://doi.org/10.1016/j.enconman.2020.113497.

[78] Okolie JA, Nanda S, Dalai AK, Berruti F, Kozinski JA. A review on subcritical and supercritical water gasification of biogenic, polymeric and petroleum wastes to hydrogen-rich synthesis gas. Renewable and Sustainable Energy Reviews 2020;119:109546. https://doi.org/10.1016/j.rser.2019.109546.

[79] Berglin E, Enderlin C, Schmidt A. Review and Assessment of Commercial Vendors/Options for Feeding and Pumping Biomass Slurries for Hydrothermal Liquefaction. Pacific Northwest National Lab. (PNNL), Richland, WA (United States); 2012.

[80] De Blasio C, Lucca G, Özdenkci K, Mulas M, Lundqvist K, Koskinen J, et al. A study on supercritical water gasification of black liquor conducted in stainless steel and nickel-chromium-molybdenum reactors. Journal of Chemical Technology & Biotechnology 2016;91:2664–78. https://doi.org/10.1002/jctb.4871.

[81] Casademont P, Sánchez-Oneto J, Scandelai APJ, Cardozo-Filho L, Portela JR. Hydrogen production by supercritical water gasification of black liquor: Use of high temperatures and short residence times in a continuous reactor. The Journal of Supercritical Fluids 2020;159:104772. https://doi.org/10.1016/j.supflu.2020.104772.

[82] Hoekman SK, Broch A, Robbins C, Zielinska B, Felix L. Hydrothermal carbonization (HTC) of selected woody and herbaceous biomass feedstocks. Biomass Conv Bioref 2013;3:113–26. https://doi.org/10.1007/s13399-012-0066-y.

[83] Basso D, Weiss-Hortala E, Patuzzi F, Castello D, Baratieri M, Fiori L. Hydrothermal carbonization of off-specification compost: A byproduct of the organic municipal solid waste treatment. Bioresource Technology 2015;182:217–24. https://doi.org/10.1016/j.biortech.2015.01.118.

[84] Funke A, Ziegler F. Heat of reaction measurements for hydrothermal carbonization of biomass. Bioresource Technology 2011;102:7595–8. https://doi.org/10.1016/j.biortech.2011.05.016.

[85] Ischia G, Cazzanelli M, Fiori L, Orlandi M, Miotello A. Exothermicity of hydrothermal carbonization: Determination of heat profile and enthalpy of reaction via high-pressure differential scanning calorimetry. Fuel 2022;310:122312. https://doi.org/10.1016/j.fuel.2021.122312.

[86] Cuvilas CA, Kantarelis E, Yang W. The Impact of a Mild Sub-Critical Hydrothermal Carbonization Pretreatment on Umbila Wood. A Mass and Energy Balance Perspective. Energies 2015;8:2165–75. https://doi.org/10.3390/en8032165.

[87] Parmar KR, Ross AB. Integration of Hydrothermal Carbonisation with Anaerobic Digestion; Opportunities for Valorisation of Digestate. Energies 2019;12:1586. https://doi.org/10.3390/en12091586.

[88] Aragón-Briceño CI, Grasham O, Ross AB, Dupont V, Camargo-Valero MA. Hydrothermal carbonization of sewage digestate at wastewater treatment works: Influence of solid loading on characteristics of hydrochar, process water and plant energetics. Renewable Energy 2020;157:959–73. https://doi.org/10.1016/j.renene.2020.05.021.

[89] Hämäläinen A, Kokko M, Kinnunen V, Hilli T, Rintala J. Hydrothermal carbonisation of mechanically dewatered digested sewage sludge—Energy and nutrient recovery in centralised biogas plant. Water Research 2021;201:117284. https://doi.org/10.1016/j.watres.2021.117284.

[90] Parmar KR, Brown AE, Hammerton JM, Camargo-Valero MA, Fletcher LA, Ross AB. Co-Processing Lignocellulosic Biomass and Sewage Digestate by Hydrothermal Carbonisation: Influence of Blending on Product Quality. Energies 2022;15:1418. https://doi.org/10.3390/en15041418.

[91] Akarsu K, Duman G, Yilmazer A, Keskin T, Azbar N, Yanik J. Sustainable valorization of food wastes into solid fuel by hydrothermal carbonization. Bioresource Technology 2019;292:121959. https://doi.org/10.1016/j.biortech.2019.121959.

[92] Cao Z, Jung D, Olszewski MP, Arauzo PJ, Kruse A. Hydrothermal carbonization of biogas digestate: Effect of digestate origin and process conditions. Waste Management 2019;100:138–50. https://doi.org/10.1016/j.wasman.2019.09.009.

[93] Zheng C, Ma X, Yao Z, Chen X. The properties and combustion behaviors of hydrochars derived from co-hydrothermal carbonization of sewage sludge and food waste. Bioresource Technology 2019;285:121347. https://doi.org/10.1016/j.biortech.2019.121347.

[94] Pecchi M, Patuzzi F, Basso D, Baratieri M. Enthalpy change during hydrothermal carbonization of biomass: a critical review. J Therm Anal Calorim 2020;141:1251–62. https://doi.org/10.1007/s10973-019-09117-4.

[95] Berge ND, Ro KS, Mao J, Flora JRV, Chappell MA, Bae S. Hydrothermal Carbonization of Municipal Waste Streams. Environ Sci Technol 2011;45:5696–703. https://doi.org/10.1021/es2004528.

[96] Rebling T, von Frieling P, Buchholz J, Greve T. Hydrothermal carbonization: combination of heat of reaction measurements and theoretical estimations. J Therm Anal Calorim 2015;119:1941–53. https://doi.org/10.1007/s10973-014-4361-7.

Appendix: Originalpublikationer/Original publications

Biomass Conversion and Biorefinery (2023) 13:12367–12394
https://doi.org/10.1007/s13399-021-02176-4

REVIEW ARTICLE

Analysis of operational issues in hydrothermal liquefaction and supercritical water gasification processes: a review

Niloufar Ghavami[1] · Karhan Özdenkçi[1] · Gabriel Salierno[1] · Margareta Björklund-Sänkiaho[1] · Cataldo De Blasio[1]

Received: 12 August 2021 / Revised: 24 November 2021 / Accepted: 30 November 2021 / Published online: 15 December 2021

Abstract
Biomass is often referred to as a carbon–neutral energy source, and it has a role in reducing fossil fuel depletion. In addition, biomass can be converted efficiently into various forms of biofuels. The biomass conversion processes involve several thermochemical, biochemical, and hydrothermal methods for biomass treatment integration. The most common conversion routes to produce biofuels include pyrolysis and gasification processes. On the other hand, supercritical water gasification (SCWG) and hydrothermal liquefaction (HTL) are best suitable for converting biomass and waste with high moisture content. Despite promising efficiencies, SCWG and HTL processes introduce operational issues as obstacles to the industrialization of these technologies. The issues include process safety aspects due to operation conditions, plugging due to solid deposition, corrosion, pumpability of feedstock, catalyst sintering and deactivation, and high production costs. The methods to address these issues include various reactor configurations to avoid plugging and optimizing process conditions to minimize other issues. However, there are only a few studies investigating the operational issues as the main scope, and reviews are seldomly available in this regard. Therefore, further research is required to address operational problems. This study reviews the main operational problems in SCWG and HTL. The objective of this study is to enhance the industrialization of these processes by investigating the operational issues and the potential solutions, i.e., contributing to the elimination of the obstacles. A comprehensive study on the operational issues provides a holistic overview of the biomass conversion technologies and biorefinery concepts to promote the industrialization of SCWG and HTL.

Keywords Biofuels · Biomass conversion · Supercritical water gasification · Hydrothermal liquefaction · Operational risks

Abbreviations

BTU	British Thermal Unit
EU	European Union
HTL	Hydrothermal liquefaction
PTG	Power to gas
CaL	Calcium looping cycle
SCWG	Supercritical water gasification
CSTR	Continuous stirred-tank reactor
SCWO	Supercritical water oxidation
LCA	Life cycle assessment
AP	Aqueous phase
SCW	Supercritical water
WBL	Weak black liquor
WGS	Water gas shift
Adt	Air-dried ton
SCWR	Supercritical water reforming
ASCWR	Autothermal supercritical water reforming
GC	Gas chromatographs
WG	Wet gas meter
TWR	Transpiring-wall reactor
HHV	High heating value
SCPW	Supercritical pressurized water
EWBB	Extracted white birch bark
SCFs	Supercritical fluids
HTL-WW	High strength hydrothermal liquefaction wastewater
PWO	Partial wet oxidation

✉ Niloufar Ghavami
niloufar.ghavami@abo.fi

[1] Faculty of Science and Engineering, Laboratory of Energy Technology, Åbo Akademi University, Rantakatu 2, 65100 Vaasa, Finland

1 Introduction

Increasing energy demand due to the world population growth and rising prosperity represents a real challenge in current times. According to the energy perspective report

[1], the global energy demand will be 675 quadrillion BTUs in 2040, increasing about 20% compared to 2017 levels. However, as the main source of energy, fossil fuel usage causes environmental problems associated with carbon emissions and other pollutants as well as fossil sources being depleted. Consequently, there is an urgent demand to eliminate the usage of fossil sources. Replacing fossil fuels with renewable resources reduces environmental effects due to greenhouse gas emissions [2]. Renewable energy consumption has increased more than 10% annually in the European Union (EU) countries, approximately one-fourth of the global renewable energy consumption. Most of the EU countries are setting goals to enhance renewable energy production [3]. By 2050, the EU intends to be climate-neutral and emit net-zero greenhouse gases. For instance, Finland is among the leading countries increasing solid biomass and bio-waste use for energy production an average of 3.6% yearly since 2010 [4, 5]. According to Sikkema et al. [4], Baltic countries surpassed their solid biomass energy share goals.

Biomass is an abundant and renewable source, thus introducing the promising potential for replacing fossil sources. Therefore, its use would contribute to the carbon neutrality of the energy sector, arising as an increasingly plausible alternative to fossil fuels [6–9]. However, there is a debate regarding sustainability and carbon-neutrality characteristics when converting 1st-generation biomass, i.e., edible biomass compromising with the food and animal feed. Processing 1st-generation biomass might cause carbon emissions equal to or even more than fossil-based production when the plant growth steps are also considered [10], despite relatively simple processes and close-to-uniform feedstock [11, 12]. Therefore, it is the 2nd-generation biomass having the potential for the complete replacement of fossil fuels, i.e., non-edible biomass and waste/by-products of existing biomass sectors. Some examples of 2nd-generation biomass include wood residues from sawmills, agricultural residues, dedicated non-edible crops, municipal sewage sludge, black liquor in the pulp mills, food waste, manure, and algae. However, traditional waste management methods such as incineration, dumping, landfilling, and composting result in environmental pollution [13–15]. In other words, managing large amounts of bio-waste and waste-to-energy conversion technologies are challenging issues in the following years. Bio-waste is generated significantly and has a high potential for biofuel production. On the other hand, valorization of 2nd-generation biomass requires advanced processes due to feedstock variety.

The 2nd-generation biomass conversion is classified as thermal, biological, and hydrothermal processes [16, 17]. The biological conversion involves enzymes or organisms converting biomass into biofuels, such as saccharification (hydrolysis of food constituents, cellulose, and hemicellulose into sugars) followed by fermentation to produce alcohols [18]. The biological conversion processes can selectively produce the desired product rather than generating numerous intermediate compounds as in thermochemical conversions. However, the biological conversion is suitable only for food waste, manure, sewage sludge, and food-related (e.g., food waste and side streams of food production plants) or digestion-related wastes (e.g., sewage sludge and manure). In contrast, processing lignocellulosic biomass is usually inefficient due to inhibiting impacts of lignin, thus requiring prior fractionation. On the other hand, perfect fractionation of 2nd-generation biomass might be unfeasible [19]. As for drawbacks from the flexibility and adaptability viewpoints, these processes require very long residence time (hours to days) and introduce issues of cell culture recovery and difficult process control. The thermal conversion methods include combustion [20], gasification [21–24], and pyrolysis [25–28]. However, burning biomass can also create pollution whereas new conversion technologies including biochemical and thermochemical methods reduce the environmental impacts [29]. For instance, comparing gasification and combustion for electricity production from forest biomass, gasification was stated to provide higher energy efficiency and cleaner gas outlet regarding NO_x and SO_x content [30]. In addition, the CO_2 produced by biomass thermochemical conversion could be integrated within power-to-gas (P2G) technologies and processed with chemical looping to produce methane [31, 32]. The gasification and pyrolysis products are further processed to produce various biofuels and chemicals [26, 33]. On other hand, the thermal processes require drying as an energy-consuming pre-treatment when processing biomass due to high moisture content. For instance, as stated by an exergy analysis of biofuels, the evaporation step is the main source of exergy loss in thermal processes, and hydrothermal processes provide higher exergy efficiency [34]. Instead, the hydrothermal processes use water as the reaction medium and avoid the evaporation or drying steps, thus providing higher energy efficiency when processing biomass [35].

The main hydrothermal processes include supercritical water gasification (SCWG) and hydrothermal liquefaction (HTL), producing syngas and bio-oil respectively. These processes are more energy-efficient than the thermal processes producing the same products, i.e., pyrolysis and thermal gasification, for biomass. The pyrolysis and gasification reactors are suitable for biomass feedstock with 10% water content, otherwise requiring drying as the pre-treatment [15, 36]. SCWG becomes more efficient than the gasification process (including the drying step) for feedstock having 30% or more moisture [37]. For instance, as an alternative treatment for black liquor to the recovery boiler treatment, gasification has the same issue of drying need despite the improvements in efficiency relative to the recovery boiler while SCWG is

more efficient than gasification as well [38–40]. In addition, HTL oil has less oxygen content than pyrolysis oil, thus requiring less hydrogen when upgrading [41].

The industrial implementation of SCWG and HTL would enable enhanced supply chains of biomass processing through the effective valorization of waste and side streams [42]. However, the industrialization of SCWG and HTL technologies is still a challenge due to operational issues. Some operational problems include plugging, corrosion, catalyst deactivation, and high production costs as the obstacles to the industrialization of these processes. In addition, other operational constraints include process safety regarding high pressure and temperature and pumpability of the feedstock. On the other hand, despite many studies investigating the product yields and/or economic performances with respect to process conditions, the obstacles are discussed briefly as additional aspects. There are only a few studies investigating the operational issues as the main scope. Therefore, further research is required to address the operational obstacles for the industrialization of SCWG and HTL processes.

The objective of this study is to investigate the operational issues and the potential solutions comprehensively, i.e., contributing to the definition and elimination of the obstacles for the industrialization of SCWG and HTL processes. After summarizing the current state-of-art in these processes, this study reviews the operational issues together with associated root causes and potential solutions for each issue. A comprehensive study on the operational issues provides a holistic overview of the biomass conversion technologies and biorefinery concepts to promote the industrialization of SCWG and HTL. In addition, this study also discusses the future aspects of further investigations on the operational issues, process integration, and biorefinery concepts. Research on constraints due to operational issues provides a framework for integrating these processes into biorefineries and for evaluating the economic and environmental performances.

2 Current state-of-art in SCWG and HTL processes

The physical properties of water play a crucial role in hydrothermal processes as water is the reaction medium [43, 44]. The state of water is pointed as sub-critical and supercritical regions from the hydrothermal conversion viewpoint: a critical point of 374 °C and 22.1 MPa. There are essential changes in the properties of water with temperature and pressure in both regions [44, 45]. The viscosity decreases with temperature. The density decreases gradually with the temperature at the sub-critical region and very sharply around the critical point while decreasing very slightly at the supercritical region. The dielectric constant also decreases with the temperature at the sub-critical region while decreasing sharply around critical temperature and remaining almost constant with the temperature at the supercritical region [44]. In addition, the stability and number of hydrogen bonds decrease with temperature as well [44]. Consequently, the solvent behavior of water becomes like a non-polar organic solvent at the supercritical region, despite individual water molecules still being polar [44]. In other words, water becomes an effective solvent for organics and gases at the supercritical region while the solubility of inorganic salts drops to parts per million scales. In contrast, the dissociation constant (or ionic product) increases with temperature at the sub-critical region from 10^{-14} at 25 °C to around 10^{-11} at close to critical temperature under a pressure of 250 bars [46]. However, the dissociation constant decreases very sharply with temperature around the critical point and slightly at the supercritical region, e.g., down to lower than 10^{-24} at 600 °C [46].

Water properties and operating conditions influence the product distribution and reaction mechanism. At HTL conditions (300–350 °C, 40–250 bars, and residence time of 15–60 min), biomass decomposition results in 30–40% bio-oil yield (dry basis by weight) as the main product while generating oxygenated organics in aqueous phase and char as the by-products. Meanwhile, in SCWG conditions (500–700 °C, 250 bars, and 1–5 min), biomass is decomposed further into gases, thus syngas being the main product. Char is a major by-product of SCWG, and the aqueous phase includes oxygenated organics in minor amounts. The biomass decomposition occurs through an ionic mechanism under HTL conditions because of the high ionic product of water. This provides an ideal condition for acid- or base-catalyzed reactions. In contrast, the SCWG conditions lead to radical mechanisms and faster decomposition due to the very low ionic product of water and higher temperature. Water acts as a reagent, solvent, and source of free radicals and hydrogen during this process [43, 47].

The hydrothermal decomposition of biomass occurs in five main steps: hydrolysis/depolymerization of polymeric substances, decomposition of monomers into intermediate compounds, gasification of those intermediates, equilibrium reactions among gases, and the reactions of char and salts. For instance, the depolymerization of lignocellulosic biomass results in phenolic compounds as lignin fragments and sugars as monomers of cellulose and hemicellulose. Hydrolysis of starch also results in glucose. In addition, glucose forms fructose through isomerization reaction [48, 49]. After the depolymerization step, the monomers generate lighter compounds such as carboxylic acids, furans, aldehydes, phenols, and alcohols through decomposition or dealkylation reactions. Then, the gases are formed through reforming reactions including steam reforming and decarboxylation. The main equilibrium reactions are methanation and water–gas-shift (WGS) reactions among the gases. The

reactions of solid substances include char gasification and repolymerization of phenolics [50, 51]. The repolymerization reactions generate mainly char at SCWG conditions whereas bio-oil is the main product of repolymerization at the temperature of HTL [52]. The overall decomposition schemes were illustrated for lignin [50] and cellulose [53], including both hydrothermal and thermal decomposition routes, and the main reactions were also illustrated in detail [54]. The product distribution is determined by the process conditions including temperature, residence time, catalyst, reactor material, biomass constituents, and biomass concentration at the reactor inlet. Meanwhile, pressure does not have a major impact on the product yields [55, 56].

Temperature is the main condition influencing the reaction kinetics, thus determining the product yields and quality. The bio-oil yield increases with temperature, at temperatures below 300 °C since the biomass decomposition is slow and/or incomplete [52]. However, high temperatures around 400 °C cause decomposition of bio-oil, and higher temperatures cause the formation of char through repolymerization instead of oil [52, 57]. Consequently, the temperature range of HTL is 300–350 °C, high temperature in the sub-critical region, as observed in HTL studies with various feedstocks [52, 57–59]. The gasification efficiency and total gas yields also increase with temperature in SCWG processes while the individual gas yields depend also on the other conditions and biomass type. For instance, temperature promotes the yields of hydrogen, methane, and carbon dioxide while carbon monoxide yield decreases with temperature, as experimented with sucrose and isoeugenol in stainless steel reactor at 500–700 °C [40]. Temperature also determines the rate-limiting step of biomass conversion. The hydrolysis rate becomes much faster than the further decomposition of monomers at supercritical water conditions while the hydrolysis step is slower and rate-limiting step at sub-critical water conditions [49, 60].

Catalyst is another important parameter influencing the product yields by promoting various decomposition steps: improving the yields and enabling lower temperatures for feasible operations. The main catalyst types include alkali metals, transition metals, activated carbon, and metal oxides as conventional catalysts used for SCWG and HTL processes [61–63]. Activated carbon is an effective catalyst for water–gas shift and methanation reactions [47]. Alkali metals promote the ionic reactions and hydrolysis step at the HTL conditions while promoting the gasification and WGS reactions at SCWG conditions [47, 64]. For instance, WGS reaction may not reach equilibrium in SCWG processes in the absence of alkali metals, thus gas products containing a significant amount of carbon monoxide, while alkali metals promote WGS reaction towards hydrogen and carbon dioxide formation at high temperature when there is excess water [40]. The alkali salts have influence on hydrogen yields as $NaOH > KOH > Ca(OH)_2 > K_2CO_3 > Na_2CO_3 > NaHCO_3$ [65]. These alkali salts are used in HTL processes as well as LiOH, CsOH, and RbOH [66]. For instance, the presence of KOH increased bio-oil yield by around 40% (by weight) while the yield was 18% without catalyst in HTL of birch sawdust [63]. The solid residue was also decreased from 33 to 12% in the presence of KOH catalyst [63]. In addition, alkali metals inhibit char and tar formation as well by inhibiting the easily-polymerizing unsaturated compounds [64]. Transition metals promote also the gasification reactions and are active at lower temperatures as well, thus enabling catalytic SCWG process at 400–500 °C [67, 68]. Transition metals can also improve hydrogen selectivity and conversion rate as well as catalyze methanation and steam reforming reactions [47]. Among the transition metals, nickel has a low cost while ruthenium has higher activity and stability [47]. In addition, the reactor wall also has a catalytic impact on biomass decomposition. For instance, the Inconel reactor promotes gasification reactions at high temperatures (600 °C or above) more than stainless steel in the case of SCWG of black liquor [40] while stainless steel is more catalytic than Inconel at 500 °C [69]. Similarly, the yields are influenced by the surface-to-volume ratio of the Inconel reactor: higher surface area with a constant volume resulting in higher yields [70]. Table 1 shows some heterogeneous catalysts used in SCWG processes together with catalyst properties and hydrogen yields.

Table 1 Heterogeneous catalysts in the SCWG process [71, 72]

Catalyst	Catalyst size (μm/nm)	BET surface area (m^2/g)	Total pore volume (mL/g)	Hydrogen yield
Ni/TiO_2	8.3 nm	32	0.1	0.7 mol H_2/mol C reacted
Ni/ZrO_2	9.6 nm	43	0.2	1 mol H_2/mol C reacted
Ru/TiO_2	8.4 nm	37	0.2	0.8 mol H_2/mol C reacted
Ru/ZrO_2	9.8 nm	51	0.3	0 mol H_2/mol C reacted
$Ni/\alpha\text{-}Al_2O_3$	118 μm	8	-	46 mol H_2/kg feed
MgO	43.1 nm	44.9	0.6	2.7 H_2/CO_2 mole ratio
Co/TiO_2	7.7 nm	32	0.1	0.6 mol H_2/mol C reacted
Co/ZrO_2	9.3 nm	42	0.2	0.7 mol H_2/mol C reacted

Residence time and biomass concentration at the reactor inlet have also a significant impact on product yields. The product yields typically increase with the residence time and decrease with the concentration, depending on the investigated range. For instance, the impact of residence time is insignificant at the 5–12-s range in SCWG of black liquor while further increase up to 120 s improves the yields [56]. However, the increases in the yields become smoother with increasing residence time at a very long residence time. In addition, long residence time at high temperatures causes char formation through repolymerization in SCWG processes [50]. Moreover, a very dilute reactor inlet (less than 10% by weight) results in a majority of the carbon in feedstock being converted to the aqueous organics in HTL processes [64].

The constituents in the feedstock play an important role in the impacts of process conditions on the reactions and product distribution. Cellulose, starch, and hemicellulose start to decompose already at 180–200 °C [64]. In contrast, proteins decompose very slowly at temperatures less than 230 °C due to peptide bonds being more stable than cellulose glycosidic bonds [64]. Moreover, lignin is the least reactive constituent of biomass, decomposing at 280–300 °C [41, 73]. At 240 °C or above, the degradation of sugars is faster than hydrolysis, i.e., generating the intermediate organics [49, 64]. In addition, lignin is stated as the main source of char formation through the repolymerization of phenolics in SCWG processes [74]. From the phenomena and kinetic modeling viewpoints, it is worth noting that the reaction mechanism and kinetics were investigated through both model compounds and real biomass. Tables 2 and 3 compile some examples of literature studies on SCWG and HTL processes of various biomass together with the concluding remarks. It is crucial to understand the interactions among the constituents when processing real biomass. However, despite the overall understanding of reaction mechanisms and the impacts of process conditions, kinetic modeling of hydrothermal biomass conversion involves difficulties due to multiple constituents interacting with each other (e.g., carbohydrates being hydrogen donor for lignin decomposition [75, 76]), extractives, and minerals affecting the product yields, very complex phenomena, and numerous intermediate compounds [43, 77]. Therefore, when assessing the techno-economic feasibility, experimental investigations are specifically needed for product yields with respect to various combinations of process conditions and each biomass type or mixtures of biomass types occurring as feedstocks. For instance, hydrothermal co-liquefaction was investigated to reduce nitrogen content in bio-oil in the case of nitrogen-containing feedstock (e.g., sewage sludge, manure, or food waste), resulting in improved yields and less nitrogen compared to a single feedstock [78, 79]. In contrast, mixing plastic and food wastes had a negative impact on energy efficiency in the SCWG process [80].

The experiments on SCWG and HTL are conducted in batch and continuous modes. The batch experiments provide simplicity for investigating the impacts of conditions on product yields: easier to conduct with less operational concerns of reactor plugging and pressurizing and pumping the feedstock [90]. For instance, some batch investigations involve an autoclave reactor with a volume of 500 mL [91], a stainless-steel vessel with a volume of 100 mL [92], a Hastelloy reactor with a volume of 200 mL [80]. However, despite being simple and suitable for qualitative analysis, the batch reactors involve techno-economic issues regarding scaling up to industrial applications [93]. Using catalysts in a batch reactor is limited due to the lack of mass transfer [94]. Moreover, the heating rate for reaching the reaction temperature strongly influences the product yields and reaction rates, especially when investigating short residence times. In addition, the process conditions do not remain constant during the operation, thus introducing difficulties in distinguishing the impacts of each condition [69]. For example, pressure increases with temperature besides the influence of heating rate. Consequently, it is not accurate to make quantitative comparisons between the yields in batch and continuous operations. Continuous operations are techno-economically more efficient for industrial applications provided that the operational issues are addressed effectively.

The optimum conditions are determined based on the compromise between the yields and costs, from the techno-economic assessment viewpoint. The reactor inlet concentration determines the equipment size and energy requirement for high pressure and high temperature while affecting the product yields as well. Dilute inlets cause higher energy demand and larger equipment despite improving the yields. Temperature also affects the energy demand while improving the process. Nevertheless, the increasing temperature usually improves the energy efficiency of the process because of enhanced yields and heat integration. The residence time and reactor material have a direct impact on the reactor cost. Increasing the residence time causes higher reactor costs while improving the yields as well. However, after some optimum values, increasing the residence time further increases the reactor costs more intensively than improving the product yields. The alkali addition can be conducted as a homogeneous catalyst dissolved in the reaction mixture; however, despite improving the bio-oil yield, homogeneous catalysts introduce separation and recovery challenges [88]. Instead, heterogeneous catalysts are suitable for bio-oil production because of easy recovery, non-corrosivity, and higher thermal stability [88]. The pressure is maintained above the vapor pressure at the reaction temperature in HTL processes. On the other hand, high pressure causes a need for tough equipment, e.g., thicker reactors

Table 2 Some SCWG studies in the literature

Ref	Research question	Feedstock	Results/findings
[43]	Performance and interaction of biomass in SCW and technical challenges	Biomass model compounds Binary or multi-component systems	Understanding the interactions within multicomponent systems
[77]	Recent development in the SCWG process	The components of biomass (carbohydrates, lignin, ash, proteins, and lipids) and real biomass	Risk analysis/catching salts and salt separation to avoid reactor plugging/integration of SCWG in a biorefinery
[81]	Degradation routs of biomass model compounds	Biomass model compounds such as cellulose and lignin	Changes reactor configurations to overcome plugging/separation of corrosive ingredients
[47]	Research on catalytic SCWG and physicochemical properties of water in sub and supercritical conditions	Glucose, glycerol, lignin, phenol, lignin and 4-propyl phenol, methanol, glycerol, glucose and wood, and cellulose	Catalysts increase hydrogen selectivity and conversion rate/more research about stable and efficient catalysts was suggested
[82]	Summarized catalytic hydrothermal gasification findings in the last two decades	Lignocellulosic biomass from different sources, sewage sludge, chicken manure, food wastes, algae, and fermentation residue	Sulfur and inorganics in biomass deactivate catalysts/moderate temperatures and long residence time increased tar/high heating rates reduce char/capillary quartz reactors are cheap and safe in high pressures
[83]	Reviewed economic costs, life cycle assessment (LCA), energy and exergy efficiencies, and thermodynamic equilibrium in SCWG	Sewage sludge, algal biomass, and black liquor	The yield of H_2 and CO_2 increased with temperature and decreased with concentration and oxygen addition/major exergy destruction is in the reactor, heat exchanger, and preheater/hydrogen production costs are lower in the SCWG
[84]	The main chemical reactions of organic compounds in supercritical water and the intermediate products in the SCWG and SCWO processes	Hydrocarbons, proteins, cellulose, lignin, phenols, alcohols, aldehydes, ketones, organic acids, and some N-, Cl-, Br-, F-, S- and P-containing organic matters	They recommended the removal of heteroatoms for organic compounds containing Cl, Br, F, S, and P to avoid pollution risks
[85]	Reviewed the role of water in converting biomass feedstock to syngas	Petrochemical waste, mixed plastics, food waste, sewage sludge, used tires, animal manure, industrial effluents, and municipal solid waste	High pressure and temperature increase corrosion/heterogeneous and homogeneous catalysts are effective, deactivation, sintering, and recovery are still challenges/biorefinery concept to reduce the costs
[86]	Reviewed the operational parameters, including reaction temperature, pressure, residence time, feed concentration, and catalysts affecting hydrogen production in the SCWG	Wastewater sludge	The high costs hinder industrialization/using a nonconventional heating source such as solar energy/clogging/plugging, corrosion, reactor design, and unsuitable material selection are considered other problems
[87]	New gasification technologies such as plasma gasification, melting gasification, fluidized bed gasification, SCWG, and microwave	Lignocellulosic biomass and residual wastes	The preferred technology for gasification is the fluidized bed because of its flexibility and large processing capacity

Table 3 Some HTL studies in the literature

Ref	Research question	Feedstock	Result
[88]	The effect of heterogeneous catalysts in hydrothermal liquefaction and bio-crude yield and quality	Lignocellulosic biomass	Homogeneous catalysts increase the bio-crude yield and quality, but the expensive recovery and corrosion are still challenging/heterogeneous catalysts are suitable for the bio-crude production process because of their easy recovery, non-corrosivity, and higher thermal stability
[78]	Summarized hydrothermal co-liquefaction of different biomass feedstock and the effect of co-liquefaction on bio-crude yield	Microalgae, macroalgae, lignocellulose, municipal sludge, food processing waste, crude glycerol, plastics waste, etc	Modeling is a useful way to investigate the co-liquefaction effect and optimize feedstock blending/hydrothermal co-liquefaction has more advantages than hydrothermal liquefaction of individual feedstock/denitrogenation is an important issue in HTL and bio-crude upgrading
[79]	Investigated the effect of biomass feedstock characteristics, hydrothermal liquefaction process parameters, and catalysts on nitrogen content in bio-crude oil	Microalgae, macroalgae, sludge, manure, and food waste	Using biomass feedstock with lower carbohydrate content reduces the nitrogen content/co-HTL of biomass with higher lipid content also results in lower nitrogen content in bio-crude/thermal hydrolysis pretreatment can decrease protein and carbohydrate
[89]	Studied the effect of the aqueous phase (AP) recirculation on the hydrothermal liquefaction process and how it affected bio-crude oil yield and properties	*S. platensis*, *C. vulgaris*, *E. prolifera*, *G. gracilis*, *C. glomerata*, *C. pyrenoidosa*, DDGS, sewage sludge, blackcurrant pomace, aspen wood, and barely straw	In HTL, AP disposal should be improved to increase the feasibility of the hydrothermal process/through aqueous phase recirculation in the HTL process, bio-crude yield can be increased considerably by organic acids and N-containing compounds in AP

and other process units as well as more energy required in feed pumps. Similarly, the pressure is maintained slightly above the critical pressure of water in SCWG processes, e.g., 25 MPa. Consequently, the promising conditions for HTL involve temperature of 300–350 °C, pressures of 4–20 MPa, reactor inlet concentration of 20–30% by weight, and residence times of 15–30 min. Meanwhile, the promising conditions for SCWG involve temperature of 600–750 °C (or 400–600 °C possible with transition metal catalysts), pressures of 23–25 MPa, reactor inlet concentration of 5–10% by weight, and residence times of 1–5 min.

The techno-economic assessments indicate SCWG and HTL processes being promising for industrial applications among the biomass conversion processes while still resulting in more expensive costs compared to fossil-based processes. For instance, SCWG is more beneficial than thermal gasification as an alternative treatment for black liquor [38]. The minimum selling price of hydrogen was calculated as low as 1.46 €/kg (price in 2018) in a preliminary feasibility study of integrating SCWG of black liquor in a pulp mill, based on the yields of lab-scale experiments [95]. Another study showed that integrating SCWG to a pulp mill can reduce the minimum selling price of air-dried pulp up to 22% [96]. In addition, the minimum selling price of hydrogen was calculated as 1.94 $/kg (price in 2019) for a stand-alone SCWG process converting soybean straw [97]. SCWG process provides a competitive minimum selling price of hydrogen compared to other renewable processes (such as water electrolysis and thermochemical water-splitting cycles) and has potential for further improvements [83]. Similarly, the HTL process provides liquid fuel production with more efficient economic performance than pyrolysis. For instance, in a detailed report conducted in 2014, the biocrude oil costs were calculated as 16 $/GJ (0.23 $/ton) for pyrolysis while the cost was 14.5 $/GJ (0.45 $/ton) for HTL in case of processing forest residue [98]. Despite higher prices per mass, HTL provides cheaper prices in terms of energy content in the bio-oil. This results from HTL oil having significantly less oxygen content than pyrolysis oil [41]. The difference in oxygen content influences the upgrading process as well: HTL oil requires less hydrogen than pyrolysis oil. Consequently, the prices of liquid fuel were reported as 26.3 $/GJ or 3.09 $/gallon gasoline-equivalent (1.1 $/ton) for the pyrolysis process and as 16.9 $/GJ or 2.00 $/gallon gasoline-equivalent (0.71 $/ton) for the pyrolysis process [98]. On the other hand, SCWG and HTL processes are not competitive yet compared to fossil-based productions. For instance, the production of hydrogen through SCWG can cost three times of hydrogen production through methane steam reforming of natural gas [99]. Similarly, the liquid fuel production through HTL was also reported to be uncompetitive compared to petroleum-based gasoline [100]. Currently, SCWG and HTL technologies are available on pilot scale to investigate the possibilities for improving the economic performances and for addressing the operational issues [68, 101–104].

The industrialization of SCWG and HTL processes requires addressing the operational issues as well as improvements in economic performance. These processes introduce operational issues due to extraordinary pressure and temperature conditions causing changes in water properties. The main operational issues include process safety matters due to extraordinary conditions, plugging, corrosion, pumpability of feedstock, and catalyst deactivation. These issues can reduce the techno-economic performances calculated in the feasibility studies for industrial capacities: reducing the product yields over time (e.g., due to catalyst deactivation), increasing the maintenance costs (e.g., corrosion and plugging), and introducing constraints to the conditions when optimizing the processes (e.g., reactor inlet concentration limited by pumpability limits).

3 Operational issues of SCWG and HTL processes

The operational issues hinder the industrialization of SCWG and HTL in a continuous mode through various effects on the processes, such as causing process safety issues, reducing the economic performance, or even ceasing the operation. Therefore, these issues can be addressed by investigating the root causes of each, the impacts on the process, and the possible solutions together. This article reviews the operational issues through a roadmap shown in Fig. 1. The main operational issues include the following:

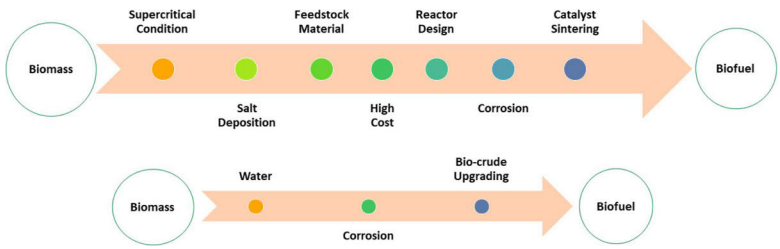

Fig. 1 Article structure and parameters studied. (Top) Supercritical water gasification operational issues. (Bottom) Hydrothermal liquefaction operational issues

- Process safety matters due to mechanical stress on the reactor
- Plugging due to solid deposition versus reactor configuration
- Corrosion due to inorganic content and water dissociation
- Pumpability of feedstock versus concentration
- Catalyst deactivation versus catalyst types
- Production costs versus biorefinery concepts
- Product quality and further upgrading/synthesis

3.1 Process safety versus operation conditions

High temperature and pressure may cause accidents during the operation due to changes in the properties of the reactor and pipeline material. The possible accidents include fracture, rupture, or burst of a pipeline or the reactor. Therefore, the mechanical properties become essential for a long-term operation at high pressure and temperature. The burst pressure is calculated based on the ultimate tensile strength of the material and the ratio of outer diameter to the wall thickness [105]. However, the burst pressure is usually calculated for a flawless material and reduces with fatigue, corrosion, and fractures on the microstructure of the material [106]. As a rule of thumb, it is suggested to operate under the pressure one-fourth of the calculated burst pressure [107]. For instance, the outer diameter-to-wall thickness ratio of stainless steel can be a maximum of around 12 for operating at 250 bars, according to the correlation derived by Oh et al. (2020) [105] and using working pressure as four times the calculated burst pressure. The ultimate strength of stainless steel was reported as 565 MPa while that of Inconel 625 is 714–1103 MPa [105, 108]. In addition, there is a need for pressure-relieving devices as a safety precaution, and the reliability of those devices becomes an issue for fluids containing also solid at high temperature and pressure [109]. Furthermore, the thermal stability of the materials is also an important parameter for long-term operations. Inconel material has good thermal stability at temperatures over 1000 °C. On the other hand, stainless steel 316L was reported to be stable up to 650 °C regarding ductility, yield strength microstructure [110], despite experimental studies of SCWG conducted in stainless steel 316L reactor at 700–750 °C [39]. Nevertheless, the thermal stability of other stainless steel types has been improved enabling the usage at temperatures up to 1150 °C through adjusting ferric and chromium contents [111].

Besides high temperature and pressure, the sudden variation of these two conditions can provoke disastrous effects as observed in the lab-scale experiments [106, 112]. The variations of temperature and pressure result from sudden mass injection into SCW conditions and partial plugging due to solid deposition in the reactor. A sudden mass injection into the reactor at supercritical conditions results in a fast expansion, which stresses the reactor metal [106]. Moreover, the fast injection of mass could also provoke a contraction of the reactor walls, which would also concern the locking system, as demonstrated in Fig. 2. At that high pressure, any variation of the metal properties might cause the reactor to release a quantity of material outside. Therefore, the reactor should certainly be shielded for hydrothermal conversion operations. In laboratory conditions, this protection is usually given to the operator by Plexiglas. Furthermore, semi-batch (i.e., stepwise injection) operations are conducted with low flow rates in the laboratory scale to avoid sudden and fast mass injections [39, 40]. Solid deposition in the reactor also causes variations in pressure and temperature due to partial plugging and control actions of the pressure valves. The solid deposition is addressed by optimizing the process conditions to minimize the char formation and applying special reactor configurations enabling the separation of solids, as determined in Sect. 3.2.

3.2 Plugging due to solid deposition versus reactor configuration

Solid-phase occurs due to the precipitation of salts in the feedstock and char formation in hydrothermal processes. The solubilities of salts decrease with temperature in hot compressed water, even to the magnitudes of ppm at SCWG temperatures [73, 113]. This causes precipitation of salts, especially in SCWG processes. The nature of the salt also affects its behavior in supercritical conditions [114]. The salts are classified as type I and type II based on melting points [115, 116]. The melting temperature of type I salts is between 800 and 1000 °C, and their solubility is slightly higher in supercritical conditions. Meanwhile, type II salts have melting points between 700 and 800 °C and are less soluble in hot compressed water [114, 115, 117, 118]. Table 4 exemplifies type I and II salts occurring in

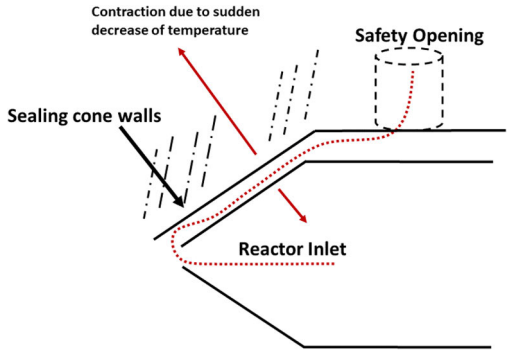

Fig. 2 Fast injection of mass effect in the reactor inlet and walls

Table 4 Type I and II salts and their characteristics

Salt component	Type	Temperature (°C)	Pressure (bar)	Ref
KOH	I	460	v.p	[123]
NaOH	I	550	v.p	[124]
K_2CO_3	I	450	v.p	[125]
LiOH	I	420	v.p	[126]
Na_2CO_3	II	540	300	[127]
Na_3PO_4	II	450	1560	[128]
Na_2SO_4	II	500	1500	[117]

"v.p." means that the phase equilibria were studied at saturated vapor pressure

supercritical water gasification of biomass [114, 116]. Type II salts cause plugging more intensively because of forming crystals instantly (also referred to as shock crystallization [119]) and sticking the hottest part of the wall while type I salts can remain as brines [118, 120, 121]. Nevertheless, the mixtures of salts behave differently from salt-water binary systems at SCW conditions; e.g., a mixture of type II salts can form type I salts [120]. For instance, the precipitated salts mainly include sodium sulfate and sodium carbonate in the case of SCWG of Kraft black liquor [112]. The other source of solid phase is char formation during biomass decomposition. Despite hydrothermal decomposition being more dominant, char is formed through pyrolysis of unhydrolyzed lignin when processing lignocellulosic feedstocks [53, 122]. Depolymerization of lignin in SCW occurs only in a few seconds but results in high char yield, i.e., char formation already at the entrance of the reactor [60]. In addition, char is formed also throughout the rector due to the repolymerization of phenolics and aromatic intermediates at high temperatures and long residence time [39, 50, 53, 122].

The solid deposition is an obstacle for SCWG processes due to introducing the risks of plugging at the reactor inlet and rupture of reactor wall [106, 112]. In a continuous operation with an isothermal reactor, the feedstock reaches SCWG conditions immediately at the reactor inlet, thus precipitating salts and char at the reactor inlet. This causes partial plugging and variations in pressure, thus introducing the safety issues mentioned in Sect. 3.1 and ultimately causing the interruption of the operation. For instance, as experimented by De Blasio et al. (2019) [112] in a plug-flow reactor, SCWG of Kraft black liquor was interrupted at 600 °C due to solid deposition and plugging while SCWG of sucrose was successfully conducted at 500–700 °C. This observation determined the impact of biomass constituents as well. In the absence of lignin and salts, the solid phase involves only char in less amount, i.e., only aromatic ring compound as the heaviest compounds and possible to decompose [112]. On the other hand, a feedstock with lignin, salts, and ash results in precipitation of salts and ash, the species impossible to decompose, as well as more intensive formation of char [112]. Moreover, even in a successful operation, solid deposition on the reactor wall increases the corrosion risk (as investigated in Sect. 3.3) and decreases the heat transfer capability [43, 117, 129, 130].

Some investigated solutions to solid deposition include stepwise injection into the reactor and separation of salts prior to the reactor. The stepwise injection (semi-batch) results in the gradual transition of the injected mass to the reaction temperature. Temperature decreases at the entrance of the reactor after each injection then adjusted via controllers until the next injections. This transition provides gradual precipitation of salts and char throughout the reactor, rather than fast precipitation at the entrance [39]. In addition, char is partly consumed in gasification reactions until the next injection. As an additional parameter, the heating rate also influences the process in semi-batch or batch processes. A high heating rate reduces char and tar formation while causing faster precipitation of solids and more variation, i.e., less time at low temperatures and reaching the SCWG temperature faster. Meanwhile, a low heating rate reduces the temperature gradient and results in gradual precipitation while reducing the efficiencies and yields due to low temperatures at the bigger part of the reactor. In the stepwise injection method, the residence time can be adjusted by changing the pumping interval of injections. However, this method can result in lower yields and efficiencies than an isothermal reactor due to fluctuations of temperature at the beginning of the reactor. Although the stepwise injection enables experimental studies in lab scale with tubular reactors, the solid deposition would be inevitable regarding long-term operations in industrial applications. Therefore, separation of solids can prevent the plugging issue as well as recover the valuable inorganics. Another solution is to separate the salts prior to the reactor, at slightly above the critical temperature and with a very short residence time of around a second, e.g., PSI process [131]. This provides the recovery of valuable inorganics and separation of substances introducing an issue for the catalysts in downstream processes [121]. The alkali nitrates are destructive for the carbon-supported catalysts, and sulfur content can cause catalyst poisoning or dealloying of reactor walls [121, 132]. In addition, nutrients can be used as fertilizers, such as potassium, phosphorous, and nitrogen. However, alkali metals catalyze the gasification reactions, i.e., undesirable to separate in advance, and char formation also causes solid deposition (more intensively for lignocellulosic feedstock).

Other measures against solid deposition include optimizing the process conditions to minimize char formation and using hydrothermal brine. The hydrothermal brine (usually a potassium salt) can catch the other salts and precipitate to the bottom of the reactor [133]. To address plugging while

capturing the salts, Wang et al. [134] patented a counter-current tank-type supercritical water reactor with a sacrificial lining containing a cylinder body and a catalyst tank. Meanwhile, process conditions play an important role in minimizing char formation. For instance, as determined for SCWG of black liquor, char formation increases with residence time (in 2–5-min range) in stainless steel reactor at high temperature (e.g., 750 °C) [39]. In contrast, the Inconel reactor suppresses the repolymerization reactions and resulted in less char formation in longer residence time at the same temperature [39]. However, residence time did not affect the char formation in the Inconel reactor at lower temperatures (e.g., 600 °C) [39]. As a result, minimum char formation was obtained at high temperature (750 °C) and long residence time (5 min) in Inconel reactor, the conditions also maximizing the thermal efficiency. Alternatively, stainless steel reactor provides minimum char formation at high temperatures with a short residence time.

The solid deposition and plugging issues can be addressed by special reactor configurations enabling solid separation. Some configurations were investigated originally for SCWO processes. A suggested configuration involves a vertical autoclave reactor of which the bottom is maintained at sub-critical conditions, thus dissolving the salts instead of precipitation [135, 136]. However, this configuration was reported to have scale-up issues [135]. Another design involves a horizontal autoclave reactor with a stirrer at the center [137]. The stirrer provides turbulent flow moving the salts with the fluid phase, instead of precipitation. This design was reported to succeed for feedstock with less than 6% organic content and less than 4% salt content in the case of SCWO, i.e., burning the content [137]. On the other hand, this design might not be applicable for solid deposition to a higher extent through salts and char formation simultaneously, as in SCWG processes. Another approach to the plugging issue is to manipulate the reactor wall only, but not the reaction zone, to prevent the precipitation of solids on the wall. For instance, a design involves a reaction chamber operating at 800 °C while the wall is maintained at 400 °C to prevent corrosion over the reinforced stainless-steel shell as designed and modeled by Cocero and Martinez (2004) [138]. As another way to manipulate the reactor wall, a design succeeded in lab scale consists of a transpiring-wall reactor (TRW) to address the plugging and corrosion problems [139, 140]. This reactor configuration avoids the contact of solids to the reactor wall by forming water film on the surface via porous, non-load-bearing cylindrical transpiring-wall elements. However, manipulating the reactor wall can cause heat transfer issues and reduction in gas yields due to temperature gradient in the reactor, despite being conducted for the exothermic SCWO process. Further designs were developed also specifically for the SCWG process. A proposed design configured a vertical tubular reactor, the reactor inlet entering from the top, and the product outlet from the bottom as shown in Fig. 3; however, this configuration caused plugging in the feed line of the condenser [141]. To address this problem, another design tilted the gasification reactor to 75° from a vertical position as shown in Fig. 4, positioning the inlet of the reactor at the bottom and the outlet of the reactor at the top (down-up configuration) as well as involving insulation and a cooling zone [142]. According to their results, the down-up configuration resulted in higher gas yield, carbon gasification efficiency, and higher hydrogen yield than the up-down configuration. Another way to prevent plugging is to use a fluidized bed reactor, providing easier continuous solid handling [90]. It can attain the same residence time values as those achieved in the traditional SCWG of biomass while improving mixing characteristics. For instance, Matsumura and Minowa (2004) [90] considered two operational modes for large and small particle size,

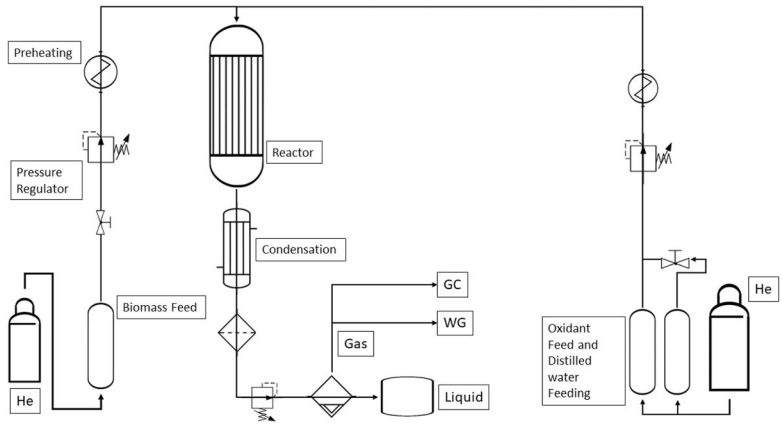

Fig. 3 Simplified Veriansyah reactor design [141]

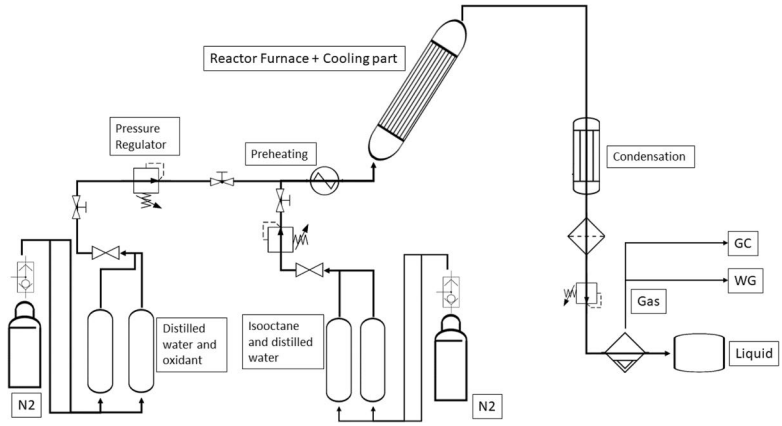

Fig. 4 Susanti et al. reactor simplified configuration [142]

bubbling/particulate bed operation for larger particle size and circulating fluidized bed for smaller particle size. Based on their results, a low-velocity bubbling fluidized bed is the optimal flow regime. Jin et al. (2010) also used a fluidized bed reactor for SCWG of coal as shown in Fig. 5 to prevent plugging issues occurring in tubular reactors. According to their results, the fluidized bed reactor enhanced mass and heat transfer in the reactor and consequently improved gasification efficiency without blockage problems. Another approach is a reactor configuration simultaneously enabling solid separation as another outlet. For example, the Verena pilot plant has a vertical pressure vessel reactor with a feedline from the top, a riser tube having an outlet at the top, and another outlet at the bottom of the reactor [101, 143]. The feedstock enters the reactor from the top and moves downwards. Then, the formed gases move upwards through the riser tube while solids precipitate towards the outlet at the bottom because of higher density.

The HTL process has less risk of plugging than SCWG because of higher solubilities of salts and less char formation under HTL conditions. Plugging was reported as a minor issue and can be controlled via a pressure letdown valve [145]. Therefore, reactor configuration is not a major concern in HTL processes. For instance, Guo et al. (2019) [146] conducted HTL of two strains of microalgae in a continuously stirred tank reactor at 24 MPa and 35 °C with a residence time of 15 min. Figure 6 shows the flow diagram. Nevertheless, the char formation can be reduced further by using co-solvent in HTL processes. The co-solvents increase bio-oil yields by improving the dissolution and hydrolysis of macromolecules and preventing repolymerization to char [147–150]. Some common co-solvents include glycerol, ethanol, methanol, and acetone. The influence of glycerol increases with the presence of alkali metals, resulting in more increase in bio-oil yield compared to the absence of alkali metals [148]. As illustrated by processing lignin and

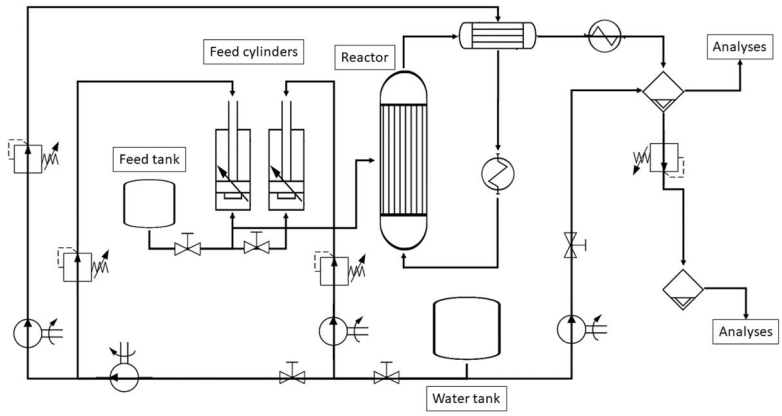

Fig. 5 The schematic diagram of the Jin et al. system [144]

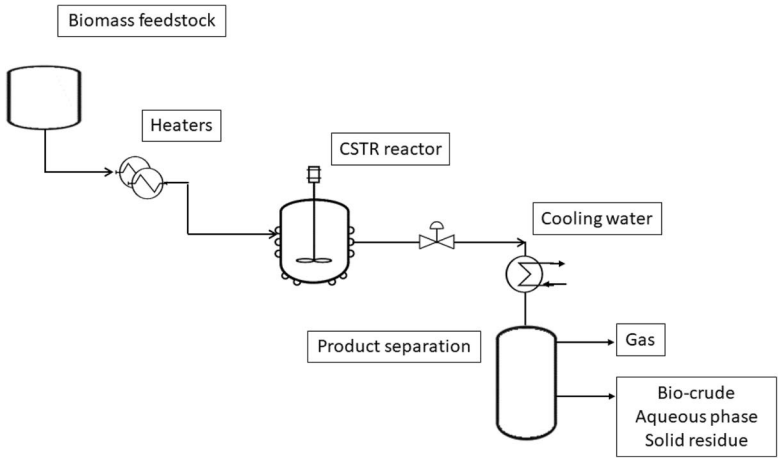

Fig. 6 Guo et al. flow diagram [146]

lignin/cellulose mixture, ethanol/water mixture increased the bio-oil yields by enhancing the hydrolysis and preventing repolymerization of lignin fragments [150]. In fact, ethanol was stated as a suitable co-solvent for any feedstock in HTL processes [150].

3.3 Corrosion types and the proposed solutions

The hydrothermal processes result in corrosion due to exposure of reactor walls and pipelines to hot compressed water, char, and alkali salts [94, 151]. The corrosion types can be classified as electrochemical and chemical corrosions. Electrochemical corrosion is a major concern in the HTL process due to the high density and polarity of water, i.e., ionic reaction mechanisms with a high concentration of hydroxide and hydronium ions as well as ions of salts [64]. In addition, the HTL process generates oxygenated compounds such as organic acids, contributing to electrochemical corrosion [145]. Chemical corrosion can occur through various phenomena including general corrosion, under-deposit corrosion, dealloying, intergranular corrosion, pitting, hydriding, and stress corrosion cracking [145, 152]. General corrosion refers to the relatively uniform degradation of metal surface material at a predictable rate. The under-deposit corrosion occurs when solids precipitate on a metal surface, thus being a major issue in SCWG. This can cause a microenvironment between the metal surface and the bulk fluid, resulting in more corrosive conditions in the microenvironment. Dealloying refers to an alloy component selectively being oxidized and dissolved under operating conditions. Dealloying can occur due to alkaline conditions or the presence of sulfide. The intergranular corrosion occurs at the metal grain boundaries in the presence of chloride, sulfate, and/or nitrate. The pitting is a localized and extensive version of corrosion occurring in the presence of chloride and sulfate under sub-critical water conditions or in the presence of chloride under SCW conditions, thus being a concern both for HTL and SCWG [151]. This corrosion might occur in stainless steel and nickel-based alloys; nickel-based alloys were stated to be more resistant to pitting than stainless steel [151]. In contrast, pitting does not occur in titanium reactors due to chloride or sulfate; however, titanium reactors have less mechanical strength [64]. Moreover, hydriding is a corrosion type associated with titanium in the presence of phosphate salts, which can result in hydrogen embrittlement: phosphate reacting with titanium dioxide layer, bare titanium reacting with water to reform the oxide, hydrogen penetrating into the titanium, and forming hydride [151]. The stress corrosion cracking occurs in the presence of mechanical stress on the material together with corrosive species. The mechanical stress can result from thermal expansion, weight loads, and bend points in piping as well as internal pressure.

Prior to industrial applications, it is crucial to investigate corrosion in SCWG and HTL processes with respect to biomass constituents, process conditions, and reactor materials. For instance, Hirose et al. [153] investigated stress corrosion cracking susceptibility and corrosion behavior of ferritic/martensitic steel F82H at 287–543 °C and 23.5 MPa supercritical pressurized water (SCPW) in Inconel625 sleeve. According to their results, F82H was the barrier between the iron-rich layer and the chromium-rich layer. Moreover, weight gain increased with temperature. Nevertheless, no signs of cracking or exfoliation were observed on the surface, and the weight gain resulted from iron-rich oxide. Similarly, Fe–Cr–Si-rich oxide(s) was observed also on various alloys in the HTL process, including 410 ferritic stainless steel, conventional-type 300 series austenitic stainless steels of varying Ni, Cr, and Mo content (301, 304L, 316L,

317L, and 347), low-Ni, high-Mn austenitic such as grades 201, and related alloys, higher-Ni austenitic (310, 800, 904L, and related high Ni, Mo, Cr grades), and the Ni-base alloys 600 and 825 [154]. Moreover, small quantities of Na, K, Cl, and Ca were also detected on those materials in the same investigation. S, Na, and Cl species caused corrosion and cracking while higher alloy Ni, Cr, and Mo contents are more resistant against corrosion. However, in the case of the existence of sulfur in the reactor, costly high-Ni alloys may not be the solution due to the risk of sulfidation attack. Therefore, Brady et al. (2014) [154] suggested reducing the nickel content and increasing the proportion of chromium and manganese in the austenitic steel, such as grade 201. Exposing nickel alloy 625 to SCW, another study also observed mass gain of 0.15 mg/cm^2 after 1000-h operation due to oxide particles at 600 °C while not observing significant mass change at 400 and 500 °C [155]. The surface morphologies also showed the size of the oxide particles on the outside surface increased with increasing test duration. Moreover, pits were also observed on the surface at 400 and 600 °C with a size of 4.3 µm and 8 µm, respectively. It can grow to 12.9 µm at 400 °C depending on the test duration, but no significant changes were observed at 600 °C.

The corrosion issue can be addressed through different approaches: optimizing the process conditions together with reactor material selection for minimum char formation, reactor configurations preventing solid species from contacting the surface, adjusting the feedstock, and adjusting the effluent [151]. Regarding the process conditions, the char formation can be reduced by optimizing the temperature, residence time, and reactor material together as well as involving catalysts, as determined in Sect. 3.2. Regarding the reactor materials, the materials stated as corrosion-resistant include stainless steels, nickel alloys, titanium, tantalum, noble metals, and ceramics [156]. Among those materials, nickel alloys (e.g., Inconel and Hastelloy), titanium, and stainless steel were the most used reactor materials because of catalytic impacts and economic aspects. The corrosion resistance of these materials depends on temperature and the species present in the reaction mixture. Nickel alloys were reported to be more corrosion-resistant and to have high strength for SCWG processes at high temperatures as well as being more catalytic while stainless steel can be more suitable to HTL processes because of higher corrosion resistance and lower cost [151, 156]. Ni alloys such as Inconel 625, Hastelloy C-276, and titanium are the most used materials to reduce corrosion [64]. Calzavara et al. (2004) [137] designed a new reactor in which there is double-shell titanium in the reactor to prevent corrosion. This new concept was suitable to prevent corrosion, observing no corrosion trace after a long-running time on the double shell. As another approach, some reactor configurations were designed to prevent corrosive species from contacting the surface. An applicable method involves the "vortex/circulating flow reactor" in which fluid motion is applied to compel the hottest environment away from the shell [151]. Other methods include transpiring wall reactor and cool wall reactor, also used to address the plugging issue as mentioned in Sect. 3.2. However, these methods have issues regarding industrial-scale applications. The other approach is to adjust the feedstock by mixing the corrosive feedstock with another non-corrosive feedstock and pre-neutralization. The pre-neutralization involves neutralizing the acidic or alkaline feedstock to address the electrochemical corrosion, relevant for HTL processes. The mixing method would at least reduce the concentrations of corrosive species, especially sulfur and chloride contents.

3.4 Pumpability of the feedstock versus concentration

One of the main challenges regarding biomass feedstock management is pumping the highly concentrated and two-phase biomass feedstock in supercritical and subcritical conditions. In addition, the feedstock concentration varies during the operation as well as occasionally containing solid particles [129, 157, 158]. The dry matter content in the biomass feedstock should be within the pumpability limits of high-pressure pumps to avoid clogging problems while optimizing the product yields versus the energy required to heat the feedstock. Otherwise, the feed may not be a steady flow into the reactor [159]. Moreover, in the case of rector clogging during SCWG of high concentrated feedstock, there will be a high amount of biomass in the reactor continuing to gasify even after turning the heaters off or stopping the inlet flows.

The pumpability limit is directly affected by the nature of biomass feedstock and the target pressure [73, 160]. In addition, the particle size of solids may cause dewatering within the pump in the case of coarse particles. However, size reduction would be costly and energy-intensive for the feedstock of hydrothermal processes. Therefore, it is advised to test the considered pumps in the specific conditions of a process in scope (the specific feedstock to be processed with biomass type and particle size to be processed, and the target pressure) [160]. Nevertheless, the particle size does not have a significant impact on the process chemistry; therefore, it is sufficient to confirm the pumpability of the feedstock with its particle size [160]. In addition, a concentrated feedstock can also be mixed with a dilute waste to control the reactor inlet concentration, as applied in a SCWO pilot plant [157]. Furthermore, the aqueous phase after product separation can be recycled to the reactor in SCWG and HTL processes.

An assessment of commercial high-pressure pumps indicated that the pumpability limit for solid content decreases with the target pressure: 45% for 130 bars and 10–18% for 206–320 bars for lignocellulosic biomass [160]. All the

assessed pumps were stated to have the ability to pump the finely ground woody feedstock up to 15% solid content; however, the industrial feedstocks have a higher particle size (2–4 mm or higher) and might require special design [160]. Nevertheless, the pumpability limit was reported as 22% for sewage sludge with a pump operating at 220–300 bars [160].

Currently, the process conditions are assessed within the pumpability limits. The optimum dry content usually has the range of 10–20% by weight for high hydrogen yields in SCWG processes, depending on the biomass type [161]. Meanwhile, HTL processes have feedstocks with higher solid contents at the optimum conditions, e.g., up to 35% [162, 163].

3.5 Catalyst deactivation versus the catalyst type

Catalyst deactivation is another issue regarding the process operation and economic performance. This issue causes a reduction in product yields and quality. Even though the feasibility studies are usually based on experimentally observed yields, catalyst deactivation reduces the product yields and quality significantly in long-term operations. Therefore, this issue is to be addressed for stable operation and optimum economic performance. Among the metals used for SCWG and HTL processes, nickel catalysts were stated to deactivate despite the high activity and cheap price [102]. As another alternative, ruthenium catalysts were stated to be more stable and to have higher activity; on the other hand, this catalyst is more expensive [102].

Catalyst deactivation can result from various phenomena including poisoning and thermal/chemical degradation as chemical deactivation as well as sintering and fouling as mechanical deactivation [164]. The poisoning occurs due to adsorption or chemisorption of intermediate organics to the catalyst surface in hydrothermal processes, thus blocking the active sites [165]. Chemical degradation refers to undesired reactions between the catalyst and the fluid or support, producing an inactive phase. Similarly, thermal degradation causes loss of surface area due to active phase-support reactions. As a mechanical deactivation, fouling refers to the deposition of unreactive species on the catalyst surface or in the pores. This becomes an issue due to the presence of char (in both HTL and SCWG processes) and salt precipitation (in SCWG processes). In addition, heterogeneous catalysts can be deactivated through sintering, i.e., the agglomeration of the catalyst particles causing a reduction in the surface area. Sintering might occur more likely at temperatures higher than 500 °C [164] while poisoning via intermediate organics becomes an issue at lower temperatures (e.g., in HTL processes or SCWG at 400 °C [165, 166]).

The approaches to address catalyst deactivation include new methods for catalyst synthesis, enhanced dispersion of the catalyst active site on the support, the addition of a transition metal in trace amounts, and bimetallic catalysts. As a new method for catalyst preparation, the synthesis of catalysts in the SCW decreases the sintering problem in Ni-based catalysts compared to the conventional sol–gel method [61]. For instance, Li et al. (2020) [61] compared the stability of various catalysts prepared in SCW and via the sol–gel method in SCWG of glycerol. The investigated catalysts included Ni-based catalysts with supports of Al_2O_3 and Mg-promoted Al_2O_3, zirconium oxides as ZrO_2, and Ce-promoted ZrO_2, carbon-based materials as activated carbon, and carbon nanotube. The catalysts prepared in SCW had higher stability during the SCWG operation and during the regeneration stage. Similarly, in situ catalyst preparation in a SCWG process overcame the sintering issue as well as provided excellent stability of crystalline structure and morphology and the good anti-coking ability [62]. Bimetallic catalysts were also investigated to address the deactivation issue by enhancing the stability of catalysts and reducing char formation. For instance, Ni/TiO_2, Ni/ZrO_2, and Ni/Ta_2O_5 catalysts were stated as "hydrothermally stable" or "hydrothermally stabilized" beds while Ni–Zr and Ni–Ta showed better persistence, activity, and anti-coking ability with increasing residence time [167]. In addition, nickel–cobalt catalyst with magnesium–aluminum support reduced fouling by decreasing char formation in SCWG as well as having a longer lifespan [168]. As a similar approach, adding a trace amount of transition metal improves the catalyst activity and stability, e.g., as experimented at 21 MPa and 350 °C by adding 1–5% ruthenium to a stabilized nickel catalyst [67]. Another approach is to optimize the dispersion of the catalyst on the support. In a comparative study on ruthenium catalysts on various supports, it was shown that the dispersion of catalyst improves the activity and stability: Ru/C with enhanced dispersion was very active without significant activity loss after a 50-h operation at 30 MPa and 450 °C [169].

3.6 Product quality and further synthesis/upgrading

From the industrial application viewpoint, it is also important to evaluate the product quality and to consider further upgrading. The carbon-neutrality would be enabled by producing biofuels with identical or close properties to those of fossil-based fuels. The main properties of HTL oil include heating value and H/C and O/C atomic ratios from the energy and chemistry viewpoint. As the desired composition, high H/C implies low aromatic content, and low O/C implies low oxidation extent [41]. Furthermore, low sulfur and nitrogen contents are desired from the environmental viewpoint. In addition, other relevant properties include acidity and viscosity from the compatibility viewpoint. The syngas properties are evaluated based on the usage because

of various options of usage. In the case of synthetic natural gas production, the methane content of syngas is the main product parameter while the hydrogen content becomes the main property in the case of pure hydrogen production [143].

The syngas produced in SCWG processes can require downstream processing depending on the usage. The production of synthetic natural gas requires a methanation reactor due to relatively high hydrogen concentration and low methane concentration in the syngas [143]. Similarly, hydrogen production requires the reforming of hydrocarbons in the syngas. Both downstream processes utilize heterogeneous catalysts sensitive against impurities (e.g., tar and sulfur in the syngas). The removal of those impurities is also necessary prior to the gas upgrading. Nevertheless, downstream upgrading might be avoided through a two-stage separation after the SCWG reactor or also including scrubber, depending on the final usage: separating as CO_2-rich gas and H_2-rich gas (hydrogen and other combustibles) [95, 101]. The CO_2-free combustible gas can be used to produce CHP. In addition, CHP and hydrogen can be obtained simultaneously by separating hydrogen (via pressure swing adsorption or chemical looping [170, 171]) and burning the off-gas.

The HTL process provides higher product quality than pyrolysis and slightly less quality than conventional crude oil, in terms of the desired energy and environmental aspects. The oxygen content of HTL oil usually varies around 10–20% while that of pyrolysis oil is 35–40% [172]. Meanwhile, crude oil has an oxygen content of 3–5% or even closer to none. Furthermore, the HTL process provides bio-oil closer to the conventional crude oil in terms of atomic ratios as shown in Fig. 7. As the main differences between HTL and pyrolysis processes, the biomass decomposition in HTL conditions results in heavier compounds, and the light oxygenated organics are separated in the aqueous phase while those compounds remain in the pyrolysis oil. The separation of light oxygenated compounds, e.g., carboxylic acids, results in more stable bio-oil than pyrolysis in terms of acidity and viscosity. On the other hand, it is required to upgrade the HTL oil for reaching the transportation fuel standards, e.g., gasoline and diesel, and for the removal of sulfur and nitrogen. The gasoline and diesel are also shown in Fig. 7 illustrating the atomic ratios, having very little oxygen and more hydrogen.

Upgrading HTL oil can be conducted through several process options including the addition of polar solvents, emulsification, hydro-cracking/catalytic cracking, hydrotreating/hydrodeoxygenation, supercritical fluids (SCFs), and zeolite cracking [178]. Comparing these technologies, it was concluded that the hydrotreating process provides more favorable upgrading [178]. Polar solvent addition and emulsification are short-term physical treatments while reaching the desired atomic ratios require chemical treatment as well. Moreover, esterification has no significant impact on

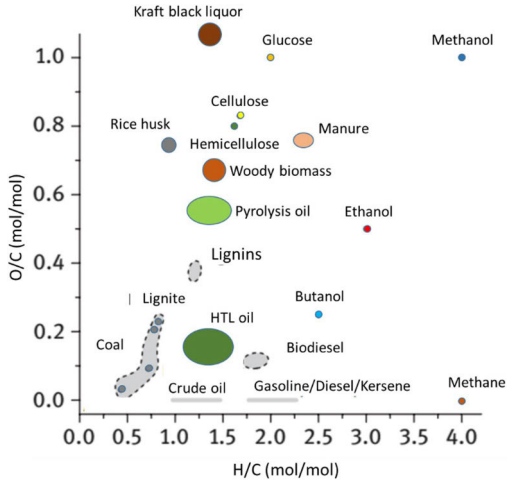

Fig. 7 The atomic ratios of various biomass feedstocks, bio-oils, and petroleum products [173–177]

denitrogenation. Nevertheless, catalytic cracking is another upgrading process with promising improvements in quality [179]. A review on the catalysts stated Ce/HZSM-5, Co/Mo/Al_2O_3, and Ni/SiO_2–Al_2O_3 to have the highest activities for denitrogenation, deoxygenation, and desulfurization, respectively [180]. However, applying a highly active and stable catalyst for this process with a long lifetime is still a challenge. Moreover, HTL oils from various feedstocks can have different upgrading challenges [181–183]. For instance, Castello et al. (2019) [181] investigated upgrading of three HTL oils originated from miscanthus, microalga Spirulina, and primary sewage sludge with NiMo/Al_2O_3 catalyst. Complete deoxygenation was achieved in the HTL oil from sewage sludge and microalgae as well as reaching remarkable deoxygenation in the HTL oil of the lignocellulosic feedstock [181]. The sewage sludge biocrude content was dominated by straight-chain hydrocarbons in the diesel range while the microalgae biocrude had also branched kinds of paraffin as jet-fuel hydrocarbons [181]. On the other hand, the bio-crude from miscanthus resulted in more aromatics in the gasoline range. Moreover, nitrogen removal still introduces a challenge despite the remarkable removal of heteroatoms [181].

3.7 Techno-economic feasibility versus process conditions and configurations

The major costs in SCWG and HTL processes are resulted from the energy demand to reach reaction temperature, the reactor cost, and the heat exchanger costs [95, 97, 98, 100].

Similarly, major exergy destruction occurs in the reactor and heat exchangers [83]. Therefore, the economic performances of SCWG and HTL processes can be improved through the optimization of process conditions associated with these costs versus revenues from the products. The process conditions introducing major impact include the biomass concentration at the reactor inlet, residence time in the reactor, the reactor material, and reaction temperature. The economic performances of SCWG and HTL are influenced by the whole set of process conditions due to inter-dependent impacts of the conditions on the equipment costs, operation costs, and product yields. Therefore, from the techno-economic viewpoint, Özdenkci et al. (2020) [39] proposed to report the product yields based on kilogram of non-inert inlet to the reactor (water being non-inert as well while ash being the only inert), rather than kilogram of dry or dry-ash-free, together with the main influencing conditions. The non-inert basis provides more accurate information on the yields regarding the reactor inlet concentration influencing the energy demand and equipment size. The residence time and reactor material directly influence the reactor cost. Temperature is also important to note in terms of the applicability of heat integration. In other words, the proposed reporting provides more accurate comparisons for preliminary selections of the promising sets of conditions. Table 5 shows some SCWG results reported as proposed. It can be observed that improving the yields on the kilogram of dry basis can differ from improving that on the kilogram of non-inert basis. Improving the economic performance requires high concentrations at the reactor inlet, high temperature, moderate residence time, and reactor material selection depending on the yields and the material costs. Thermal efficiency can be optimized through heat integration and energy recovery [83, 86]. In addition, the operation costs due to energy needs can also be reduced through non-conventional heat sources such as solar energy [86]. Moreover, the product yields are required to be verified also in a pilot scale to investigate the impact of the surface-area-to-volume ratio of the reactor. The industrial vessel reactors would provide a much less surface area-to-volume ratio compared to the lab-scale tubular reactors.

The techno-economic performances of SCWG and HTL processes are limited by operational issues determining the applicable ranges of process conditions. As a major constraint on the economic performance, the reactor inlet concentration is restricted by the pumpability limits as described in Sect. 3.4. The pumpability limits decrease with pressure, thus introducing a major constraint for SCWG. Consequently, the concentrations of more than 20% are currently disabled by the pumpability limits in SCWG processes. In addition, the maximum limit can be slightly less depending on the feedstock, e.g., lignocellulosic biomass. Nevertheless, the HTL conditions have higher pumpability limits depending on the pressure. As a process safety restriction, the material constraints at high temperature and pressure affect the equipment and pipeline costs through thickness of process units and suitable material selection. For instance, temperatures higher

Table 5 The results from SCWG of Kraft black liquor (RT: residence time)

Reactor feed	P (MPa)	T (°C)	Reactor material	RT (s)	Hydrogen yield (mol H_2/kg non-inert) Energy yield (kj/kg non-inert)	Hydrogen yield (mol/kg organics) Energy yield (kj/kg organics)	Reference
KBL 4.25 wt%	25	750	Inconel 625	300	0.646 458	24.92 17,644	[39]
KBL 4.25 wt%	25	750	Inconel 625	133	0.440 315	16.93 12,162	[39]
KBL 4.25 wt%	25	750	Stainless steel	133	0.370 310	14.27 11,963	[39]
KBL 12.3 wt%	25	700	Inconel 625	77	1.238 912	14.43 10,627	[40]
KBL 12.3 wt%	25	700	Stainless steel	77	1.232 793	14.36 9240	[40]
KBL 12.3 wt%	25	600	Inconel 625	91	1.478 750	17.22 8736	[40]
KBL 0.81 wt%	23.3	700	Inconel 625	25	0.162 75	33.62 15,521	[184]
KBL 1.62 wt%	23.4	700	Inconel 625	25	0.195 81	20.10 16,786	[184]

than 650 °C requires Inconel or modified stainless steel reactors for ensuring thermal stability. Moreover, the diameter-to-thickness ratio of process units and pipelines is to be determined based on the operating pressure and tensile strength of the materials. As another major constraint resulting from reactor thickness, it is unfeasible to conduct indirect heating to the reactor. Consequently, the reactor inlet should be heated to the reaction temperature prior to the reactor. This introduces another heat exchanger operating with a high-pressure stream. Moreover, heating the feed stream to SCWG temperatures causes solid precipitation in the heat exchanger and pipelines. This results in process configurations in which the biomass feed and recycling SCW are introduced to the reactor as separate inlet flows as shown in Fig. 8. The reactor outlet shown in Fig. 8 is configured in the same way as the Verena pilot plant to enable solid separation [101, 143]. The biomass feedstock and recycling SCW are mixed at the beginning of the reactor. However, the SCW inlet is to be heated to higher temperature than the reaction temperature to ensure the reaction mixture temperature at the desired value, e.g., through heat exchange with the flue gas (shown as "FLUEGASH" in Fig. 8).

The selection of conversion technology depends extensively on the biomass feedstock and the desired products. SCWG and HTL have different advantages and disadvantages while both processes are suitable for high-moisture biomass without consuming energy for drying. Figure 9 summarizes the pros and cons of these processes. The SCWG product is in the gas phase that can be directly used as a biofuel or to produce other biochemicals. HTL is conducted at lower temperatures than SCWG, so there is no requirement for special reactor and piping materials mentioned in the supercritical conditions. On the other hand, corrosion in HTL is more severe than SCWG. HTL process results in the production of solid, aqueous, and gaseous by-products. The aqueous phase and solid by-product contain most of the nutrients of biomass feedstock [185]. Moreover, a significant portion of the carbon in feedstock remains in the aqueous phase in HTL processes, i.e., remarkable loss in

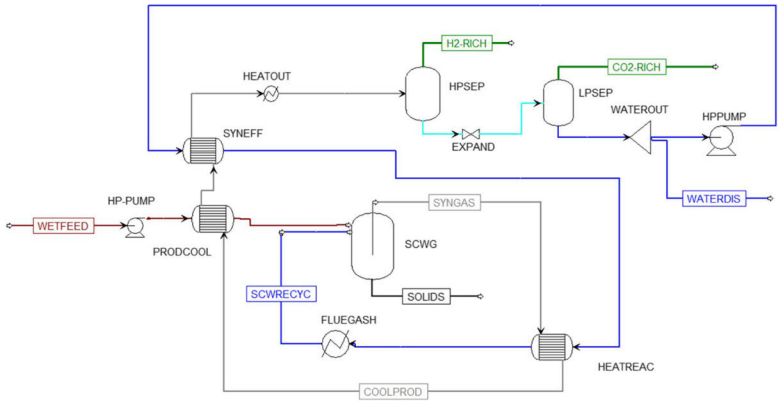

Fig. 8 The process configuration of SCWG with the reactor having two inlets and a riser tube for the gas outlet: brown streams representing the biomass feedstock, blue streams representing the aqueous phase, gray streams representing syngas, and green streams representing gas products after separation

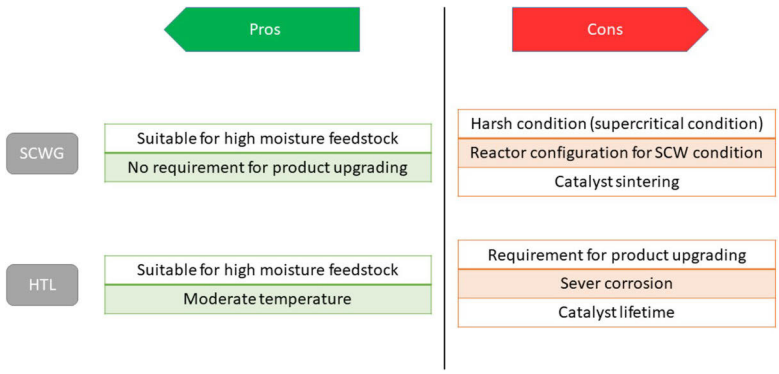

Fig. 9 SCWG and HTL pros and cons

energy content of the feedstock and environmental issue in discharging this phase [186]. Therefore, processing the solid and aqueous phases is important in this process in order to improve the energy efficiency of HTL [187].

SCWG and HTL processes can be integrated with various ways to achieve flexibility regarding product demand and to improve efficiency. The SCWG and HTL reactors can operate in parallel to produce syngas and bio-oil simultaneously. The proportion of inlets to SCWG and HTL can be adjusted in accordance with the demand on bio-oil and syngas, hydrogen, or CHP. Alternatively, the aqueous phase of HTL can be processed in SCWG to recover more energy. In the case of integrated HTL and upgrading, SCWG of the aqueous phase provides hydrogen needed in bio-oil upgrading [188].

Biomass feedstock can introduce a major cost in SCWG and HTL processes, besides other operational costs [86]. For instance, the feedstock cost was around half or more of the operational costs in SCWG of soybean straw and HTL of wood [97, 100]. Similarly, SCWG of black liquor can result in feedstock cost close to half of the operational costs, despite being integrated into a pulp mill [95]. On the other hand, the low-value wastes or residues have also low bulk density, thus increasing the transportation costs to the plants and greenhouse gas emissions [189]. The feedstock transportation was investigated as sub-problem optimization of biomass supply chains [190, 191]. The two-echelon delivery scheme was stated as functional for biomass transportation and the reduction of greenhouse gas emissions: transportation of feedstocks from farmlands to collection stations and from collection stations to the processing plants. Furthermore, the whole supply chain involves transportation of feedstocks to the conversion plants, biomass conversion at these plants, and transportation of products to the demand sites. Sustainable biorefinery concepts require the optimization of the whole chain, e.g., the balance between the transportation costs and chemical conversion costs. The supply chain network design refers to optimizing the locations and capacities of production plants with respect to sustainability measures (e.g., economic and/or environmental indicators), on the constraints of the locations and amounts of feedstocks and amounts of desired products [192–194].

4 Future aspects of SCWG and HTL operations

The future target of biorefineries is stated to achieve sustainable production of fuels, energy, and chemicals from biomass sources. The sustainability of biorefineries is determined with several features including fossil-independent productions and supply chains, minimum environmental impacts and carbon neutrality, no compromise with food and animal feed sectors, and the ability to adapt to the variations in biomass availability and market demand. In fact, the biomass conversion processes play a crucial role to meet these features. To enable sustainable replacement of fossils, the conversion processes are desired to involve multi-feed-multi-product operations and to process a wide spectrum of feedstocks as well as the techno-economic feasibility. In other words, effective biomass conversion processes are required to achieve a sustainable and fossil-independent industry. Figure 10 shows the links among the biomass conversion processes, sustainable supply chain, and socio-economic impacts. From the socio-economic viewpoint, processing

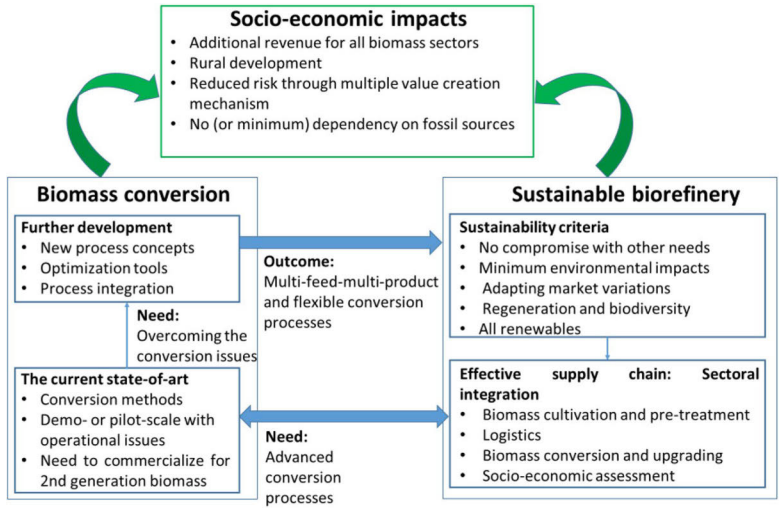

Fig. 10 The inter-relations among biomass conversion processes, sustainable biorefinery, and socio-economic impacts

the wastes and side streams of various sectors, effective biomass conversion processes can increase the economic and environmental performances of those sectors simultaneously. On the other hand, the conversion processes have operational issues affecting techno-economic performances. Therefore, it would be a very critical milestone to address the operational issues of promising conversion processes.

The hydrothermal processes provide effective conversion routes of biomass feedstocks with respect to sustainability features as well as being suitable to the high-moisture nature of biomass. Among those processes, SCWG and HTL produce syngas and crude bio-oil as the vital platform substances for the production of CHP, biofuels, and chemicals. Therefore, syngas and bio-oil have inevitable and increasing demand. In addition, SCWG and HTL processes produce these substances of higher quality than the thermal process alternatives. Furthermore, these processes can also convert various biomass feedstocks including agricultural wastes, forest residues, sewage sludge, manure, and algae as well as waste streams or by-products of other production plants (e.g., black liquor in pulp mills and olive mill wastewater). Consequently, it is desirable to improve the techno-economic feasibility of these processes for industrial applications, to address high costs compared to fossil-based productions. However, the commercialization of SCWG and HTL processes is hindered by operational issues introducing constraints on the applicable process conditions, blocking the operation or/and affecting the process configurations. Further research and novel concepts are required to address the operational issues of SCWG and HTL processes besides the currently investigated solutions.

The main phenomena behind most of the operational issues are char formation and the impacts of inorganic salts: causing variations in reactor pressure and plugging in SCWG, corrosion in both SCWG and HTL processes, catalyst deactivation, and affecting product quality. This requires a special reactor configuration enabling solid separation simultaneously with the hydrothermal conversion. The reactor concept of the Verena pilot plant is designed to separate the solids from the bottom. This concept can further be modified considering the techno-economic aspects: catalytic impact of reactor materials, surface area-volume ratio, and the prices of reactor materials. Figure 11 shows a potential reactor concept for enabling solid separation while having a catalytic impact as well. The outer reactor wall can be stainless steel because of its cheaper price and insignificant surface-area-to-volume ratio. The riser tubes can be multiple and coil-shaped made of Inconel material to provide more surface area for the catalytic material. Both the outer and inner surfaces of the riser tubes can function to catalyze the reactors in this concept. Moreover, SCWG reactors should have two inlets for the biomass feedstock at subcritical temperature and SCW to avoid solid precipitation in the pipelines and heat exchangers while a single inlet can be sufficient for HTL processes.

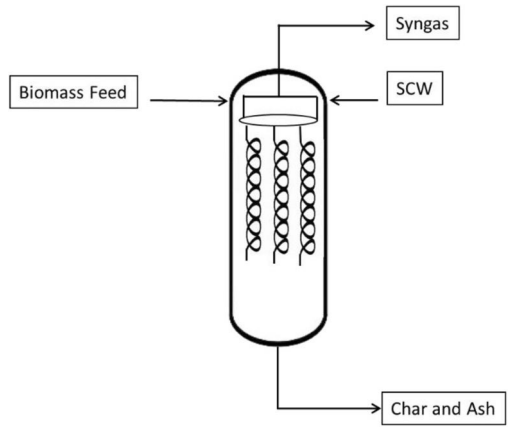

Fig. 11 The reactor concept with multiple, coil-shaped riser tubes

Besides the reactor configuration, the process concept can also be enhanced to reduce the char formation and to improve the economic performance of the hydrothermal conversion. For instance, Özdenkçi et al. (2017) [42] proposed partial wet oxidation (PWO) prior to SCWG and HTL reactors. Figure 12 shows the block diagram of the process concept. PWO is an exothermic process at 170–240 °C, thus providing self-heating the feedstock up to this temperature range. Moreover, oxidizing the sulfur content in PWO can provide sulfur-free bio-oil or syngas. The reduction of oxidized sulfur does not occur to a significant extent at temperatures lower than 900 °C [195]. Consequently, the oxidized sulfur can occur in the salts, i.e., either precipitating in SCWG or dissolved in the aqueous phase in HTL. Furthermore, PWO can reduce char formation in SCWG and HTL reactors by breaking down the large molecules in advance. The light and oxygenated molecules are gasified to a higher extent than the long-chain organics and aromatics [196]. Consequently, char formation can be reduced by introducing the biomass into SCWG or HTL reactor after partial decomposition via PWO. In addition, in the case of lignocellulosic feedstocks, some part of PWO downstream can be used for recovering lignin as another product as applied in pulp mills. Lignin precipitates in black liquor when reducing pH to 9–10 [197] while PWO enhances the filtering of lignin and enables sulfur-free product [198].

As future aspects, the investigations on SCWG and HTL processes can be directed towards new concepts and solutions to address the operational issues and to extend the application range of process conditions. As a major part of investment costs, the reactor costs can be reduced

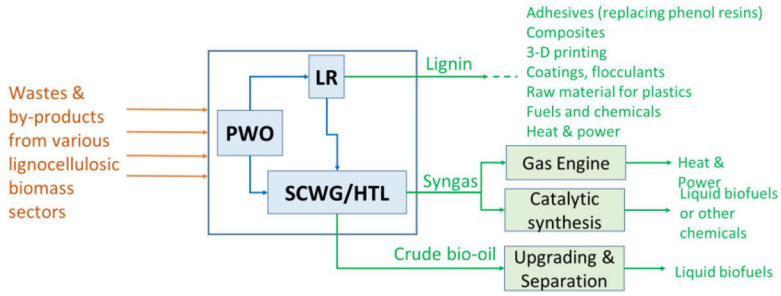

Fig. 12 The block diagram of a process concept involving PWO prior to HTL and SCWG (LR: lignin recovery)

by improving the tensile strength and thermal stability of the materials, thus enabling a higher diameter-to-thickness ratio. This might increase the range of economically feasible residence times for optimizing the process conditions. Meanwhile, the solutions against catalyst deactivation and corrosion would make the product yields of lab-scale studies applicable in industrial processes. As a major operational issue, solid deposition can be addressed by special reactor configurations, partial decomposition of biomass prior to the SCWG or HTL reactor, and recovering the major source of char formation in biomass (i.e., lignin) as another product. From the process development viewpoint, the future scope can involve the proof of concept in Fig. 12 through the experiments of PWO followed by SCWG or HTL for various feedstocks, to validate sulfur-free products and reduce char formation while enhancing the gas and bio-oil yields. Afterward, the whole process is to be optimized with respect to conditions in PWO and SCWG or HTL. In addition, the reactor configuration Fig. 11 can also be implemented in a pilot-scale process to verify the solid separation simultaneously with catalytic conversion of biomass.

5 Conclusion

Biomass represents an abundant and renewable source for replacing fossil sources and enabling carbon-neutrality. Sustainability aspects emphasize the usage of 2nd-generation biomass in chemical, fuel, and energy production. However, conversion of 2nd-generation of biomass requires advanced processes and currently results in higher production costs than conventional fossil-based processes. Therefore, it is crucial to select suitable conversion technologies with respect to the biomass feedstock and to enhance the techno-economic performance of these processes.

The hydrothermal processes present promising conversion routes because of the high moisture content of biomass feedstocks: high energy efficiencies, product yields, and quality compared to thermal processes. The SCWG and HTL processes produce syngas and bio-oil as crucial platform chemicals from waste streams and residues of biomass sectors. Commercial implementation of these processes can improve the biomass supply chains from environmental and economic viewpoints. However, these processes undergo operational issues reducing the economic performance and/or endangering process safety. In other words, the operational issues are obstacles to the process development of SCWG and HTL technologies. Therefore, a holistic investigation is required to determine the obstacles, root causes, and potential solutions comprehensively.

This study reviews the operational issues of SCWG and HTL processes together with the phenomena causing the issues and solutions addressing these issues. The main issue is process safety regarding thermal and mechanical stress on the reactor due to high pressure and temperature. Addressing this issue requires proper selection of reactor material and diameter-to-thickness ratio considering the operating pressure and the tensile strength of materials at the operating temperature. Regarding the reactor and pipeline material, corrosion is another issue regarding long-term operation. Corrosion results from the presence of alkali salts, char formation, and corrosive inorganics (sulfur, chloride, or nitrate). This issue is currently addressed through corrosion-resistant material selection and optimum conditions minimizing char formation as well as adjusting the feedstock via mixing with another non-corrosive feedstock or pre-neutralization. Catalyst deactivation is another long-term issue reducing the product yields. This can occur due to chemical degradation (chemisorption of intermediate organics on active sites), sintering of heterogeneous catalysts at high temperatures, or fouling (due to deposition of unreactive species on catalyst surface). The catalyst deactivation can be reduced through different catalyst preparation methods, and enhanced dispersion, adding a trace amount of transition metals to alkali metal catalysts and bimetallic catalysts. In addition, the biomass concentration into a reactor inlet is restricted by pumpability limits to high pressure. This issue introduces a constraint to the applicable concentration range when investigating the optimum

conditions. Moreover, solid deposition is the main obstacle increasing the occurrence risks of other issues as well. Solid deposition results from char formation (in SCWG and HTL) and precipitation of inorganic salts (in SCWG). This issue causes mechanical stress on the reactor through variation of pressure, under-deposit corrosion, dealloying in case of sulfide, and catalyst deactivation through fouling. Addressing this issue requires special reactor configurations enabling solid separation simultaneously with the reactions while providing a surface area of catalytic wall in an economically feasible way, besides optimum conditions minimizing the char formation.

The future aspects can include new concepts of integrating SCWG and HTL, enhanced reactor configurations. As a new concept, PWO of the feedstock prior to the SCWG or HTL reactor can reduce the char formation and provide sulfur-free products as well as slightly improve the energy efficiency. As an enhanced reactor configuration, the reactor can have two outlets: to collect the products through multiple, coil-shaped riser tubes while solids precipitate to the bottom outlet. Addressing the operational issues will also improve the techno-economic performances of SCWG and HTL processes. The further scope can be to investigate these processes involving the new solutions, e.g., experiments of PWO followed by SCWG or HTL with various feedstocks and a new reactor configuration. In other words, the operational issues present the main obstacle also affecting economic feasibility. Therefore, effective solutions can enable the efficient implementation of SCWG and HTL processes, thus improving the biomass supply chains.

The commercialization of SCWG and HTL processes will improve the biomass supply chains as well: the whole chain of transporting the residues/wastes from the fields to conversion plants, the processes converting these feedstocks into intermediates, and/or final products, and transportation of the final product. The techno-economic performances of biorefineries can be evaluated through profitability measures, exergy analysis, and LCA within the whole supply chain. It is essential to optimize the supply chain network, and conversion processes are the heart of these chains.

Acknowledgements We acknowledge the Regional Council of Ostrobothnia for their support in conducting the EU-ERUF project named "Implementation of a hydrothermal carbonization process for the disposal sludge and wet organic streams."

Funding Open access funding provided by Abo Akademi University (ABO). This work received financial support from the University Foundation in Ostrobothnia (Högskolestiftelsen) [28600114K1], EU Commission, and the Aktia Foundation [28600114K3].

Declarations

Competing interests The authors declare no competing interests.

References

1. Exxonmobil (2019) Outlook for energy: a perspective to 2040
2. Butera G, Fendt S, Jensen SH et al (2020) Flexible methanol production units coupling solid oxide cells and thermochemical biomass conversion via different gasification technologies. Energy 208:118432. https://doi.org/10.1016/j.energy.2020.118432
3. Liu L, Wu L (2021) Forecasting the renewable energy consumption of the European countries by an adjacent non-homogeneous grey model. Appl Math Model 89:1932–1948. https://doi.org/10.1016/j.apm.2020.08.080
4. Sikkema R, Proskurina S, Banja M, Vakkilainen E (2021) How can solid biomass contribute to the EU's renewable energy targets in 2020, 2030 and what are the GHG drivers and safeguards in energy- and forestry sectors? Renewable Energy 165:758–772. https://doi.org/10.1016/j.renene.2020.11.047
5. Energy Policies of IEA Countries: Finland 2018 Review. In: IEA Webstore. https://webstore.iea.org/energy-policies-of-iea-countries-finland-2018-review. Accessed 2 Jan 2021
6. Ma J, Wei H, Liu Y et al (2020) Application of Co3O4-based materials in electrocatalytic hydrogen evolution reaction: a review. Int J Hydrogen Energy 45:21205–21220. https://doi.org/10.1016/j.ijhydene.2020.05.280
7. Meng J, Mäkelä MR, de Vries RP (2020) Molecular engineering to improve lignocellulosic biomass based applications using filamentous fungi. In: Advances in Applied Microbiology. Academic Press
8. Mailaram S, Kumar P, Kunamalla A et al (2021) 3 - Biomass, biorefinery, and biofuels. In: Dutta S, Mustansar Hussain C (eds) Sustainable Fuel Technologies Handbook. Academic Press, pp 51–87
9. Ganguly P, Sarkhel R, Das P (2021) 2 - The second- and third-generation biofuel technologies: comparative perspectives. In: Dutta S, Mustansar Hussain C (eds) Sustainable Fuel Technologies Handbook. Academic Press, pp 29–50
10. Luque R, Herrero-Davila L, Campelo JM et al (2008) Biofuels: a technological perspective. Energy Environ Sci 1:542–564. https://doi.org/10.1039/B807094F
11. Cherubini F (2010) The biorefinery concept: using biomass instead of oil for producing energy and chemicals. Energy Convers Manage 51:1412–1421. https://doi.org/10.1016/j.enconman.2010.01.015
12. Elliott DC (2004) Biomass, chemicals from C. J. Cleveland. Elsevier Inc, Oxford
13. Aggarwal S, Hakovirta M (2021) Supercritical carbon dioxide drying of municipal sewage sludge – novel waste-to-energy

valorization pathway. J Environ Manage 285:112148. https://doi.org/10.1016/j.jenvman.2021.112148
14. Byun J, Kwon O, Park H, Han J (2021) Food waste valorization to green energy vehicles: sustainability assessment. Energy Environ Sci. https://doi.org/10.1039/D1EE00850A
15. Yaashikaa PR, Kumar PS, Varjani S, Saravanan A (2020) A critical review on the biochar production techniques, characterization, stability and applications for circular bioeconomy. Biotechnology Reports 28:e00570. https://doi.org/10.1016/j.btre.2020.e00570
16. Shahbaz M, Al-Ansari T, Aslam M et al (2020) A state of the art review on biomass processing and conversion technologies to produce hydrogen and its recovery via membrane separation. Int J Hydrogen Energy 45:15166–15195. https://doi.org/10.1016/j.ijhydene.2020.04.009
17. Das P, V.p. C, Mathimani T, Pugazhendhi A (2021) Recent advances in thermochemical methods for the conversion of algal biomass to energy. Science of The Total Environment 766:144608. https://doi.org/10.1016/j.scitotenv.2020.144608
18. Ishola MM, Brandberg T, Taherzadeh MJ (2015) Simultaneous glucose and xylose utilization for improved ethanol production from lignocellulosic biomass through SSFF with encapsulated yeast. Biomass Bioenerg 77:192–199. https://doi.org/10.1016/j.biombioe.2015.03.021
19. Zheng Y, Pan Z, Zhang R (2009) Overview of biomass pretreatment for cellulosic ethanol production. Int J Agric Biol Eng 2:51–68. https://doi.org/10.25165/ijabe.v2i3.168
20. Ma W, Ma C, Liu X et al (2021) Nox formation in fixed-bed biomass combustion: Chemistry and modeling. Fuel 290:119694. https://doi.org/10.1016/j.fuel.2020.119694
21. Sharma P, Gupta B, Pandey M, et al (2020) Downdraft biomass gasification: a review on concepts, designs analysis, modelling and recent advances. Mater Today: Proc. https://doi.org/10.1016/j.matpr.2020.08.789
22. Habibollahzade A, Ahmadi P, Rosen MA (2021) Biomass gasification using various gasification agents: optimum feedstock selection, detailed numerical analyses and tri-objective grey wolf optimization. J Clean Prod 284:124718. https://doi.org/10.1016/j.jclepro.2020.124718
23. Galvagno A, Prestipino M, Maisano S et al (2019) Integration into a citrus juice factory of air-steam gasification and CHP system: energy sustainability assessment. Energy Convers Manage 193:74–85. https://doi.org/10.1016/j.enconman.2019.04.067
24. Galvagno A, Prestipino M, Chiodo V et al (2017) Energy performance of CHP system integrated with citrus peel air-steam gasification: a comparative study. Energy Procedia 126:485–492. https://doi.org/10.1016/j.egypro.2017.08.233
25. Grammelis P, Margaritis N, Kourkoumpas D-S (2018) 4.27 Pyrolysis energy conversion systems. In: Dincer I (ed) Comprehensive Energy Systems. Elsevier, Oxford, pp 1065–1106
26. Balat M, Balat M, Kırtay E, Balat H (2009) Main routes for the thermo-conversion of biomass into fuels and chemicals. Part 1: Pyrolysis systems. Energy Convers Manage 50:3147–3157. https://doi.org/10.1016/j.enconman.2009.08.014
27. Kılıç M, Pütün AE, Uzun BB, Pütün E (2014) Converting of oil shale and biomass into liquid hydrocarbons via pyrolysis. Energy Convers Manage 78:461–467. https://doi.org/10.1016/j.enconman.2013.11.002
28. Bridgwater AV (2012) Review of fast pyrolysis of biomass and product upgrading. Biomass Bioenerg 38:68–94. https://doi.org/10.1016/j.biombioe.2011.01.048
29. Zafar MW, Sinha A, Ahmed Z et al (2021) Effects of biomass energy consumption on environmental quality: the role of education and technology in Asia-Pacific Economic Cooperation countries. Renew Sustain Energy Rev 142:110868. https://doi.org/10.1016/j.rser.2021.110868
30. Briones-Hidrovo A, Copa J, Tarelho LAC, et al (2021) Environmental and energy performance of residual forest biomass for electricity generation: gasification vs. combustion. J Clean Prod 289:125680. https://doi.org/10.1016/j.jclepro.2020.125680
31. Bareschino P, Mancusi E, Urciuolo M et al (2020) Life cycle assessment and feasibility analysis of a combined chemical looping combustion and power-to-methane system for CO2 capture and utilization. Renew Sustain Energy Rev 130:109962. https://doi.org/10.1016/j.rser.2020.109962
32. Cormos C-C (2020) Techno-economic implications of flexible operation for super-critical power plants equipped with calcium looping cycle as a thermo-chemical energy storage system. Fuel 280:118293. https://doi.org/10.1016/j.fuel.2020.118293
33. Balat M, Balat M, Kırtay E, Balat H (2009) Main routes for the thermo-conversion of biomass into fuels and chemicals. Part 2: gasification systems. Energy Convers Manage 50:3158–3168. https://doi.org/10.1016/j.enconman.2009.08.013
34. Saidur R, BoroumandJazi G, Mekhilef S, Mohammed HA (2012) A review on exergy analysis of biomass based fuels. Renew Sustain Energy Rev 16:1217–1222. https://doi.org/10.1016/j.rser.2011.07.076
35. Lepage T, Kammoun M, Schmetz Q, Richel A (2021) Biomass-to-hydrogen: a review of main routes production, processes evaluation and techno-economical assessment. Biomass Bioenerg 144:105920. https://doi.org/10.1016/j.biombioe.2020.105920
36. Gagliano A, Nocera F, Bruno M (2018) 2 - simulation models of biomass thermochemical conversion processes, gasification and pyrolysis, for the prediction of the energetic potential. In: Yahyaoui I (ed) Advances in Renewable Energies and Power Technologies. Elsevier, pp 39–85
37. Yoshida Y, Dowaki K, Matsumura Y et al (2003) Comprehensive comparison of efficiency and CO2 emissions between biomass energy conversion technologies—position of supercritical water gasification in biomass technologies. Biomass Bioenerg 25:257–272. https://doi.org/10.1016/S0961-9534(03)00016-3
38. Naqvi M, Yan J, Dahlquist E (2010) Black liquor gasification integrated in pulp and paper mills: a critical review. Biores Technol 101:8001–8015. https://doi.org/10.1016/j.biortech.2010.05.013
39. Özdenkçi K, Prestipino M, Björklund-Sänkiaho M et al (2020) Alternative energy valorization routes of black liquor by stepwise supercritical water gasification: effect of process parameters on hydrogen yield and energy efficiency. Renew Sustain Energy Rev 134:110146. https://doi.org/10.1016/j.rser.2020.110146
40. De Blasio C, Lucca G, Özdenkci K et al (2016) A study on supercritical water gasification of black liquor conducted in stainless steel and nickel-chromium-molybdenum reactors. J Chem Technol Biotechnol 91:2664–2678. https://doi.org/10.1002/jctb.4871
41. Tekin K, Karagöz S, Bektaş S (2014) A review of hydrothermal biomass processing. Renew Sustain Energy Rev 40:673–687. https://doi.org/10.1016/j.rser.2014.07.216
42. Özdenkçi K, De Blasio C, Muddassar HR et al (2017) A novel biorefinery integration concept for lignocellulosic biomass. Energy Convers Manage 149:974–987. https://doi.org/10.1016/j.enconman.2017.04.034
43. Hu Y, Gong M, Xing X et al (2020) Supercritical water gasification of biomass model compounds: a review. Renew Sustain Energy Rev 118:109529. https://doi.org/10.1016/j.rser.2019.109529
44. Kruse A, Dahmen N (2015) Water – a magic solvent for biomass conversion. J Supercrit Fluids 96:36–45. https://doi.org/10.1016/j.supflu.2014.09.038

45. Rogers GFC, Mayhew YR (1994) Thermodynamic and transport properties of fluids: S. I. Units, 5th edition. Wiley-Blackwell, Oxford
46. Marshall WL, Franck E (1981) Ion product of water substance, 0–1000 C, 1–10,000 Bars. New International Formulation and Its Background. https://doi.org/10.1063/1.555643
47. Guo Y, Wang SZ, Xu DH et al (2010) Review of catalytic supercritical water gasification for hydrogen production from biomass. Renew Sustain Energy Rev 14:334–343. https://doi.org/10.1016/j.rser.2009.08.012
48. Kabyemela BM, Adschiri T, Malaluan RM, Arai K (1999) Glucose and fructose decomposition in subcritical and supercritical water: detailed reaction pathway, mechanisms, and kinetics. Ind Eng Chem Res 38:2888–2895. https://doi.org/10.1021/ie9806390
49. Sasaki M, Kabyemela B, Malaluan R et al (1998) Cellulose hydrolysis in subcritical and supercritical water. J Supercrit Fluids 13:261–268. https://doi.org/10.1016/S0896-8446(98)00060-6
50. Fang Z, Sato T, Smith RL et al (2008) Reaction chemistry and phase behavior of lignin in high-temperature and supercritical water. Biores Technol 99:3424–3430. https://doi.org/10.1016/j.biortech.2007.08.008
51. Yanik J, Ebale S, Kruse A et al (2007) Biomass gasification in supercritical water: part 1. Effect of the nature of biomass. Fuel 86:2410–2415. https://doi.org/10.1016/j.fuel.2007.01.025
52. Akhtar J, Amin NAS (2011) A review on process conditions for optimum bio-oil yield in hydrothermal liquefaction of biomass. Renew Sustain Energy Rev 15:1615–1624. https://doi.org/10.1016/j.rser.2010.11.054
53. Savage PE, Levine RB, Huelsman CM (2010) Chapter 8:hydrothermal processing of biomass. In: Thermochemical Conversion of Biomass to Liquid Fuels and Chemicals. pp 192–221
54. Simsek Kus N (2012) Organic reactions in subcritical and supercritical water. Tetrahedron 68:949–958. https://doi.org/10.1016/j.tet.2011.10.070
55. Sricharoenchaikul V (2009) Assessment of black liquor gasification in supercritical water. Biores Technol 100:638–643. https://doi.org/10.1016/j.biortech.2008.07.011
56. Cao C, Guo L, Chen Y et al (2011) Hydrogen production from supercritical water gasification of alkaline wheat straw pulping black liquor in continuous flow system. Int J Hydrogen Energy 36:13528–13535. https://doi.org/10.1016/j.ijhydene.2011.07.101
57. Yin S, Dolan R, Harris M, Tan Z (2010) Subcritical hydrothermal liquefaction of cattle manure to bio-oil: effects of conversion parameters on bio-oil yield and characterization of bio-oil. Biores Technol 101:3657–3664. https://doi.org/10.1016/j.biortech.2009.12.058
58. Zhou D, Zhang L, Zhang S et al (2010) Hydrothermal liquefaction of macroalgae Enteromorpha prolifera to bio-oil. Energy Fuels 24:4054–4061. https://doi.org/10.1021/ef100151h
59. Zhang L, Champagne P, (Charles) Xu C, (2011) Bio-crude production from secondary pulp/paper-mill sludge and waste newspaper via co-liquefaction in hot-compressed water. Energy 36:2142–2150. https://doi.org/10.1016/j.energy.2010.05.029
60. Yong TL-K, Matsumura Y (2012) Reaction kinetics of the lignin conversion in supercritical water. https://pubs.acs.org/doi/full/https://doi.org/10.1021/ie300921d. Accessed 28 Mar 2019
61. Li S, Zhu B, Wang W et al (2020) Efficient and stable supercritical-water-synthesized Ni-based catalysts for supercritical water gasification. J Supercrit Fluids 160:104790. https://doi.org/10.1016/j.supflu.2020.104790
62. Zhu B, Li S, Wang W, Zhang H (2019) Supercritical water synthesized Ni/ZrO2 catalyst for hydrogen production from supercritical water gasification of glycerol. Int J Hydrogen Energy 44:30917–30926. https://doi.org/10.1016/j.ijhydene.2019.10.044
63. Nazari L, Yuan Z, Souzanchi S et al (2015) Hydrothermal liquefaction of woody biomass in hot-compressed water: catalyst screening and comprehensive characterization of bio-crude oils. Fuel 162:74–83. https://doi.org/10.1016/j.fuel.2015.08.055
64. Toor SS, Rosendahl L, Rudolf A (2011) Hydrothermal liquefaction of biomass: a review of subcritical water technologies. Energy 36:2328–2342. https://doi.org/10.1016/j.energy.2011.03.013
65. Muangrat R, Onwudili JA, Williams PT (2010) Influence of alkali catalysts on the production of hydrogen-rich gas from the hydrothermal gasification of food processing waste. Appl Catal B 100:440–449. https://doi.org/10.1016/j.apcatb.2010.08.019
66. Wang Y, Wang H, Lin H et al (2013) Effects of solvents and catalysts in liquefaction of pinewood sawdust for the production of bio-oils. Biomass Bioenerg 59:158–167. https://doi.org/10.1016/j.biombioe.2013.10.022
67. Elliott DC, Hart TR, Neuenschwander GG (2006) Chemical processing in high-pressure aqueous environments. 8. Improved Catalysts for Hydrothermal Gasification. Ind Eng Chem Res 45:3776–3781. https://doi.org/10.1021/ie060031o
68. Luterbacher JS, Fröling M, Vogel F et al (2009) Hydrothermal gasification of waste biomass: process design and life cycle asessment. Environ Sci Technol 43:1578–1583. https://doi.org/10.1021/es801532f
69. Castello D, Rolli B, Kruse A, Fiori L (2017) Supercritical water gasification of biomass in a ceramic reactor: long-time batch experiments. Energies 10:1734. https://doi.org/10.3390/en10111734
70. Tuan Abdullah TA, Croiset E (2014) Evaluation of an Inconel-625 Reactor and its wall effects on ethanol reforming in supercritical water. Ind Eng Chem Res 53:2121–2129. https://doi.org/10.1021/ie403305d
71. Lee CS, Conradie AV, Lester E (2021) Review of supercritical water gasification with lignocellulosic real biomass as the feedstocks: Process parameters, biomass composition, catalyst development, reactor design and its challenges. Chem Eng J 415:128837. https://doi.org/10.1016/j.cej.2021.128837
72. Mastuli MS, Kamarulzaman N, Kasim MF et al (2017) Catalytic gasification of oil palm frond biomass in supercritical water using MgO supported Ni, Cu and Zn oxides as catalysts for hydrogen production. Int J Hydrogen Energy 42:11215–11228. https://doi.org/10.1016/j.ijhydene.2017.02.174
73. Yakaboylu O, Harinck J, Smit KG, De Jong W (2015) Supercritical water gasification of biomass: a literature and technology overview. Energies 8:859–894. https://doi.org/10.3390/en8020859
74. Karayıldırım T, Sınağ A, Kruse A (2008) Char and coke formation as unwanted side reaction of the hydrothermal biomass gasification. Chem Eng Technol 31:1561–1568. https://doi.org/10.1002/ceat.200800278
75. Yoshida T, Matsumura Y (2001) Gasification of cellulose, xylan, and lignin mixtures in supercritical water. Ind Eng Chem Res 40:5469–5474. https://doi.org/10.1021/ie0101590
76. Kruse A, Dahmen N (2018) Hydrothermal biomass conversion: Quo vadis? J Supercrit Fluids 134:114–123. https://doi.org/10.1016/j.supflu.2017.12.035
77. Rodriguez Correa C, Kruse A (2018) Supercritical water gasification of biomass for hydrogen production – review. J Supercrit Fluids 133:573–590. https://doi.org/10.1016/j.supflu.2017.09.019
78 Yang J (Sophia), He Q, Yang L (2019) A review on hydrothermal co-liquefaction of biomass. Appl Energy 250:926–945. https://doi.org/10.1016/j.apenergy.2019.05.033
79. Leng L, Zhang W, Peng H et al (2020) Nitrogen in bio-oil produced from hydrothermal liquefaction of biomass: a review.

Chem Eng J 401:126030. https://doi.org/10.1016/j.cej.2020.126030
80. Su H, Kanchanatip E, Wang D et al (2020) Production of H2-rich syngas from gasification of unsorted food waste in supercritical water. Waste Manage 102:520–527. https://doi.org/10.1016/j.wasman.2019.11.018
81. Reddy SN, Nanda S, Dalai AK, Kozinski JA (2014) Supercritical water gasification of biomass for hydrogen production. Int J Hydrogen Energy 39:6912–6926. https://doi.org/10.1016/j.ijhydene.2014.02.125
82. Azadi P, Farnood R (2011) Review of heterogeneous catalysts for sub- and supercritical water gasification of biomass and wastes. Int J Hydrogen Energy 36:9529–9541. https://doi.org/10.1016/j.ijhydene.2011.05.081
83. Chen J, Liang J, Xu Z, E J, (2020) Assessment of supercritical water gasification process for combustible gas production from thermodynamic, environmental and techno-economic perspectives: a review. Energy Convers Manage 226:113497. https://doi.org/10.1016/j.enconman.2020.113497
84. Wei N, Xu D, Hao B et al (2021) Chemical reactions of organic compounds in supercritical water gasification and oxidation. Water Res 190:116634. https://doi.org/10.1016/j.watres.2020.116634
85. Okolie JA, Nanda S, Dalai AK et al (2020) A review on subcritical and supercritical water gasification of biogenic, polymeric and petroleum wastes to hydrogen-rich synthesis gas. Renew Sustain Energy Rev 119:109546. https://doi.org/10.1016/j.rser.2019.109546
86. Ibrahim ABA, Akilli H (2019) Supercritical water gasification of wastewater sludge for hydrogen production. Int J Hydrogen Energy 44:10328–10349. https://doi.org/10.1016/j.ijhydene.2019.02.184
87. Shahabuddin M, Alam MT, Krishna BB et al (2020) A review on the production of renewable aviation fuels from the gasification of biomass and residual wastes. Biores Technol 312:123596. https://doi.org/10.1016/j.biortech.2020.123596
88. Scarsella M, de Caprariis B, Damizia M, De Filippis P (2020) Heterogeneous catalysts for hydrothermal liquefaction of lignocellulosic biomass: a review. Biomass Bioenerg 140:105662. https://doi.org/10.1016/j.biombioe.2020.105662
89. Leng S, Leng L, Chen L et al (2020) The effect of aqueous phase recirculation on hydrothermal liquefaction/carbonization of biomass: a review. Biores Technol 318:124081. https://doi.org/10.1016/j.biortech.2020.124081
90. Matsumura Y, Minowa T (2004) Fundamental design of a continuous biomass gasification process using a supercritical water fluidized bed. Int J Hydrogen Energy 29:701–707. https://doi.org/10.1016/j.ijhydene.2003.09.005
91. Li J, Chen J, Chen S (2018) Supercritical water treatment of heavy metal and arsenic metalloid-bioaccumulating-biomass. Ecotoxicol Environ Saf 157:102–110. https://doi.org/10.1016/j.ecoenv.2018.03.069
92. Zhang H, Gong M, Ding L, Su Y (2020) Energy recovery and phosphorus phase behaviour from catalytic gasification of cyanobacterial biomass in supercritical water. Biomass Bioenerg 134:105477. https://doi.org/10.1016/j.biombioe.2020.105477
93. Adar E, Ince M, Bilgili MS (2020) Supercritical water gasification of sewage sludge by continuous flow tubular reactor: a pilot scale study. Chem Eng J 391:123499. https://doi.org/10.1016/j.cej.2019.123499
94. Pinkard BR (2019) Supercritical water gasification: practical design strategies and operational challenges for lab-scale, continuous flow reactors. 32
95. Özdenkçi K, De Blasio C, Sarwar G et al (2019) Techno-economic feasibility of supercritical water gasification of black liquor. Energy 189:116284. https://doi.org/10.1016/j.energy.2019.116284
96. Magdeldin M, Järvinen M (2020) Supercritical water gasification of Kraft black liquor: process design, analysis, pulp mill integration and economic evaluation. Appl Energy 262:114558. https://doi.org/10.1016/j.apenergy.2020.114558
97. Okolie JA, Nanda S, Dalai AK, Kozinski JA (2021) Techno-economic evaluation and sensitivity analysis of a conceptual design for supercritical water gasification of soybean straw to produce hydrogen. Biores Technol 331:125005. https://doi.org/10.1016/j.biortech.2021.125005
98. Tews IJ, Zhu Y, Drennan C, et al (2014) Biomass direct liquefaction options. TechnoEconomic and Life Cycle Assessment. Pacific Northwest National Lab. (PNNL), Richland, WA (United States)
99. Spath PL, Mann MK, Amos WA (2003) Update of hydrogen from biomass -- determination of the delivered cost of hydrogen. National Renewable Energy Lab., Golden, CO. (US)
100. Zhu Y, Biddy MJ, Jones SB et al (2014) Techno-economic analysis of liquid fuel production from woody biomass via hydrothermal liquefaction (HTL) and upgrading. Appl Energy 129:384–394. https://doi.org/10.1016/j.apenergy.2014.03.053
101. Boukis N, Galla U, Müller H, et al (2007) Biomass gasification in supercritical water. Experimental progress achieved with the verena pilot plant. 4
102. Matsumura Y (2015) Chapter 9 - hydrothermal gasification of biomass. In: Pandey A, Bhaskar T, Stöcker M, Sukumaran RK (eds) Recent advances in thermo-chemical conversion of biomass. Elsevier, Boston, pp 251–267
103. Anastasakis K, Biller P, Madsen RB et al (2018) Continuous hydrothermal liquefaction of biomass in a novel pilot plant with heat recovery and hydraulic oscillation. Energies 11:2695. https://doi.org/10.3390/en11102695
104. Elliott DC, Biller P, Ross AB et al (2015) Hydrothermal liquefaction of biomass: developments from batch to continuous process. Biores Technol 178:147–156. https://doi.org/10.1016/j.biortech.2014.09.132
105. Oh DH, Race J, Oterkus S, Chang E (2020) A new methodology for the prediction of burst pressure for API 5L X grade flawless pipelines. Ocean Eng 212:107602. https://doi.org/10.1016/j.oceaneng.2020.107602
106. De Blasio C, Salierno G, Magnano A (2021) Implications on feedstock processing and safety issues for semi-batch operations in supercritical water gasification of biomass. Energies 14:2863. https://doi.org/10.3390/en14102863
107. Deterimine Tubing Burst Pressure and Working Pressure | TBL Plastics. https://www.tblplastics.com/how-to-determine-tubing-burst-pressure-and-working-pressure/. Accessed 18 Nov 2021
108. Steel M Inconel vs Stainless Steel: Which is Stronger? https://www.marlinwire.com/blog/inconel-vs-stainless-steel-which-is-stronger. Accessed 3 Nov 2021
109. Li Y, Wang S, Xu T et al (2021) Novel designs for the reliability and safety of supercritical water oxidation process for sludge treatment. Process Saf Environ Prot 149:385–398. https://doi.org/10.1016/j.psep.2020.10.049
110. Wang S, Li J, Cao Y et al (2018) Thermal stability and tensile property of 316L stainless steel with heterogeneous lamella structure. Vacuum 152:261–264. https://doi.org/10.1016/j.vacuum.2018.03.040
111. Kosmač A (2012) Stainless steels at high temperatures. Euro Inox, Brussels
112. De Blasio C, De Gisi S, Molino A et al (2019) Concerning operational aspects in supercritical water gasification of kraft black liquor. Renew Energy 130:891–901. https://doi.org/10.1016/j.renene.2018.07.004

113. Waldeck WF, Lynn G, Hill AE (1932) Aqueous solubility of salts at high temperatures. I. SOLUBILITY OF SODIUM CARBONATE FROM 50 TO 348°1. J Am Chem Soc 54:928–936. https://doi.org/10.1021/ja01342a012
114. Voisin T, Erriguible A, Ballenghien D et al (2017) Solubility of inorganic salts in sub- and supercritical hydrothermal environment: application to SCWO processes. J Supercrit Fluids 120:18–31. https://doi.org/10.1016/j.supflu.2016.09.020
115. Marshall WL (1975) Water and its solutions at high temperatures and pressures. Chemistry 48:6–12
116. Valyashko VM (2004) Chapter 15 - Phase equilibria of water-salt systems at high temperatures and pressures. In: Palmer DA, Fernández-Prini R, Harvey AH (eds) Aqueous Systems at Elevated Temperatures and Pressures. Academic Press, London, pp 597–641
117. Zhang Y, Wang S, Song W et al (2019) Characteristics of sodium sulfate deposition in hydrogen production from supercritical water gasification: a review. Int J Hydrogen Energy 44:29467–29482. https://doi.org/10.1016/j.ijhydene.2019.05.125
118. Hodes M, Marrone PA, Hong GT et al (2004) Salt precipitation and scale control in supercritical water oxidation—part A: fundamentals and research. J Supercrit Fluids 29:265–288. https://doi.org/10.1016/S0896-8446(03)00093-7
119. Armellini FJ, Tester JW, Hong GT (1994) Precipitation of sodium chloride and sodium sulfate in water from sub- to supercritical conditions: 150 to 550 °C, 100 to 300 bar. J Supercrit Fluids 7:147–158. https://doi.org/10.1016/0896-8446(94)90019-1
120. Schubert M, Regler JW, Vogel F (2010) Continuous salt precipitation and separation from supercritical water. Part 2. Type 2 salts and mixtures of two salts. J Supercrit Fluids 52:113–124. https://doi.org/10.1016/j.supflu.2009.10.003
121. Schubert M, Regler JW, Vogel F (2010) Continuous salt precipitation and separation from supercritical water. Part 1: type 1 salts. J Supercrit Fluids 52:99–112. https://doi.org/10.1016/j.supflu.2009.10.002
122. Resende FLP, Fraley SA, Berger MJ, Savage PE (2008) Noncatalytic gasification of lignin in supercritical water. Energy Fuels 22:1328–1334. https://doi.org/10.1021/ef700574k
123. Kruse A, Meier D, Rimbrecht P, Schacht M (2000) Gasification of pyrocatechol in supercritical water in the presence of potassium hydroxide. Ind Eng Chem Res 39:4842–4848. https://doi.org/10.1021/ie0001570
124. Watanabe M, Inomata H, Osada M et al (2003) Catalytic effects of NaOH and ZrO2 for partial oxidative gasification of n-hexadecane and lignin in supercritical water☆. Fuel 82:545–552. https://doi.org/10.1016/S0016-2361(02)00320-4
125. Sınağ A, Kruse A, Schwarzkopf V Key Compounds of the hydropyrolysis of glucose in supercritical water in the presence of K2CO3 | Industrial & Engineering Chemistry Research. https://pubs.acs.org/doi/abs/https://doi.org/10.1021/ie030079r. Accessed 25 Feb 2021
126. Miyaoka H, Nakajima K, Yamaguchi S, et al Catalysis of lithium chloride and alkali metal borohydrides on hydrogen generation of ammonia and lithium hydride system | The Journal of Physical Chemistry C. https://pubs.acs.org/doi/abs/https://doi.org/10.1021/acs.jpcc.5b05572. Accessed 25 Feb 2021
127. Xu D, Wang S, Hu X et al (2009) Catalytic gasification of glycine and glycerol in supercritical water. Int J Hydrogen Energy 34:5357–5364. https://doi.org/10.1016/j.ijhydene.2008.08.055
128. Ebadi AG, Hisoriev H, Zarnegar M, Ahmadi H Hydrogen and syngas production by catalytic gasification of algal biomass (Cladophora glomerata L.) using alkali and alkaline-earth metals compounds. https://iahr.tandfonline.com/doi/full/https://doi.org/10.1080/09593330.2017.1417495#.YDfaiWgzaM8. Accessed 25 Feb 2021
129. Vadillo V, Sánchez-Oneto J, Portela JR, Martínez de la Ossa EJ (2013) Problems in supercritical water oxidation process and proposed solutions. Ind Eng Chem Res 52:7617–7629. https://doi.org/10.1021/ie400156c
130. Xu D, Huang C, Wang S et al (2015) Salt deposition problems in supercritical water oxidation. Chem Eng J 279:1010–1022. https://doi.org/10.1016/j.cej.2015.05.040
131. Vogel F (2017) Hydrothermal conversion of biomass. In: Meyers RA (ed) Encyclopedia of Sustainability Science and Technology. Springer, New York, New York, pp 1–46
132. Marrone PA, Hong GT (2009) Corrosion control methods in supercritical water oxidation and gasification processes. 21
133. Kruse A, Forchheim D, Gloede M et al (2010) Brines in supercritical biomass gasification: 1. Salt extraction by salts and the influence on glucose conversion. J Supercrit Fluids 53:64–71. https://doi.org/10.1016/j.supflu.2010.01.001
134. Wang S, Gong Y, Ma H, et al (2014) Countercurrent tank type supercritical water reactor with a sacrificial lining
135. Barner HE, Huang CY, Johnson T et al (1992) Supercritical water oxidation: an emerging technology. J Hazard Mater 31:1–17. https://doi.org/10.1016/0304-3894(92)87035-E
136. Huang C-Y (1992) Apparatus and method for supercritical water oxidation
137. Calzavara Y, Joussot-Dubien C, Turc H-A et al (2004) A new reactor concept for hydrothermal oxidation. J Supercrit Fluids 31:195–206. https://doi.org/10.1016/j.supflu.2003.11.001
138. Cocero MJ, Martínez JL (2004) Cool wall reactor for supercritical water oxidation: modelling and operation results. J Supercrit Fluids 31:41–55. https://doi.org/10.1016/j.supflu.2003.09.023
139. Wellig B, Lieball K, von Rohr R, Ph, (2005) Operating characteristics of a transpiring-wall SCWO reactor with a hydrothermal flame as internal heat source. J Supercrit Fluids 34:35–50. https://doi.org/10.1016/j.supflu.2004.07.003
140. Xu D, Wang S, Huang C et al (2014) Transpiring wall reactor in supercritical water oxidation. Chem Eng Res Des 92:2626–2639. https://doi.org/10.1016/j.cherd.2014.02.028
141. Veriansyah B, Kim J, Kim J-D, Lee Y-W (2008) Hydrogen production by gasification of isooctane using supercritical water. Int J Green Energy 5:322–333. https://doi.org/10.1080/15435070802229084
142. Susanti RF, Veriansyah B, Kim J-D et al (2010) Continuous supercritical water gasification of isooctane: a promising reactor design. Int J Hydrogen Energy 35:1957–1970. https://doi.org/10.1016/j.ijhydene.2009.12.157
143. Boukis N, Stoll IK (2021) Gasification of biomass in supercritical water, challenges for the process design—lessons learned from the operation experience of the first dedicated pilot plant. Processes 9:455. https://doi.org/10.3390/pr9030455
144. Jin H, Lu Y, Liao B et al (2010) Hydrogen production by coal gasification in supercritical water with a fluidized bed reactor. Int J Hydrogen Energy 35:7151–7160. https://doi.org/10.1016/j.ijhydene.2010.01.099
145. Lee A, Lewis D, Kalaitzidis T, Ashman P (2016) Technical issues in the large-scale hydrothermal liquefaction of microalgal biomass to biocrude. Curr Opin Biotechnol 38:85–89. https://doi.org/10.1016/j.copbio.2016.01.004
146. Guo B, Walter V, Hornung U, Dahmen N (2019) Hydrothermal liquefaction of Chlorella vulgaris and Nannochloropsis gaditana in a continuous stirred tank reactor and hydrotreating of biocrude by nickel catalysts. Fuel Process Technol 191:168–180. https://doi.org/10.1016/j.fuproc.2019.04.003
147. Kosinkova J, Ramirez JA, Nguyen J et al (2015) Hydrothermal liquefaction of bagasse using ethanol and black liquor as solvents. Biofuels, Bioprod Biorefin 9:630–638. https://doi.org/10.1002/bbb.1578

148. Cao L, Zhang C, Hao S et al (2016) Effect of glycerol as co-solvent on yields of bio-oil from rice straw through hydrothermal liquefaction. Biores Technol 220:471–478. https://doi.org/10.1016/j.biortech.2016.08.110
149. Wang X, Xie X, Sun J, Liao W (2019) Effects of liquefaction parameters of cellulose in supercritical solvents of methanol, ethanol and acetone on products yield and compositions. Biores Technol 275:123–129. https://doi.org/10.1016/j.biortech.2018.12.047
150. Feng S, Wei R, Leitch M, Xu CC (2018) Comparative study on lignocellulose liquefaction in water, ethanol, and water/ethanol mixture: roles of ethanol and water. Energy 155:234–241. https://doi.org/10.1016/j.energy.2018.05.023
151. Marrone PA, Hong GT (2009) Corrosion control methods in supercritical water oxidation and gasification processes. J Supercrit Fluids 51:83–103. https://doi.org/10.1016/j.supflu.2009.08.001
152. Kritzer P (2004) Corrosion in high-temperature and supercritical water and aqueous solutions: a review. J Supercrit Fluids 29:1–29. https://doi.org/10.1016/S0896-8446(03)00031-7
153. Hirose T, Shiba K, Enoeda M, Akiba M (2007) Corrosion and stress corrosion cracking of ferritic/martensitic steel in super critical pressurized water. J Nucl Mater 5
154. Brady MP, Keiser JR, Leonard DN et al (2014) Corrosion considerations for thermochemical biomass liquefaction process systems in biofuel production. JOM 66:2583–2592. https://doi.org/10.1007/s11837-014-1201-y
155. Chang K-H (2012) Corrosion behavior of Alloy 625 in supercritical water environments. Progr Nucl Energy 12
156. Ferreira-Pinto L Experimental basic factors in the production of H2 via supercritical water gasification. i n t e r n a t i o n a l j o u r n a l o f h y d r o g e n e n e r g y 19
157. Vadillo V, García-Jarana MB, Sánchez-Oneto J et al (2012) New feed system for water-insoluble organic and/or highly concentrated wastewaters in the supercritical water oxidation process. J Supercrit Fluids 72:263–269. https://doi.org/10.1016/j.supflu.2012.09.011
158. Cocero MJ (2018) Supercritical water processes: future prospects. J Supercrit Fluids 134:124–132. https://doi.org/10.1016/j.supflu.2017.11.018
159. Xu X, Matsumura Y, Stenberg J, Antal MJ (1996) Carbon-catalyzed gasification of organic feedstocks in supercritical water †. Ind Eng Chem Res 35:2522–2530. https://doi.org/10.1021/ie950672b
160. Berglin E, Enderlin C, Schmidt A (2012) Review and assessment of commercial vendors/options for feeding and pumping biomass slurries for hydrothermal liquefaction. Pacific Northwest National Lab. (PNNL), Richland, WA (United States)
161. Kruse A (2009) Hydrothermal biomass gasification. J Supercrit Fluids 47:391–399. https://doi.org/10.1016/j.supflu.2008.10.009
162. Elliott DC, Hart TR, Schmidt AJ et al (2013) Process development for hydrothermal liquefaction of algae feedstocks in a continuous-flow reactor. Algal Res 2:445–454. https://doi.org/10.1016/j.algal.2013.08.005
163. Seiple TE, Skaggs RL, Fillmore L, Coleman AM (2020) Municipal wastewater sludge as a renewable, cost-effective feedstock for transportation biofuels using hydrothermal liquefaction. J Environ Manage 270:110852. https://doi.org/10.1016/j.jenvman.2020.110852
164. Bartholomew CH (2001) Mechanisms of catalyst deactivation. Appl Catal A 212:17–60. https://doi.org/10.1016/S0926-860X(00)00843-7
165. Yoshida T, Oshima Y, Matsumura Y (2004) Gasification of biomass model compounds and real biomass in supercritical water. Biomass Bioenerg 26:71–78. https://doi.org/10.1016/S0961-9534(03)00063-1
166. Cao L, Zhang C, Chen H et al (2017) Hydrothermal liquefaction of agricultural and forestry wastes: state-of-the-art review and future prospects. Biores Technol 245:1184–1193. https://doi.org/10.1016/j.biortech.2017.08.196
167. Li S, Savage PE, Guo L (2019) Stability and activity maintenance of sol-gel Ni-MxOy (M=Ti, Zr, Ta) catalysts during continuous gasification of glycerol in supercritical water. J Supercrit Fluids 148:137–147. https://doi.org/10.1016/j.supflu.2019.02.028
168. Kang K, Azargohar R, Dalai AK, Wang H (2017) Hydrogen generation via supercritical water gasification of lignin using Ni-Co/Mg-Al catalysts. Int J Energy Res 41:1835–1846. https://doi.org/10.1002/er.3739
169. Peng G, Ludwig C, Vogel F (2016) Ruthenium dispersion: a key parameter for the stability of supported ruthenium catalysts during catalytic supercritical water gasification. ChemCatChem 8:139–141. https://doi.org/10.1002/cctc.201500995
170. Darmawan A, Ajiwibowo MW, Biddinika MK et al (2019) Black liquor-based hydrogen and power co-production: combination of supercritical water gasification and syngas chemical looping. Appl Energy 252:113446. https://doi.org/10.1016/j.apenergy.2019.113446
171. Ajiwibowo MW, Darmawan A, Aziz M (2019) Co-production of hydrogen and power from black liquor via supercritical water gasification, chemical looping and power generation. Energy Procedia 158:2299–2304. https://doi.org/10.1016/j.egypro.2019.01.259
172. Lehto J, Oasmaa A, Solantausta Y, et al Fuel oil quality and combustion of fast pyrolysis bio-oils. VTT Technical research Center of Finland
173. Vendra Singh S, Chaturvedi S, Dhyani VC, Kasivelu G (2020) Pyrolysis temperature influences the characteristics of rice straw and husk biochar and sorption/desorption behaviour of their biourea composite. Biores Technol 314:123674. https://doi.org/10.1016/j.biortech.2020.123674
174. Wu K, Zhang X, Yuan Q, Liu R (2020) Investigation of physico-chemical properties of hydrochar and composition of bio-oil from the hydrothermal treatment of dairy manure: effect of type and usage volume of extractant. Waste Manage 116:157–165. https://doi.org/10.1016/j.wasman.2020.08.004
175. Rinaldi R, Schüth F (2009) Design of solid catalysts for the conversion of biomass. Energy Environ Sci 2:610–626. https://doi.org/10.1039/B902668A
176. Ramirez JA, Brown RJ, Rainey TJ (2015) A review of hydrothermal liquefaction bio-crude properties and prospects for upgrading to transportation fuels. Energies 8:6765–6794. https://doi.org/10.3390/en8076765
177. Santos RB, Gomide JL, Hart PW (2015) Kraft pulping of reduced metal content eucalyptus wood: process impacts. BioResources 10:6538–6547
178. Arvindnarayan S, Sivagnana Prabhu KK, Shobana S et al (2017) Upgrading of micro algal derived bio-fuels in thermochemical liquefaction path and its perspectives: a review. Int Biodeterior Biodegrad 119:260–272. https://doi.org/10.1016/j.ibiod.2016.08.011
179. Saber M, Nakhshiniev B, Yoshikawa K (2016) A review of production and upgrading of algal bio-oil. Renew Sustain Energy Rev 58:918–930. https://doi.org/10.1016/j.rser.2015.12.342
180. Xu D, Lin G, Guo S et al (2018) Catalytic hydrothermal liquefaction of algae and upgrading of biocrude: a critical review. Renew Sustain Energy Rev 97:103–118. https://doi.org/10.1016/j.rser.2018.08.042
181. Castello D, Haider MS, Rosendahl LA (2019) Catalytic upgrading of hydrothermal liquefaction biocrudes: different challenges for different feedstocks. Renew Energy 141:420–430. https://doi.org/10.1016/j.renene.2019.04.003

182. Duan P, Savage PE (2011) Upgrading of crude algal bio-oil in supercritical water. Biores Technol 102:1899–1906. https://doi.org/10.1016/j.biortech.2010.08.013
183. Yang C, Li R, Cui C et al (2016) Catalytic hydroprocessing of microalgae-derived biofuels: a review. Green Chem 18:3684–3699. https://doi.org/10.1039/C6GC01239F
184. Casademont P, Sánchez-Oneto J, Scandelai APJ et al (2020) Hydrogen production by supercritical water gasification of black liquor: use of high temperatures and short residence times in a continuous reactor. The J Supercrit Fluids 159:104772. https://doi.org/10.1016/j.supflu.2020.104772
185. López Barreiro D, Bauer M, Hornung U et al (2015) Cultivation of microalgae with recovered nutrients after hydrothermal liquefaction. Algal Res 9:99–106. https://doi.org/10.1016/j.algal.2015.03.007
186. Duan P-G, Yang S-K, Xu Y-P et al (2018) Integration of hydrothermal liquefaction and supercritical water gasification for improvement of energy recovery from algal biomass. Energy 155:734–745. https://doi.org/10.1016/j.energy.2018.05.044
187. Davidson SD, Lopez-Ruiz JA, Zhu Y et al (2019) Strategies to valorize the hydrothermal liquefaction-derived aqueous phase into fuels and chemicals. ACS Sustainable Chem Eng 7:19889–19901. https://doi.org/10.1021/acssuschemeng.9b05308
188. Ong BHY, Walmsley TG, Atkins MJ, Walmsley MRW (2020) A Kraft mill-integrated hydrothermal liquefaction process for liquid fuel co-production. Processes 8:1216. https://doi.org/10.3390/pr8101216
189. Sun F, Aguayo MM, Ramachandran R, Sarin SC (2018) Biomass feedstock supply chain design – a taxonomic review and a decomposition-based methodology. Int J Prod Res 56:5626–5659. https://doi.org/10.1080/00207543.2018.1475766
190. Li S, Wang Z, Wang X et al (2019) Integrated optimization model of a biomass feedstock delivery problem with carbon emissions constraints and split loads. Comput Ind Eng 137:106013. https://doi.org/10.1016/j.cie.2019.106013
191. Aguayo MM, Sarin SC, Cundiff JS (2019) A branch-and-price approach for a biomass feedstock logistics supply chain design problem. IISE Trans 51:1348–1364. https://doi.org/10.1080/24725854.2019.1589656
192. Sharma B, Ingalls RG, Jones CL, Khanchi A (2013) Biomass supply chain design and analysis: basis, overview, modeling, challenges, and future. Renew Sustain Energy Rev 24:608–627. https://doi.org/10.1016/j.rser.2013.03.049
193. Kim J, Realff MJ, Lee JH et al (2011) Design of biomass processing network for biofuel production using an MILP model. Biomass Bioenerg 35:853–871. https://doi.org/10.1016/j.biombioe.2010.11.008
194. You F, Wang B (2011) Life cycle optimization of biomass-to-liquid supply chains with distributed–centralized processing networks. Ind Eng Chem Res 50:10102–10127. https://doi.org/10.1021/ie200850t
195. Wrobel CL (2000) Modeling total reduced sulfur and sulfur dioxide emissions from a kraft recovery boiler using an artificial neural network and Investigating volatile organic compounds in an urban intermountain valley using a TD/GC/MS methodology and intrinsic tracer molecules. University of Montana
196. Chakinala AG, Kumar S, Kruse A et al (2013) Supercritical water gasification of organic acids and alcohols: the effect of chain length. J Supercrit Fluids 74:8–21. https://doi.org/10.1016/j.supflu.2012.11.013
197. Tomani P (2010) The LignoBoost process. Cellul Chem Technol 44:53–58
198. Kouisni L, Gagné A, Maki K et al (2016) LignoForce system for the recovery of lignin from black liquor: feedstock options, odor profile, and product characterization. ACS Sustainable Chem Eng 4:5152–5159. https://doi.org/10.1021/acssuschemeng.6b00907

International Journal of Heat and Mass Transfer 183 (2022) 122200

Contents lists available at ScienceDirect

International Journal of Heat and Mass Transfer

journal homepage: www.elsevier.com/locate/hmt

Supercritical Water Gasification of glycerol: Continuous reactor kinetics and transport phenomena modeling

Gabriel Salierno[a,*], Fabrizio Marinelli[b], Blaž Likozar[c], Niloufar Ghavami[a], Cataldo De Blasio[a]

[a] Laboratory of Energy Technology, Faculty of Science and Engineering, Åbo Akademi University, Rantakatu 2; Vaasa 65100, Finland
[b] WS Atkins, 500 Park Avenue the Hub, Bristol BS324R, United Kingdom
[c] Department of Catalysis and Chemical Reaction Engineering, National Institute of Chemistry, Hajdrihova 19, Ljubljana 1001, Slovenia

II

ARTICLE INFO

Article history:
Received 30 June 2021
Revised 12 October 2021
Accepted 31 October 2021
Available online 24 November 2021

Keywords:
Supercritical Water Gasification
Glycerol
Compartment model
Inconel-625

ABSTRACT

Supercritical Water Gasification of glycerol is carried out on a continuous tubular reactor at 25 MPa and 610 °C. A design of experiments is performed at three levels of glycerol concentration (2.5; 5; and 10%) and three levels of inflow rate (125; 250; and 375 mL/min). The process outputs are the molar production of H_2; CH_4; CO_2; CO; and C_2H_6. The influence of Stainless Steel 316 and Inconel-625 as reactor materials is compared. A compartment model is implemented considering the system as a heat exchanger in series with a wall reactor. Heat transfer influence on reactivity is successfully captured. The results are useful and accurate in describing global stoichiometry. H_2, CH_4, and CO_2 productivity are fairly predicted. The catalytic effect of Inconel-625 manifests from the CO_2 to CO ratio when compared with Stainless Steel 316. Inconel-625 is 50% more productive in terms of C2 hydrocarbons and 40% more active towards CH_4 production, which is detrimental in 50% of the H_2 yield.

1. Introduction

The Circular Economy (CE) is considered the optimal approach to overcome the environmental impact of consumption and production patterns [69–71]. In contrast with the current linear economy, the CE concept strives to minimize waste production and better use natural resources in a closed loop. Biodiesel emerged as a renewable and potentially circular alternative to fossil fuels for transportation, is produced through trans-esterification of triglycerides with methanol or ethanol [70]. Glycerol, the by-product of biodiesel production, is an industrial chemical with several applications, including the food industry, pharmaceutical, and cosmetics [28,72–74]. Paradigm shifts to sustainable biofuels such as biodiesel and value-added biochemicals due to environmental concerns, subsequently increasing glycerol production. Therefore, the sustainable valorization of crude glycerol results in value-added products that support biodiesel production economically and environmentally.

According to the literature, every 10 tonnes of biodiesel produced during the trans-esterification reaction generates approximately 1 tonne of crude glycerol [76]. The glycerol market size is valued at USD 2.6 billion in 2019 and will grow 4.0% from 2020 to 2027 [77]. However, the crude glycerol derived from biodiesel production has low value. It contains impurities, including methanol, fatty acid methyl esters (FAMEs), soap and water, heavy metals, glycerides, ash, and free fatty acids (FFAs). The variability in composition makes biodiesel glycerol residue purification complicated and expensive [28,75]. Direct combustion of glycerol has low efficiency and produces high amounts of coke [13,38]. Therefore, alternative energetic valorization routes for crude glycerol have great importance in supporting the circular production of biodiesel (Sharma et al., 2021).

Several thermochemical methods can produce syngas and value-added chemicals from glycerol, including hydrothermal gasification, in subcritical or supercritical conditions, steam reforming, partial oxidation reforming, oxidative steam reforming, and autothermal reforming [72,81]. The steam reforming process is highly endothermic with a high operating cost of steam reformers; autothermal steam reforming by adding a limited amount of oxygen and exothermic partial oxidation decreases the energy and coke formation. However, there is still coking [19,58]). In supercritical water reforming, hydrogen is produced with high efficiency beyond the critical point of water. Reduced dielectric constant, low viscosity and large diffusivity in the critical point of water create a homogeneous reaction condition [12,78].

* Corresponding author.
E-mail address: gabriel.salierno@abo.fi (G. Salierno).

https://doi.org/10.1016/j.ijheatmasstransfer.2021.122200

Nomenclature

Latin symbols

a	power law pre-exponential parameter (-)
a_w	reactor wall surface to volume ratio (m^2/m^3)
b	power law exponent parameter (-)
C_{gly}	glycerol concentration (M)
C_{int}	acetaldehyde intermediate concentration (M)
C_o	initial glycerol concentration (M)
C_p	molar heat capacity ($J \cdot mol^{-1} \cdot °C^{-1}$)
Da_I	Damköhler number: $\frac{(k_1+k_2)\cdot C_o}{K_m \cdot a_w}$
E_{a1} to E_{a5}	activation energy (kJ/mol)
$F_{gly,in}$	glycerol molar inflow rate (mol/min)
$F_{Prod,j}$	molar production rate of j-th product (mol/min)
G_m	molar flux ($mol \cdot m^{-2} \cdot sec^{-1}$)
h_c	convective heat transfer coefficient ($W \cdot m^{-2} \cdot °C^{-1}$)
k_1; k_2; k_5	1st order reaction rate constants (min^{-1})
k_3; k_4	second-order reaction rate constants ($M^{-1}\ min^{-1}$)
K_m	global mass transfer coefficient ($mol \cdot m^{-2} \cdot sec^{-1}$)
L	length (m)
L_{Tube}	tube length (m)
Nu_i	internal Nusselt number: $\frac{h_c \cdot r_i}{\lambda}$
Pr	Prandtl number: $\frac{\mu \cdot C_p}{\lambda}$
r	radius (m)
Re	Reynolds number: $\frac{2r \cdot u \cdot \rho}{\mu}$
St_h	Stanton number for heat transfer: $\frac{Nu_i}{Re \cdot Pr}$
St_m	Stanton number for mass transfer: $\frac{K_m}{G_m}$
t	time (min; sec)
T	temperature (°C)
u	velocity (m / sec)
V_m	molar volume (dm^3/mol)
X_f	final conversion (-)
X_g	glycerol conversion (-)
z	axial position (m)

Acronyms

CE	circular economy
IIPF	ideal isothermal plug flow
MFC	mass flow controller
SCWG	supercritical water gasification
SS-316	stainless steel 316

Greek symbols

ε_1; ε_2	reaction expansion factors (-)
δ	discrete difference (-)
Δ_F	fluid dynamic boundary layer thickness (m)
Δ_T	thermal boundary layer thickness (m)
Φ_R	reactive zone ratio (-)
Φ_m	mass transfer efficiency (-)
λ	thermal conductivity ($W \cdot m^{-1} \cdot °C^{-1}$)
ν	stoichiometric coefficient (-)
μ	viscosity ($Pa \cdot sec$)
π	pi number (-)
P	density (kg/m^3)
T	residence time (sec)

Subscripts

bulk	bulk fluid
c	convective
C	critical point
e	external
FD	fluid dynamic
gly	glycerol
h	heat transfer
HE	heat exchanger compartment
i	internal
j	j-th product
m	mass transfer
mix	mixture
$prod_j < -gly$	glycerol to the j-th product
ref	reference
R	reactive compartment
SC	supercritical
w	wall material
we	wall, external side
wi	wall, internal side
z	axial position

Gong et al. (2021) investigated the SCWG reaction mechanism for the biomass model compounds, including glycerol, guaiacol, alanine, glucose, and humic acid. Based on their results, glycerol exhibited the best gas yield (7.44 mol/kg organic matter), and glucose showed the best hydrogen yield (3.15 mol/kg organic matter); the hydrogen yield of glycerol reached 2.71 mol H_2 per kg of organic matter. Jin et al. [24] developed a computational fluid dynamic model and numerical study of SCWG of glycerol. They studied the effect of operating parameters (feedstock flow rate, preheated water flow rate, reactor wall temperature of 650 °C, and preheated water temperature of 426 °C) in a tubular reactor. The experimental results validated the combined model. They also discussed two bottlenecks that hinder the complete SCWG. They concluded the short residence time and a side-reaction region in the feeding inlet are the reasons for incomplete gasification. Based on their results, a 135° feeding angle and high preheated water temperature (600 °C) prevent side-reaction. Almeida et al. (2018) studied crude glycerol gasification and used steam as an oxidant. They conducted the gasification experiments in a fixed bed reactor and compared the technical glycerol with the crude glycerol steam reforming. Based on their results, no significant difference was observed. However, the cold gas efficiency for crude glycerol (in the range of 100 –110%) was higher than technical glycerol.

The general objective of this work is to construct a dynamical description of glycerol Supercritical Water Gasification (SCWG) in a continuous flow through a tubular reactor. Results obtained by high-end simulations demonstrated a high degree of confidence [12,24,37,64]. However, robust calculation techniques based on correlations are sometimes preferred. The available information acquired from industrially relevant and cost-effective sensors is usually inadequate to validate complex and time-consuming computational models [21,79,80]). The literature on SCWG is extensive. However, industrially relevant reactor materials are not always utilized [9,68].

Moreover, most glycerol SCWG studies are in batch or continuous mode of operation with rather long residence times [22,44,51]. The effect of transport properties on global efficiency is seldom addressed. This work proposes a simplified method that allows the extraction of useful information to design and monitor SCWG reactors in a continuous mode of operation. This contribution aims to explain the productivity of glycerol SCWG in continuous mode utilizing an integral model involving a heat exchanger compartment in series with a tubular wall reactor. The results are also useful to describe the relationships within the most relevant gas components of the product. The influence of Stainless Steel 316 (SS-316) and Inconel-625 as reactor materials are compared under the same operative conditions of temperature, pressure, and glycerol molar

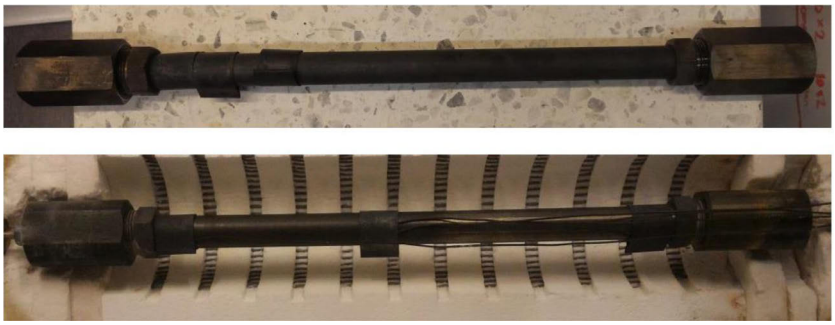

Fig. 1. Tubular reactors employed. Stainless Steel 316 (above) and Inconel-625 (below).

inflow range. The impact of heat transfer properties and catalytic activity of the wall material on the reactor performance is assessed from the experimental and model results.

2. Materials and methods

Glycerol SCWG is performed through a laboratory-scale continuous tubular flow reactor at the Process and Systems Engineering Laboratory at the Åbo Akademi University (Turku, Finland).

2.1. Experimental setup

The experiments have been conducted using two different reactors with the same shape but made of different types of Steel: SS-316 (Fig. 1 - above) and Inconel-625 (Fig. 1 - below). The total inner volume of the reactors is 83 ml, and their length is 0.51 m. Piping and fittings are provided by Swagelok (Stockholm, Sweden), having an internal diameter of 3 mm and an outside diameter of 6 mm with a working pressure of 420 bar.

The SCWG setup (Fig. 2) is equipped with a suitable pneumatic injection system based on compressed nitrogen and feed cylinders. The main function of the feed cylinders is to ensure that the feed is not handled directly by a pump, avoiding issues related to obstruction and corrosion phenomena. The feed cylinders are a DOT-3A 5000 (Swagelok; Stockholm, Sweden), which have a maximum pressure tolerance of 40 MPa. One cylinder is enough to perform the experiments. Nevertheless, the presence of a second cylinder facilitates start-up and cleaning operations.

The experimental setup has two cylinders with a capacity of 500 mL each. In this way, it is possible to ensure a continuous flow into the reactor. They are appropriately separated via valves so that, when a cylinder is in use, the other can be filled and pressurized. In addition, they are equipped with a bottom ball valve to previously feeding the water-glycerol mixture and let the compressed nitrogen enter, a top ball valve connecting to the reactor line, and a disc safety valve, which protects sample cylinders from over pressurization by venting the cylinder contents to the atmosphere. When the tests are terminated, a cleaning cycle is performed by pumping distilled water from the top to remove the eventual un-reacted feed that can compromise the results of the following experiments.

Once the feed cylinder is filled and pressurized, the top valve is open, and the mixture is pushed into the reactor by the compressed nitrogen, contained in a steel-lined carbon fiber-wrapped pressure vessel (Linde, Sweden), with a nominal capacity of 20 dm^3 and a nominal pressure of 300 bar. It is encased in a High-Density Polyethylene jacket and equipped with gas identification rings. An alarm sounds when the contents are low. In addition, the tank is equipped with a regulation valve attached to the exit nozzle to regulate the outlet pressure accordingly. The feed flow rate is pneumatically set by a mass flow controller (MFC) EL-FLOW F-231M (Bronkhorst High-Tech BV; Ruurlo, Netherlands). The MFC consists of a thermal mass flow sensor, a precise control valve, and a microprocessor-based pc-board with signal and Fieldbus conversion. This MFC is suitable for accurate measurements and control of flow between 10 and 500 mL/min at ambient pressure and 200–1000 L/min at high operating pressures (up to 400 bar).

Operating temperature is controlled by a Fibrothal HAS 100/500/114 heating system (Kanthal; Hallstahammar, Sweden), with a resistance R20 with a maximum power of 2600 W. The heating system is constituted of a cylindrical insulated case with embedded electrical resistances positioned in the inner wall of the case. The insulation material is a ceramic fiber, able to withstand a maximum temperature of 1150 °C, with a thermal conductivity varying between 0,10 and 0,21 W/(m.°C) with a temperature ranging from 400 up to 800 °C. The electronic control unit allows controlling and regulating the heating rate and maintaining a constant temperature. In this case, to avoid thermal shocks and deformation of the piping and reactor materials, the heating rate is set to 140 °C/h. The electrical energy required to heat the reactor and keep the setpoint temperature is measured by an electricity meter and maintained constant during the experiments. Before every experiment, the plant and the reactor are filled with water to avoid thermophysical damages to the piping and reactor. Moreover, by doing so, the plant is pressurized and ready for the injection of the feed coming from the cylinder.

The thermocouples used to monitor temperature at the outer walls of the reactor are of K-type. They can perform measurements between -200 and 1260 °C with a sensitivity of 41 μV/°C. Thermocouples are positioned on the reactor's outer wall using custom-made ducts; temperatures are measured along the reactor right after the inlet, middle, and right before the outlet. A relief valve R3A from Swagelok was positioned after the cooling section of the system and before the outlet gas sampling section. During the start-up phase of the system, the pressure on the nitrogen line has to be controlled and regulate by changing the volume flow rate of the nitrogen. The control is done with the help of a manometer installed close to the top valve. The temperature measurement at the inlet of the reactor is the most important since the entry of the feed into the reactor causes a sharp decrease in temperature. Hence, it is crucial to check if the inlet temperature does not fall below the critical point. The data acquisition system is the NI-DAQ mix (National Instruments, Austin, United States automatically saves the values of temperatures and pressures. The check and the control of temperature are made through LabView software to acquire and store both the temperature and pressure measurements.

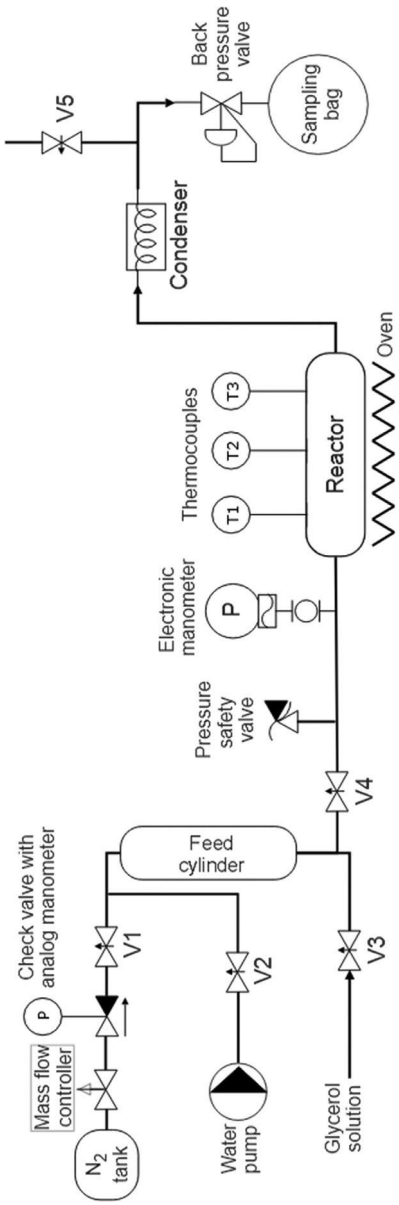

Fig. 2. Layout of the experimental setup.

In addition, this software allows directly controlling the temperatures and the pressures during the experiment through a user-friendly graphical interface.

After exiting the reactor, the stream pass through a coiled pipe heat exchanger immersed in a water container under ambient conditions. The collection of the effluents is made by using a plastic bag, Tedlar®, attached to the outlet nozzle downstream the relief valve. Afterward, the bag's volume is measured before and after a syringe extracts the gas. The way of cooling and depressurizing the effluent can modify the final composition because of the solubility of the gases in the liquid phase. Hence, the collection is made at ambient conditions since, at high pressure, the CO_2 is soluble in the liquid phase.

2.2. Operational conditions

For each reactor material, experiments are carried out in three flowrates and three compositions, totalizing nine operational conditions. The mass flow controller is set at 125, 250, and 375 mL/min. Aqueous solutions of glycerol 2.5%, 5%, and 10% w/w are prepared before every experiment and left at least one hour with a stirrer to make them homogenous. The weight of distilled water and 87% glycerol (technical grade, Sigma) is recorded to know their composition precisely.

The first step of the procedure is aimed at reaching the thermodynamic conditions. Therefore, in the start-up phase, the system is filled with distilled water and put under pressure by slowly opening valve V2 (see Fig. 2) and with attention to avoid hydraulic shocks. Then the valve V4 for the filling of the reactor until the system is full of water. Finally, closing the feed valves and those in contact with the external environment makes it possible to put the system under pressure. Every sampling bag is replaced every 20 min with a flow rate of 375 mL/min, every 30 min with a flow rate of 250 mL/min, and every 45 min with a 125 mL/min flow rate. The sampling time is recorded to get a precise measure of the gas productivity.

2.3. Product gas composition

The analysis of the gas product is carried out by a Perkin Elmer Claurus 500 Gas Chromatographer equipped with a molecular sieve 13 × 45/60 packed column and a Thermal Conductivity Detector. The method employs nitrogen as the carrier gas, and the oven temperature is set at 250 °C.

The chromatograph calibration is performed by injecting gas from reference bottles of known composition. For every operational condition of initial flow and composition, the sampling bags are analyzed to quantify the amount of hydrogen, carbon monoxide, carbon dioxide, methane, ethane, and ethylene. Measurements are performed by quadruplicate.

3. Results and discussion

The mass yield of individual gaseous products is calculated by combining the product gas volume of the sampling bag with the composition relationship. Considering that the mass yield is steady during the sampling time, it is possible to estimate the molar production (F_{Prod}) of hydrogen, carbon monoxide, carbon dioxide, methane, ethane, and ethylene. The design of experiment response curve analysis indicated that the only relevant variable is the first-order interaction of residence time and glycerol inlet content; thus, the natural variable to explore is the glycerol molar inflow rate. Statistical analysis of the experiment results and the compartment model are implemented in MATLAB R2020b (The MathWorks Inc., Natick, Massachusetts, United States of America).

3.1. Operational conditions effect on individual gas productivity

The productivity of hydrogen (Fig. 3A) is observed higher on stainless steel compared with Inconel-625, suggesting that the catalytic activity of the latter wall material would be towards hydrogenation of C2 intermediates. The production of carbon monoxide (Fig. 3B) and carbon dioxide (Fig. 3C) are significantly similar for

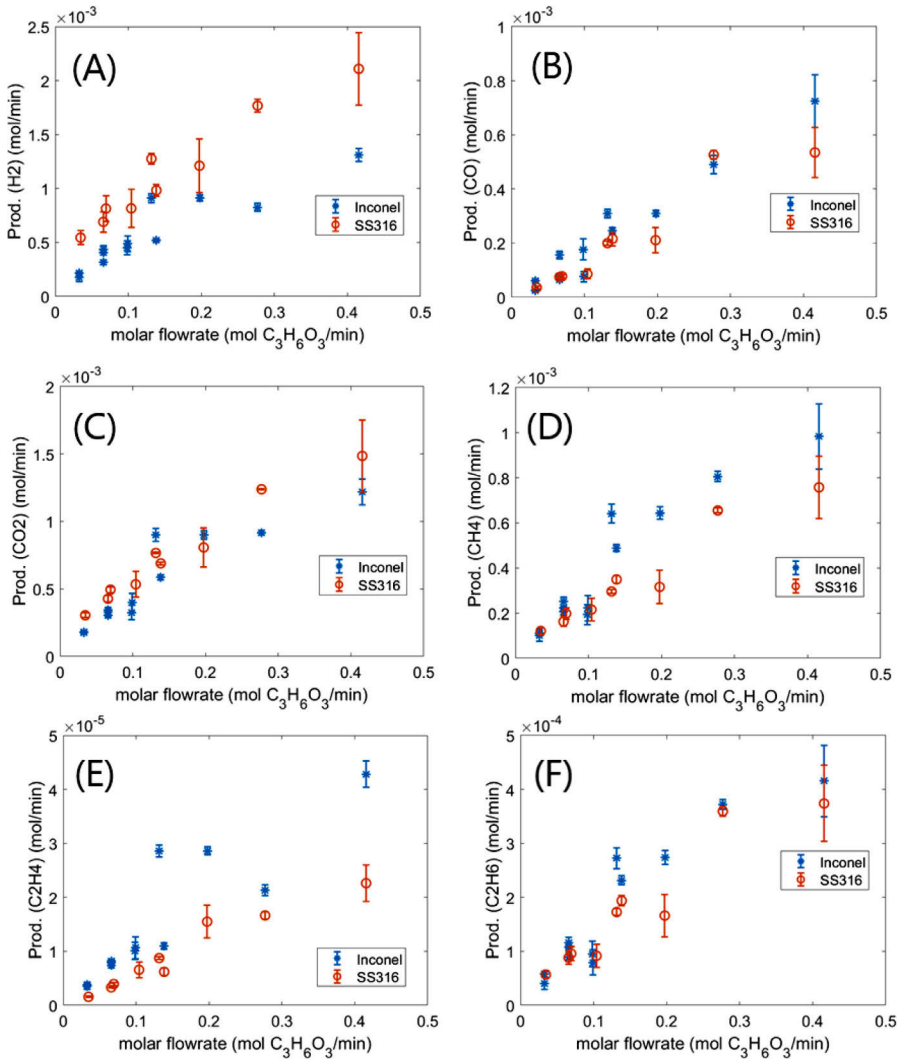

Fig. 3. Molar production as a function of the glycerol molar inflow rate: (A) hydrogen; (B) carbon monoxide; (C) methane; (D) carbon dioxide; (E) ethylene; (F) ethane.

both reactor materials within the operational window, signifying that there is no catalytic effect of Inconel-625 over water gas shift or methanation.

The productivity of methane (Fig. 3D) and ethylene (Fig. 3E) is observed higher in the case of using Inconel-625, suggesting undoubtedly a catalytic activity of the reactor material towards cracking and the hydrogenation of the acetaldehyde intermediate. The high nickel content of Inconel-625 could explain the enhancement of hydrocarbon production to the detriment of the hydrogen yield. At glycerol molar flow rates higher than 0.1 mol/min, Inconel-625 shows higher CH_4, C_2H_4, and C_2H_6 productivity.

A reasonable explanation for this behavior could be the catalytic activity of the Inconel wall towards the hydrogenation of C2 intermediates [9]. However, at glycerol molar inflow rates lower than 0.1 mol/min, there is no significant difference in methane and ethylene productivities. In any case, considering the noticeable amount of produced C2 hydrocarbons, the acetaldehyde intermediate appears to be rather active towards hydrogenation independently of the wall material. Another plausible explanation of the observed productivity of methane could be the accumulation of acetaldehyde that could decompose into methane and carbon monoxide [8,17,18].

The interpretation of the ethane production, shown in Fig. 3F, appears to be less straightforward. There is a slight difference favoring Inconel-625 between 0.1 and 0.2 mol glycerol per minute, but the differences are not significant between reactor materials

outside this range. Ethane production depends upon three reactions after glycerol pyrolysis: acetaldehyde reduction and dehydration, followed by ethylene hydrogenation. Therefore, the impact of the catalytic effect of Inconel-625 might be observed as less profound. In addition, ethane is a minor product.

The productivity of each gas is approximately linear with glycerol molar flow rates. However, in the case of H_2, CO, and CO_2, the linear tendency breaks around 0.2 mol/min, adopting a lower slope when the residence time of the substrate decreases.

4. Dynamical interpretation of gas production in terms of heat exchanger-reactor compartments

Guo et al. [18] fully characterized the glycerol SCWG pathways (Eqs. (1) and (4)). The glycerol anoxic pyrolysis reactions are endothermic [28] and irreversible, providing H_2, CO, CO_2, H_2O, and a C2 intermediate (Eq. (1)), which is acetaldehyde [8,16,17]. In these cases, reaction rates have order one with respect to glycerol and do not require water as a reagent.

$$\begin{aligned} &C_3H_8O_3 \xrightarrow{k_1} CO_2 + 2H_2 + CH_3CHO \; k_1(600^\circ C) \\ &= 15.24 \; min^{-1} \; E_{a1} = 53 \pm 2 \; kJ/mol \end{aligned}$$

$$\begin{aligned} &C_3H_8O_3 \xrightarrow{k_2} CO + H_2 + H_2O + CH_3CHO \; k_2(600^\circ C) \\ &= 9.48 \; min^{-1} \; E_{a2} = 60 \pm 3 \; kJ/mol \end{aligned} \quad (1)$$

Considering an ideal isothermal plug flow (IIPF) reactor, glycerol pyrolysis conversion is related to the residence time (T) according to an integral relation (Eq. (2)), adapted from Levenspiel [32]:

$$T = \int_0^{X_f} \frac{dX_g}{[k_1(1+\varepsilon_1 X_g) + k_2(1+\varepsilon_2 X_g)](1-X_g)} \quad (2)$$

Where T is the residence time, X_g is the glycerol conversion towards pyrolysis, X_f is the final glycerol conversion, and ε is the expansion factor of each reaction, considering the molar volume (V_m) stoichiometric change of each reaction (Eq. (3)).

$$\varepsilon = \frac{\sum_{j=1}^{N_{prod}} (\nu_j \cdot V_{m,j})}{V_{m,gly}} \quad (3)$$

Acetaldehyde conversion pathways (Eq. (4)) are also irreversible [8,18]. It is observed that the thermal decomposition into CO and CH_4 (pathway 5) has much lower activation energy than the hydrolytic pathways 3 and 4, which produce hydrogen, carbon monoxide, and carbon dioxide; thus, pathway 5 is expected to be the preferred route for the conversion of the acetaldehyde intermediate [39]. Yet, considering the water content inside the reactor, closer to water molar density, hydrogen production from acetaldehyde should be faster than that of glycerol. However, acetaldehyde pyrolysis is limited by glycerol conversion, and the observed C2 hydrocarbon products point out to a highly competitive acetaldehyde hydrogenation.

$$\begin{aligned} &CH_3CHO + H_2O \xrightarrow{k_3} 2CO + 3H_2 \; k_3(600^\circ C) \\ &= 36.7 \; M^{-1} \; min^{-1} E_{a3} = 114 \pm 4 \; kJ/mol \end{aligned}$$

$$\begin{aligned} &CH_3CHO + 3H_2O \xrightarrow{k_4} 2CO_2 + 5H_2 \; k_4(600^\circ C) \\ &= 24.5 \; M^{-1} \; min^{-1} \; E_{a4} = 110 \pm 2 \; kJ/mol \end{aligned}$$

$$CH_3CHO \xrightarrow{k_5} CO + CH_4 \; k_5(600^\circ C) = 84 \; min^{-1} \; E_{a5} = 67 \pm 2 \; kJ/mol \quad (4)$$

If the hypotheses of the IIPF were fulfilled, the estimated residence times would be sufficient to achieve a production of 2.5 to 7 moles of hydrogen per mole of glycerol. Observed hydrogen productions are around 1% of the ideal value. Devising a compartment model is a reasonable approach to understand this apparent discrepancy in productivity.

The expected temperature profile (Fig. 4 - above) suggest that a non-reactive heat exchanger in series with a reactor with partial active volume (Fig. 4 - below) is the simplest compartment model that could address a tubular reactor electrically heated from the outside, treating a cold stream that needs to be warmed up to relevant temperatures for gasification. In this case, we will consider that there will be sensible reactivity only after the system overpasses the critical temperature of water ($T_{C,\ H2O}$ = 386 °C) and glycerol ($T_{C,\ gly}$ = 452 °C) at the mean operating pressure of 25 MPa. Above those temperatures, it can be considered that the system can react towards gasification in supercritical conditions.

The velocity and thermal profiles usually differ from an ideal plug flow in the vicinity of the wall. However, since there is an unrestricted mass transfer in the radial direction, there is no difference in residence times between the two zones of the reactive compartment. Therefore, heat exchange calculations of the fluid flowing through the tubular reactor are conducted to estimate the temperature profiles and, therefore, understand the distribution of the active volumes within the equipment. As discussed earlier, thermocouples provide the temperature of the outer surface of the reactor during the process of gasification. The temperature control setpoint is defined at the center of the outer reactor wall, and it is set at 610 °C, fluctuating less than 2% throughout the experiments (Temp. 2 - Fig. 5). The thermocouple located downstream (Temp. 3 - Fig. 5) is observed to differ less than 5% from the setpoint temperature. On the other hand, the thermocouple is located towards the entrance of the reactor (Temp. 1 - Fig.5) is 90 °C lower than the setpoint, indicating the effect of the cold inlet on the reactor wall temperature.

Knowing the outer wall temperature makes it possible to estimate the thermal axial profiles for the reactor wall and the fluid. By knowing the thermal conductivity (λ) of the reactor materials and the thermophysical properties of the fluid components, the heat transfer rate through the reactor wall can be estimated. A linear gradient in the axial direction is assumed on the outer wall around the first thermocouple. Both the thermal conductivities of SS-316 and Inconel-625, λ_w, follow a fairly linear relationship below their melting points [3,27].

Thermophysical water and product gases are sourced from the National Institute of Standards and Technology open online database [40]. Glycerol liquid phase density, thermal conductivity, and heat capacity at 25 MPa are determined from equations reported in the recent literature [47]. Glycerol and acetaldehyde vapor properties are estimated by following the generalized Lydersen corresponding states method [43]. Since the vapor pressure of glycerol-water mixtures follows a fairly linear relationship with composition [65], densities and heat capacities of the solutions can be approximated as the weighted mean of the individual pure component values.

The axial temperature profile at the inner wall of the reactor (T_{wi}) can be estimated stepwise by performing an energy balance on a discrete wall element [26]. Considering that the tube is submerged in a thermal well and the heat flux is uniform around a sufficiently small discrete tube element, the rectangular rule numerical recipe described in Eq. (5) can be utilized:

$${}^{z+\delta z}T_{wi} = \left(\frac{\lambda_w \cdot {}^{z}T_{we}}{r_e - r_i} + \frac{h_c \cdot {}^{z}T_{bulk}}{\ln(r_e/r_i)}\right) \Big/ \left(\frac{\lambda_w}{r_e - r_i} + \frac{h_c}{\ln(r_e/r_i)}\right) \quad ; z \in (0; L_R) \quad (5)$$

Where r_e and r_i are the external and the internal radius of the tube; L_R is the reactor length; λ_w is the mean thermal conduc-

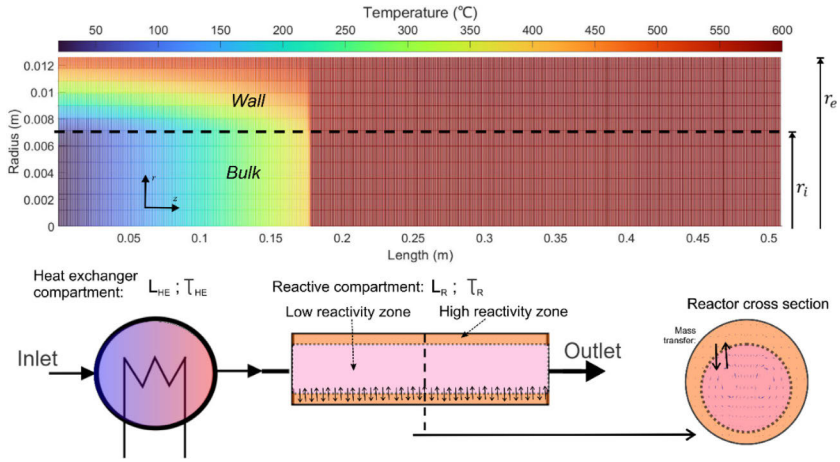

Fig. 4. Reactor temperature profile (above) for 10% (w/w) of glycerol and 375 mL/min flowrate. Heat exchange - mixed flow reactor compartment model (below).

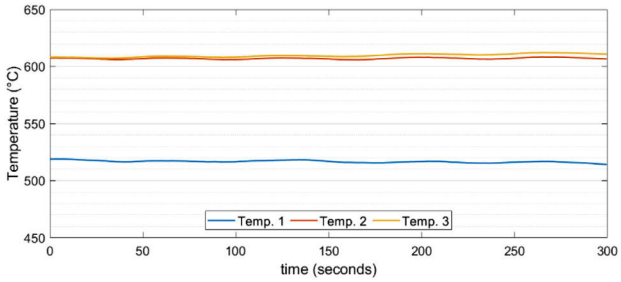

Fig. 5. Temperature measurement at the outer wall of the reactor.

tivity of the wall material, linearly interpolated between the wall external temperature (T_{we}) and the inner wall temperature (T_{wi}). The dominant heat transfer mechanism within the fluid is convective since the Nusselt number is over 200 at the inlet and can range up to 10,000 at the outlet. To estimate the heat transfer coefficient (h_c - Eq. (6)), the Sieder-Tate equation [43,53] is employed within subcritical temperatures since the Reynolds number is lower than 2000 under that condition, even considering the acceleration of the stream due to thermal expansion. Yamagata correlation is found most suitable to estimate the h_c parameter at supercritical temperatures [30,62].

$$h_c = \begin{cases} 1.86 \cdot Re^{1/3} Pr^{1/3} \left(\frac{4r_i}{L}\right)^{1/3} \left(\frac{\mu_{bulk}}{\mu_w}\right)^{0.14} \left(\frac{\lambda_{mix}}{2r_i}\right) & \text{if } T_{bulk} < T_c)_{H2O} \\ 0.0135 \cdot Re^{0.8} Pr^{0.8} \cdot \left(\frac{\lambda_{mix}}{r_i}\right) & \text{if } T_{bulk} \geq T_C)_{H2O} \end{cases}$$
$$Re = \frac{2r_i \cdot u_z \cdot \rho_{mix}}{\mu_{mix}} \; ; \; Pr = \frac{\mu_{mix} \cdot C_{p,mix}}{\lambda_{mix}} \quad (6)$$

The fluid thermal conductivity (λ_{mix}), viscosity (μ_{mix}), heat capacity ($C_{p,mix}$), density (ρ_{mix}), and thus the Prandtl number is estimated from the thermophysical properties of the glycerol-water mixture at the mean fluid temperature (T_{bulk}), which is recalculated in every step following Eq. (7):

$$^{z+\delta z}T_{bulk} - {}^{z}T_{bulk} = \left(\frac{\lambda_w 2\pi r_i \cdot ({}^{z}T_{we} - {}^{z}T_{wi})}{r_e - r_i} \cdot \frac{\delta z}{u_z}\right) \Big/ \left(\pi r_i^2 \cdot \rho_{mix} \cdot C_{p,mix}\right) \quad ; z \in [0; L_{Tube}) \quad (7)$$

From detailed investigations on heat transfer in horizontal tubes involving water at supercritical conditions [15,52,63], buoyancy effects have a minor impact on the radial temperature profile in tubes of inner diameters smaller than 20 mm, so a fully developed plug flow can be considered in the bulk annulus. The Reynolds number is recalculated, taking into account the evolution of the thermophysical properties of the glycerol-water mixture and the increment of the mean fluid velocity (u_z) due to thermal expansion. After the system overpasses the critical water temperature, the fluid velocity can be considered constant since the outer wall temperature, and the inner temperature does not differ significantly. Fig. 6 illustrates the result of the estimations in the form of mean axial temperature profiles, considering axial steps (δz) of one millimeter, and the initial condition $^{z=0}T_{wi} = {}^{z=0}T_{bulk}$. An inlet temperature of 50 °C was estimated by thermal imaging.

The calculated bulk temperature differs significantly from the estimated inner wall temperature only at the first tenth of the re-

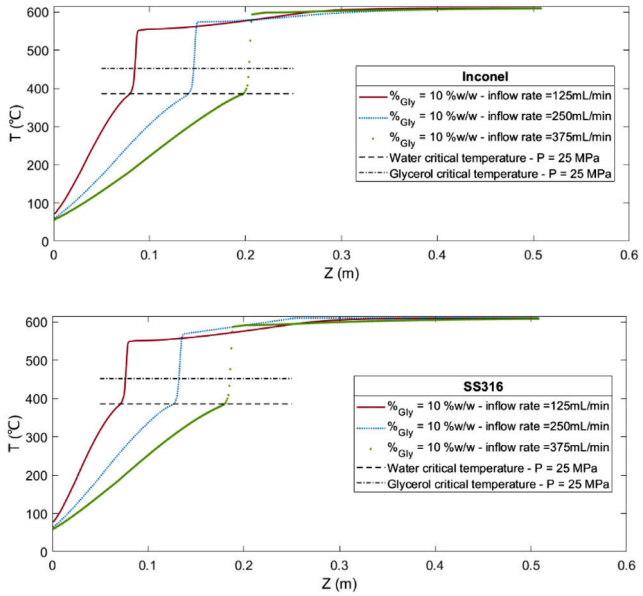

Fig. 6. Axial profiles of the temperature inside both reactors: Inconel-625 (above) and SS-316 (below).

actor length in both cases. This result is in concordance with the findings of Yukananto et al. [64] in their detailed simulation of SCWG in a tubular reactor, in which the thermal profile presents a radial gradient at the beginning of the operation and swiftly become an ideal plug flow both in terms of velocity and temperature distribution.

Residence time distributions can be estimated considering that the velocity profile is affected by the thermal expansion of the fluid (Eq. (8)), obeying the continuity condition of a non-isothermal incompressible flow as follows:

$$u_{(z+\delta z)} = u(z) \cdot \frac{\rho_{mix}|_{z+\delta z T_{bulk}}}{\rho_{mix}|_{z T_{bulk}}} \tag{8}$$

Where $\rho_{mix}|_{z+\delta z T_{bulk}}$ and $\rho_{mix}|_{z T_{bulk}}$ are the reacting mixture densities evaluated at the axial slice outlet temperature and inlet temperature, respectively. The finite axial differential is chosen so the fluid velocity can be considered constant in every slice, avoiding complex iterative sub-routines. Therefore, the time step is simply $\delta z/u(z)$.

Fig. 7 illustrates the temperature time evolution of the fluid inside each reactor, considering the density variation with temperature. The obtained temperature profile in the vicinity of the critical point is similar to the results obtained by Sallevelt et al. [50].

At supercritical conditions, the Reynolds number increase abruptly. The Prandtl number is corrected by turbulence, under the suggestion of Bird et al. [6]. Water is the dominant driver of thermal behavior in supercritical conditions. Since the observed glycerol conversion and the residence time at supercritical temperatures are low, the effect of the composition variability on the results is negligible.

The approximation utilized to estimate the axial temperature profiles of Fig. 6 and the temperature time evolution of Fig. 7 is based on the assumption that the thermal expansion of the fluid is intense enough to neglect the effect of back mixing and axial diffusion. However, it provides insights that enforce the heat exchanger - reactor compartment hypothesis to describe glycerol SCWG under continuous operation. In addition, it also points out the importance of the reactor wall material properties beyond the classical mechanical endurance and corrosion resistance. Differences are slight in space, but the impact of the thermal conductivity of the reactor wall material on the heat transfer rate can be appreciated in the residence time distribution on the proposed compartments. It can be seen that the material has some extent of influence on the compartment distribution, being the heat exchange compartment up to 15% longer. In addition, Inconel-625 requires longer residence times to reach the critical temperature. It is explained by the lower thermal conductivity of Inconel-625 compared with SS-316 when the fluid is colder than the oven temperature. In supercritical conditions, wall thermal conductivities do not differ greatly. Also, the heat transport within the supercritical fluid is highly efficient, so the residence times only depend upon the initial flow rate. Table 1 summarizes the axial distribution of the heat exchanger and the reactor compartments with their respective residence times.

By combining the kinetic parameters provided by Guo et al. [18] and the integral relation described in Eq. (2), the required residence time of an IIPF reactor can be estimated. The direct computation of Eq. (3) is implemented in Wolfram|Alpha as definite integrals series. Calculation results are shown in Fig. 8 for different temperatures within the supercritical window of the reactor.

The compartmentalized approach allows the interpretation of the observed conversion as a product of efficiencies (Φ) correcting an ideal reference conversion [14,32]. Glycerol pyrolysis is highly endothermic [28,58,59], which points naturally at the reactor wall area as the most reactive zone since it is localized closest to the

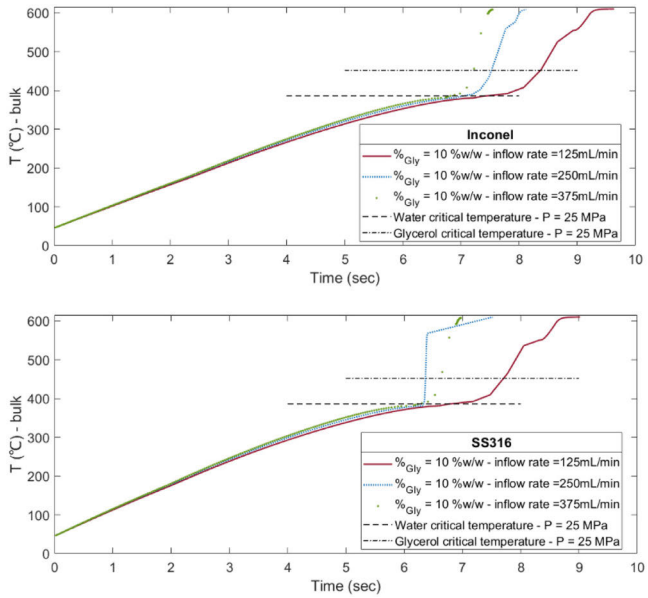

Fig. 7. Temperature time evolution inside each reactor: Inconel-625 (above) and SS-316 (below).

Table 1
Estimation of the compartment longitudes and their respective residence times.

Inflow rate (mL/min)	Glycerol content (% w/w)	Inconel-625		SS-316		Inconel-625		SS-316	
		L_{HE} (m)	L_R (m)	L_{HE} (m)	L_R (m)	T_{HE}(s)	T_R(s)	T_{HE}(s)	T_R(s)
125	2,5	0,08	0,43	0,08	0,43	7,5	2,4	6,8	2,4
250	2,5	0,15	0,36	0,13	0,37	7,1	1,0	6,4	1,1
375	2,5	0,20	0,30	0,19	0,32	7,0	0,6	6,2	0,6
125	5	0,08	0,43	0,07	0,43	7,4	2,4	6,8	2,4
250	5	0,15	0,36	0,13	0,38	7,1	1,0	6,4	1,1
375	5	0,20	0,30	0,18	0,32	6,8	0,6	6,2	0,6
125	10	0,08	0,43	0,07	0,43	7,2	2,4	6,6	2,4
250	10	0,15	0,36	0,13	0,38	6,9	1,0	6,3	1,1
375	10	0,20	0,31	0,18	0,32	6,7	0,6	6,2	0,6

heat source. Thus, the thermal boundary layer (Δ_T) can be considered the active zone of the reactor compartment, which size can be related to the fluid dynamic viscous layer (Δ_{FD}) by the $Pr^{-1/3}$ rule ([6] p.389). In turn, it is assumed that $\Delta_{FD}/r_i = 13.77 \cdot Re^{-1/2}$ if we consider the thickness of the buffer zone [6] p.166; [25] p.504; [33,66]), where $Re = 2r_i\rho_{mix}u_z/\mu_{mix}$ and the fluid properties are determined at the inner wall temperature. Therefore, it is possible to define a reactive zone ratio (Φ_R) following Eq. ((9):

$$\Phi_R = \frac{\Delta_T}{r_i} = \frac{\Delta_{FD}}{r_i \cdot Pr^{\frac{1}{3}}} \approx \frac{13.77}{Re^{\frac{1}{2}} \cdot Pr^{\frac{1}{3}}} \quad T_{bulk} \rightarrow T_{wi}$$

		Glycerol content (%w/w)		
	Φ_R	2.5%	5.0%	10%
Initial Flowrate mL/min	125	0.035	0.034	0.034
	250	0.024	0.024	0.024
	375	0.020	0.020	0.019

(9)

From the result determined in Eq. (9), only 2 to 3% of the reactor compartment is effectively utilized. Φ_R is observed almost independent of the glycerol content since it has a very slight impact on the Prandtl in supercritical conditions. In contrast, the initial flow rate impact on Φ_R is more noticeable since the velocities range under thermal expansion greatly influences the final Reynolds number.

After defining the reactive zone, it is worth assessing the mass exchange between the highly reactive zone and the bulk. Fluid to wall mass transfer efficiency (Φ_{MT}) can be addressed by considering that the heat transfer Stanton number (St_h) is equal to the mass transfer Stanton number (St_m), both defined in Eq. (10). It is a well-established methodology to estimate mass transfer coefficients from heat transfer information, known as the Reynolds analogy ([36] p.351).

$$St_h = \frac{Nu_i}{Re \cdot Pr}; \; Nu_i = \frac{h_c \cdot r_i}{\lambda_{mix}}; \; St_m = \frac{\widehat{K_m}}{G_m}; \; St_h = St_m \quad (10)$$

G_m is the molar flux (in moles per unit time per cross-section area) and $\widehat{K_m}$ is the global mass transfer coefficient (in moles per unit time per boundary layer area). Nusselt number (Nu_i) is defined as the ratio between the convective heat transfer rate and

Table 2
Mass transfer and kinetic quantities relevant to the Damköhler number estimation.

Glycerol % w/w	Inflow rate (mL/min)	St	G_m(mol/(min · m²))	a_w(m²/m³)	$k_1 + k_2$(min⁻¹)	C_o(M)	Da_I
2.5	125	0.0015	373	278	24.72	0.019	$4{\cdot}10^{-06}$
2.5	250	0.0016	682	278	24.72	0.019	$5{\cdot}10^{-06}$
2.5	375	0.0018	1166	278	24.72	0.019	$6{\cdot}10^{-06}$
5	125	0.0015	373	278	24.72	0.038	$4{\cdot}10^{-06}$
5	250	0.0016	682	278	24.72	0.038	$5{\cdot}10^{-06}$
5	375	0.0018	1166	278	24.72	0.038	$6{\cdot}10^{-06}$
10	125	0.0015	373	278	24.72	0.076	$4{\cdot}10^{-06}$
10	250	0.0016	689	278	24.72	0.076	$5{\cdot}10^{-06}$
10	375	0.0018	1177	278	24.72	0.076	$6{\cdot}10^{-06}$

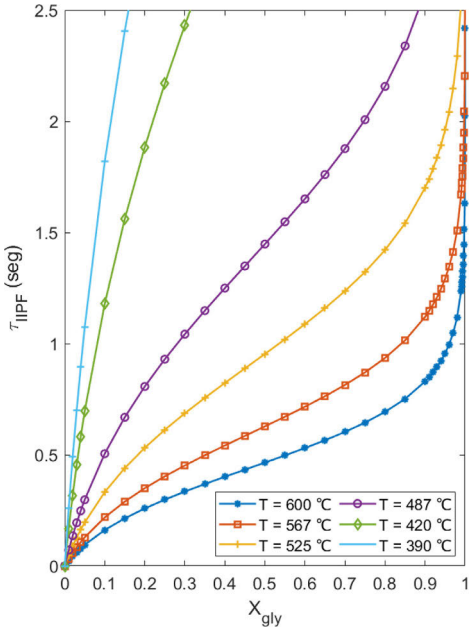

Fig. 8. Required residence time vs. conversion for glycerol pyrolysis in an IIPF reactor.

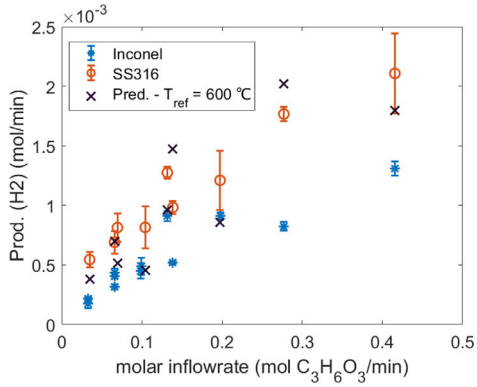

Fig. 9. Comparison between predicted and experimental values of H_2 production.

the internal conductive heat transfer rate at the bulk temperature. The obtained Stanton numbers are aligned with those predicted by heat transfer correlations in supercritical flow through tubes [48,60]. The relation between the reaction rate to the convective mass transfer rate, known as the first Damköhler number (Da_I) is a measure that allows verifying mass transfer limitations [14]. Since the glycerol pyrolysis reactions are both first order with respect to glycerol Eq. (1)), the Damköhler number expression follows Eq. ((11):

$$Da_I = \frac{(k_1 + k_2) \cdot C_o}{\widehat{K_m} \cdot a_w} = \frac{(k_1 + k_2) \cdot C_o}{St \cdot G_m \cdot 2 \cdot r_i^{-1}} \tag{11}$$

Where k_1 and k_2 are the reaction rates of the glycerol pyrolysis pathways Eq. (1)), and a_w is the reactor wall surface to volume ratio. If the reaction were faster than the mass transfer mechanism, it would certainly impact the gasification efficiency. Table 2 summarizes the comparison between the mass transfer and reaction rates, showing that the Da_I is much lower than one, which means that there are no mass transfer limitations between the bulk and the wall. In summary, the predicted production of the j-th gas component (F_{prod_j}) from glycerol SCWG is expressed in Eq. ((12):

$$F_{prod_j} = F_{Gly.in} \cdot \overline{\nu_{prod_j <- gly}} \cdot \Phi_R \cdot \Phi_m \cdot {}^{Tref}X_{gly}(T_R) \tag{12}$$

Where ${}^{Tref}X_{gly}(T_R)$ is a reference conversion calculated from the IIPF curves at the residence time of the reactor compartment. Since the Damköhler number is several orders of magnitude lower than one for every operational condition, it can be considered that $\Phi_m = 1$. $F_{Gly.in}$ is the glycerol molar flow rate at the entrance of the reactor compartment. Table 3 summarizes the reference conversions within the thermal window corresponding to reactor materials and the explored volumetric inflow rates.

The logarithmic mean of the temperature within the thermal boundary layer suggests 600 °C as the reference temperature. Fig. 9 shows the hydrogen production predicted by the compartment model in comparison with the experimental values. It can be readily seen that the model captures the mean trend. van Bennekom et al. [58] found that the glycerol conversion increased when increasing temperature and residence time in supercritical water reforming in an Incoloy-825 reactor. The conversion was nearly independent of the feed concentration, which is in line with the current results. Differences between experimental and predicted values are expected mostly due to density fluctuations introduced by the action of pressure regulators. In the vicinity of the critical point, water density and heat capacity change steeply, greatly influencing the fluid mechanics and the heat transfer rate of the system [45], which in turn could distort the expected reactivity depending on the magnitude of the pressure fluctuations [10].

Table 3
IIPF conversions at reference temperatures as a function of the volumetric inflow rate for both reactor materials.

Reactor Material	Inflow rate (mL/min)	$^{390^\circ C}X_{gly}$	$^{420^\circ C}X_{gly}$	$^{487^\circ C}X_{gly}$	$^{525^\circ C}X_{gly}$	$^{567^\circ C}X_{gly}$	$^{590^\circ C}X_{gly}$	$^{600^\circ C}X_{gly}$
Inconel-625	125	0.15	0.30	0.82	0.98	~1	~1	~1
Inconel-625	250	0.05	0.08	0.30	0.55	0.85	0.90	0.97
Inconel-625	375	0.03	0.04	0.13	0.25	0.45	0.55	0.7
SS-316	125	0.15	0.30	0.82	0.98	~1	~1	~1
SS-316	250	0.05	0.10	0.30	0.60	0.85	0.91	0.97
SS-316	375	0.03	0.04	0.13	0.25	0.45	0.55	0.7

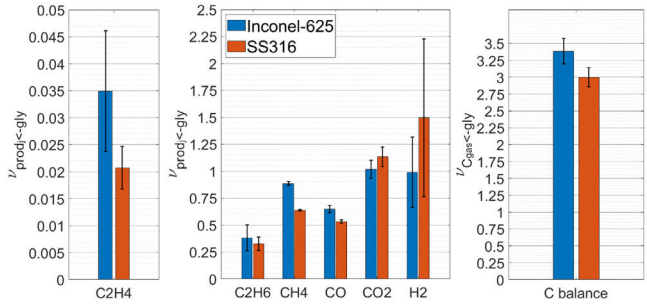

Fig. 10. Empirical stoichiometric coefficients and carbon balance.

If only the glycerol pyrolysis reactions are considered, the stoichiometric value $\overline{\nu_{H_2<-gly}} = 1.5$ can be used since pathways 1 and 2 of Eq. (1) can be considered equiprobable for having similar activation energies and rates. A fair agreement exists between the model and the experimental results regarding orders of magnitude in this context. However, a coincidence should not be considered solely as proof of mechanism. Most of the products can subsequently be converted. This is especially the case of hydrogen, involved in the methanation of carbon monoxide and the reduction of the acetaldehyde intermediate. Therefore, the prediction based on the stoichiometry of glycerol gasification might differ from the experimental results. The ratio between the predicted values at $\nu = 1$ and the experimental results could be employed to determine global stoichiometric coefficients ($\overline{\nu_{prod_j<-gly}}$) summarized in Fig. 10, which are useful to understand the influence of the operational conditions on the selectivity of glycerol SCWG towards gaseous products.

5. Influence of the wall material on the continuous SCWG productivity

The stoichiometric coefficients obtained for the SS-316 reactor are reasonable if considered non-catalytic towards hydrogenation based on carbon balance. The atomic balance for hydrogen in SS-316 shows the expected H_2 production that would come exclusively from the glycerol pyrolysis pathways. However, the error of the prediction shown in Fig. 10 reflects the difficulty of describing the behavior of hydrogen gas. The depletion of CO by water-gas shift (Pathway 6, Eq. (13)) and methanation (Pathway 7, Eq. (14)) reactions fairly explain that the CO_2 to CO ratio is about 40% less than expected. According to the extensive characterization performed by Guo et al. [18] in similar working conditions, both reactions are considered slightly reversible and have similar activation energies [49].

Moreover, water-gas shift reaction natural displacement towards CO consumption is enhanced by the saturation environment due to the presence of a high concentration of water [34]. Moreover, Pathway 6 is catalyzed by nickel, which impact over glycerol gasification is well characterized by Iliuta and Iliuta [23]. On the other hand, Pathway 7 is limited by hydrogen, although it is catalyzed to a lesser extent by the presence of nickel.

$$CO + H_2O \underset{k_{-6}}{\overset{k_6}{\rightleftarrows}} CO_2 + H_2$$

$$\begin{aligned} k_6(600^\circ C) &= 0.21\ M^{-1}\ min^{-1} & E_{a6} &= 77\ kJ/mol \\ k_{-6}(600^\circ C) &= 0.009\ M^{-1}\ min^{-1} & E_{a-6} &= 145\ kJ/mol \\ k_{6*}(600^\circ C; cat) &= 4\ M^{-1}\ min^{-1} Kg_{Ni}^{-1} & E_{a6*} &= 15\ kJ/mol \end{aligned} \quad (13)$$

$$CO + 3H_2 \underset{k_{-7}}{\overset{k_7}{\rightleftarrows}} CH_4 + H_2O$$

$$\begin{aligned} k_7(600^\circ C) &= 59.9\,M^{-1}\ min^{-1} & E_{a7} &= 74\ kJ/mol \\ k_{-7}(600^\circ C) &= 0.006\,M^{-1}\ min^{-1} & E_{a-7} &= 83\ kJ/mol \\ k_{7*}(600^\circ C; cat) &= 7.2\,M^{-1}\ min^{-1} Kg_{Ni}^{-1} & E_{a7*} &= 31\ kJ/mol \end{aligned} \quad (14)$$

Carbon balance was successfully captured for the case of using SS-316 as wall material, enforcing the idea of acetaldehyde total conversion at the active zone of the reactor compartment. The carbon imbalance observed in Inconel-625 might be assignable to nickel susceptibility to either altering the mechanism of glycerol conversion to alternative intermediates or to coke formation [21,31,56,58,67,68], which could have been accumulated over duty. However, coke formation from CO is also limited by the rather low concentration of hydrogen. It is observed that a residence time is required on the order of hours to obtain measurable amounts of carbon [41,42], mostly because it implies hydrogen consuming polymerization reactions [57]. Moreover, it is well known that nickel catalyze carbon SCWG [67], and the excess of supercritical water inhibits the formation of carbon.

$$CO + H_2 \underset{fast}{\overset{slow}{\rightleftarrows}} C + H_2O \quad (15)$$

Inconel-625 seemingly depletes the produced hydrogen, at least partially; its high nickel content is likely accelerating subsequent pathways that consume formerly produced hydrogen. Methane productivity is favored when Inconel-625 is employed as reactor material, coinciding with its catalytic effect to the detriment of hydrogen productivity. Pathways 3 and 4 of Eq. (4) are considered

equiprobable due to presenting similar activation energies (114 and 110 kJ/mol, respectively), which are less probable than pathway 5 (67 kJ/mol). Therefore, it is unclear if the higher methane relation can be attributed to methanation activity or if the acetaldehyde pyrolysis (pathway 5 in Eq. (4)) is favored at the high nickel content reactor wall. In addition, acetaldehyde hydrogenation reactions are very fast [54], present even lower activation energies than pathway 5 (Eq. (4)), and are favored at high pressures [5]. Thus, methane and C2 hydrocarbon production suggest that the aldehyde intermediate is mostly converted without producing hydrogen.

Ethylene is obtained from the reduction of the acetaldehyde intermediate, followed by dehydration (Eq. (16)). Reduction of acetaldehyde can be achieved either by hydrogenation (Pathway 8a) or by disproportionation reaction (Pathway 8b) involving remnant glycerol as hydrogen donor from its hydroxyl groups [55]. Eq. (16) shows estimations of uncatalyzed acetaldehyde reduction pathways, in which activation energies come about to be fairly comparable to Pathways 3 and 4. Although ethylene is observed as a minor product, it is another indicator of the Inconel-625 catalytic activity, not only due to their dominant nickel presence catalyzing hydrogenations [11] but also chromium content could enhance the activity towards Pathway 8b [55]. It is worth recalling that the major portion of Inconel-625 is made of nickel (61.4%) and chromium (21%), followed by molybdenum (8.5%), iron (4.5%), and niobium (3.8%), among several other trace elements. Moreover, chromium presence is incremented on the surface of Inconel alloys when exposed to corrosive environments, such as supercritical water [19,61]. Also, water acts as a catalyst of ethanol steam reforming and dehydration in supercritical conditions [4], which is worth mentioning, although this affects both reactor materials similarly.

$$\begin{matrix} CH_3CHO + H_2 \overset{k_{8a}}{\rightarrow} C_2H_5OH \overset{fast}{\rightarrow} (CH_2)_2 + H_2O & E_{a8a} \sim 86\ kJ/mol \\ CH_3CHO + C_3H_8O_3 \overset{k_{8b}}{\rightarrow} & E_{a8b} \sim 100\ kJ/mol \end{matrix} \quad (16)$$

Overall production of C2 hydrocarbons seems to be enhanced by more than 50% when the empirical stoichiometric coefficients of SS-316 and Inconel-625 are compared. Ethylene hydrogenation (Eq. (17)) kinetic data available in the literature fairly explains the excess observed in the productivity of ethane, despite the low availability of ethylene and hydrogen. The nickel surface lowers the activation energy for ethylene hydrogenation abruptly (Pathway 9a, [20])compared to an iron surface (Pathway 9b,[35]).

$$(CH_2)_2 + H_2 \begin{matrix} \overset{k_{9a}}{\rightarrow} \\ \overset{k_{9b}}{\rightarrow} \end{matrix} (CH_3)_2 \begin{matrix} E_{a9a} = 23\ kJ/mol \\ E_{a9b} = 72\ kJ/mol \end{matrix} \quad (17)$$

Gasification reaction networks are naturally complex, especially for hydrogen. Pinkard et al. [45] implemented in-line Raman spectroscopy, which allowed to faster follow the continuous gasification productivity of primary alcohols without the issue of gas sampling; it was found that the dispersion of the observed hydrogen productivity can be as high as 50% in the case of a simpler model compound such as ethanol. The chaotic behavior of hydrogen comes from its high reactivity involved in most subsequent pathways as a reagent or product. Eq. (18) summarizes the contributions for hydrogen productivity, where the individual pathways will be influenced by several factors, such as pressure fluctuations [10], mixing regimes [46], and catalytic activity of the reactor wall surface, especially in the case of Pathways 5 to 9 within a reactor made of a highly complex composition, such as the Inconel family, among other nickel-based alloys made for high-pressure and corrosion resistance [19,61].

$$\frac{dC_{H2}}{dt} = (2k_1 + k_2)C_{gly} + [(3k_3 + 5k_4)C_{int} + k_6C_{CO}]C_w - \left[3k_7C_{CO} + k_{8a}C_{int} + k_9C_{(C2H4)}\right]C_{H2} \quad (18)$$

The manifest tendency of Inconel-625 to facilitate hydrogen consumption mechanisms is well known, and it has been observed in the present work. However, nickel-rich alloys are preferred despite being ten times more expensive than stainless steel [1,2] for their resistance to high pressures and corrosion [3]. Retarded heat transfer can be easily handled by adjusting the length and wall thickness of the reactor. On the other hand, moderating undesired catalytic effects is more complex. In an effort to increase the gasification efficiency of Inconel-625 towards hydrogen production, an initiative such as pretreatment of the inner reactor with hydrogen peroxide might have positive results in terms of reproducibility [7]. Reductive pretreatment, such as hydrogenolysis of the wall material, improved gasification efficiencies [57]; however, the supercritical water re-oxidizes the nickel metal. Surface modification of heavy-duty resistant nickel-based alloys focused on controlling undesired hydrogen-consuming pathways is currently a very active topic in the field of Supercritical Water Gasification [29,45].

6. Conclusions

Supercritical Water Gasification of glycerol was carried out in laboratory-scale tubular reactors made of industrially relevant materials, such as Stainless Steel 316 and Inconel-625. The reactors were operated in a continuous mode at 25 MPa inside an electric oven set at a temperature of 610 °C. Experiments were conducted at molar inflow rates between 0.03 and 0.4 mol glycerol per minute with water to substrate relation between 10 and 50.

An integral model was implemented considering the tubular equipment as a heat exchanger compartment in series with a wall reactor; this conception captures the global dynamics of the system. Heat transfer characteristics of the reactor wall had little influence on the relative size of the compartments. On the other hand, thermal conductivity has a significant impact on the residence time distribution. Inconel-625 transfers heat 20% slower than SS-316, so it takes a longer time to reach the supercritical condition. Thus, the heat transfer characteristics of the wall material have to be considered in the sizing of the reactor. The length of the heat transfer portion enlarges when the fluid velocity increases. Glycerol content is observed to have an inappreciable influence on both compartment sizes and residence time distribution. Initial flow rates have a modest effect on the residence time distribution.

Overall efficiency was successfully estimated considering that the active zone of the reactor compartment is inside the thermal boundary layer adjacent to the tube wall. First Damköhler numbers in the order of 10^{-6} point to a highly efficient mass transfer between the active and low reactivity zones inside the reactor compartment. Considering that the temperature distribution within the reactor compartment does not vary significantly, the fluid velocity has the most sensible impact on the thermal boundary layer thickness and thus on the reactor efficiency.

Hydrogen productivity was fairly predicted despite its complex behavior. Beside explaining gasification productivity in continuous non-isothermal operation, this tool allows obtaining empirical stoichiometric coefficients to understand the gaseous product output. Atomic balance of carbon, hydrogen, and oxygen suggests that the residence time on the active zone of the reactor compartment is enough for complete glycerol pyrolysis. Acetaldehyde intermediate is mostly converted to hydrocarbons and carbon monoxide. However, the reactor's active zone is just a fraction of the volume concentrated in the vicinity of the reactor wall, which explains the observed conversion and the remarkable effect of the reactor wall material on the hydrogen empirical stoichiometric coefficients. Using Inconel-625 as reactor wall material, methane, ethane, and ethylene productivities are enhanced, which is well explained by the hydrogenolysis and thermal decomposition of the acetalde-

hyde intermediate. Inconel-625 produces 50% more C2 hydrocarbons and 40% more CH_4, reducing a 50% the H_2 yield. The catalytic effect of Inconel-625 is detrimental to hydrogen productivity since it increases the rate of subsequent pathways that use the produced hydrogen as a reagent. The high amount of nickel content in Inconel-625 explains the majority of the difference between both reactor materials.

Declaration of Competing Interest

The authors declare that they have no known competing financial interests or personal relationships that could have appeared to influence the work reported in this paper.

CRediT authorship contribution statement

Gabriel Salierno: Formal analysis, Writing – original draft, Conceptualization, Methodology. **Fabrizio Marinelli:** Formal analysis, Data curation, Investigation. **Blaž Likozar:** Writing – review & editing, Visualization. **Niloufar Ghavami:** Writing – original draft. **Cataldo De Blasio:** Data curation, Writing – review & editing, Funding acquisition, Supervision, Project administration, Resources.

Acknowledgments

Financial support from Åbo Akademi University, Högskolestiftelsen i Österbotten (2804720/28600122), the Harry Schaumans Foundation (2804720/28002257), Suomen Kulttuurirahasto (00210970), and the Slovenian Research Agency (P2-0152) is gratefully appreciated.

References

[1] Alibaba.com, 2021a. Inconel-625 tubing [WWW Document]. URL https://www.alibaba.com/trade/search?fsb=y&IndexArea=product_en&Catld=&SearchText=inconel-625+tubes (accessed 9.29.21).
[2] Alibaba.com, 2021b. Stainless steel 316 tubing [WWW Document]. URL https://www.alibaba.com/trade/search?fsb=y&IndexArea=product_en&Catld=&SearchText=stainless+steel+316+tubing (accessed 9.29.21).
[3] T.R. Allen, Y. Chen, X. Ren, K. Sridharan, L. Tan, G.S. Was, E. West, D. Guzonas, Material performance in supercritical water, in: Comprehensive Nuclear Materials, Elsevier, 2012, pp. 292–338, doi:10.1016/B978-0-08-102865-0.00115-1.
[4] T. Arita, K. Nakahara, K. Nagami, O. Kajimoto, Hydrogen generation from ethanol in supercritical water without catalyst, Tetrahedron Lett. 44 (2003) 1083–1086, doi:10.1016/S0040-4039(02)02704-1.
[5] T. Bentz, F. Striebel, M. Olzmann, Shock-tube study of the thermal decomposition of CH $_3$CHO and CH $_3$CHO + H Reaction, J. Phys. Chem. A 112 (2008) 6120–6124, doi:10.1021/jp802030z.
[6] R.B. Bird, W.E. Stewart, E.N. Lightfoot, Transport Phenomena, 2nd. ed., Wiley, New York, 2007 Rev.
[7] N. Boukis, V. Diem, W. Habicht, E. Dinjus, Methanol reforming in supercritical water, Ind. Eng. Chem. Res. 42 (2003) 728–735, doi:10.1021/ie020557i.
[8] Y.C. Chang, A.N. Ko, Vapor phase reactions of acetaldehyde over type X zeolites, Appl. Catal. A Gen. 190 (2000) 149–155, doi:10.1016/S0926-860X(99)00293-8.
[9] C. De Blasio, G. Lucca, K. Özdenkci, M. Mulas, K. Lundqvist, J. Koskinen, M. Santarelli, T. Westerlund, M. Järvinen, A study on supercritical water gasification of black liquor conducted in stainless steel and nickel-chromium-molybdenum reactors, J. Chem. Technol. Biotechnol. 91 (2016) 2664–2678, doi:10.1002/jctb.4871.
[10] C. De Blasio, G. Salierno, A. Magnano, Implications on feedstock processing and safety issues for semi-batch operations in supercritical water gasification of biomass, Energies 14 (2021) 2863, doi:10.3390/en14102863.
[11] B. Dou, V. Dupont, G. Rickett, N. Blakeman, P.T. Williams, H. Chen, Y. Ding, M. Ghadiri, Hydrogen production by sorption-enhanced steam reforming of glycerol, Bioresour. Technol. 100 (2009) 3540–3547, doi:10.1016/j.biortech.2009.02.036.
[12] I.D. Dumbrava, C.C. Cormos, A. Imre-Lucaci, A.M. Cormos, CFD modelling of supercritical water reforming of glycerol for hydrogen production, Int. J. Hydrog. Energy (2021), doi:10.1016/j.ijhydene.2021.05.143.
[13] D.R. Emberson, J. Wyndorps, A. Ahmed, K.O. Pires Bjørgen, T. Løvås, Detailed examination of the combustion of diesel and glycerol emulsions in a compression ignition engine, Fuel 291 (2021) 120147, doi:10.1016/j.fuel.2021.120147.
[14] H.S. Fogler, Elements of Chemical Reaction Engineering, 5th ed., Prentice Hall, Boston, 2016.
[15] Z. Gao, J. Bai, Numerical analysis on nonuniform heat transfer of supercritical pressure water in horizontal circular tube, Appl. Therm. Eng. 120 (2017) 10–18, doi:10.1016/j.applthermaleng.2017.03.109.
[16] T. Gejo, H. Bitto, J.R. Huber, Quantum beats in the S1 dynamics of acetaldehyde, Chem. Phys. Lett. 261 (1996) 443–449, doi:10.1016/0009-2614(96)00991-8.
[17] Z. Geng, M. Zhang, Y. Yu, Theoretical investigation on pyrolysis mechanism of glycerol, Fuel 93 (2012) 92–98, doi:10.1016/j.fuel.2011.08.021.
[18] S. Guo, L. Guo, J. Yin, H. Jin, Supercritical water gasification of glycerol: intermediates and kinetics, J. Supercrit. Fluids 78 (2013) 95–102, doi:10.1016/j.supflu.2013.03.025.
[19] S. Guo, D. Xu, Y. Liang, Y. Li, J. Yang, G. Chen, D.D. Macdonald, Corrosion characteristics of typical Ni–Cr Alloys and Ni–Cr–Mo alloys in supercritical water: a review, Ind. Eng. Chem. Res. 59 (2020) 18727–18739, doi:10.1021/acs.iecr.0c04292.
[20] C.J. Heard, S. Siahrostami, H. Grönbeck, Structural and energetic trends of ethylene hydrogenation over transition metal surfaces, J. Phys. Chem. C 120 (2016) 995–1003, doi:10.1021/acs.jpcc.5b09735.
[21] T. Hou, S. Zhang, Y. Chen, D. Wang, W. Cai, Hydrogen production from ethanol reforming: catalysts and reaction mechanism, Renew. Sustain. Energy Rev. 44 (2015) 132–148, doi:10.1016/j.rser.2014.12.023.
[22] Y. Hu, M. Gong, X. Xing, H. Wang, Y. Zeng, C.C. Xu, Supercritical water gasification of biomass model compounds: a review, Renew. Sustain. Energy Rev. 118 (2020) 109529, doi:10.1016/j.rser.2019.109529.
[23] I. Iliuta, M.C. Iliuta, Biosyngas production in an integrated aqueous-phase glycerol reforming/chemical looping combustion process, Ind. Eng. Chem. Res. 52 (2013) 16142–16161, doi:10.1021/ie402114k.
[24] H. Jin, S. Guo, L. Guo, C. Cao, A mathematical model and numerical investigation for glycerol gasification in supercritical water with a tubular reactor, J.Supercrit. Fluids 107 (2016) 526–533, doi:10.1016/j.supflu.2015.06.028.
[25] W.M. Kays, M.E. Crawford, Convective Heat And Mass Transfer, 3rd ed., McGraw-Hill, New York, 1993 McGraw-Hill series in mechanical engineering.
[26] W.M. Kays, M.E. Crawford, B. Weigand, Convective Heat And Mass Transfer, 4th ed., McGraw-Hill Higher Education, Boston, 2005 McGraw-Hill series in mechanical engineering.
[27] R.J.M. Konings, R.E. Stoller, Comprehensive Nuclear Materials, Elsevier, San Diego, 2020.
[28] A.L. Leal, M.A. Soria, L.M. Madeira, Autothermal reforming of impure glycerol for H2 production: thermodynamic study including *in situ* CO_2 and/or H_2 separation, Int. J. Hydrog. Energy 41 (2016) 2607–2620, doi:10.1016/j.ijhydene.2015.11.132.
[29] C.S. ee, A.V. Conradie, E. Lester, Review of supercritical water gasification with lignocellulosic real biomass as the feedstocks: process parameters, biomass composition, catalyst development, reactor design and its challenges, Chem. Eng. J. 415 (2021) 128837, doi:10.1016/j.cej.2021.128837.
[30] X. Lei, H. Li, N. Dinh, W. Zhang, A study of heat transfer scaling of supercritical pressure water in horizontal tubes, Int. J. Heat Mass Transf. 114 (2017) 923–933, doi:10.1016/j.ijheatmasstransfer.2017.06.052.
[31] R.V. Lelo, G.K. Maron, A. Thesing, J.H. Alano, L. da Silva Rodrigues, B. da Silveira Noremberg, M.T. Escote, A. Valentini, L.F.D. Probst, N.L.V. Carreño, Vanadium effect over γ-Al_2O_3-supported Ni catalysts for valorization of glycerol, Fuel Process. Technol. 216 (2021) 106773, doi:10.1016/j.fuproc.2021.106773.
[32] O. Levenspiel, Chemical Reaction Engineering, 3rd ed., Wiley, New York, 1999.
[33] C. Lin, R. Moulton, G. Putnam, Mass transfer between solid wall and fluid streams. Interferometric measurements of concentration profiles in turbulent and streamline flow, Ind. Eng. Chem. 45 (1953) 640–646, doi:10.1021/ie50519a600.
[34] S. Liu, L. Guo, H. Jin, L. Li, G. Li, L. Yu, Hydrogen production by supercritical water gasification of coal: a reaction kinetic model including nitrogen and sulfur elements, Int. J. Hydrog. Energy 45 (2020) 31732–31744, doi:10.1016/j.ijhydene.2020.08.166.
[35] J.M.H. Lo, T. Ziegler, Theoretical studies of the formation and reactivity of C_2 hydrocarbon species on the Fe(100) surface, J. Phys. Chem. C 111 (2007) 13149–13162, doi:10.1021/jp073757m.
[36] W.L. McCabe, J.C. Smith, P. Harriott, Unit Operations of Chemical Engineering, 5th ed., McGraw-Hill, New York, 1993 McGraw-Hill chemical engineering series.
[37] E.M. Moghaddam, A. Goel, M. Siedlecki, K. Michalska, O. Yakaboylu, W. de Jong, Supercritical water gasification of wet biomass residues from farming and food production practices: lab-scale experiments and comparison of different modelling approaches, Sustain. Energy Fuels 5 (2021) 1521–1537, doi:10.1039/D0SE01635G.
[38] R. Moreira, F. Bimbela, L.M. Gandía, A. Ferreira, J.L. Sánchez, A. Portugal, Oxidative steam reforming of glycerol. a review, Renew. Sustain. Energy Rev. 148 (2021) 111299, doi:10.1016/j.rser.2021.111299.
[39] Y. Nagai, S. Morooka, N. Matubayasi, M. Nakahara, Mechanisms and kinetics of acetaldehyde reaction in supercritical water: noncatalytic disproportionation, condensation, and decarbonylation, J. Phys. Chem. A 108 (2004) 11635–11643, doi:10.1021/jp046117h.
[40] NIST Standard Reference Database 69: NIST Chemistry WebBook, 2021. Thermophysical properties of fluid Systems [WWW Document]. URL https://webbook.nist.gov/chemistry/fluid/ (accessed 5.5.21).
[41] C. Park, R.T.K. Baker, Carbon deposition on iron–nickel during interaction with ethylene–carbon monoxide–hydrogen mixtures, J. Catal. 190 (2000) 104–117, doi:10.1006/jcat.1999.2735.
[42] C. Park, R.T.K. Baker, Carbon deposition on iron–nickel during interaction with ethylene–hydrogen mixtures, J. Catal. 179 (1998) 361–374, doi:10.1006/jcat.1998.2226.

[43] R.H. Perry, D.W. Green, J.O Maloney, Perry's Chemical Engineers' Handbook, 7th ed., McGraw-Hill, New York, 1997.
[44] B.R. Pinkard, D.J. Gorman, K. Tiwari, J.C. Kramlich, P.G. Reinhall, I.V. Novosselov, Review of gasification of organic compounds in continuous-flow, supercritical water reactors, Ind. Eng. Chem. Res. 57 (2018) 3471–3481, doi:10.1021/acs.iecr.8b00068.
[45] B.R. Pinkard, D.J. Gorman, K. Tiwari, E.G. Rasmussen, J.C. Kramlich, P.G. Reinhall, I.V. Novosselov, Supercritical water gasification: practical design strategies and operational challenges for lab-scale, continuous flow reactors, Heliyon 5 (2019) e01269, doi:10.1016/j.heliyon.2019.e01269.
[46] B.R. Pinkard, J.C. Kramlich, I.V. Novosselov, Gasification pathways and reaction mechanisms of primary alcohols in supercritical water, ACS Sustain. Chem. Eng. 8 (2020) 4598–4605, doi:10.1021/acssuschemeng.0c00445.
[47] N.M.C.T. Prieto, T.A. Souza, A.P. Egas, A.G.M. Ferreira, L.Q. Lobo, A.T.A. Portugal, Liquid glycerol: experimental densities at pressures of up to 25MPa, and some derived thermodynamic properties, J. Chem. Thermodyn. 101 (2016) 64–77, doi:10.1016/j.jct.2016.05.006.
[48] A. Pucciarelli, W. Ambrosini, A successful general fluid-to-fluid similarity theory for heat transfer at supercritical pressure, Int. J. Heat Mass Transf. 159 (2020) 120152, doi:10.1016/j.ijheatmasstransfer.2020.120152.
[49] F.L.P. Resende, P.E. Savage, Kinetic model for noncatalytic supercritical water gasification of cellulose and lignin, AIChE J. (2010) 2412–2420, doi:10.1002/aic.12165.
[50] J.L.H.P. Sallevelt, J.A.M. Withag, E.A. Bramer, D.W.F. Brilman, G. Brem, One-dimensional model for heat transfer to a supercritical water flow in a tube, J. Supercrit.Fluids 68 (2012) 1–12, doi:10.1016/j.supflu.2012.04.003.
[51] S.K. Sansaniwal, M.A. Rosen, S.K. Tyagi, Global challenges in the sustainable development of biomass gasification: an overview, Renew. Sustain. Energy Rev. 80 (2017) 23–43, doi:10.1016/j.rser.2017.05.215.
[52] Z. Shang, S. Chen, Numerical investigation of diameter effect on heat transfer of supercritical water flows in horizontal round tubes, Appl. Therm. Eng. 31 (2011) 573–581, doi:10.1016/j.applthermaleng.2010.10.020.
[53] E.N. Sieder, G.E. Tate, Heat transfer and pressure drop of liquids in tubes, Ind. Eng. Chem. 28 (1936) 1429–1435, doi:10.1021/ie50324a027.
[54] R. Sivaramakrishnan, J.V. Michael, S.J. Klippenstein, Direct observation of roaming radicals in the thermal decomposition of acetaldehyde, J. Phys. Chem. A 114 (2010) 755–764, doi:10.1021/jp906918z.
[55] L. Sominsky, E. Rozental, H. Gottlieb, A. Gedanken, S. Hoz, uncatalyzed meerwein–ponndorf–oppenauer–verley reduction of aldehydes and ketones under supercritical conditions, J. Org. Chem. 69 (2004) 1492–1496, doi:10.1021/jo035251f.
[56] J. Tarr, M. Kaufman, Diamond film deposition from the reaction of hydrogen atoms with acetaldehyde, Diam. Relat. Mater. 7 (1998) 1328–1332, doi:10.1016/S0925-9635(98)00194-0.
[57] T.A. Tuan Abdullah, E. Croiset, Evaluation of an Inconel-625 reactor and its wall effects on ethanol reforming in supercritical water, Ind. Eng. Chem. Res. 53 (2014) 2121–2129, doi:10.1021/ie403305d.
[58] J.G. van Bennekom, R.H. Venderbosch, D. Assink, H.J. Heeres, Reforming of methanol and glycerol in supercritical water, J. Supercrit. Fluids 58 (2011) 99–113, doi:10.1016/j.supflu.2011.05.005.
[59] H. Wang, X. Wang, M. Li, S. Li, S. Wang, X. Ma, Thermodynamic analysis of hydrogen production from glycerol autothermal reforming, Int. J. Hydrog. Energy 34 (2009) 5683–5690 2nd International Conference on Hydrogen Safety, doi:10.1016/j.ijhydene.2009.05.118.
[60] G. Xie, X. Xu, X. Lei, Z. Li, Y. Li, B. Sunden, Heat transfer behaviors of some supercritical fluids: a review, Chin. J.Aeronaut. (2021), doi:10.1016/j.cja.2020.12.022.
[61] T. Xu, S. Wang, X. Tang, Y. Li, J. Yang, J. Li, Y. Zhang, Corrosion mechanism of Inconel 600 in oxidizing supercritical aqueous systems containing multiple salts, Ind. Eng. Chem. Res. 58 (2019) 23046–23056, doi:10.1021/acs.iecr.9b04527.
[62] K. Yamagata, K. Nishikawa, S. Hasegawa, T. Fujii, S. Yoshida, Forced convective heat transfer to supercritical water flowing in tubes, Int. J.Heat Mass Transf. 15 (1972) 2575–2593, doi:10.1016/0017-9310(72)90148-2.
[63] S. Yu, H. Li, X. Lei, Y. Feng, Y. Zhang, H. He, T. Wang, Influence of buoyancy on heat transfer to water flowing in horizontal tubes under supercritical pressure, Appl. Therm. Eng. 59 (2013) 380–388, doi:10.1016/j.applthermaleng.2013.05.034.
[64] R. Yukananto, A.K. Pozarlik, G. Brem, Computational fluid dynamic model for glycerol gasification in supercritical water in a tee junction shaped cylindrical reactor, J. Supercrit. Fluids 133 (2018) 330–342, doi:10.1016/j.supflu.2017.11.001.
[65] M. Zaoui-Djelloul-Daouadji, A. Negadi, I. Mokbel, L. Negadi, Vapor-liquid) equilibria and excess Gibbs free energy functions of (ethanol+glycerol), or (water+glycerol) binary mixtures at several temperatures, J. Chem. Thermodyn. 69 (2014) 165–171, doi:10.1016/j.jct.2013.09.046.
[66] Y. Zhang, H. Tan, Y. Li, S. Shan, Y. Liu, A modified heat transfer correlation for flow boiling in small channels based on the boundary layer theory, Int. J. Heat Mass Transf. 132 (2019) 107–117, doi:10.1016/j.ijheatmasstransfer.2018.11.148.
[67] B. Zhu, S. Li, W. Wang, H. Zhang, Supercritical water synthesized Ni/ZrO_2 catalyst for hydrogen production from supercritical water gasification of glycerol, Int. J. Hydrog. Energy 44 (2019) 30917–30926, doi:10.1016/j.ijhydene.2019.10.044.
[68] C. Zhu, R. Wang, H. Jin, X. Lian, L. Guo, J. Huang, Supercritical water gasification of glycerol and glucose in different reactors: The effect of metal wall, Int. J. Hydrog. Energy 41 (2016) 16002–16008 Special Issue: 16th China Hydrogen Energy Conference (CHEC 2015), November 2015, Zhenjiang City, Jiangsu Province, China, doi:10.1016/j.ijhydene.2016.06.085.
[69] European Union, P.O. of the E., 2019. Masterplan for a competitive transformation of EU energy-intensive industries enabling a climate-neutral, circular economy by 2050. URL: https://op.europa.eu/en/publication-detail/-/publication/be308ba7-14da-11ea-8c1f-01aa75ed71a1.
[70] J. Mahabir, N. Koylass, N. Samaroo, K. Narine, K. Ward, Towards resource circular biodiesel production through glycerol upcycling, Energ. Convers Manage 233 (2021) 113930, doi:10.1016/j.enconman.2021.113930.
[71] Z. Sverko Grdic, M. Krstinic Nizic, E. Rudan, Circular Economy Concept in the Context of Economic Development in EU Countries, Sustainability 12 (2020) 3060, doi:10.3390/su12073060.
[72] K.S. Avasthi, R.N. Reddy, S. Patel, Challenges in the Production of Hydrogen from Glycerol – A Biodiesel Byproduct Via Steam Reforming Process, Procedia Engineering, Chemical, Civil and Mechanical Engineering Tracks of 3rd Nirma University International Conference on Engineering (NUiCONE2012) 51 (2013) 423–429, doi:10.1016/j.proeng.2013.01.059.
[73] M. Grilc, B. Likozar, J. Levec, Kinetic model of homogeneous lignocellulosic biomass solvolysis in glycerol and imidazolium-based ionic liquids with subsequent heterogeneous hydrodeoxygenation over NiMo/Al2O3 catalyst, Catal. Today 256 (2015) 302–314, doi:10.1016/j.cattod.2015.02.034.
[74] A. Tamošiūnas, D. Gimžauskaitė, R. Uscila, M. Aikas, Thermal arc plasma gasification of waste glycerol to syngas, Appl. Energ 251 (2019) 113306, doi:10.1016/j.apenergy.2019.113306.
[75] S.B. Costa-Gutierrez, J.M. Saez, J.D. Aparicio, E.E. Raimondo, C.S. Benimeli, M.A. Polti, Glycerol as a substrate for actinobacteria of biotechnological interest: Advantages and perspectives in circular economy systems, Chemosphere 279 (2021) 130505, doi:10.1016/j.chemosphere.2021.130505.
[76] L.R. Kumar, R. Kaur, R.D. Tyagi, P. Drogui, Identifying economical route for crude glycerol valorization: Biodiesel versus polyhydroxy-butyrate (PHB), Bioresource Technol. 323 (2021) 124565, doi:10.1016/j.biortech.2020.124565.
[77] Williams, A., 2020. Biofuels Market Size, Share, Outlook & Industry Growth Report. URL https://www.bccresearch.com/market-research/energy-and-resources/liquid-biofuels-outside-north-america-report.html.
[78] D. Unlu, N.D. Hilmioglu, Application of aspen plus to renewable hydrogen production from glycerol by steam reforming, International Journal of Hydrogen Energy, Hydrogen Energy Technologies for Mitigating Global Warming (2020), doi:10.1016/j.ijhydene.2019.02.106.
[79] M. Dudukovič, P. Mills, Scale-up and multiphase reaction engineering, Curr. Opin. Chem. Eng. 9 (2015) 49–58, doi:10.1016/j.coche.2015.08.002.
[80] S. Roy, P. Kamalanathan, M. Al-Dahhan, Integration of phase distribution from gamma-ray tomography technique with monolith reactor scale modeling, Chem. Eng. Sci. 200 (2019) 27–37, doi:10.1016/j.ces.2018.12.053.
[81] E. Markočič, B. Kramberger, J.G. van Bennekom, H. Jan Heeres, J. Vos, Ž. Knez, Glycerol reforming in supercritical water; a short review, Renew. Sust. Energ. 23 (2013) 40–48, doi:10.1016/j.rser.2013.02.046.

Energy Conversion and Management 270 (2022) 116215

Contents lists available at ScienceDirect

Energy Conversion and Management

journal homepage: www.elsevier.com/locate/enconman

Process simulation of hydrothermal carbonization of digestate from energetic perspectives in Aspen Plus

Niloufar Ghavami [a,*], Karhan Özdenkçi [a], Simeone Chianese [b], Dino Musmarra [b], Cataldo De Blasio [a]

[a] Faculty of Science and Engineering, Åbo Akademi University, Rantakatu 2, 65100 Vaasa, Finland
[b] Department of Engineering, University of Campania "Luigi Vanvitelli", Via Roma 29, 81031 Aversa, Italy

ARTICLE INFO

Keywords:
Hydrothermal carbonization
Energetic yield
Digestate
Circular economy
Hydrochar

ABSTRACT

Digestate, a nutrient-rich substance, is a potential resource of income in biogas plants. It can be utilized as a soil amendment and solid biofuel due to containing inorganic and organic compounds. However, concerning the environmental regulations, there is a requirement for further processes, including hydrothermal carbonization (HTC). Regarding the selection of optimum conditions from the experimental data, this study proposes the energetic yield as the performance indicator from the techno-economic viewpoint, taking solid load and relative equipment size comparison into account as well as the heating value of hydrochar. The energetic yield is the energy content in hydrochar as the heating value per unit mass of reactor inlet, MJ/kg reactor inlet. Among the investigated data for various digestates, the optimum feedstock and conditions were HTC agricultural residue (with 5.02 Energetic yield MJ/kg reactor inlet) at 200 °C and the residence time of 1 h with 30 % solid load based on the energetic yields, i.e. selected for process simulation. This study also investigates required experimental data for enabling mass balance and simulation models. In addition to yield and proximate analysis of feedstock and hydrochar, the characterization of process water is important for representing the dissolved organics. The available data influences the accuracy and closure of elemental mass balances for process simulation. In addition, this study also investigates simulation aspects for producing hydrochar with 20 % moisture content as well: the impact of property method on energy balance, the heat of reaction compared to the literature values, and heat integration concepts. SRK, PSRK, NRTL, and IDEAL methods reported the same value, −122 kW, as the heat duty of the reactor. This value corresponds to −1.46 MJ/kg dry solid and −1.74 MJ/kg dry-ash-free solid inlet as the heat of reaction.

III

1. Introduction

Sustainable development is defined by the United Nations [1] as "*the development that meets the needs of the present without compromising the ability of future generations to meet their own needs*." Therefore, sustainable development goals are designed to mitigate the excessive usage of fossil fuels, providing affordable and clean energy, environmental protection, and socioeconomic development [2,3]. In the current linear economic model that non-renewable resources are used; they end up as waste material that produces large amounts of pollutants and waste [4,5]. On the contrary, a circular economy (CE) is based on recycling wastes and energy production from renewable resources [6]. In this regard, international organizations, including European Union (EU), set guidelines according to UN Agenda [7] to reduce the negative effects of non-renewable resources and move towards CE and sustainable development.

To address the negative effects of non-renewables and move towards sustainability, there is a need for renewable alternatives like biofuels. Biochemical conversion technologies and making use of enzymes of microorganisms is an appropriate closed-loop process in the CE concept

Abbreviations: AGR, Agricultural residue; AD, Anaerobic digestion; BMP, Biochemical methane potential; COD, Chemical oxygen demand; CE, Circular economy; CMD, Cow manure digestate; ECD, Energy crops digestate; EU, European Union; FWD, Food waste digestate; HHV, Higher heating value; HTC, Hydrothermal carbonization; Mtoe, Mega tonnes of oil equivalent; MSW, Municipal solid waste; NC solids, Non-conventional solids; OHWD, Organic household waste digestate; SS, Sewage sludge; SCWG, Supercritical water gasification; TOC, Total organic carbon; VGF, Vegetable, garden, and fruit waste; WS, Wheat straw; YW, Yard waste.

* Corresponding author.
E-mail address: Niloufar.ghavami@abo.fi (N. Ghavami).

https://doi.org/10.1016/j.enconman.2022.116215
Received 10 June 2022; Received in revised form 20 August 2022; Accepted 5 September 2022
Available online 18 September 2022

[8]. Anaerobic digestion (AD), composting, and fermentation are considered the default processes for converting organic waste feedstock, including agricultural waste, manure, animal slurry, and municipal solid waste (MSW), into biofuels [9–11]. Biogas and digestate, the products of the AD process, have dual benefits in energy production and waste management [12]. Biogas is a vital energy contributor in the transition to renewable energy resources and toward sustainable development in many countries. According to assessments and potentials in the EU [13], biogas production is expected to increase from 28.8 to 40.2 Mtoe in 2030 (the current production level is 14.9 Mtoe). Digested sludge, digestate, which is rich in nutrients, is commonly used for agricultural application or incineration [14,15]. According to statistics, there is no accurate data for digestate production; however, based on estimations for EU28, approximately 180 million tons of digestate are produced annually [16].

Development of the AD process for energy production increased volumes of the generated digestate year by year. However, environmental restrictions limited the direct usage of the digestate. The restrictions are imposed by the presence of high amounts of nitrogen, heavy metals, organisms, and pathogens due to the contaminants and pollution of soil and water [17,18]. Storage and transportation of the oversupplied digestate lead to high costs [19,20]; therefore, there is a need for further process.

Digestates can be treated via physicochemical, biological, and mechanical methods to recover and remove nutrients [21,22]. Among physicochemical technologies, thermochemical treatments are feasible technologies for managing organic wastes to produce valuable biofuels, heat, and power. Especially, hydrothermal treatments using water as a solvent and reactant are specialized for handling the high moisture content of wastes, that reviewed by many scientists [23–29]. Among the hydrothermal processes, analysis of operational problems in hydrothermal liquefaction (HTL) and supercritical water gasification (SCWG) processes concluded that the hydrothermal carbonization (HTC) process, with lower operating conditions, reduces the risk of operational problems reviewed by Ghavami et al. (2021) [30]. In addition, processing digestate through HTC reduces the global warming potential and increases the exergy efficiency compared to composting digestate [31]. HTC is a viable thermochemical process to convert the digestate to hydrochar and recover solid carbon and energy without drying pretreatment [32–35]. Hydrochar could be replaced as a substitute for fossil fuels due to its higher carbon content, HHV, lower ash, and the richer oxygenated functional group as compared to digestate [36–38]. Meanwhile, it is suitable for use in conventional combustion processes due to the similarity of the energy content and chemical structure of hydrochar to natural coal [39]. In recent years, the HTC has been investigated to produce remediation and conditioner agent for soil improvement and fertilizer [40–42]. The HTC process is followed by densification or palletization processes to improve the storage and transportation properties of the solid fuel [43].

Various types of digestate feedstock can be used in the HTC process. Comparing HTC of municipal solid waste (MSW) digestate and agricultural residue (cow dung) digestate at 200 °C temperature for 4.5 h residence time, Pawlak-Kruczek et al. [44] concluded that wet MSW digestate is more profitable for energy purposes because of higher energy densification (1.406 for MSW digestate and 1.123 for agricultural residue digestate). Among the feedstocks, including digestates of organic household waste (OHWD), energy crops (ECD), and cow manure (CMD), ECD showed the highest solid yield while OHWD showed the lowest solid recovery, as observed in the experiments by Cao et al. [17]. The severity of the reaction increased the carbon content of hydrochars from OHWD and ECD [17]. In another study on HTC at 150–250 °C, with a solid load of 10–30 % by weight and with 1 h residence time, the highest heating value (HHV) was obtained from agricultural residue (AGR) digestate among different digestates, such as sewage sludge (SS), AGR, vegetable, garden, and fruit waste (VGF), and residual municipal solid waste (MSW) [45]. Sewage sludge digestate resulted in a low HHV hydrochar compared to higher lignin-containing feedstock; meanwhile, AGR digestate had a lower ash content corresponding to higher carbon content [46]. However, despite HTC being implemented industrially for sewage sludge by TerraNova company in Germany [47] and for pulp and paper sludge in Finland [48,49], further progress on HTC of digestates requires process simulation, integration, and techno-economic assessment based on the experimental results.

The physicochemical properties of hydrochar strongly depend on the digestate, its origin, and the process conditions. These properties can guide the selection of optimum feedstock and conditions as well as the end-use application of the hydrochar [50,51]. HTC process is governed by various factors including temperature and residence time. An increase in temperature reaction increases energy yield due to enhancement of the HHV and decreases solid yield, and significantly decreases hydrochar yield [52]. The combined effect of residence time and temperature on hydrochar properties is still not clear; therefore, further research is needed. Residence time and the reaction temperature are defined by a single factor which is the severity of the HTC reaction (Equation 1):

$$R_0 = t_{res}.\,exp\left(\frac{T_{HTC} - 100}{14.75}\right) \quad \text{Severity factor} \tag{1}$$

where R_0 is the severity factor, T_{HTC} is the HTC temperature (°C), and t_{res} is the residence time (min). The increase of the severity factor has a positive effect on the dry basis carbon content [17,53]. At high temperatures, higher reaction activity leads to the transition of water-soluble components into aqueous and gaseous phases and transferring of organic matter [54,55]. Increased temperature enhances hydrochar thermal stability due to increased carbonization and devolatilization, according to Nzediegwu et al. [56].

Digestate origin also influences the hydrochar properties [17]. The higher carbon content feedstock results in higher energy density in hydrochar [57]. For instance, sewage sludge digestate results in a low HHV hydrochar compared to lignin-containing feedstock, while digestates with lower ash content results in higher carbon content in hydrochar [46]. Meanwhile, according to Fujiwara et al. [58], a high amount of lignin and hemicellulose is identified as the limiting factor in the anaerobic process, i.e. non-lignocellulosic feedstocks being more suitable for the AD process. The degradability of cellulose, hemicellulose, and lignin are affected by the rigid structure of the pseudo-components to be used in AD.

During the HTC process, the digestate is carbonized at relatively low temperatures and autogenous pressure. The HTC process is conducted in the subcritical condition in which the water characteristics change dramatically. An increase in the temperature below the critical point (374 °C) results in weakening water's hydrogen bonds, an increase in dielectric constant, and produces high ionization constants. The subcritical condition increases H^+ concentration which boosts acid-catalyzed reactions [59]. The overall behavior of the HTC reaction is exothermic, in which the hydrogen and oxygen content is reduced by various reaction mechanisms [60,61]. These mechanisms include hydrolysis, dehydration, decarboxylation, aromatization, condensation, and polymerization [35]. The first stage is hydrolysis, in which the biomass feedstock is degraded to oligomers and monomers; in this stage monomers like 2-furfural and 5- hydroxymethylfurfural (5-HMF) are produced. In the dehydration process, the amount of OH groups decreases, causing a lower O/C ratio [62]. The decarboxylation stage reduces C═O and COOH groups leading to decreasing O/C ratio of the solid product [63]. According to Ahmed et al. [33], the HTC process temperature range is capable of treatment of polluted problematic biomass, including sewage sludge, and the problematic compounds transform or thermally degrade during the HTC process. In addition, the necessary treatment is provided by the HTC process to recover nutrients and produce energy while addressing sterilization and sanitation. In another study, Lu et al. [64] applied co-HTC of SS and polyvinyl chloride (PVC) to transform heavy metals and chlorine. Mn and Zn were removed

effectively, the toxicity of Ni and As was reduced, and dechlorination efficiency improved by the addition of PVC.

Reviewing the simulated models of HTC of organic waste and biomass, Ischia and Fiori [60] concluded the lack of focus on the HTC system and specifically the reactor as the heart of the process. Regarding the phenomena in the reactor, chemical kinetics and heat transfer are weakly understood, thus complicating or even preventing the mechanistic models. For instance, the inorganics in trace amounts are usually neglected when investigating the reaction mechanism and kinetics, such as N, P, Na, Si, K, Ca, and Mg. Transformation of these species can catalyze or affect hydrochar formation, structure, and other product pathways. Few studies are conducted on each pathway, and process development for various value-added products is time-consuming and expensive [65]. Moreover, the heat of reaction is obtained only based on the overall reaction while missing the heat of reaction versus the space in a reactor or residence time, i.e. the stages of reactions [27]. In addition, heat transfer models are affected by a lack of information on the changes in density, porosity, and permeability of biomass due to unexplored reactions [27]. There is also a lack of information on component interactions and reactions in different process severities during hydrothermal processes. Most HTC experiments are carried out in bench-scale batch reactors; however, commercialization and industrialization of the HTC process require more investigations on the continuous process for validation of product yields. Meanwhile, the separation of HTC products (hydrochar, process water, and gas product) has great importance as well. The experimental studies conduct complete dewatering for characterization purposes with the methods suitable only for lab-scale (such as microfilters and oven-drying the solid), while industrially applicable dewatering requires specific investigation. Comparing innovative methods for dewatering, Gao et al. [66] considered different operational modes and concluded dewatering hydrochar at the same hydrothermal temperature by mechanical compression resulted in the lowest moisture content (45.49 %) in hydrochar. It is worth mentioning that the hydrothermal fluid was transferred before the dewatering process. A better understanding of the HTC process and gaps provides information for future research and investigation to improve the process and upgrade the products.

Due to the complicated reaction kinetics and mechanisms, simulation models are simplified based on the experimental results rather than mechanistic kinetic models. Simulations based on experimental results require sufficient characterization data of hydrochar, process water, and gases to enable the mass balance. However, some experimental studies might focus on the impacts of process conditions on hydrochar yield and quality rather than presenting a complete set of data sufficient for mass balance. Nevertheless, it is possible to simulate the HTC process based on experimental results involving adequate characterization of hydrochar and process water [67–69]. Meanwhile, the gas yield is typically calculated by differences in experimental studies [45,57,62]. In addition, the gas is assumed to be carbon dioxide only due to other gases being generated in negligible amounts. However, the gas composition was observed to include 70–90 % of carbon dioxide by the studies also investigating the gas outlet of the HTC process [70,71]. To sum up, it is needed to investigate the required characterization data regarding mass balance and the impact of experimental data on the accuracy of the process simulations.

Constructing a representative simulation model is crucial in energy balances and selecting the optimum process conditions and integration concepts. However, the simulation models of HTC involve simplifications that can influence the energy balance results sharply. For instance, McGaughy and Reza [72] simulated HTC of food waste in Aspen Plus based on the experimental yields obtained in a batch reactor at 200–260 °C with a residence time of 30 min. Moreover, digestate and hydrochar are defined as non-conventional solids in the simulations; however, default values are considered for heating values calculated by Aspen Plus through empirical relations instead of user-defined values. As a matter of fact, the empirical relations in Aspen Plus are derived originally for coal [73]. This affects the heat of the reaction calculated by the simulation model. Therefore, there is a need for simulation models as representative as possible based on the experimental results.

Besides the sufficient characterization of products and dewatering data, simulating an HTC process also requires selecting optimum conditions. It is beneficial to have a clear indication enabling the comparison of various conditions from the techno-economic viewpoint at an early stage to filter the promising sets of conditions for further process design and feasibility assessment. Some performance parameters include energy densification, energy recovery, and carbon recovery. On the other hand, the current process performance parameters do not include the combined impact of process conditions from the techno-economic viewpoint. The energy densification does not explicitly determine the optimum temperature due to the opposite trend of hydrochar heating value and yield with temperature. Meanwhile, dry-basis yield and carbon recovery do not involve the impact of solid load and residence time on the equipment sizes. Therefore, it is needed to determine a criterion implying the relative comparison of equipment sizes as well as hydrochar outcome.

This study aims to illustrate a simulation model for the HTC of digestates regarding the industrial application, to determine experimental data required for the simulation, and to define an evaluation criterion for selecting the optimum feedstock and conditions from the technical viewpoint. The study complies with the data of various feedstocks processed at various conditions, establishes the optimum feedstock conditions set via the defined criterion, and presents the process simulation results. The digested feedstock and optimum conditions are selected based on the calculation of energetic yield per reactor inlet as well as considering residence time. The simulation results include energy balance, heat and electricity requirements for the process, and the impact of the thermodynamic method. The simulation model also involves dewatering followed by thermal drying of hydrochar down to 20 % moisture content in the final product. HTC of organic waste is an emerging technology to move towards sustainability and a circular economy. In this regard, process modeling and simulation provide information to predict and optimize the process conditions and products. This research article provides a reliable simulation for the commercialization of the HTC process as well as a proper criterion for selecting the promising sets of conditions and required characterization data for mass balances.

2. Selection of feedstock and process conditions

This study compares various digestates as feedstock and process conditions studied in the literature, such as digestates of food waste, sewage sludge, and agricultural residue (mixture of maize, grass silage, and manure). Table 1 summarizes the elemental composition and the chemical energy content (HHV) of different types of digestates tested in various studies, and Table 2 gives the related properties of resulting hydrochar in different operational conditions and product yields as obtained in the studies listed in Table 1. In addition, Table 2 also gives the calculated energetic yields for each set of feedstock-condition experiments. This study illustrates the comparison of feedstock and process conditions based on energetic yield; however, the various digestates have been tested under different conditions in different studies. It should be noted that proper comparison can be made when all the digestates are tested under the same conditions. Nevertheless, the comparison in this study is still useful for selecting promising sets of conditions and observing the impact of conditions.

Table 2 introduces a process performance indicator, namely energetic yield, as the criterion for the selection of optimum process conditions. This performance parameter gives an indication of techno-economic comparison at the early stage of process development, while dry-based yield is more informative on conversion and chemistry. For instance, a techno-economic assessment on supercritical water gasification (SCWG) of Kraft black liquor showed that the economically

Table 1
Elementary composition of different digestates.

Digestate sample	HHV (MJ/Kg)	C	H	N	S	O	Ash	Ref.
Energy crops (ECD)	16.4	40.3	4.6	2.1	0.3	24.0	28.7	[17]
Cow manure (CMD)	17.0	42.6	5.0	2.0	0.4	34.3	15.7	
Organic household waste (OHWD)	13.4	34.3	4.0	1.9	0.2	23.8	35.8	
Wheat straw (WS)	20.1	41.7	5.6	0.9	0.2	37.8	13.8	[74]
Food waste (FWD)	13.2	32.9	3.0	4.0	0.2	29.4	30.5	[75]
Yard waste (YW)	16.7	39.4	5.3	10	0.5	32.2	12.6	
Mix FW & YW	14.95	36.2	4.2	7.0	0.3	30.8	21.5	
Agricultural residue (AGR)	17.8	44.1	5.1	3.2	0.3	31.3	16.0	[45]
Municipal solid waste (MSW)	15.6	24.1	1.7	1.5	0.2	16.9	55.6	
Sewage sludge (SS)	14.9	28.6	3.1	3.4	1.5	16.5	46.9	
Vegetable, garden and fruit waste (VGF)	14.9	29.5	3.0	2.0	0.3	21.4	43.8	
Manure	14.6	26.8	3.4	1.7	0.4	22.9	44.8	[54]
Manure & whey	15.9	28.2	3.6	1.7	0.5	20.3	45.7	

*C, H, O, N, S and ash are reported based on weight percent dry basis.

optimum hydrogen production was not achieved at the process conditions of maximum dry-based hydrogen yield because of lower revenue by the off-gas than the optimum set of conditions [76]. Consequently, it was proposed to determine the hydrogen and energy yields on a non-inert basis (ash being the only inert) for SCWG processes together with residence time and reactor material [77]. This is also applicable to other hydrothermal processes when selecting the optimum conditions. The ash amount is relatively less in SCWG and to be separated within the reactor, i.e. not affecting the majority of the process equipment. Meanwhile, HTC of digestate involves higher ash content, and the ash is split between process water and hydrochar. Therefore, this study introduces the energetic yield on the basis of the total inlet to the reactor. The energetic yield represents the energy content of hydrochar via its heating value per unit mass of reactor inlet, in MJ/kg reactor inlet. The energy content takes the combination of hydrochar yield and heating value into account while the reactor inlet basis takes the relative equipment size into account. For instance, for processing a defined amount of dry feedstock, low solid load results in streams with high flow rates, i.e. larger equipment and energy requirement. Similarly, the residence time is also a direct indication of reactor size together with the energy yield parameter. When the energetic yields are close, the residence time is another parameter to compare the sets of conditions. For example, HTC of energy crop digestate resulted in the same energetic yield at 210 °C with 2-hour and 5-hour residence times, i.e. no reason to consider higher residence time and larger reactor. Similarly, HTC of wheat straw digestate resulted in the same energetic yield at 240 °C with 2-hour residence time and at 260 °C with 8-hour residence time. Among the feedstocks and condition sets in Table 2, the HTC process gives the most efficient outcome for AGR digestate at 200 °C, 30 % solid load, and 1-hour residence time, i.e. 5.02 MJ/kg reactor inlet.

3. Process description and simulation

Prior to the simulation, it is needed to define the capacity, the components, and thermodynamic methods. Therefore, a process model is simulated in Aspen Plus V11.1 based on the following assumptions:

- The process is simulated in steady-state mode.
- The property method and free-water methods are PSRK (Predictive Soave-Redlich-Kwong) equation of state and STEAMNBS, respectively.
- The stream class is defined as 'MIXNC', i.e. mixed of conventional and non-conventional compounds.
- The digestate feedstock rate was considered as 1000 kg/h with 30 % solid load, i.e. 700 kg/h water and 300 kg/h of dry feedstock.
- The dissolved organics in process water are represented as one non-conventional compound.
- The chemical and physical properties of hydrochar, digestate, and ash, considered non-conventional solids (NC solids), are estimated by 'HCOALGEN' and 'DCOALIGT' (with codes of 6 for user input values of HHV of these components).
- The HTC reactor is considered a RYIELD block based on the mass balance with experimental results.
- The gas product of the HTC process is considered as 90 % CO_2, 6 % CO, 3 % CH_4, and 1 % H_2 by volume for enabling the mass balances.
- Air is defined as 79 % nitrogen and 21 % oxygen gases by volume.
- The target product is hydrochar with a maximum of 20 % moisture content.

The component list involves conventional substances of water, carbon dioxide, carbon monoxide, methane, hydrogen, oxygen, and nitrogen, besides non-conventional substances of digestate, hydrochar, dissolved organics, and ash. The digestate and hydrochar are defined to represent the dry-ash-free part, while ash is defined as a separate component. Since ash is split to process water and hydrochar, it can be more convenient to define ash separately when using a split block in the simulation model, i.e. distributing ash as a component.

An appropriate thermodynamic property method is required to model a process simulation and achieve reliable results. Physical property methods facilitate the interpretation of component behavior under process conditions. Property methods are chosen based on the involved components and simulation conditions. Consequently, selecting the property method was one of the basic and critical steps.'IDEAL' based method [57,62] and SRK [72] were used in some studies for the HTC process. However, the existence of non-conventional components (digestate, ash, and hydrochar) and moderate pressure do not support the selection of the 'IDEAL' base method. Alternatively, SRK and PSRK are suitable for mild or high-pressure processes, including polar and non-polar components and light gases. This study compares different property methods, including SRK, PSRK, NRTL, and 'IDEAL' base, to achieve more accurate data. Soave-Redlich-Kwong (SRK) equation of state gained wide popularity and occupied many thermodynamic packages, including Aspen Plus, due to its simplicity and engineering flexibility [78]. Moreover, this method is recommended for high-pressure conditions [79]. The SRK property method can be used for non-polar or mildly polar mixtures and provides reasonable results in all temperatures and pressures consistent in the critical region [80,81]. Predictive Soave–Redlich–Kwong equation of state (PSRK) was developed by Gmehling based on the SRK equation and used the UNIFAC method in calculating mixture parameters [82]. This equation of state is able to capture the non-ideal interactions and predicts the properties of pseudo-components [83]. In addition, the PSRK method can predict binary interactions at any pressure and can be used for the mixture of polar, non-polar, and light gases. This property method provides accurate results in high temperatures and pressures and is also close to the critical point [84]. The nonrandom two-liquid (NRTL) property method has been widely used in vapor–liquid and liquid–liquid equilibrium (VLE and LLE) to characterize the critical solution temperature and LLE immiscibility [85,86]. It is also recommended for a highly non-ideal chemical system by Aspen Plus.

The process simulation for HTC of AGR digestate involves the heat exchange between the reactor downstream and feed stream, heating the feed further to reach the reaction temperature, the reactor, separation of the solid product, and thermal drying to decrease the moisture content

Table 2
Properties of hydrochars from HTC of digestates as conducted by the studies referred in Table 1.

Feedstock digestate	*HTC conditions*			*Hydrochar*				*Process performance*	
	T_{HTC} (°C)	t_{res} (h)	Solid load (%)	C (%)	H (%)	O (%)	HHV (MJ/kg)	Yield (% dry basis)	Energetic yield (MJ/kg reactor inlet)
ECD	210	2	15	41.2	3.9	21.9	23.1	79.5	1.92
		5		42.4	3.8	20.2	24.0	77.8	1.92
	230	2		40.8	3.5	20.4	23.2	71.8	1.68
		5		42.0	3.4	16.8	24.9	66.1	1.61
	250	2		41.6	3.2	15.8	25.1	61.3	1.47
		5		42.0	3.1	14.0	25.9	58.6	1.41
CMD	210	2	15	46.9	4.6	27.5	22.7	75.3	2.10
		5		47.2	4.2	26.3	22.6	71.2	1.95
	230	2		47.7	4.0	24.1	23.3	65.7	1.81
		5		50.7	4.0	19.1	25.8	58.3	1.75
	250	2		51.0	3.8	17.9	26.1	52.7	1.57
		5		52.4	3.9	16.1	27.2	52.4	1.63
OHWD	210	2	15	32.7	3.0	21.1	20.4	79.2	1.41
		5		35.6	3.2	19.2	22.4	75.5	1.52
	230	2		33.6	2.9	17.1	22.3	72.8	1.35
		5		34.6	2.7	14.4	23.7	68.9	1.32
	250	2		34.3	2.6	13.1	24.4	67.9	1.29
		5		35.7	2.7	12.6	25.2	65.8	1.32
WS	220	2		59.9	5.3	33.4	23.4	55.3	1.94
		4		64.0	5.5	28.8	25.5	48.8	1.87
		6		67.2	5.1	26.1	26.3	57.9	2.28
		8		70.3	5.1	22.9	27.7	53.3	2.21
	240	2		70.6	4.7	23.0	27.3	56.8	2.33
		4	15	73.2	4.8	20.1	28.6	51.6	2.21
		6		74.1	5.1	18.8	29.5	49.3	2.18
		8		74.5	5.0	18.5	29.5	50.5	2.23
	260	2		64.2	4.0	30.0	23.3	45.9	1.60
		4		71.4	4.7	22.2	27.6	51.1	2.12
		6		70.6	4.1	23.6	26.3	57.6	2.27
		8		74.0	4.9	19.2	29.1	55.3	2.33
FWD	250	2	10	34.4	3.6	12.0	13.9	51.0	0.71
YW				54.4	5.2	18.9	20.7	47.0	0.97
Mix FW & YW				44.1	4.6	15.7	18.9	44.0	0.83
AGR	200	1	10	52.0	6.9	23.1	21.6	60.0	1.30
			20	50.8	6.0	24.4	20.7	67.8	2.81
			30	51.2	6.1	22.8	20.9	80.1	5.02
	250		10	57.3	6.3	11.5	24.0	47.2	1.13
			20	57.1	6.6	12.0	24.2	51.1	2.47
			30	56.7	5.8	12.7	23.3	49.4	3.45
MSW	200	1	10	22.6	1.6	11.7	15.5	85.0	1.32
			20	21.4	1.6	13.9	15.6	87.1	2.72
			30	24.0	1.8	12.2	15.4	85.7	3.96
	250		10	23.0	1.6	9.7	15.6	82.0	1.28
			20	21.7	1.6	7.9	15.6	84.1	2.62
			30	23.4	1.7	7.8	15.5	83.5	3.88
SS	200	1	10	34.0	4.2	13.0	15.0	72.6	1.09
			20	34.0	4.2	14.0	15.1	76.1	2.30
			30	35.2	4.4	12.7	15.4	78.0	3.60
	250		10	34.4	4.0	9.2	15.2	65.6	1.00
			20	34.7	4.1	10.6	15.3	67.9	2.08
			30	36.4	4.3	9.0	15.7	69.5	3.27
VGF	200	1	10	26.3	2.7	14.4	14.8	79.5	1.18
			20	32.2	3.3	13.3	15.1	80.9	2.44
			30	30.4	3.1	12.5	14.9	79.8	3.57
	250		10	26.4	2.6	8.3	14.8	71.1	1.05
			20	27.8	2.7	9.0	14.9	71.4	2.13
			30	29.1	2.9	5.4	15.0	73.7	3.32
Manure	180	1	25	28.9	3.4	16.2	11.4	79.5	2.26
	210			31.4	3.5	9.1	13.0	75.7	2.46
	240			32.5	3.3	3.2	13.7	65.7	2.25
Manure & Whey	180	1	25	36.7	4.2	12.9	15.5	86.6	3.36
	210			35.5	3.8	13.6	14.5	81.1	2.95
	240			37.7	3.9	6.0	16.1	68.3	2.75

of hydrochar. The process simulation model is depicted in Fig. 1. The stream "FEED" is pumped to a pressure of 45 bars to ensure the liquid phase at the reaction temperature and exposed to heat exchange with the reactor downstream as represented by the units "HE1" and "HE2". The feedstock reaches the temperature of 180 °C after this heat exchange by specifying 20 °C. Afterwards, the heating conducted in the "HEATER" unit represents the external heating to reach the reaction temperature of 200 °C. The reactor unit "HTC" operates at the constant temperature of 200 °C, thus resulting downstream at the same temperature. The reactor is represented with a RYIELD block with user-defined yields based on experimental data. After heat exchange with the feedstock, the reaction mixture goes through expansion and separation. The dewatering is represented as a split block to separate process water, namely "DEWATER". Then, separating process water as the stream "PWATER",

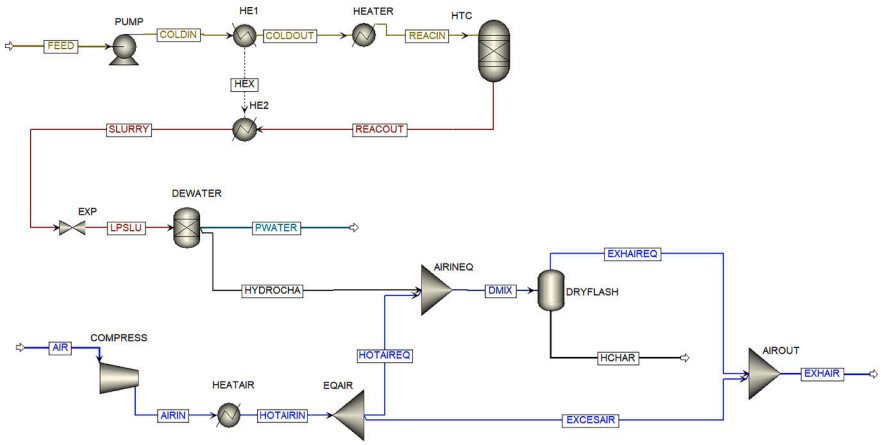

Fig. 1. Simulation model of HTC process.

the hydrochar goes through thermal drying with air. The dryer is represented as air compressed to 1.2 bars and heated to 110 °C, hydrochar-air contact, and flash separation to separate dried hydrochar and humid air. Aspen Plus calculates this part in equilibrium while the industrial driers operate with excess air to reduce the equipment size. The stream "EXCESAIR" represents the excess air in the dryer. The drying is conducted to reduce the moisture content down to 20 % moisture to avoid molding in case the product is transported or stored before further usage.

The mass balance is required to define the yields on a non-inert basis for Aspen Plus simulation and to determine the representation of organics in the process water stream. The experimental results include the ultimate analysis of digestate and hydrochar, the yields, and process water characterization for HTC of AGR digestate [45]. The data used in mass balance are shown in Table 3.

The mass balance involves the following steps based on the available characterization data:

I). determining the hydrochar, gas, and liquid flow rates using the yield data and total mass balance
II). nitrogen elemental balance to determine the nitrogen amount in process water
III). carbon amount in process water calculated with C:N ratio
IV). elemental balance of sulphur to determine the sulphur amount in process water
V). elemental balance of carbon to determine carbon in gas, i.e. carbon dioxide
VI). determining the mass flow rates of gas species via the carbon element amount and composition of gas
VII). calculating the hydrogen and oxygen content of organics in process water by using chemical oxygen demand (COD) and biochemical methane potential (BMP) data (i.e. writing hydrogen amount in terms of COD and other elements, then using solver function in excel to reach the BMP data by adjusting oxygen content)
VIII). determining the water amount in process water via the liquid flow rate and organic and ash content

Conducting these steps includes a few assumptions as well. The gas is assumed to have no nitrogen and sulphur as H_2S or NO_x, i.e. all the nitrogen and sulphur in feedstock being split between hydrochar and process water. In addition, the lab-scale experiments involved oven drying of hydrochar after complete dewatering through microfilters, i.e. the amount of evaporated water representing the difference between gas flow rate calculated from the yield and carbon dioxide flow rate calculated from carbon balance. In addition, the experimental BMP is utilized as the theoretical one to enable the calculation despite the small error in the elemental balances of hydrogen and oxygen.

Table 3
Characterization results of feedstock, process water, and hydrochar [45].

Sample	Ultimate analysis (wt% dry)					Proximate analysis (wt% dry)			
	C (%)	H (%)	O (%)	N (%)	S (%)	Ash (%)	FC	VM	HHV (MJ/kg)
Feedstock	44.1	5.1	31.3	3.2	0.3	16.0	13.8	70.2	17.8
Hydrochar	51.2	6.1	22.8	3.5	0.10	16.3	17.0	66.7	20.9
Process water									
C:N	5.8		TOC	18.8 g/L		BMP_{exp}	178.6 Nml CH_4/g COD		
TN	3.3 g/L		COD	54.6 g/L					
Yields									
Hydrochar	80.1 wt% dry-based								
Liquid	16.8 wt% dry-based								
Gas	3.1 wt% dry-based								

4. Result and discussion

4.1. Mass balance for the reactor using the experimental results

The methodology of mass balance depends on the available characterization data. The extent of sample analysis also determines the accuracy of mass balances. The total mass balance is enabled with yields of hydrochar and liquid as well as ultimate and proximate analysis of feedstock and hydrochar. To determine the components and yields for the process simulation, the next step is to identify the process water. The carbon, nitrogen, and sulphur contents are directly calculated from the elemental balances, while the hydrogen and oxygen occur as generated water and in the organic content. With the available data for this case, the hydrogen and oxygen content of dissolved organics are calculated via experimental BMP and COD. From the energetic viewpoint, an insignificant mismatch in hydrogen and oxygen balances is caused by utilizing the experimental BMP in a stoichiometric calculation. Alternatively, a more accurate determination can be enabled by CHNS analysis of the dissolved content in process water. Moreover, CHNS analysis and experimental BMP together provide biodegradability information of the process water as well: theoretical BMP from the elemental composition versus experimentally measured value. This is an important consideration regarding recycling the process water to the anaerobic digester in a biogas production plant. Another assumption in the mass balance is the gas composition due to the unavailability of gas composition analysis. This can also cause a slight mismatch in the elemental balances of carbon and hydrogen. Most of the experimental HTC studies determine the gas yield by difference through total mass balance, not measuring the composition. The HTC studies analyzing the gas compositions observed that carbon dioxide is the most dominant one (90 % by volume or more), followed by carbon monoxide (3–8 % by volume), and the remaining amount as hydrogen and methane [87,88]. Moreover, trace amounts of light hydrocarbons can also occur only in severe conditions [88]. The mismatch in determining the gas can be considered relatively insignificant from the preliminary mass balance and energetic viewpoints focusing on hydrochar production, despite gas composition being important from the environmental viewpoint. On the other hand, this slightly affects also the identifying process water as well for recycling or disposal, especially when CHNS analysis is not available for process water.

The mass balance for the HTC reactor is shown in Fig. 2, defining ash as a separate component and inert, i.e. digestate and hydrochar non-conventional components representing dry-ash-free portions of feedstock and solid product. Table 4 shows the ultimate and proximate analysis of non-conventional compounds defined in the simulation model. Representing ash separately, the digestate and feedstock compositions are calculated to represent dry-ash-free portions of those. In addition, all the organic content in process water is represented as a single non-conventional compound, namely organics, to enable mass balance. This might have a slight impact on the energy balance since the heating value of the organics is then calculated empirically within the simulation model. Another alternative could be introducing a set of conventional compounds per the functional groups in process water. However, this representation does not ensure a precise representation regarding elemental balance and heating value. Moreover, this requires a more intensive characterization of process water. Ash is the only inert component; Table 5 shows the yields defined in the simulation model on a non-inert basis. The non-inert-based yields are calculated as the mass flow rate of a product divided by total inlet except ash, i.e. the sum of water and dry-ash-free amounts. These yields are introduced as the input values to the RYIELD block of the simulation model. The calculations are determined in Supplementary Material for the mass balance around the reactor and the yields.

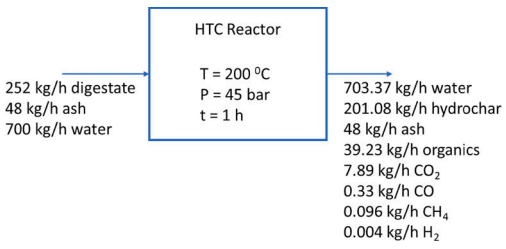

Fig. 2. Mass balance for the HTC reactor.

4.2. Dewatering and thermal drying

The reactor downstream has slightly over 70 % water content, as shown in Fig. 2. Therefore, hydrochar product is obtained after dewatering and thermal drying. The dewatering in this study is based on the experimental filtration results presented by Aragon-Briceno et al. (2022) [62]. The water content of the hydrochar stream is reduced to 50 % in the dewatering unit while recovering 85 % of the dry solid inlet in the hydrochar by spending 79.09 kJ/kg of dry solid. Afterwards, thermal drying is applied to reduce the moisture content down to 20 % by weight. The heat requirement for thermal drying is assumed as 3.82 MJ/kg of water evaporated based on the energy balance of HTC of sewage sludge at 200 °C with a residence time of 45 min, as presented by Zhao et al. (2014) [89]. Despite the different feedstock and slightly shorter residence time, this heat requirement is reasonable for preliminary assessment since the energy amount is obtained experimentally by drying the hydrochar. Nevertheless, this amount of energy was calculated when drying the hydrochar completely, while drying down to 20 % moisture content might require less energy. Fig. 3 shows the mass and energy balance for dewatering and thermal drying. The calculations are determined in Supplementary Material for the energy requirements of dewatering and thermal drying.

4.3. Energy balance and the impact of the thermodynamic property method

The process was simulated with four property methods mentioned in Section 3 to compare the convenience of these methods for the HTC process. Table 6 shows the heat duties of heat exchangers and power consumptions pump and compressor when the process is simulated with PSRK, SRK, NTRL, and IDEAL methods. NTRL and IDEAL methods result in the same heat and power values, while the results with SRK and PSRK methods differ for pump and heat exchangers involving the feedstock and reactor outlet. This study selects the PSRK method for evaluating energy balances because of temperature and pressure conditions and non-conventional compounds.

The heat of reaction plays an important role in heat integration; therefore, it is important to validate the calculated values. The heat of reaction is obtained via two methods: Hess's law based on the formation enthalpies and differential calorimetry measurements [90]. Calculating the heat of reaction via Hess's law requires proper representation of organics in process water and accurate measurement of the heating value of hydrochar. Meanwhile, calorimetry measurements require proper imitation of HTC conditions regarding temperature and residence time. Therefore, improvements are needed in the heat of reaction aspect. The simulation model calculates the heat duty of the reactor based on the enthalpies, i.e. Hess's law. For the case in this study, all investigated thermodynamic methods result in the same value, −122 kW, as the heat duty of the reactor. This value corresponds to −1.46 MJ/kg dry solid and −1.74 MJ/kg dry-ash-free solid inlet. The calculated heat of reaction is within the range of reported ones in the literature despite the need for more verification. For instance, the heat of reaction was measured as −1.07 MJ/kg dry-ash-free cellulose (with 9 % standard deviation) and −0.76 MJ/kg dry-ash-free wood (with 32 % standard

Table 4
Non-conventional compounds in the simulation model.

NC components	Ultimate analysis (wt%)					Proximate analysis (wt%)			
	C	H	N	S	O	Ash	FC	VM	HHV (MJ/kg)
Digestate	52.5	6.07	3.81	0.36	37.3	–	16.4	83.6	21.19
Hydrochar	61.2	7.29	4.18	0.12	27.2	–	20.3	79.7	24.97
Ash	–	–	–	–	–	100	–	–	–
Organics	17.6	9.57	3.0	1.7	68.1	–	–	100	Default value

Table 5
The calculated yields as defined in the simulation.

Component	Yield (kg/kg non-inert)
Hydrochar	0.2113
Water	0.7390
Organics	0.04122
CO_2	0.008289
H_2	0.000004186
CH_4	0.0001005
CO	0.0003516

deviation) at 240 °C with 10-hour residence time assuring the complete reaction [91]. It was also observed that the heat of the reaction increases with residence time and temperature as well. The measured heat of the reaction varied from −0.59 to −1.33 MJ/kg-cellulose at the temperature range of 180–240 °C with a 3-hour residence time [92]. Similarly, the heat of the reaction was measured as −2.53 and −3.47 MJ/kg of dry wood at 180 °C with 2.5-hour and 5.83-hour (350 min) residence times, respectively [93].

After selecting the thermodynamic method, the stream temperatures are also determined based on the energy balances. The simulation is based on processing 1000 kg/h wet digestate of AGR with 30 % solid load at 25 °C. The 'FEED' stream is pumped to a pressure of 45 bar, causing a one-degree increase in temperature. The heat exchange of the feedstock and reactor outlet cools the reactor outlet down to 49 °C while the feedstock is heated to 180 °C. The feedstock is further heated to 200 °C and transferred into the reactor. The reactor is assumed to operate isothermally while exothermic conversion results in heat release in the reactor. For instance, this excess heat from the reactor can be used to heat the air inlet for thermal drying, thus covering around three fourth of the heat required for thermal drying. The reactor outlet cooled down to 49 °C goes through dewatering and thermal drying. For thermal drying, the air temperature increases from 25 °C to 46 °C when compressing to 1.2 bars. In addition, the hydrochar product is calculated to be at 33 °C due to the evaporation of water, and exhaust air is at 70 °C.

The energy need of the process can be determined through the energy balances as heat and electricity requirements. The pump and the compressor require electricity. Meanwhile, the external heat requirements include heating the feedstock to the reaction temperature ("Heater" unit) and heating the air for thermal drying ("HEATAIR" unit) while the reactor releases heat because of exothermic conversion ("HTC" unit). As a further heat integration, the heat released by the reactor can also be utilized to heat the air inlet for thermal drying. This will reduce the external heat requirement for thermal drying. Table 7 shows the energy balance and net energy requirements of the process.

Table 6
Comparison of different property methods.

Property method	PUMP	HE1,2	HEATER	HEATAIR	HTC	COMPRESS
	Power (kW)	Heat (kW)	Heat (kW)	Heat (kW)	Heat (kW)	Power (kW)
PSRK	1.75	150	21	162	−122	56.4
SRK	1.37	170	24	162	−122	56.4
NRTL	1.32	162	25	162	−123	56.4
'IDEAL'	1.32	162	25	162	−123	56.4

Table 7
Heat and power requirements of the HTC process.

Electricity requirement	
PUMP	1.75 kW
COMPRESS	56.4 kW
Total electricity consumption	58.15 kW
Heat requirement	
HEATER	21 kW
HEATAIR	162 kW
HTC	−122 kW
Net heat consumption	61 kW

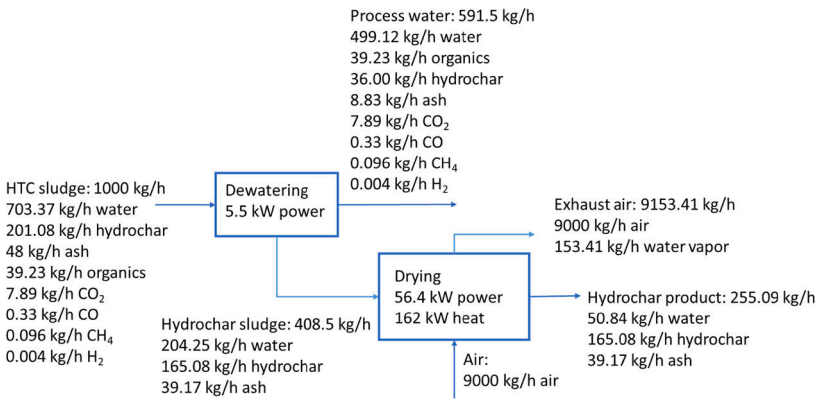

Fig. 3. Block diagram of dewatering and thermal drying.

When configuring the heat integration and energy balance, an operational issue is the pumpability of the feedstock with respect to solid load and target pressure. The energy balance shown in Table 7 assumes that the digestate is fluid and pressurized with a pump; however, a high solid load can cause the stream to be sludge rather than fluid, depending on the biomass nature and the pump type. The pumpability limits (maximum solid load) decrease with target pressure and particle size [94]. An assessment of high-pressure pumps for HTL processes stated the pumpability limit for sewage sludge is 22 % solid load at 220–300 bars while lignocellulosic biomass has the pumpability limit of 10–18 % solid load at 206–320 bars [94]. A similar assessment is required specifically for digestates and HTC conditions to investigate the pumpability limits. In the case of the digestate feedstock and reactor downstream being not pumpable as high solid load as 30 %, a single exchanger might not be applicable for heat transfer from the reactor downstream to the feedstock, thus requiring another heat integration concept. Fig. 4 shows an example of heat integration for the slurries not being pumpable and transferred by other means, e.g. screwdrivers or pistons, with the same stream names as in the simulation model illustrated in Fig. 1. This integration involves utility water cooling the reactor downstream and heating the However, this heat transfer is conducted with two heat exchangers, thus slightly increasing the investment cost. Moreover, this heat integration will increase the need for energy needed for heating the feedstock to the reaction temperature. The feedstock is heated to 160 °C instead of 180 °C, i.e. 40 °C gap to the reaction temperature instead of 20 °C. The energy balance showed that 21 kW is needed to heat the feedstock from 180 °C to 200 °C. Meanwhile, this requirement will increase to 42 kW when using the heat integration in Fig. 4.

5. Future perspectives

The HCT process is a prominent alternative for waste valorization from a technical viewpoint. Meanwhile, based on the aforementioned discussions in previous sections, some identified challenges and future recommendations are listed below.

- **Reaction kinetics and mechanism**

Due to the complicated phenomena inside the reactor (including reaction mechanism, kinetics, and heat and mass transfer), rather than mechanistic models, reactor design is based on empirical studies in laboratories providing limited insight into the nature and function of the reactions. This causes issues for in-process scale-up. The lab-scale results also need to be verified in pilot-scale reactors, or the yields are to be modified based on the results of pilot-scale reactors when scaling up the process.

- **Batch and continuous processes**

Most experiments on the HTC process are limited to laboratory scale and batch processes. Comparing batch and continuous processes, it can be concluded that the limitations of the batch process are limited heat recovery, limited feedstock load, and long heat-up and cool-down. Lack of information on continuous mode is a great challenge in industrialization and commercialization, and more importantly, reaching optimum conditions in the continuous process is also challenging.

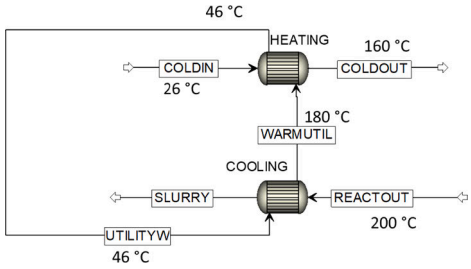

Fig. 4. An alternative heat integration for slurries over the pumpability limits.

- **Pumpability of feedstock**

Pumping wet biomass feedstock containing organic solid waste at high temperatures is another challenge, specifically in a continuous process. Considering operational problems reviewed by Ghavami et al. (2021) [30], pumping two-phase and highly concentrated feedstock in the subcritical condition is one of the main challenges in dealing with biomass feedstock to avoid clogging and maintain a steady flow rate into the reactor. The pumpability of feedstock and product sludges will influence the heat integration as well. Therefore, an assessment of high-pressure pumps is required specifically for digestates and HTC conditions to investigate the pumpability limits.

- **Integration of HTC and dewatering**

The integration of the HTC process with the dewatering section can reduce the moisture of the final product. Most post-dewatering methods include filter press by a piston, centrifuge separation, and pressurized HTC, which decrease the moisture content in hydrochar only up to 20 % compared to the biomass feedstock and require a lot of energy for water evaporation [62,66]. Dewatering in hot conditions directly and in-situ mechanical compression is one of the methods that are rarely studied and reported in the literature. However, it is also worth considering that no clear trend was reported for the relation between potential water recovery and thermal treatment and retention time. To the authors' knowledge, the dewaterability properties of different biomass feedstock are not widely investigated.

The aqueous phase contains secondary hydrochar and some organic components that can be recovered to reduce the economic cost of the HTC process.

- **Energetic applications of hydrochar**

Hydrochar has been used for combustion, gasification, and pyrolysis; however, according to reports, its reactivity is not adequate in combustion [95]. In addition, the conversion of N and S for air pollution components requires more work to control the combustion [96]. Some organic additives such as citric acid are needed to add to the hydrochar to make it more stable for combustion [97]. Moreover, a detailed analysis of ash composition shows the possibility of some operational problems like corrosion, slagging, and fouling during combustion [98]. On the other hand, the pyrolysis and gasification processes require low moisture biomass; high moisture and low-energy–density biomass cannot be utilized in these processes. Nevertheless, hydrochar has higher hydrophobicity, grindability, and energy density than biochar produced via torrefaction [99]. The upgraded biomass in the HTC process can improve the performance of gasification and pyrolysis processes.

- **Hydrochar as a fertilizer**

The impacts of hydrochar in soil include nutrient release, mineralization, carbon sequestration, higher fertilizer efficiency, water holding capacity, and lowering N_2O emissions in the presence of animal manure [27]. The high amount of remaining nitrogen and phosphorous in hydrochar shows its potential as a nutrient provider. It can also be added to the soil to improve the effectiveness of the fertilizer and decrease fertilizer loss [100]. The nutrient is slowly released into the soil over the time that the plant grows by hydrochar [101]. The controlled release of

nitrogen improves the efficiency of the fertilizer and, more importantly, reduces the risk of pollution and environmental damages [102].

An important issue is heavy metal concentrations when applying hydrochar as a fertilizer. Nevertheless, heavy metal concentrations of hydrochar from digestates are usually within the standards. HTC of the sewage sludge digestate of a biogas plant located in Turku (Finland) resulted in hydrochars with low enough heavy metal contents to fulfill the EU standards regardingfertilizers [103]. Meanwhile, many other digestates have much lower ash and heavy metal content than the sewage sludge digestate, including the AGR digestate simulated in this study.

However, negative impacts were also observed depending on the plant type, the dose of hydrochar and the C:N ratio [104]. For instance, using manure digestates can cause overfertilization due to high nitrogen content, while sewage sludge digestates can be more suitable for soil amendment [61]. This can be addressed by engineering the hydrochar or using activated carbon [27].

- **HTC integration**

Integration of waste valorization processes has great importance in the bioeconomy to produce value-added products [105]. In addition, intermediate products produced in regional processes play a crucial role in the overall biomass supply chain network [105]. There is much potential in this regard and fewer studies that require more research and investigations [106]. For instance, the integration of the AD process followed by HTC is still under evaluation. According to the literature, applying a hydrothermal treatment as a post-treatment after AD could extract the energy from biomass digestate [107–109]. Compared from a techno-economic and life cycle assessment point of view, integration of the HTC system for sewage sludge reduces environmental impact, according to Medina-Martos et al. [110]. Furthermore, considering that plastic wastes are also a major problem, co-HTC of biomass and halogenated plastics improves the hydrochar quality by enhancing the removal of chlorine and inorganics [28].

6. Conclusion

More research and studies are recently driven to conversion of digestate from AD into value-added products due to the increase of AD process for organic waste/biomass treatment and the environmental restrictions for its direct usage. Hydrothermal carbonization is proper for high-moisture feedstock as a prominent method for waste valorization in the subcritical region.

This research article investigates the simulation aspects of the HTC process of the digestate to estimate the optimum condition and to formulate mass and energy balances. Regarding the selection of optimum conditions, the energetic yield is defined as the energy content in hydrochar per reactor inlet from the techno-economic viewpoint: implying the relative equipment sizes and the optimum compromise of the opposite impact of temperature on hydrochar yield and heating value. It is concluded that mass balance is enabled by adequate characterization of process water as well as the feedstock and hydrochar. In addition, the accuracy of mass balance can be increased with more data on process water (e.g. CHNS) and gas composition. The accuracy of mass balance influences the simulation model as well since the reactor outlet is defined based on the experimental results. The adequate characterization will provide accurate elemental balances by representing organics in process water accurately and defining the observed gas composition rather than assuming. The energy balance is obtained through the simulation results after formulating the mass balance. Due to the importance of the heat of the reaction in heat integration, the heat duty of the reactor was estimated based on the reactor inlet and outlet as well as the heating values of the feedstock and hydrochar. The heat of the reaction is also verified by comparing the data reported in the literature for model compounds and similar biomass feedstocks.

The main challenges and future aspects include investigating the product yields in a continuous, pilot-scale reactor and verifying the heat of reaction with the real biomass under the scope. The product yields might differ in an industrial application from the lab-scale results due to different reactor configurations and heat integration. Therefore, the feasibility assessments should be conducted with the pilot-scale results closer to the industrial process. In addition, even though the heat of reaction can be justified by comparing the literature values, the accuracy of energy balance can be improved by measuring the exact heat of reaction for the real biomass feedstock and reaction conditions. In addition, more investigations are needed on the reaction kinetics, different reaction pathways, and transport phenomena to enable mechanistic or semi-mechanistic models.

CRediT authorship contribution statement

Niloufar Ghavami: Writing – original draft, Writing – review & editing, Conceptualization, Methodology, Software, Investigation. **Karhan Özdenkçi:** Writing – original draft, Writing – review & editing, Conceptualization, Methodology, Software. **Simeone Chianese:** Writing – review & editing, Visualization. **Dino Musmarra:** Supervision, Funding acquisition. **Cataldo De Blasio:** Project administration, Supervision, Funding acquisition, Writing – review & editing.

Declaration of Competing Interest

The authors declare that they have no known competing financial interests or personal relationships that could have appeared to influence the work reported in this paper.

Data availability

Data will be made available on request.

Acknowledgements

We gratefully acknowledge the financial support of Kaute Foundation [20210185], Finland and the University Foundation in Ostrobothnia (Högskolestiftelsen) [28600148], Finland. We also acknowledge the Regional Council of Ostrobothnia for their support in conducting the EU-ERUF project named “Implementation of a hydrothermal carbonization process for the disposal sludge and wet organic streams” [28400198K1], Finland. The authors would like to thank the VALERE “VAnviteLli pEr la RicErca” PROGRAMME and 2021-2022 Call for Visiting Professors/Researchers at the University of Campania Luigi Vanvitelli, Italy.

Appendix A. Supplementary material

Supplementary material is provided to determine the mass balance and energy consumption in the dewatering and drying sections. Supplementary data to this article can be found online at https://doi.org/10.1016/j.enconman.2022.116215.

References

[1] Sustainability | United Nations n.d. https://www.un.org/en/academic-impact/sustainability [accessed July 25, 2022].
[2] Solarte-Toro JC, Cardona Alzate CA. Biorefineries as the base for accomplishing the sustainable development goals (SDGs) and the transition to bioeconomy: Technical aspects, challenges and perspectives. Bioresour Technol 2021;340:125626. https://doi.org/10.1016/j.biortech.2021.125626.
[3] Zeng Y, Maxwell S, Runting RK, Venter O, Watson JEM, Carrasco LR. Environmental destruction not avoided with the Sustainable Development Goals. Nat Sustain 2020;3:795–8. https://doi.org/10.1038/s41893-020-0555-0.
[4] Naveenkumar R, Baskar G. Process optimization, green chemistry balance and technoeconomic analysis of biodiesel production from castor oil using heterogeneous nanocatalyst. Bioresour Technol 2021;320:124347. https://doi.org/10.1016/j.biortech.2020.124347.

[5] De Pascale A, Arbolino R, Szopik-Depczyńska K, Limosani M, Ioppolo G. A systematic review for measuring circular economy: The 61 indicators. J Cleaner Prod 2021;281:124942. https://doi.org/10.1016/j.jclepro.2020.124942.

[6] Rezvani Ghomi E, Khosravi F, Tahavori MA, Ramakrishna S. Circular Economy: a Comparison Between the Case of Singapore and France. Mater Circ Econ 2021;3:2. https://doi.org/10.1007/s42824-020-00016-w.

[7] United Nations Official Document n.d. https://www.un.org/ga/search/view_doc.asp?symbol=A/RES/70/1&Lang=E [accessed December 8, 2021].

[8] Sam A, Barik D. Chapter 2 - Toxic Waste From Municipality. In: Barik D, editor. Energy from Toxic Organic Waste for Heat and Power Generation. Woodhead Publishing; 2019. p. 7–16. https://doi.org/10.1016/B978-0-08-102528-4.00002-X.

[9] Gómez-Camacho CE, Pirone R, Ruggeri B. Is the Anaerobic Digestion (AD) sustainable from the energy point of view? Energy Convers Manage 2021;231:113857. https://doi.org/10.1016/j.enconman.2021.113857.

[10] Rajendran K, Mahapatra D, Venkatraman AV, Muthuswamy S, Pugazhendhi A. Advancing anaerobic digestion through two-stage processes: Current developments and future trends. Renew Sustain Energy Rev 2020;123:109746. https://doi.org/10.1016/j.rser.2020.109746.

[11] Zhang C, Shao M, Wu H, Wang N, Chen Q, Xu Q. Management and valorization of digestate from food waste via hydrothermal. Resour Conserv Recycl 2021;171:105639. https://doi.org/10.1016/j.resconrec.2021.105639.

[12] Roopnarain A, Rama H, Ndaba B, Bello-Akinosho M, Bamuza-Pemu E, Adeleke R. Unravelling the anaerobic digestion 'black box': Biotechnological approaches for process optimization. Renew Sustain Energy Rev 2021;152:111717. https://doi.org/10.1016/j.rser.2021.111717.

[13] Kampman B, Leguijt C, Scholten T, Tallat-Kelpsaite J, Brückmann R, Maroulis G, et al. An assessment of the potential of biogas from digestion in the EU beyond 2020 n.d.:158.

[14] Vázquez-Rowe I, Golkowska K, Lebuf V, Vaneeckhaute C, Michels E, Meers E, et al. Environmental assessment of digestate treatment technologies using LCA methodology. Waste Manage 2015;43:442–59. https://doi.org/10.1016/j.wasman.2015.05.007.

[15] Provenzano MR, Cavallo O, Malerba AD, Fabbri C, Zaccone C. Unravelling (maize silage) digestate features throughout a full-scale plant: A spectroscopic and thermal approach. J Cleaner Prod 2018;193:372–8. https://doi.org/10.1016/j.jclepro.2018.05.081.

[16] Catenacci A, Boniardi G, Mainardis M, Gievers F, Farru G, Asunis F, et al. Processes, applications and legislative framework for carbonized anaerobic digestate: Opportunities and bottlenecks. A critical review. Energy Convers Manage 2022;263:115691. https://doi.org/10.1016/j.enconman.2022.115691.

[17] Cao Z, Jung D, Olszewski MP, Arauzo PJ, Kruse A. Hydrothermal carbonization of biogas digestate: Effect of digestate origin and process conditions. Waste Manage 2019;100:138–50. https://doi.org/10.1016/j.wasman.2019.09.009.

[18] Tan F, Zhu Q, Guo X, He L. Effects of digestate on biomass of a selected energy crop and soil properties. J Sci Food Agric 2021;101:927–36. https://doi.org/10.1002/jsfa.10700.

[19] Sambusiti C, Monlau F, Ficara E, Musatti A, Rollini M, Barakat A, et al. Comparison of various post-treatments for recovering methane from agricultural digestate. Fuel Process Technol 2015;137:359–65. https://doi.org/10.1016/j.fuproc.2015.04.028.

[20] Herbes C, Roth U, Wulf S, Dahlin J. Economic assessment of different biogas digestate processing technologies: A scenario-based analysis. J Cleaner Prod 2020;255:120282. https://doi.org/10.1016/j.jclepro.2020.120282.

[21] Monfet E, Aubry G, Ramirez AA. Nutrient removal and recovery from digestate: a review of the technology. Biofuels 2018;9:247–62. https://doi.org/10.1080/17597269.2017.1336348.

[22] Romio C, Kofoed MVW, Møller HB. Digestate Post-Treatment Strategies for Additional Biogas Recovery: A Review. Sustainability 2021;13:9295. https://doi.org/10.3390/su13169295.

[23] Park M, Kim N, Lee S, Yeon S, Seo JH, Park D. A study of solubilization of sewage sludge by hydrothermal treatment. J Environ Manage 2019;250:109490. https://doi.org/10.1016/j.jenvman.2019.109490.

[24] Huang H, Yuan X. The migration and transformation behaviors of heavy metals during the hydrothermal treatment of sewage sludge. Bioresour Technol 2016;200:991–8. https://doi.org/10.1016/j.biortech.2015.10.099.

[25] Kumar M, Olajire Oyedun A, Kumar A. A review on the current status of various hydrothermal technologies on biomass feedstock. Renew Sustain Energy Rev 2018;81:1742–70. https://doi.org/10.1016/j.rser.2017.05.270.

[26] Tekin K, Karagöz S, Bektaş S. A review of hydrothermal biomass processing. Renew Sustain Energy Rev 2014;40:673–87. https://doi.org/10.1016/j.rser.2014.07.216.

[27] Heidari M, Dutta A, Acharya B, Mahmud S. A review of the current knowledge and challenges of hydrothermal carbonization for biomass conversion. J Energy Inst 2019;92:1779–99. https://doi.org/10.1016/j.joei.2018.12.003.

[28] Shen Y. A review on hydrothermal carbonization of biomass and plastic wastes to energy products. Biomass Bioenergy 2020;134:105479. https://doi.org/10.1016/j.biombioe.2020.105479.

[29] Krylova AY, Zaitchenko VM. Hydrothermal Carbonization of Biomass: A Review. Solid Fuel Chem 2018;52:91–103. https://doi.org/10.3103/S0361521918020076.

[30] Ghavami N, Özdenkçi K, Salierno G, Björklund-Sänkiaho M, De Blasio C. Analysis of operational issues in hydrothermal liquefaction and supercritical water gasification processes: a review. Biomass Conv Bioref 2021. https://doi.org/10.1007/s13399-021-02176-4.

[31] Stobernack N, Mayer F, Malek C, Bhandari R, Himanshu H. Hydrothermal carbonization of biowaste as an alternative treatment path to current waste management practices in Germany. Energy Convers Manage 2021;244:114433. https://doi.org/10.1016/j.enconman.2021.114433.

[32] Li J, Zhu X, Li Y, Tong YW, Ok YS, Wang X. Multi-task prediction and optimization of hydrochar properties from high-moisture municipal solid waste: Application of machine learning on waste-to-resource. J Cleaner Prod 2021;278:123928. https://doi.org/10.1016/j.jclepro.2020.123928.

[33] Ahmed M, Andreottola G, Elagroudy S, Negm MS, Fiori L. Coupling hydrothermal carbonization and anaerobic digestion for sewage digestate management: Influence of hydrothermal treatment time on dewaterability and bio-methane production. J Environ Manage 2021;281:111910. https://doi.org/10.1016/j.jenvman.2020.111910.

[34] Funke A, Ziegler F. Hydrothermal carbonization of biomass: A summary and discussion of chemical mechanisms for process engineering. Biofuels, Bioprod Biorefin 2010;4:160–77. https://doi.org/10.1002/bbb.198.

[35] Sharma HB, Sarmah AK, Dubey B. Hydrothermal carbonization of renewable waste biomass for solid biofuel production: A discussion on process mechanism, the influence of process parameters, environmental performance and fuel properties of hydrochar. Renew Sustain Energy Rev 2020;123:109761. https://doi.org/10.1016/j.rser.2020.109761.

[36] Wang L, Li A, Chang Y. Hydrothermal treatment coupled with mechanical expression at increased temperature for excess sludge dewatering: Heavy metals, volatile organic compounds and combustion characteristics of hydrochar. Chem Eng J 2016;297:1–10. https://doi.org/10.1016/j.cej.2016.03.131.

[37] Zhang S, Zhu X, Zhou S, Shang H, Luo J, Tsang DCW. Chapter 15 - Hydrothermal Carbonization for Hydrochar Production and Its Application. In: Ok YS, Tsang DCW, Bolan N, Novak JM, editors. Biochar from Biomass and Waste, Elsevier; 2019, p. 275–94. https://doi.org/10.1016/B978-0-12-811729-3.00015-7.

[38] Xia Y, Yang T, Zhu N, Li D, Chen Z, Lang Q, et al. Enhanced adsorption of Pb(II) onto modified hydrochar: Modeling and mechanism analysis. Bioresour Technol 2019;288:121593. https://doi.org/10.1016/j.biortech.2019.121593.

[39] Zhao P, Shen Y, Ge S, Chen Z, Yoshikawa K. Clean solid biofuel production from high moisture content waste biomass employing hydrothermal treatment. Appl Energy 2014;131:345–67. https://doi.org/10.1016/j.apenergy.2014.06.038.

[40] Ok YS, Tsang DCW, Bolan N, Novak JM. Biochar from Biomass and Waste: Fundamentals and Applications. Elsevier; 2018.

[41] Yahav Spitzer R, Mau V, Gross A. Using hydrothermal carbonization for sustainable treatment and reuse of human excreta. J Cleaner Prod 2018;205:955–63. https://doi.org/10.1016/j.jclepro.2018.09.126.

[42] Saha N, McGaughy K, Davis SC, Reza MT. Assessing hydrothermal carbonization as sustainable home sewage management for rural counties: A case study from Appalachian Ohio. Sci Total Environ 2021;781:146648. https://doi.org/10.1016/j.scitotenv.2021.146648.

[43] Kambo HS, Dutta A. A comparative review of biochar and hydrochar in terms of production, physico-chemical properties and applications. Renew Sustain Energy Rev 2015;45:359–78. https://doi.org/10.1016/j.rser.2015.01.050.

[44] Pawlak-Kruczek H, Niedzwiecki L, Sieradzka M, Mlonka-Mędrala A, Baranowski M, Serafin-Tkaczuk M, et al. Hydrothermal carbonization of agricultural and municipal solid waste digestates – Structure and energetic properties of the solid products. Fuel 2020;275:117837. https://doi.org/10.1016/j.fuel.2020.117837.

[45] Parmar KR, Ross AB. Integration of Hydrothermal Carbonisation with Anaerobic Digestion. Opportunities for Valorisation of Digestate Energies 2019;12:1586. https://doi.org/10.3390/en12091586.

[46] Wilk M, Magdziarz A, Jayaraman K, Szymańska-Chargot M, Gökalp I. Hydrothermal carbonization characteristics of sewage sludge and lignocellulosic biomass. A comparative study. Biomass Bioenergy 2019;120:166–75. https://doi.org/10.1016/j.biombioe.2018.11.016.

[47] Schnell M, Horst T, Quicker P. Thermal treatment of sewage sludge in Germany: A review. J Environ Manage 2020;263:110367. https://doi.org/10.1016/j.jenvman.2020.110367.

[48] Mendoza Martinez CL, Sermyagina E, Vakkilainen E. Hydrothermal Carbonization of Chemical and Biological Pulp Mill Sludges. Energies 2021;14:5693. https://doi.org/10.3390/en14185693.

[49] Mäki E, Saastamoinen H, Melin K, Matschegg D, Pihkola H. Drivers and barriers in retrofitting pulp and paper industry with bioenergy for more efficient production of liquid, solid and gaseous biofuels: A review. Biomass Bioenergy 2021;148:106036. https://doi.org/10.1016/j.biombioe.2021.106036.

[50] Seruga P, Krzywonos M, Seruga A, Niedźwiecki Ł, Pawlak-Kruczek H, Urbanowska A. Anaerobic Digestion Performance: Separate Collected vs. Mechanical Segregated Organic Fractions of Municipal Solid Waste as Feedstock. Energies 2020;13:3768. https://doi.org/10.3390/en13153768.

[51] Danso-Boateng E, Holdich RG, Martin SJ, Shama G, Wheatley AD. Process energetics for the hydrothermal carbonisation of human faecal wastes. Energy Convers Manage 2015;105:1115–24. https://doi.org/10.1016/j.enconman.2015.08.064.

[52] Bhakta Sharma H, Panigrahi S, Dubey BK. Food waste hydrothermal carbonization: Study on the effects of reaction severities, pelletization and framework development using approaches of the circular economy. Bioresour Technol 2021;333:125187. https://doi.org/10.1016/j.biortech.2021.125187.

[53] Zhuang X, Liu J, Zhang Q, Wang C, Zhan H, Ma L. A review on the utilization of industrial biowaste via hydrothermal carbonization. Renew Sustain Energy Rev 2022;154:111877. https://doi.org/10.1016/j.rser.2021.111877.

[54] Belete YZ, Mau V, Yahav Spitzer R, Posmanik R, Jassby D, Iddya A, et al. Hydrothermal carbonization of anaerobic digestate and manure from a dairy farm

on energy recovery and the fate of nutrients. Bioresour Technol 2021;333: 125164. https://doi.org/10.1016/j.biortech.2021.125164.
[55] Román S, Ledesma B, Álvarez A, Coronella C, Qaramaleki SV. Suitability of hydrothermal carbonization to convert water hyacinth to added-value products. Renewable Energy 2020;146:1649–58. https://doi.org/10.1016/j.renene.2019.07.157.
[56] Nzediegwu C, Naeth MA, Chang SX. Carbonization temperature and feedstock type interactively affect chemical, fuel, and surface properties of hydrochars. Bioresour Technol 2021;330:124976. https://doi.org/10.1016/j.biortech.2021.124976.
[57] Aragón-Briceño CI, Grasham O, Ross AB, Dupont V, Camargo-Valero MA. Hydrothermal carbonization of sewage digestate at wastewater treatment works: Influence of solid loading on characteristics of hydrochar, process water and plant energetics. Renewable Energy 2020;157:959–73. https://doi.org/10.1016/j.renene.2020.05.021.
[58] Fujiwara M, Koyama M, Akizuki S, Ban S, Toda T. Influence of lignocellulosic components on the anaerobic digestibility of aquatic weeds: Comparison with terrestrial crops. Ind Crops Prod 2022;178:114576. https://doi.org/10.1016/j.indcrop.2022.114576.
[59] Wang T, Zhai Y, Zhu Y, Li C, Zeng G. A review of the hydrothermal carbonization of biomass waste for hydrochar formation: Process conditions, fundamentals, and physicochemical properties. Renew Sustain Energy Rev 2018;90:223–47. https://doi.org/10.1016/j.rser.2018.03.071.
[60] Ischia G, Fiori L. Hydrothermal Carbonization of Organic Waste and Biomass: A Review on Process, Reactor, and Plant Modeling. Waste Biomass Valor 2021;12: 2797–824. https://doi.org/10.1007/s12649-020-01255-3.
[61] Kruse A, Dahmen N. Hydrothermal biomass conversion: Quo vadis? J Supercrit Fluids 2018;134:114–23. https://doi.org/10.1016/j.supflu.2017.12.035.
[62] Aragon-Briceño C, Pożarlik A, Bramer E, Brem G, Wang S, Wen Y, et al. Integration of hydrothermal carbonization treatment for water and energy recovery from organic fraction of municipal solid waste digestate. Renewable Energy 2022;184:577–91. https://doi.org/10.1016/j.renene.2021.11.106.
[63] Reza MT, Andert J, Wirth B, Busch D, Pielert J, Lynam JG, et al. Hydrothermal Carbonization of Biomass for Energy and Crop Production. Appl Bioenergy 2014; 1. https://doi.org/10.2478/apbi-2014-0001.
[64] Lu X, Ma X, Qin Z, Chen X, Chen L, Tian Y. Co-hydrothermal carbonization of sewage sludge and polyvinyl chloride: Hydrochar properties and fate of chlorine and heavy metals. J Environ Chem Eng 2021;9:106143. https://doi.org/10.1016/j.jece.2021.106143.
[65] Munir MT, Mansouri SS, Udugama IA, Baroutian S, Gernaey KV, Young BR. Resource recovery from organic solid waste using hydrothermal processing: Opportunities and challenges. Renew Sustain Energy Rev 2018;96:64–75. https://doi.org/10.1016/j.rser.2018.07.039.
[66] Gao N, Li Z, Quan C, Miskolczi N, Egedy A. A new method combining hydrothermal carbonization and mechanical compression in-situ for sewage sludge dewatering: Bench-scale verification. J Anal Appl Pyrol 2019;139:187–95. https://doi.org/10.1016/j.jaap.2019.02.003.
[67] Kambo HS, Minaret J, Dutta A. Process Water from the Hydrothermal Carbonization of Biomass: A Waste or a Valuable Product? Waste Biomass Valor 2018;9:1181–9. https://doi.org/10.1007/s12649-017-9914-0.
[68] Wang F, Wang J, Gu C, Han Y, Zan S, Wu S. Effects of process water recirculation on solid and liquid products from hydrothermal carbonization of Laminaria. Bioresour Technol 2019;292:121996. https://doi.org/10.1016/j.biortech.2019.121996.
[69] Heidari M, Salaudeen S, Dutta A, Acharya B. Effects of Process Water Recycling and Particle Sizes on Hydrothermal Carbonization of Biomass. Energy Fuels 2018; 32:11576–86. https://doi.org/10.1021/acs.energyfuels.8b02684.
[70] Basso D, Weiss-Hortala E, Patuzzi F, Baratieri M, Fiori L. In Deep Analysis on the Behavior of Grape Marc Constituents during Hydrothermal Carbonization. Energies 2018;11:1379. https://doi.org/10.3390/en11061379.
[71] Erses Yay AS, Birinci B, Açıkalın S, Yay K. Hydrothermal carbonization of olive pomace and determining the environmental impacts of post-process products. J Cleaner Prod 2021;315:128087. https://doi.org/10.1016/j.jclepro.2021.128087.
[72] McGaughy K, Toufiq RM. Hydrothermal carbonization of food waste: simplified process simulation model based on experimental results. Biomass Conv Bioref 2018;8:283–92. https://doi.org/10.1007/s13399-017-0276-4.
[73] Safarian S, Rydén M, Janssen M. Development and Comparison of Thermodynamic Equilibrium and Kinetic Approaches for Biomass Pyrolysis Modeling. Energies 2022;15:3999. https://doi.org/10.3390/en15113999.
[74] Reza MT, Mumme J, Ebert A. Characterization of hydrochar obtained from hydrothermal carbonization of wheat straw digestate. Biomass Conv Bioref 2015; 5:425–35. https://doi.org/10.1007/s13399-015-0163-9.
[75] He M, Zhu X, Dutta S, Khanal SK, Lee KT, Masek O, et al. Catalytic co-hydrothermal carbonization of food waste digestate and yard waste for energy application and nutrient recovery. Bioresour Technol 2022;344:126395. https://doi.org/10.1016/j.biortech.2021.126395.
[76] Özdenkçi K, De Blasio C, Sarwar G, Melin K, Koskinen J, Alopaeus V. Techno-economic feasibility of supercritical water gasification of black liquor. Energy 2019;189:116284. https://doi.org/10.1016/j.energy.2019.116284.
[77] Özdenkçi K, Prestipino M, Björklund-Sänkiaho M, Galvagno A, De Blasio C. Alternative energy valorization routes of black liquor by stepwise supercritical water gasification: Effect of process parameters on hydrogen yield and energy efficiency. Renew Sustain Energy Rev 2020;134:110146. https://doi.org/10.1016/j.rser.2020.110146.
[78] Chen X, Li H. Improved Prediction of Saturated and Single-Phase Liquid Densities of Water through Volume-Translated SRK EOS. Fluid Phase Equilib 2021;528: 112852. https://doi.org/10.1016/j.fluid.2020.112852.
[79] Sadjadi S, Hosseinpour M, Mohammadnezhad F, Ahmadi SJ, Khazayi MA. Hydrogen-Deuterium chemical exchange in supercritical water: Thermodynamic considerations for optimizing the synthesis of high degree deuterated benzene. J Supercrit Fluids 2017;125:96–103. https://doi.org/10.1016/j.supflu.2017.02.010.
[80] Lozano EM, Pedersen TH, Rosendahl LA. Generic approach for the modeling of liquefied thermochemical products and biomass heat of formation. Case study: HTL biocrude, Pyrolysis oil and assessment of energy requirements n.d.:18.
[81] Soave G. Equilibrium constants from a modified Redlich-Kwong equation of state. Chem Eng Sci 1972;27:1197–203. https://doi.org/10.1016/0009-2509(72)80096-4.
[82] Holderbaum T, Gmehling J. PSRK: A Group Contribution Equation of State Based on UNIFAC. Fluid Phase Equilib 1991;70:251–65. https://doi.org/10.1016/0378-3812(91)85038-V.
[83] Vella JR, Marshall BD. Prediction of the Distillation Curve and Vapor Pressure of Alcohol-Gasoline Blends Using Pseudocomponents and an Equation of State. Ind Eng Chem Res 2020;59:8361–73. https://doi.org/10.1021/acs.iecr.0c00226.
[84] Gmehling J, Li J, Fischer K. Further development of the PSRK model for the prediction of gas solubilities and vapor-liquid -equilibria at low and high pressures II. Fluid Phase Equilib 1997;141:113–27. https://doi.org/10.1016/S0378-3812(97)00204-5.
[85] Alshbuki EH, Bey MM, Mohamed AAla. Simulation Production of Dimethylether (DME) from Dehydration of Methanol Using Aspen Hysys. SIJCMS 2020;03:13–8. https://doi.org/10.36348/sijcms.2020.v03i02.002.
[86] Dadmohammadi Y, Gebreyohannes S, Neely BJ, Gasem KAM. Application of Modified NRTL Models for Binary LLE Phase Characterization. Ind Eng Chem Res 2018;57:7282–90. https://doi.org/10.1021/acs.iecr.8b00683.
[87] Hoekman SK, Broch A, Robbins C, Zielinska B, Felix L. Hydrothermal carbonization (HTC) of selected woody and herbaceous biomass feedstocks. Biomass Conv Bioref 2013;3:113–26. https://doi.org/10.1007/s13399-012-0066-y.
[88] Basso D, Weiss-Hortala E, Patuzzi F, Castello D, Baratieri M, Fiori L. Hydrothermal carbonization of off-specification compost: A byproduct of the organic municipal solid waste treatment. Bioresour Technol 2015;182:217–24. https://doi.org/10.1016/j.biortech.2015.01.118.
[89] Zhao P, Shen Y, Ge S, Yoshikawa K. Energy recycling from sewage sludge by producing solid biofuel with hydrothermal carbonization. Energy Convers Manage 2014;78:815–21. https://doi.org/10.1016/j.enconman.2013.11.026.
[90] Pecchi M, Patuzzi F, Basso D, Baratieri M. Enthalpy change during hydrothermal carbonization of biomass: a critical review. J Therm Anal Calorim 2020;141: 1251–62. https://doi.org/10.1007/s10973-019-09117-4.
[91] Funke A, Ziegler F. Heat of reaction measurements for hydrothermal carbonization of biomass. Bioresour Technol 2011;102:7595–8. https://doi.org/10.1016/j.biortech.2011.05.016.
[92] Ischia G, Cazzanelli M, Fiori L, Orlandi M, Miotello A. Exothermicity of hydrothermal carbonization: Determination of heat profile and enthalpy of reaction via high-pressure differential scanning calorimetry. Fuel 2022;310: 122312. https://doi.org/10.1016/j.fuel.2021.122312.
[93] Cuvilas CA, Kantarelis E, Yang W. The Impact of a Mild Sub-Critical Hydrothermal Carbonization Pretreatment on Umbila Wood. A Mass and Energy Balance Perspective. Energies 2015;8:2165–75. https://doi.org/10.3390/en8032165.
[94] Berglin E, Enderlin C, Schmidt A. Review and Assessment of Commercial Vendors/Options for Feeding and Pumping Biomass Slurries for Hydrothermal Liquefaction. Pacific Northwest National Lab. (PNNL), Richland, WA (United States); 2012.
[95] Volpe M, Luz FC, Saha N, Reza MT, Mosonik MC, Volpe R, et al. Enhancement of energy and combustion properties of hydrochar via citric acid catalysed secondary char production. Biomass Conv Bioref 2021. https://doi.org/10.1007/s13399-021-01816-z.
[96] Zhang Z, Yang J, Qian J, Zhao Y, Wang T, Zhai Y. Biowaste hydrothermal carbonization for hydrochar valorization: Skeleton structure, conversion pathways and clean biofuel applications. Bioresour Technol 2021;324:124686. https://doi.org/10.1016/j.biortech.2021.124686.
[97] Wilk M, Śliz M, Lubieniecki B. Hydrothermal co-carbonization of sewage sludge and fuel additives: Combustion performance of hydrochar. Renewable Energy 2021;178:1046–56. https://doi.org/10.1016/j.renene.2021.06.101.
[98] Magdziarz A, Gajek M, Nowak-Woźny D, Wilk M. Mineral phase transformation of biomass ashes – Experimental and thermochemical calculations. Renewable Energy 2018;128:446–59. https://doi.org/10.1016/j.renene.2017.05.057.
[99] Kambo HS, Dutta A. Comparative evaluation of torrefaction and hydrothermal carbonization of lignocellulosic biomass for the production of solid biofuel. Energy Convers Manage 2015;105:746–55. https://doi.org/10.1016/j.enconman.2015.08.031.
[100] Fang J, Zhan L, Ok YS, Gao B. Minireview of potential applications of hydrochar derived from hydrothermal carbonization of biomass. J Ind Eng Chem 2018;57: 15–21. https://doi.org/10.1016/j.jiec.2017.08.026.
[101] Wu L, Wei W, Wang D, Ni B-J. Improving nutrients removal and energy recovery from wastes using hydrochar. Sci Total Environ 2021;783:146980. https://doi.org/10.1016/j.scitotenv.2021.146980.
[102] Wu W, Yan B, Sun Y, Zhong L, Lu W, Chen G. Potential of yak dung-derived hydrochar as fertilizer: Mechanism and model of controlled release of nitrogen.

Sci Total Environ 2021;781:146665. https://doi.org/10.1016/j.scitotenv.2021.146665.
[103] Hämäläinen A, Kokko M, Kinnunen V, Hilli T, Rintala J. Hydrothermal carbonisation of mechanically dewatered digested sewage sludge—Energy and nutrient recovery in centralised biogas plant. Water Res 2021;201:117284. https://doi.org/10.1016/j.watres.2021.117284.
[104] Bargmann I, Rillig MC, Kruse A, Greef J-M, Kücke M. Effects of hydrochar application on the dynamics of soluble nitrogen in soils and on plant availability. J Plant Nutr Soil Sci 2014;177:48–58. https://doi.org/10.1002/jpln.201300069.
[105] Özdenkçi K, De Blasio C, Muddassar HR, Melin K, Oinas P, Koskinen J, et al. A novel biorefinery integration concept for lignocellulosic biomass. Energy Convers Manage 2017;149:974–87. https://doi.org/10.1016/j.enconman.2017.04.034.
[106] Drabold E, McGaughy K, Agner J, Sellars D, Johnson R, Hajer AA, et al. Challenges and process economics for algal carbon capture with novel integration: Hydrothermal carbonization. Bioresource Technol Reports 2020;12:100556. https://doi.org/10.1016/j.biteb.2020.100556.
[107] Aragón-Briceño CI, Ross AB, Camargo-Valero MA. Mass and energy integration study of hydrothermal carbonization with anaerobic digestion of sewage sludge. Renewable Energy 2021;167:473–83. https://doi.org/10.1016/j.renene.2020.11.103.
[108] Lucian M, Volpe M, Merzari F, Wüst D, Kruse A, Andreottola G, et al. Hydrothermal carbonization coupled with anaerobic digestion for the valorization of the organic fraction of municipal solid waste. Bioresour Technol 2020;314:123734. https://doi.org/10.1016/j.biortech.2020.123734.
[109] Cao Z, Hülsemann B, Wüst D, Illi L, Oechsner H, Kruse A. Valorization of maize silage digestate from two-stage anaerobic digestion by hydrothermal carbonization. Energy Convers Manage 2020;222:113218. https://doi.org/10.1016/j.enconman.2020.113218.
[110] Medina-Martos E, Istrate I-R, Villamil JA, Gálvez-Martos J-L, Dufour J, Mohedano ÁF. Techno-economic and life cycle assessment of an integrated hydrothermal carbonization system for sewage sludge. J Cleaner Prod 2020;277:122930. https://doi.org/10.1016/j.jclepro.2020.122930.

Energy 291 (2024) 130221

Contents lists available at ScienceDirect

Energy

journal homepage: www.elsevier.com/locate/energy

Process simulation of co-HTC of sewage sludge and food waste digestates and supercritical water gasification of aqueous effluent integrated with biogas plants

Niloufar Ghavami *, Karhan Özdenkçi, Cataldo De Blasio

Faculty of Science and Engineering, Åbo Akademi University, Rantakatu 2, 65100, Vaasa, Finland

ARTICLE INFO

Handling Editor: Krzysztof (K.J.) Ptasinski

Keywords:
Biorefinery
Co-hydrothermal carbonization
Integration of hydrothermal processes
Nutrient recovery
Process simulation

ABSTRACT

The objective of this article is to investigate the integration of a digestate treatment with a biogas plant processing sewage sludge and food waste via process simulations: co-HTC of mixed digestates and supercritical water gasification (SCWG) of the aqueous effluent. The optimum co-HTC conditions are selected based on the energetic yields, comparing relative equipment sizes besides the hydrochar product. The selected conditions are 200 °C, 30 % solid load, and 1-h residence time for the mixing ratios in scope: energetic yields of 3.58–3.59 MJ/kg reactor inlet. These conditions result in more than 60 % K, P, and N recovery on hydrochar. SCWG of the aqueous effluent provides complete mineral recovery in the solid form and surplus energy production through syngas while causing some nitrogen loss as N_2 gas. Although the co-HTC data is calculated from individual HTC results, the synergetic effect on the energetic yield does not affect the selection of optimum conditions as investigated through co-HTC of sewage sludge and food waste (the origins of the digestates). Consequently, biogas plants can evolve into multi-product biorefineries through the proposed integration. Meanwhile, this study can guide future co-HTC experiments of food waste and sewage sludge digestates and reduce the required runs.

IV

1. Introduction

Solid waste management has become a significant concern due to increasing waste amounts related to population growth, widespread urbanization, and the massive consumption of resources [1–7]. Two major wastes, sewage sludge (SS) and food waste (FW), are directly related to the population. According to FAO (The Food and Agriculture Organization of the United Nations), the global generation of FW and SS are 1.6 billion tonnes and 45 million dry tons per year, respectively [8,9]. SS and FW are complex wastes containing proteins, lipids, and carbohydrates. Moreover, SS contains high ash and harmful contaminants, such as pharmaceuticals, heavy metals, and microplastics [10,11]. Similarly, conventional disposal of FW produces greenhouse gases, foul odor, and leaching [12,13]. Therefore, it is crucial to reduce and reuse waste through effective strategies.

Organic wastes are widely treated via anaerobic digestion (AD) to produce biogas: deriving 25 % of all bioenergy from biogas is possible based on EU policy estimates [14,15]. Increasing the application of AD implies increasing digestate discharge (a by-product of AD). Statistics for EU28 pointed to approximately 180 million tons of digestate generation annually [16]. Therefore, the valorization of the digestate becomes a significant concern [17,18]. Furthermore, nutrient recovery is crucial in waste management: phosphorus and nitrogen as the basis of fertilizers. However, supply problems can occur due to limited phosphorus resources and the energy-intensive production of nitrogen-based fertilizers [19]. Efficient recovery of critical elements is essential regarding the sustainability of food supply and circular economy [20,21]. Aragón-Briceño et al. suggested hydrothermal carbonization (HTC) as a prominent option for enhanced nutrient recovery [22].

HTC gains attention due to its capability of treating wet biomass, cost-effectiveness, efficient energy consumption, and less toxicity [23–25]. It produces a coal-like, energy-dense hydrochar product at 180–250 °C temperatures in autogenous pressure [26,27]. Six companies have already applied the HTC process on an industrial scale for nitrogen and phosphorus recovery, mainly processing SS and integrating it with wastewater treatment plants [22]. Some other concepts include producing hydrochar within the ISO/TS17225-8 standards from FW via HTC coupled with AD [28] and energy recovery from SS via integrating HTC and aqueous phase reforming [29]. Reviewing sustainable

* Corresponding author. Åbo Akademi, Faculty of Science and Engineering, Vaasa, , Finland.
E-mail address: niloufar.ghavami@abo.fi (N. Ghavami).

https://doi.org/10.1016/j.energy.2023.130221
Received 10 July 2023; Received in revised form 28 December 2023; Accepted 30 December 2023
Available online 1 January 2024

List of abbreviation

Anaerobic digestion AD
Biochemical methane potential BMP
Combined heat and power CHP
Chemical oxygen demand COD
Co-hydrothermal carbonization Co-HTC
Carbon retention CR
Energy yield EY
Food waste FW
Food waste digestate FWD
Heavy metals HMs
Higher heating value HHV
Hydrothermal carbonization HTC
Mixing ratio MR
Predictive Soave-Redlich-Kwong PSRK
Process water PW
Retention R
Synergistic coefficient SC
Synergistic effect SE
Supercritical water SCW
Supercritical water gasification SCWG
Sewage sludge SS
Sewage sludge digestate SSD

management of food waste digestate (FWD), HTC was stated to be the most promising valorization option, including direct application to land, composting, and pyrolysis [30]. Therefore, HTC of various digestates are investigated for integrating biogas plants [31].

Since biogas plants typically process multiple wastes, HTC of mixed digestates (co-HTC) is essential and results in a synergetic effect (SE). Co-hydrothermal carbonization (co-HTC) is a favorable technique to improve the hydrochar properties, compared to HTC of a single feedstock, elevating the yield, higher heating value (HHV), and thermal behavior of hydrochar [32]. For instance, adding 50 % cellulose or hemicellulose to SS increased HHV by 111–117 % and reduced the ash content from 71.2 % to 34.7–48.5 % [33]. Co-HTC of SS and model compounds of FW resulted in only 20 % of nitrogen remaining in hydrochar [34]. The Co-HTC of SS and banana stalk improved hydrochar properties and migration of heavy metals (HMs) [35]. The feedstock mixing ratio acted as an important parameter affecting the hydrochar yield, HHV, and energy yield (EY). Increasing the SS to FW ratio showed an upward trend in hydrochar fuel properties and combustion performance.

Similarly, adding lignocellulosic biomass improved the yield and properties of hydrochar produced via co-HTC of SS and lignocellulosic biomass [36]. Kavindi et al. [37] applied hydrochar from co-HTC of rice straw and sewage sludge digestate (SSD) to remediate solid form Cr(VI) from agricultural soil, observing better microbial activity with the rice straw:SSD mass ratio of 1:1. Zhao et al. [38] observed hydrochar characteristics improved because of the SE of distillers grains and SS: fuel ratio, activity, HHV, and combustion efficiency of the hydrochar increasing with the proportion of distillers grains. To sum up, the effects of co-HTC are different and highly dependent on the composition of the feedstock combinations. Nutrient-rich SS and FW are related to population and urbanization, thus implying many large-capacity biogas plants are processing these wastes. For instance, a biogas plant in Finland (Stormossen) processes FW and SS in different digesters, thus having two digestates [39].

Meanwhile, more experimental studies on co-HTC of FWD and SSD must be conducted. However, conducting co-HTC experiments in a vast combination range of mixing ratios, temperature, residence time, and solid load would be too costly and time-consuming. Therefore, the promising sets of conditions can be selected for the experimental verification by using individual HTC results as a preliminary assessment.

HTC discharges a high amount of process water (PW) containing considerable dissolved organic compounds, minerals, and nutrients. PW contains about 15 % of the feedstock energy, 20–50 % of biomass organics, and high nutrients such as phosphorus and nitrogen [40–42]. Nutrient recovery supports the sustainable usage of resources and reduces environmental pollution by replacing conventional fertilizers. In other words, PW needs further treatment due to containing toxic compounds and needing to recover nutrients [43]. The first option is watering the fields nearby after treating PW to remove the organic content. However, this might cause overdosing of the soil with the same element recovered dominantly in PW [44]. Another option is recirculating PW to the HTC process [45] or the AD reactor [46]. However, circulating the PW to the AD reactor introduces a risk since biological processes are sensitive to toxic compounds and heavy metals [47] despite the potential to increase biogas yield.

Meanwhile, circulating the PW to the HTC reactor increased the hydrochar mass yield and HHV without damaging the carbon content in hydrochar [48,49]. Some studies achieved a 5–10 % increase in hydrochar mass yield [50] and up to 15 % increase in the hydrochar energy yield [51] by recirculating PW to the HTC process. In addition, PW recirculation reduces wastewater production [43] and is an effective method for heat recovery [52]. This option is suitable when operating with a low solid load, i.e., diluting the dewatered digestate. However, the optimum reaction conditions might not require dilution of the digestate feedstock. For instance, the optimum conditions of HTC were determined as 30 % solid load when counting relative equipment size and energy requirements [53]. Alternatively, the minerals can be recovered effectively through precipitation or electrochemically [54,55]. Meanwhile, dissolved organics are still to be treated after these methods. In other words, there is a need for PW treatment to recover minerals and nutrients in a solid form as well as energy recovery utilizing the organic content.

Considering its high water content, PW can be treated through another hydrothermal process. Supercritical water gasification (SCWG) is a promising technology that produces syngas while recovering the minerals and nutrients in a solid outlet. This method has great importance both in energy production and fertilizers. SCWG occurs at higher temperatures and pressure than the critical point of water (374 °C and 22.1 MPa). SCW becomes a suitable solvent for organics and gases but has no solubility for salts [56]. The impact of pressure is relatively minor when operating at 23–29 MPa [57,58]. Temperature is usually around 400–500 °C for catalytic SCWG (e.g., ruthenium and nickel) and higher without a heterogeneous catalyst [59]. The syngas yield increases with temperature and residence time, while too long residence time can cause char formation via repolymerization [60–62]. A main operational issue is the risk of reactor plugging due to char formation and solid deposition [63].

Nevertheless, char formation is reduced since a process's aqueous effluent contains smaller molecules than the primary feedstock [64]. Some studies investigated the integration of SCWG with the HTC process for various feedstocks, e.g., SS and FW, e.g., enhanced syngas production and complete recovery from the digestate stream [65–67]. In addition, a SCWG reactor enabling solid separation (e.g., configuration proposed by Ghavami et al. [63]) would provide the recovery of char, including minerals and nutrients. The char outlet can be transferred to the fields nearby or far away, like hydrochar.

This study aims to construct and simulate a process integration concept valorizing the digestates of a biogas plant processing SS and FW to reach circularity. The integrated process cases involve co-HTC of the digestates with or without SCWG of PW, enabling complete circularity

or only digestate treatment with a relatively low investment cost. The optimum conditions for co-HTC of SSD and FWD are selected based on combining the individual HTC results of each digestate due to the lack of experimental co-HTC data of these digestates. This selection helps obtain preliminary results of the proposed concept and directs future co-HTC experiments towards promising sets of conditions.

2. Material and method

2.1. The integration concept and the selection of optimum co-HTC conditions

The scope of this study is to integrate a co-HTC process into a biogas plant, processing SS and FW in parallel. The biogas plant generates digestates dewatered to 30 % solid content. The proposed integration scenario is depicted in Fig. 1. The aqueous effluent (i.e., PW) is the outlet stream of the simulated process when integrating only co-HTC. The other scenario is the co-HTC of digestates and SCWG of PW: recovering the nutrients and minerals in solid products and producing syngas from the organic content in PW.

The co-HTC data is generated based on the individual HTC results of the digestates. Supplementary Material 1provides the complete list of experimental HTC results from various studies and generated co-HTC data at the matching conditions [6,31,36,68–77]. The co-HTC data cover the range of 150–250 °C, 10–30 % solid load, and 0.5–2 h of residence time. Table 1 shows the analysis of digestates used in generating co-HTC data.

The optimum conditions are selected based on the energetic yields of co-HTC data. The energetic yield is defined as the energy content of hydrochar per unit mass of the reactor inlet [53]. The co-HTC hydrochar yields and heating values are calculated as the mass-weighted average of individual results, as shown in Equations (1) and (2), where MR represents the mixing ratio. Then, the energetic yields are calculated, as shown in Equation (3). Finally, the co-HTC conditions resulting in the maximum energetic yield are selected for the simulations.

$$co-HTC\ Yield\ (\%)=\frac{(Yield_{SSD}\ x\ MR_{SSD})+(Yield_{FWD}\ x\ MR_{FWD})}{MR_{SSD}+MR_{FWD}} \quad (1)$$

Table 1
Analysis of the selected digestate samples (dry basis).

Digestate	HHV (MJ/kg)	C (%)	H (%)	N (%)	S (%)	O (%)	Ash (%)	Ref.
SSD1	14.9	28.9	3.2	3.4	1.5	16.1	46.9	[31]
SSD2	14.4	33.3	4.6	4	1.2	20.3	36.7	[68]
SSD4	11.5	30.3	4.2	3.5	2.3	18.8	40.9	[6]
SSD7	14.3	29.6	4.3	4.4	1.6	20.1	40.1	[36]
FWD1	14.9	29.5	3.0	2.0	0.3	21.3	43.9	[31]
FWD3	19.7	46.0	6.5	2.7	0.3	36.6	8.0	[75]
FWD4	13.4	34.3	4	1.9	0.2	23.8	35.8	[76]

As an important parameter, the SE is evaluated by the synergistic coefficient (SC), comparing between the experimental co-HTC results and calculated values from the individual HTC results. This study introduces SC on the energetic yield (i.e., the proposed selection criteria) to evaluate the reliability of calculated co-HTC data as shown in Equation (4): where Energetic $yield_{experimental}$ and Energetic $yield_{calculated}$ represents the values calculated from the experimental co-HTC data and from combining the individual HTC data, respectively. However, due to the lack of experimental co-HTC data on SSD and FWD, the co-HTC data on SS and FW reported by Zheng et al. [78] are used to investigate the SC on energetic yield concerning temperature and mixing ratios.

$$SC\ on\ energetic\ yield\ (\%)=\frac{Energetic\ yield_{experimental}-Energetic\ yield_{calculated}}{Energetic\ yield_{calculated}}x100 \quad (4)$$

2.2. Process simulation

This study investigates the process integration to a biogas plant generating 300 kg/h SSD and 300 kg/h FWD on a dry basis. To investigate the possible capacity increase and SE effect, the co-HTC simulations involve the mixing ratios of SSD:FWD as.

- 1:1 (300 and 300 kg/h dry)
- 1:3 (300 and 900 kg/h dry)
- 3:1 (900 and 300 kg/h dry)

$$co-HTC\ HHV\ \left(\frac{MJ}{kg}\right)=\frac{(Yield_{SSD}\ x\ HHV_{SSD}\ x\ MR_{SSD})+(Yield_{FWD}\ x\ HHV_{SSD}\ x\ MR_{FWD})}{(Yield_{SSD}\ x\ MR_{SSD})+(Yield_{FWD}\ x\ MR_{FWD})} \quad (2)$$

$$Energetic\ yield\ \left(\frac{MJ}{kg\ reactor\ inlet}\right)=\frac{(co-HTC\ Yield)\ x\ (co-HTC\ HHV)\ x\ Solid\ load\ (\%)}{100\ x\ 100} \quad (3)$$

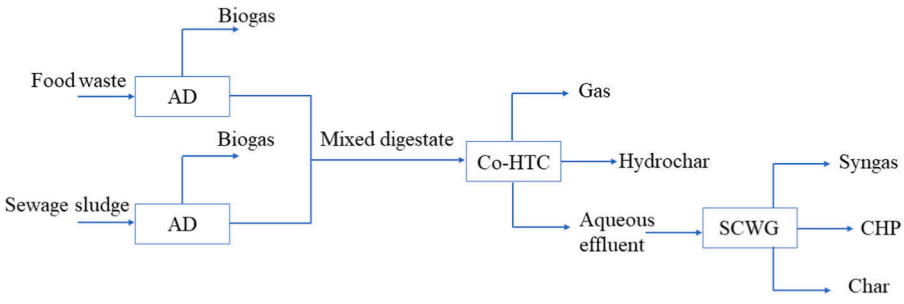

Fig. 1. Process integration block diagram.

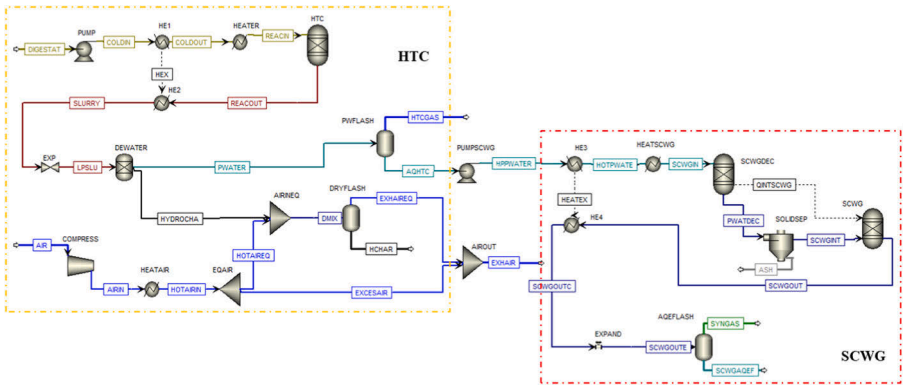

Fig. 2. Process simulation of Co-HTC and SCWG.

Fig. 2 shows the integrated processes simulated in Aspen Plus V11.1. The co-HTC section consists of pressurizing and heating the feedstock, reactor, dewatering, and thermal drying the hydrochar down to 20 % moisture content. The simulation starts with pumping and two-step feedstock heating to the reaction conditions. The first heating step is the heat exchange with the reactor outlet ('REACTOUT'), and the second is the external heat ('HEATER'). The reactor operates at a constant temperature, i.e., isothermal reactor, and is represented by a RYIELD block. After heat exchange with the feedstock ('HE1' and 'HE2'), the reactor outlet is conducted to the dewatering unit ('DEWATER') to separate hydrochar and PW, reducing the hydrochar moisture content to 50 % with the energy requirement of 79.09 kJ/kg dry solid [79]. Some portion of hydrochar remains in the PW, calculated based on the dewatering concept [79]. Finally, the hydrochar is dried by hot air (P = 1.2 bar, T = 110 °C) to reach 20 % moisture. Since industrial dryers operate with excess air, the heat requirement of thermal drying is assumed to be 3.82 MJ/kg water evaporated [80]. Therefore, the air flowrate ('AIR') is adjusted so that the heat duty of the 'HEATAIR' unit corresponds to the mentioned requirement. The air flow is split as the equilibrium ('HOTAIREQ') and the excess air ('EXCESAIR'). The outlet drying streams are the hydrochar product ('HCHAR') and the exhaust air ('EXHAIR'). When integrating only co-HTC, the stream 'PWATER' is an outlet stream. For the 1:1 mixing ratio, the simulation continues with the SCWG of PW, as shown in Fig. 2. The 'PWATER' stream is conducted to the flash separation to remove gases ('PWFLASH') and pressurized to 250 bars ('PUMPSCWG'). Afterwards, the stream is exposed to heat exchange with the reactor outlet ('HE3' and 'HE4') and external heating ('HEATSCWG') to reach the desired temperature. Since the SCWG reaction is endothermic, the SCWG inlet is heated to 625 °C, and the outlet of an adiabatic reactor is at 600 °C. The SCWG reactor is first simulated with a yield reactor to decompose non-conventional components into elemental ones ('SCWGDEC'). After separating the ash in the solid separator ('SOLIDSEP'), the remaining components are conducted to the SCWG reactor represented by a RGIBBS block ('SCWG'), determining the outlet by minimizing Gibbs free energy. After cooling down via heat exchange with the PW, the SCWG outlet stream is expanded to 1 bar ('EXPAND') and conducted to the flash separator to separate syngas and aqueous phase ('AQEFLASH').

The component list and thermodynamic property method are selected similarly to the previous article on HTC of agricultural residue digestate [53]. The components include water, digestate, and hydrochar as dry-ash-free, ash, dissolved organics, CO_2, H_2, CH_4, CO, N_2, O_2, H_2S, and NH_3. Ash is an inert and a separate component to facilitate the mass balance. Additionally, the dissolved organics in PW are defined as a single, non-conventional component. The mixed digestates, organics, and hydrochar are defined as dry-ash-free, non-conventional components. The physical properties of non-conventionals are estimated via 'HCOALGEN' and 'DCOALIGT'. The heating values of digestates and hydrochars are calculated as the mass-weighted average of the individual heating values, while the heating value of ash is introduced as 0. Heating values of dissolved organics are calculated based on a correlation valid for a wide range of substances [53]. The thermodynamic property method is selected as Predictive Soave-Redlich-Kwong (PSRK), except the RYIELD and RGIBBS reactors representing the SCWG reactor simulated with the IDEAL method.

At the selected co-HTC conditions and flow rates of each digestate, conducting a mass balance using the experimental HTC results determines the reactor yields (per unit mass of non-inert) and ultimate and proximate analysis of non-conventionals. Supplementary Material 2shows the individual HTC mass balances and the co-HTC balance at the selected conditions and digestates. The mass balance is conducted through the following steps.

- Hydrochar, liquid, and gas flow rates based on total mass balance and yield data
- Nitrogen elemental balance to determine the nitrogen content in PW
- Gas flow rates calculated based on the assumed mole fractions as CO_2: 0.9, H_2: 0.01, CH_4: 0.03, CO: 0.06 [81].
- Assuming no ash, sulfur, and nitrogen in gas product [82].
- Carbon and sulfur mass flows in PW calculated via elemental balances
- Hydrogen and oxygen contents of organics in the PW estimated based on chemical oxygen demand (COD) and biochemical methane potential (BMP)

The simulation results are evaluated regarding the products and energy requirements. The recovery measures are carbon retention and the recovery of fertilizer elements (K, P, N). The retention of elements can be calculated as shown in Equation (5) [83]. The recovery of each component can be calculated similarly, i.e., the percentage of an element in hydrochar relative to the carbon in the feedstock.

$$Retention\ (R) = \frac{Mass\ of\ element\ in\ hydrochcar}{Mass\ of\ element\ in\ feedstock} x100 \quad (5)$$

The energy requirements are obtained from the simulation results. Electricity is required to operate the pumps pressurizing the reactor inlets ('PUMP' and 'PUMPSCWG'), the dewatering ('DEWATER'), and the air compressor in the HTC section ('COMPRESS'). External heat is required to heat the feedstock after heat exchange with the co-HTC reactor outlet ('HEATER'), to heat the air introduced for hydrochar

drying ('HEATAIR'), and to heat the SCWG reactor inlet after heat exchange with the outlet ('HEATSCWG'). The heat duty in HEATSCWG heater is 25 % electricity and 75 % heat requirement due to high-temperature heating compromising the combined heat and power (CHP) production via steam. The split is based on the conventional CHP plants with steam turbines: 25 % electricity, 60 % heat, and 15 % heat loss [84]. Moreover, CHP production via syngas can fulfill the energy requirement. Similarly, the energy generation from syngas combustion is 25 % electricity and 60 % heat. Meanwhile, the co-HTC reactor releases heat when operating isothermally because of exothermic reactions, thus causing a negative heat requirement.

3. Result and discussion

3.1. Selection of optimum co-HTC conditions

Selecting the optimum conditions plays a crucial role in the economic performance. Determining optimum conditions at the early stage of process development is beneficial. However, the impacts of conditions are comprehensive and interdependent. In particular, temperature has the opposite effect on the hydrochar yield and heating value: the yield decreases with temperature while the heating value increases. Moreover, increasing residence time slightly improves the yield and heating value [6,75]; however, increasing residence time can also decrease the yield at long residence times (e.g., more than 2 h) or high temperatures [75,76].

Furthermore, it is crucial to compare the relative equipment size and energy requirement, i.e., implicitly the investment and operation costs. The residence time directly affected the reactor size. In addition, the equipment size is directly influenced by the solid load of the reactor inlet, not counted in dry-based or dry-ash-free yields. The impact of solid load on the equipment size is very dominant compared to a slight effect on the product. Therefore, stating the need for a comprehensive methodology, Özdenkçi et al. (2020) [61] evaluated the conditions of SCWG based on hydrogen and energy yields with the basis of a non-inert reactor inlet.

Similarly, Ghavami et al. (2022) [53] introduced the energetic yield as the energy content of hydrochar per unit mass of the reactor inlet. The energetic yield is the first criterion when selecting the optimum conditions: compiling the impacts of conditions on the product yield, heating value, and relative equipment size. When different sets of conditions give close energetic yields, the other criteria are the residence time (comparing the reactor size), the reactor material, and the catalyst load [53,61].

The co-HTC of FWD and SSD is simulated at the optimum conditions with maximum energetic yields. Table 2 shows the energetic yields concerning the conditions and mixing ratios. The optimum energetic yields are obtained as 3.59, 3.58, and 3.59 MJ/kg reactor inlet for the SSD1:FWD1 ratios of 1:1, 1:3, and 3:1, respectively, at 200 °C with 30 % solid load and 1-h residence time. Meanwhile, it is worth noting that the proper comparison can be made when the specific digestates of a biogas plant are exposed to co-HTC experiments, considering that the feedstocks at different studies are not identical. Nevertheless, this study is still helpful for selecting the sets of promising conditions and introducing the comparison methodology.

Due to the SE of different constituents, the feedstock types and mixing ratio are important factors influencing the hydrochar yields and heating values [32,35]. For instance, a co-HTC review listed SCs on hydrochar yield and CR for various mixed wastes, e.g., swine manure-sawdust, textile-waste paper, waste-textile-FW, and SS-pine wood [85]. However, no experimental data exists on the co-HTC of FWD and SSD. Nevertheless, the mixture of SS and FW can cause a similar synergetic impact with the mix of SSD and FWD, as the origins of these digestates. An investigation on co-HTC of SS and FW presented experimental results at 180–280 °C and 7 % solid load with the SS:FW ratios of 70:30, 50:50, and 30:70 [78]. Increasing the SS ratio resulted in higher hydrochar yield due to higher inorganic content: the highest yield with 70 % SS. Meanwhile, FW contributed to the increase in the product heating value.

Since this study selects the optimum conditions based on the energetic yield, the SC on the energetic yield indicates the role of SE in the optimum conditions. Therefore, Fig. 3 shows the SCs on the energetic yields for the experimental results of co-HTC of SS and FW presented by Zheng et al. (2019) [78]. The complete data is given in Supplementary Material 3, including the digestate analysis, hydrochar yields, and heating values. It can be seen that the SC decreases with temperature, except for 70 % SS feedstock at 280 °C. The SCs are 10.2–11.9 % at 180 °C and reduce to negative values at higher temperatures.

Nevertheless, SC on the energetic yield does not affect the choice of optimum temperature, except for 70 % SS feedstock. Furthermore, the SC would potentially be very close to zero at 200 °C, i.e., SE introducing only a minor impact on the energetic yields. Therefore, it can be expected that the optimum conditions of co-HTC of SSD and FWD can be selected by combining the individual HTC data for the preliminary investigations, which enables the selection of promising conditions for future co-HTC experiments.

3.2. Mass balances

The co-HTC reactor yields are calculated by using the data on the defined mixing ratios (SSD1:FWD1 as 1:1, 1:3, 3:1) and the selected conditions (200 °C, 30 % solid load, and 1 h for all the mixing ratios), presented by Parmar and Ross [31]. The properties of non-conventionals are also determined through these calculations, as shown in Supplementary Material 2. These are introduced as inputs to the simulation models. Table 3 shows the feedstock and hydrochar properties with

Table 2
The co-HTC results and the energetic yields for the SSD:FWD ratios of 1:1, 1:3 and 3:1, respectively.

Feedstock	Conditions			Hydrochar		Process performance
	T (°C)	Solid load (%)	t_{res} (h)	Yield (% dry)	HHV(MJ/kg)	Energetic yield (MJ/kg reactor inlet)
SSD1:FWD1	200	10	1	76.1 77.8 74.3	14.89 14.85 14.94	1.13 1.15 1.11
		20		78.5 79.7 77.3	15.10 15.10 15.10	2.37 2.41 2.33
		30		78.9 79.4 78.5	14.99 15.02 15.27	**3.59 3.58 3.59**
	250	10		68.4 69.7 67.0	15.15 14.89 15.09	1.02 1.04 1.01
		20		69.7 70.5 68.8	15.09 15.00 15.20	2.10 2.12 2.09
		30		71.6 72.3 70.6	15.34 15.17 15.52	3.29 3.31 3.28
SSD7:FWD1	150	20	1	89.8 89.4 90.2	15.10 15.05 15.15	2.71 2.69 2.73
	200			79.0 79.9 78.0	15.15 15.12 15.17	2.39 2.42 2.37
	250			71.0 71.1 70.7	15.05 14.97 15.12	2.13 2.13 2.14
SSD1:FWD3	200	10	1	57.9 50.6 65.3	18.77 21.48 16.67	1.09 1.09 1.09
SSD2:FWD3	250	10	0.5	54.8 44.6 64.9	19.42 22.47 17.33	1.06 1.00 1.12
SSD4:FWD4	210	15	2	83.8 81.5 86.0	11.64 11.76 11.52	1.46 1.44 1.48
	230			75.2 74.0 76.5	11.94 12.16 11.71	1.35 1.35 1.34
	250			69.9 68.9 71.0	12.44 12.57 12.32	1.31 1.30 1.31

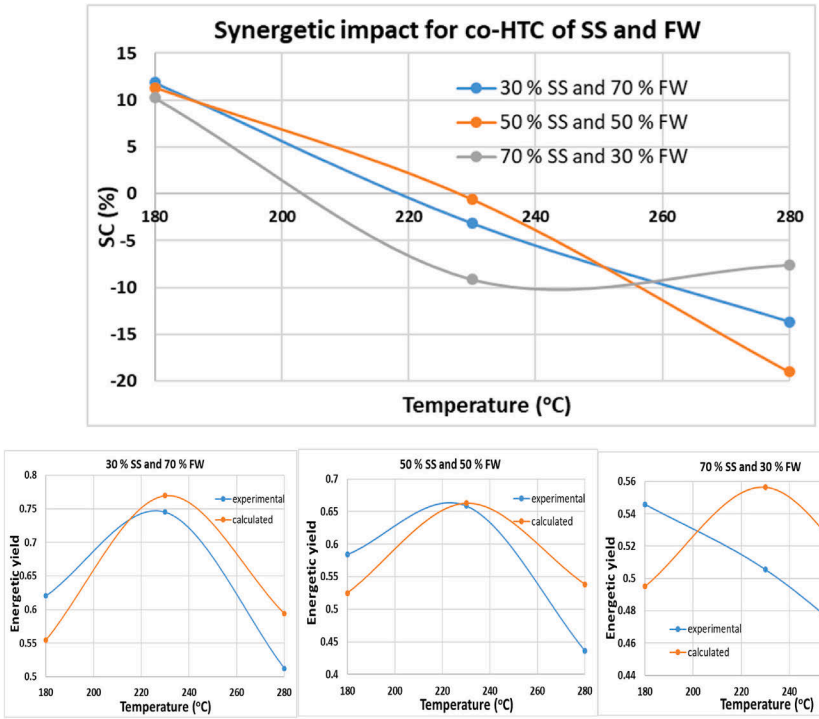

Fig. 3. The energetic yields (MJ/kg reactor inlet) and SE on the energetic yields (%).

Table 3
Feedstock and hydrochar properties (daf).

Material		C (%)	H (%)	O (%)	N (%)	S (%)	HHV(MJ/kg)
1:1	Digestate	53.48	5.68	34.25	4.94	1.65	27.29
	Hydrochar	62.73	7.14	24.67	4.13	1.34	29.31
1:3	Digestate	53.03	5.51	36.13	4.24	1.08	26.92
	Hydrochar	63.28	6.83	25.43	3.56	0.89	30.27
3:1	Digestate	53.95	5.85	32.31	5.67	2.23	27.67
	Hydrochar	62.21	7.42	23.94	4.68	1.75	28.40

Table 4
The elemental analysis and heating values of organics.

SSD:FWD ratio	Dissolved organics (dry-ash-free)					
	C (%)	H (%)	O (%)	N (%)	S (%)	HHV (MJ/kg)
1:1	24.84	2.61	58.03	10.76	3.76	4.29
1:3	28.61	2.96	57.35	8.79	2.29	6.70
3:1	19.86	2.15	58.92	13.37	5.70	1.10

different mixing ratios. Table 4 gives the elemental analysis and heating value of the dissolved organics. Table 5 reports the co-HTC reactor yields introduced in the RYIELD block in kg/kg non-inert.

An essential aspect of processing the experimental data is prioritizing the characterization data and determining the simulation inputs [53]. For instance, the mass balance in this study reveals a mismatching carbon amount in the organics when calculated through carbon elemental balance or nitrogen elemental balance and the C:N ratio of PW, i.e., affecting the hydrogen and oxygen calculations and causing

Table 5
Calculated yields in kg/kg non-inert.

Component	*SSD:FWD ratio*		
	1:1	1:3	3:1
Hydrochar	0.140	0.136	0.145
Water	0.809	0.809	0.808
Organics	0.033	0.038	0.029
CO_2	0.017	0.016	0.017
H_2	8.479E-06	8.291E-06	8.668E-06
CH_4	0.0002	0.0002	0.0002
CO	0.0007	0.0007	0.0007

errors in elemental balances. Therefore, this study conducts mass balance with the priority as follows: total mass balance to define the flow rates, digestate and hydrochar analysis to identify the feed and product, assumed gas composition, elemental balances around the reactor to determine elemental contents of PW, and finally using COD and BMP data to determine the content of hydrogen and oxygen in the dissolved organics and water amount in the PW stream. The ultimate and proximate analysis on solid samples is reliable because drying at low temperatures avoids further decomposition. In contrast, CHNS analysis of PW can involve higher uncertainty since light organics can evaporate during sample drying. The accuracy can be improved further through a more profound analysis of PW and ash. Ash is considered inert despite including some inorganic carbon.

Meanwhile, equilibrium reactions also convert inorganic carbon to carboxylates [86]. Consequently, it is beneficial regarding accuracy to utilize the most reliable characterization data first. The mass balance

results are sufficient for the preliminary assessment despite requiring further improvements.

After determining the inputs, the process is simulated to determine the mass and energy balances. Table 6 shows the flowrates following the block diagram depicted in Fig. 4. The digestate flowrate is based on the mass balance calculation (determined in Supplementary Material 2), and the rest is extracted from the simulation. The mass balance indicates several aspects of the process. Comparing the reactor inlet and outlet shows that water participates in the reactions. A small amount of water is consumed in the SSD:FWD ratios of 1:1 and 3:1 while being generated to a smaller extent in the mixing ratio of 1:3. Additionally, SSD causes slightly more gas formation than FWD while FWD results in slightly more dissolved organics. Dissolved organics is another aspect since PW has 4.7–5.4 % of organics, i.e., potential for further recovery. Furthermore, Table 6 indicates that most ash is recovered within the hydrochar, which encourages the usage of hydrochar as a fertilizer.

After flash separation, the PW is conducted to SCWG, removing the dissolved gases for the mixing ratio 1:1. The stream information is reported in Table 7. The mass balance indicates that 61 kg/h water is consumed in SCWG reactions, thus contributing to the formation of syngas. This observation is consistent with the experimental studies observing hydrogen and oxygen gasification efficiencies as more than 100 %, i.e., elements of water being converted besides the solid content [86]. The carbon representing char is observed in negligible amounts in the simulation. It is beneficial to process the aqueous effluent in SCWG to reduce the char formation, rather than the original feedstock, because it includes dissolved and smaller molecules. Meanwhile, the SCWG reactor may not reach equilibrium, and unhydrolyzed content (e.g., hydrochar in PW) may cause a char outlet. Therefore, SCWG results are to be validated through experimenting with the specific stream, although simulations are helpful for preliminary assessment.

The mineral and nutrient recovery is improved through the ash outlet of the SCWG reactor. In the case of a reactor configuration enabling solid separation, the minerals can be recovered entirely because of no solubility in SCW. Meanwhile, nitrogen recovery introduces a challenge due to distribution into different phases. Nitrogen gas is observed due to ammonia decomposition as an equilibrium reaction. The PW includes 9.2 kg/h nitrogen element. According to the SCWG results, most nitrogen element is converted into gas, 8.85 kg/h of N_2. Despite observing fewer amounts, the experimental studies also reported nitrogen gas formation. For instance, a survey of SCWG of SS

Table 6
Mass flows of the co-HTC process in kg/h.

Stream	Component	*SSD:FWD ratio*		
		1:1	1:3	3:1
DIGESTATE	Digestate	327.6	664.2	646.2
	Ash	272.4	535.8	553.8
	Water	1400	2800	2800
HTCOUT	Hydrochar	242.75	470.66	500.34
	Ash	272.4	535.8	553.8
	Water	1396.95	2803.1	2784.7
	Organics	57.30	130.44	98.76
	Gases	30.60	60.00	62.40
PWATER	Water	999.43	2000.44	1997.27
	Ash	45.35	57.86	123.54
	Hydrochar	72.34	145.94	143.20
	Organics	57.30	130.44	98.76
	Gases	30.60	60.00	62.40
HCSLUDGE	Water	397.52	802.66	787.43
	Ash	227.05	477.94	430.26
	Hydrochar	170.41	324.72	357.14
AIR	Air	17550	35450	34760
EXHAUSTAIR	Air	17550	35450	34760
	Water	298.43	603.7	591.02
HCPRODUCT	Water	99.09	198.96	196.41
	Ash	227.05	477.94	430.26
	Hydrochar	170.41	324.72	357.14

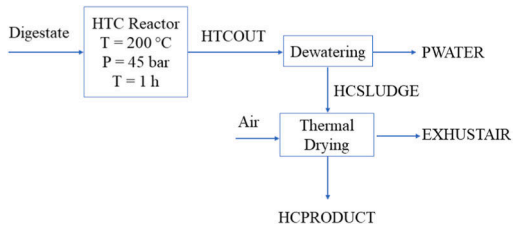

Fig. 4. The block diagram of the integrated co-HTC process.

Table 7
Mass flows in the SCWG section for 1:1 SSD:FWD ratio.

	Flow rates (kg/h)		
Component	HPPWATER	SYNGAS	SCWGAQEF
Water	997.71	51.06	885.79
Ash	45.35	-	-
Hydrochar	72.34	-	-
Organics	57.30	-	-
CO_2	0.62	143.40	0.15
CO	0.0009	2.14	0.0001
CH_4	0.0004	26.27	0.002
H_2	1.26e-5	6.63	0.0004
N_2	-	8.85	0.0003
H_2S	-	3.31	0.01
NH_3	-	0.17	0.19

observed 10–20 % nitrogen recovery in the solid phase, the majority in liquid, and significant amounts in gas [87]. Thus, a considerable portion of nitrogen is converted into gas, although the ammonia decomposition might not reach equilibrium. Nitrogen transformation depends on the feedstock composition during the HTC and SCWG processes. Nitrogen retention rate is higher in co-HTC of SS with different feedstocks, including FW and garden waste, due to various interactions between organic waste and SS [41]. In the co-HTC of SS and FW model compounds, about 67 % of the nitrogen is transformed to the PW in the form of NH_4^+ and organic-N, and only 20 % to the hydrochar, resulting in a 36–60 % rise in nitrogen retention [34].

Additionally, nitrogen transformation is affected by temperature: 47.3 % of nitrogen transformed to the aqueous product at 160 °C, while 69.2 % transformed at 250 °C during HTC of SS [88]. In this study, about 38 % of the nitrogen in the digestate is transferred to the dissolved organics, i.e., inlet to the SCWG reactor. Table 8 reports the retentions in hydrochar for carbon, potassium, phosphorus, and nitrogen. It can be seen that increasing SSD promotes carbon, potassium, and nitrogen retention; however, FWD promotes phosphorus retention.

Regarding the usage of hydrochar from co-HTC of SSD and FWD, its utilization as a fertilizer is potentially more suitable than energetic usage. The heating values of hydrochar products are relatively low due to high ash content, causing a longer time for complete combustion [89]. Meanwhile, the hydrochar recovers most the nutrients and minerals, thus making it feasible to transport to the agricultural fields. The remaining nutrients and minerals in PW can also be recovered as a solid product, e.g., through SCWG, as in this study or a precipitation process.

Table 8
Retention of different elements.

	SSD-FWD ratio		
Retention (%)	1:1	1:3	3:1
Carbon	86.91	84.56	89.28
Potassium	66.97	63.97	70.77
Phosphorus	67.23	75.70	62.92
Nitrogen	61.93	59.35	63.92

3.3. Energy balance

The energy balances are obtained from the simulation results. Table 9 and Table 10 present the energy requirements of the co-HTC process for all the mixing ratios and the SCWG section for the 1:1 mixing ratio, respectively. The energy requirements in the co-HTC section are proportional to flow rates with only minor deviations regarding the mixing ratio, except for the reactor. Contrarily, the reactor heat duty differs sharply depending on the mixing ratio: the heat of reaction increases with SSD proportion. From the heat integration viewpoint, the released heat from the reactor can sufficiently cover the heat required for thermal drying in all the mixing ratios. Heating the feedstock requires different utility due to the temperature range; nevertheless, the heat released from the reactor exceeds the sum of this requirement and the need in drying, except the SSD:FWD ratio of 1:3. The SCWG of PW provides more energy production. The net heating value of the syngas is 9.03 MJ/kg. The CHP production from syngas covers most of the power consumption and provides extra heat. The net power requirement reduces from 124.9 to 16 kW and increases the net heat production by 331 kW.

It is essential to determine the heat of reaction and verify it with the literature. It can be determined through Hess's law (the enthalpy change between reactants and products) or by calculating the system's exchanged thermal power [90]. The calculated heat duty of the reactor is reported in Table 9, which is equivalent to −2.56, −2.12, and −2.90 $MJ/kg_{dry\text{-}solid}$ and −4.69, −3.83, −5.39 $MJ/kg_{dry\text{-}ash\text{-}free\text{-}solid}$ for 1:1, 1:3, and 3:1 SSD:FWD ratios, respectively. There is a lack of information about the heat of reaction of co-HTC of SSD and FWD; nevertheless, the obtained heat of reactions is within the reported ranges for FW (−1.19 $MJ/kg_{dry\text{-}solid}$), SS (−2.62 $MJ/kg_{dry\text{-}solid}$), organic waste (−7.30 $MJ/kg_{dry\text{-}solid}$), and glucose (−1.06 $MJ/kg_{dry\text{-}solid}$) [90–92]. The heat of reaction differs depending on the severity of conditions and the feedstock composition. For instance, the experimental condition for SS was 250 °C and 20 h residence time [91].

The energy balance calculations are functional for preliminary analysis despite uncertainties in non-conventional properties. The possible errors due to non-conventional properties are minimized since water dominates the streams. For instance, the duties of heat exchangers involve a minor uncertainty because of the specific heat of non-conventionals calculated via the empirical correlations meant for coal. Moreover, the dissolved organics introduce uncertainty in its heating value. Therefore, the results help select the optimum conditions and feasibility assessments. At the same time, further improvements can include validating of energy balances on a pilot scale and a more accurate representation of non-conventional properties, e.g., temperature dependence of specific heats.

3.4. Operational aspects and simulation limitations

Although this study provides a valuable methodology to select the optimum conditions and process simulation models, it is worth noting the limitations: verification of synergetic impact, stream rheology, and SCWG limitations, including solid recovery, thermodynamic method, and reaching the equilibrium state.

Table 9
Co-HTC energy requirements.

	SSD-FWD ratio		
	1:1	1:3	3:1
Electricity requirement (kW)			
PUMP	3.5	7	7
COMPRESS	110.0	222.3	217.9
DEWATER	11.4	22.1	23.2
Total	124.9	251.4	248.1
Heat requirement (kW)			
HAETER	40.45	80.8	80.9
HEATAIR	316.26	638.8	626.4
CO-HTC	−427.2	−706.8	−967.1
Total	−70.49	12.8	−259.8

Table 10
SCWG energy balance.

Electricity requirement (kW)		Heat requirement (kW)	
HTC Section	124.9	HTC Section	−70.49
PUMPSCWG	31.5	–	
0.25 × HEATSCWG	11	0.75 × HEATSCWG	33
Electricity outcome (kW)		Heat outcome (kW)	
0.25 × SYNGAS	151.68	0.6 × SYNGAS	364.05

The reliability of the generated co-HTC data is verified by using the experimental co-HTC of the origins (SS and FW) due to the lack of data on the co-HTC of these digestates. The SCs on the energetic yield are near zero around the optimum temperature, and the waste types have similar constituents. Meanwhile, verifying the synergetic impacts of those digestates through the co-HTC experiments is essential.

Stream rheology is important for biorefinery design, specifically in piping, heat requirement, and pumping. Slurries with more than 20 % solid load behave like non-Newtonian fluids [93]. It depends on the feedstock, particle size, and sludge concentration, and the energy requirement increases with sludge concentration [94]. This study simulates co-HTC integration with a 30 % solid load. If the feedstock slurry is too viscous to pump, the process can be integrated with a lower solid load (e.g., 20 %). However, lowering the solid load will proportionally increase the energy requirements and equipment sizes due to the increased flow rates. Another alternative is transporting the feedstock through screwdrivers and modifying the heat integration, as shown in Fig. 5. This increases the external heat requirement and requires extra power for the screwdriver while saving investment and operation costs through relatively smaller equipment sizes.

The simulation of SCWG assumes reaching equilibrium. The minerals accelerate some reactions in the conversion mechanism, e.g., water gas shift reaction and steam reforming, and suppress the char formation [59]. The feasible residence time of SCWG is relatively short, e.g., up to 5 min, due to high pressure causing high reactor cost [61,95]. Meanwhile, the decomposition of intermediates might be kinetic-limited. Moreover, char is negligible in the simulation results; however, the unhydrolyzed portion of organics can form char, of which the

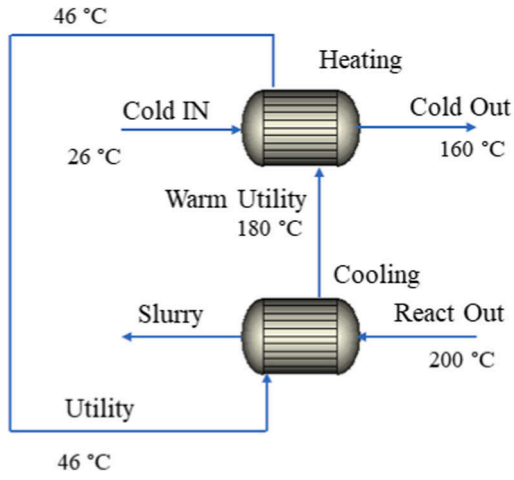

Fig. 5. Alternative heat integration for a viscous slurry [53].

gasification is kinetic-limited. In addition, ammonia decomposition depends on the residence time and might not reach equilibrium, e.g., less nitrogen loss in syngas. Therefore, the results of SCWG of PW can be experimentally verified as a further investigation. Another simulation limitation is the assumption of complete solid recovery. This requires a particular reactor configuration, e.g., multiple riser tubes for gas outlets while precipitating the solids [63].

Despite high pressure and polar compounds, the SCWG reactor units are simulated with the IDEAL method. However, several other methods implied exothermic reactions. Only the IDEAL method provided reasonable results regarding temperature, dropping from 625 to 600 °C. This is consistent with the simulations of SCWG of black liquor conducted using the PSRK method, resulting in a 15 °C temperature drop [95].

4. Future aspects

Co-HTC of FWD and SSD is an innovative approach for waste management and energy production. Integrating the co-HTC process with SCWG enables nutrient recovery and syngas production. This study is a preliminary assessment of integrating co-HTC of SSD and FWD followed by SCWG of PW with biogas plants. It can enlighten the further process development steps.

- Experimental data

Simulation studies provide a practical preliminary assessment, while experiments can verify the simulations. First, experiments at promising condition sets can address the lack of experimental data on the co-HTC of SSD and FWD. The experiments can cover a range of conditions around the selected optimum values: e.g., 180–220 °C, 0.5–1.5 h, and 20–30 % solid load. Furthermore, experiments on the SCWG of PW are needed for more accurate syngas and solid outlets. The accuracy can be improved through deeper characterization of ash and PW and temperature dependences of physical properties of non-conventional components.

- Feedstock variation and co-processing with other wastes

SSD and FWD have various compositions affecting the process efficiency and product. The particular waste should be specifically experimented with when developing the process integration. Furthermore, a biomass supply chain requires multi-feed-multi-product processes to enable a circular economy [96]. Therefore, a future aspect can involve another waste into the SCWG or the co-HTC reactor. This can increase the capacity and improve the economic performance but requires co-processing experiments [97].

- Commercial viability and scale-up

The proposed integration has shown promise at the lab-scale and industrial implementations. HTC is applied commercially by several companies, i.e., being economically feasible [41,98]. Similarly, SCWG was stated as economically feasible even for a more challenging feedstock (black liquor), provided the operational issues are addressed effectively [95]. SCWG introduces high investment costs due to high flow rates and pressure [99]. The integration of co-HTC can be an option when preferring lower investment costs. Meanwhile, SCWG of PW enables a high amount of CHP production and complete recovery of the minerals despite increasing the investment cost.

5. Conclusion

This study investigates integrating co-hydrothermal carbonization of digestates and supercritical water gasification of process water with a biogas plant processing sewage sludge and food waste in parallel. The hydrochar can be used as a fertilizer, while syngas can provide CHP production. The optimum co-hydrothermal carbonization conditions are selected based on the energetic yields, comparing the relative equipment sizes besides the product yield and quality. The co-hydrothermal carbonization data is generated from the individual HTC data of each digestate due to the lack of co-hydrothermal carbonization experimental data on sewage sludge digestate and food waste digestate. The results indicated that the optimum co-hydrothermal carbonization conditions were 200 °C, 1-h residence time, and 30 % solid load. These conditions provide remarkable nutrient recovery on the hydrochar: 64–71 % potassium, 63–76 % phosphorus, and 59–64 % nitrogen recoveries.

Furthermore, supercritical water gasification of process water provides further mineral and nutrient recovery in solid form, which is beneficial for logistics. Additionally, using syngas for combined heat and power production provides surplus energy. Meanwhile, supercritical water gasification sharply increases the investment cost, i.e., it is an effective option for large-capacity plants.

Despite the uncertainties, this study is helpful for preliminary assessment and directing the co-hydrothermal carbonization experiments towards promising ranges of conditions. Two main uncertainty factors are the heat of reaction in the co-hydrothermal carbonization and the synergistic effect of mixing feedstocks. The heat of reaction from the simulations (−2.56, −2.12, and −2.90 MJ/$kg_{dry\text{-}solid}$ and −4.69, −3.83, −5.39 MJ/$kg_{dry\text{-}ash\text{-}free\text{-}solid}$ for 1:1, 1:3, and 3:1 sewage sludge digestate and food waste digestate ratios, respectively) matches with the literature values for similar feedstocks and model compounds. Similarly, this study investigates the synergistic coefficient on the energetic yields for co-hydrothermal carbonization of sewage sludge and food waste due a to lack of data on co-hydrothermal carbonization of sewage sludge digestate and food waste digestate. The synergistic coefficient decreases with temperature in all mixing ratios and is close to zero at the selected co-hydrothermal carbonization temperature. This investigation determines that the SE has no significant impact on choosing the optimum conditions. Therefore, future co-hydrothermal carbonization experiments can involve narrow ranges of conditions around the selected optimum (e.g., 180–220 °C, 20–30 % solid load, and 0.5–1.5 h residence time) rather than numerous experiments.

In conclusion, biogas plants can be evolved into multi-product biorefinery facilities through the hydrothermal treatment of digestate. Hydrothermal carbonization is the option for producing hydrochar with a relatively low investment cost, followed by supercritical water gasification of process water providing energy production and further recovery of nutrients.

CRediT authorship contribution statement

Niloufar Ghavami: Writing – review & editing, Writing – original draft, Validation, Software, Methodology, Investigation, Data curation, Conceptualization. **Karhan Özdenkçi:** Writing – review & editing, Writing – original draft, Validation, Supervision, Software, Methodology, Investigation, Formal analysis, Data curation, Conceptualization. **Cataldo De Blasio:** Writing – review & editing.

Declaration of competing interest

The authors declare that they have no known competing financial interests or personal relationships that could have appeared to influence the work reported in this paper.

Data availability

Data will be made available on request.

Acknowledgements

We gratefully acknowledge the financial support of Kaute

Foundation [20220122] and the University Foundation of Ostrobothnia (Högskolestiftelsen) [28600148] in Finland. We are also very grateful to the EU Regional Council of Ostrobothnia for their support in conducting the EU-ERUF project named "Implementation of a hydrothermal carbonization process for the disposal sludge and wet organic streams" [28400198K1].

Appendix A. Supplementary data

Supplementary data to this article can be found online at https://doi.org/10.1016/j.energy.2023.130221.

References

[1] Arya S, Chavan D, Vishwakarma S, Kumar S. 20 - an approach for integrating sustainable development goals (SDGs) through organic waste management. In: Hussain C, Hait S, editors. Advanced organic waste management. Elsevier; 2022. p. 331–50. https://doi.org/10.1016/B978-0-323-85792-5.00010-1.

[2] Orejuela-Escobar LM, Landázuri AC, Goodell B. Second generation biorefining in Ecuador: circular bioeconomy, zero waste technology, environment and sustainable development: the nexus. Journal of Bioresources and Bioproducts 2021;6:83–107. https://doi.org/10.1016/j.jobab.2021.01.004.

[3] Kaza S, Yao L, Bhada-Tata P, Woerden FV. What a waste 2.0: a global snapshot of solid waste management to 2050. World Bank Publications; 2018.

[4] Yu Z, Khan SAR, Ponce P, Zia-ul-haq HM, Ponce K. Exploring essential factors to improve waste-to-resource recovery: a roadmap towards sustainability. J Clean Prod 2022;350:131305. https://doi.org/10.1016/j.jclepro.2022.131305.

[5] Khosravi A, Zheng H, Liu Q, Hashemi M, Tang Y, Xing B. Production and characterization of hydrochars and their application in soil improvement and environmental remediation. Chem Eng J 2022;430:133142. https://doi.org/10.1016/j.cej.2021.133142.

[6] Hämäläinen A, Kokko M, Kinnunen V, Hilli T, Rintala J. Hydrothermal carbonisation of mechanically dewatered digested sewage sludge—energy and nutrient recovery in centralised biogas plant. Water Res 2021;201:117284. https://doi.org/10.1016/j.watres.2021.117284.

[7] Saqib NU, Sharma HB, Baroutian S, Dubey B, Sarmah AK. Valorisation of food waste via hydrothermal carbonisation and techno-economic feasibility assessment. Sci Total Environ 2019;690:261–76. https://doi.org/10.1016/j.scitotenv.2019.06.484.

[8] FAO - News Article: Food wastage: Key facts and figures n.d. https://www.fao.org/news/story/en/item/196402/icode/(accessed September 27, 2023), ISBN 978-92-5-107752-8, p. 11–16.

[9] Ferrentino R, Langone M, Fiori L, Andreottola G. Full-scale sewage sludge reduction technologies: a review with a focus on energy consumption. Water 2023;15:615. https://doi.org/10.3390/w15040615.

[10] Mejías C, Martín J, Santos JL, Aparicio I, Alonso E. Occurrence of pharmaceuticals and their metabolites in sewage sludge and soil: a review on their distribution and environmental risk assessment. Trends in Environmental Analytical Chemistry 2021;30:e00125. https://doi.org/10.1016/j.teac.2021.e00125.

[11] Wang X, Chi Q, Liu X, Wang Y. Influence of pyrolysis temperature on characteristics and environmental risk of heavy metals in pyrolyzed biochar made from hydrothermally treated sewage sludge. Chemosphere 2019;216:698–706. https://doi.org/10.1016/j.chemosphere.2018.10.189.

[12] Bhakta Sharma H, Panigrahi S, Dubey BK. Food waste hydrothermal carbonization: study on the effects of reaction severities, pelletization and framework development using approaches of the circular economy. Bioresour Technol 2021;333:125187. https://doi.org/10.1016/j.biortech.2021.125187.

[13] Ding A, Zhang R, Ngo HH, He X, Ma J, Nan J, et al. Life cycle assessment of sewage sludge treatment and disposal based on nutrient and energy recovery: a review. Sci Total Environ 2021;769:144451. https://doi.org/10.1016/j.scitotenv.2020.144451.

[14] Liu Y, Li X, Wu S, Tan Z, Yang C. Enhancing anaerobic digestion process with addition of conductive materials. Chemosphere 2021;278:130449. https://doi.org/10.1016/j.chemosphere.2021.130449.

[15] Mao C, Feng Y, Wang X, Ren G. Review on research achievements of biogas from anaerobic digestion. Renew Sustain Energy Rev 2015;45:540–55. https://doi.org/10.1016/j.rser.2015.02.032.

[16] Catenacci A, Boniardi G, Mainardis M, Gievers F, Farru G, Asunis F, et al. Processes, applications and legislative framework for carbonized anaerobic digestate: opportunities and bottlenecks. A critical review. Energy Convers Manag 2022;263:115691. https://doi.org/10.1016/j.enconman.2022.115691.

[17] Malhotra M, Aboudi K, Pisharody L, Singh A, Banu JR, Bhatia SK, et al. Biorefinery of anaerobic digestate in a circular bioeconomy: opportunities, challenges and perspectives. Renew Sustain Energy Rev 2022;166:112642. https://doi.org/10.1016/j.rser.2022.112642.

[18] Zhu X, He M, Xu Z, Luo Z, Gao B, Ruan R, et al. Combined acid pretreatment and co-hydrothermal carbonization to enhance energy recovery from food waste digestate. Energy Convers Manag 2022;266:115855. https://doi.org/10.1016/j.enconman.2022.115855.

[19] Ersahin ME, Cicekalan B, Cengiz AI, Zhang X, Ozgun H. Nutrient recovery from municipal solid waste leachate in the scope of circular economy: recent developments and future perspectives. J Environ Manag 2023;335:117518. https://doi.org/10.1016/j.jenvman.2023.117518.

[20] Robles Á, Aguado D, Barat R, Borrás L, Bouzas A, Giménez JB, et al. New frontiers from removal to recycling of nitrogen and phosphorus from wastewater in the Circular Economy. Bioresour Technol 2020;300:122673. https://doi.org/10.1016/j.biortech.2019.122673.

[21] Orner KD, Smith SJ, Breunig HM, Scown CD, Nelson KL. Fertilizer demand and potential supply through nutrient recovery from organic waste digestate in California. Water Res 2021;206:117717. https://doi.org/10.1016/j.watres.2021.117717.

[22] Aragón-Briceño CI, Pozarlik AK, Bramer EA, Niedzwiecki L, Pawlak-Kruczek H, Brem G. Hydrothermal carbonization of wet biomass from nitrogen and phosphorus approach: a review. Renew Energy 2021;171:401–15. https://doi.org/10.1016/j.renene.2021.02.109.

[23] Huezo L, Vasco-Correa J, Shah A. Hydrothermal carbonization of anaerobically digested sewage sludge for hydrochar production. Bioresour Technol Rep 2021;15:100795. https://doi.org/10.1016/j.biteb.2021.100795.

[24] Jiang H, Deng F, Luo Y, Xie Z, Chen Y, Zhou P, et al. Hydrothermal carbonization of corn straw in biogas slurry. J Clean Prod 2022:131682. https://doi.org/10.1016/j.jclepro.2022.131682.

[25] Yusuf I, Flagiello F, Ward NI, Arellano-García H, Avignone-Rossa C, Felipe-Sotelo M. Valorisation of banana peels by hydrothermal carbonisation: potential use of the hydrochar and liquid by-product for water purification and energy conversion. Bioresour Technol Rep 2020;12:100582. https://doi.org/10.1016/j.biteb.2020.100582.

[26] Zhuang X, Liu J, Zhang Q, Wang C, Zhan H, Ma L. A review on the utilization of industrial biowaste via hydrothermal carbonization. Renew Sustain Energy Rev 2022;154:111877. https://doi.org/10.1016/j.rser.2021.111877.

[27] He C, Zhang Z, Ge C, Liu W, Tang Y, Zhuang X, et al. Synergistic effect of hydrothermal co-carbonization of sewage sludge with fruit and agricultural wastes on hydrochar fuel quality and combustion behavior. Waste Manag 2019;100:171–81. https://doi.org/10.1016/j.wasman.2019.09.018.

[28] Mannarino G, Sarrion A, Diaz E, Gori R, De la Rubia MA, Mohedano AF. Improved energy recovery from food waste through hydrothermal carbonization and anaerobic digestion. Waste Manag 2022;142:9–18. https://doi.org/10.1016/j.wasman.2022.02.003.

[29] Oliveira AS, Sarrión A, Baeza JA, Diaz E, Calvo L, Mohedano AF, et al. Integration of hydrothermal carbonization and aqueous phase reforming for energy recovery from sewage sludge. Chem Eng J 2022:136301. https://doi.org/10.1016/j.cej.2022.136301.

[30] Dutta S, He M, Xiong X, Tsang DCW. Sustainable management and recycling of food waste anaerobic digestate: a review. Bioresour Technol 2021;341:125915. https://doi.org/10.1016/j.biortech.2021.125915.

[31] Parmar KR, Ross AB. Integration of hydrothermal carbonisation with anaerobic digestion; opportunities for valorisation of digestate. Energies 2019;12:1586. https://doi.org/10.3390/en12091586.

[32] Bardhan M, Novera TM, Tabassum M, Islam MdA, Islam MdA, Hameed BH. Co-hydrothermal carbonization of different feedstocks to hydrochar as potential energy for the future world: a review. J Clean Prod 2021;298:126734. https://doi.org/10.1016/j.jclepro.2021.126734.

[33] Lu X, Ma X, Chen X. Co-hydrothermal carbonization of sewage sludge and lignocellulosic biomass: fuel properties and heavy metal transformation behaviour of hydrochars. Energy 2021;221:119896. https://doi.org/10.1016/j.energy.2021.119896.

[34] Wang Z, Huang J, Wang B, Hu W, Xie D, Liu S, et al. Co-hydrothermal carbonization of sewage sludge and model compounds of food waste: influence of mutual interaction on nitrogen transformation. Sci Total Environ 2022;807:150997. https://doi.org/10.1016/j.scitotenv.2021.150997.

[35] Zhang C, Zheng C, Ma X, Zhou Y, Wu J. Co-hydrothermal carbonization of sewage sludge and banana stalk: fuel properties of hydrochar and environmental risks of heavy metals. J Environ Chem Eng 2021;9:106051. https://doi.org/10.1016/j.jece.2021.106051.

[36] Parmar KR, Brown AE, Hammerton JM, Camargo-Valero MA, Fletcher LA, Ross AB. Co-processing lignocellulosic biomass and sewage digestate by hydrothermal carbonisation: influence of blending on product quality. Energies 2022;15:1418. https://doi.org/10.3390/en15041418.

[37] Kavindi GAG, Lei Z, Yuan T, Shimizu K, Zhang Z. Use of hydrochar from hydrothermal co-carbonization of rice straw and sewage sludge for Cr(VI) bioremediation in soil. Bioresour Technol Rep 2022;18:101052. https://doi.org/10.1016/j.biteb.2022.101052.

[38] Zhao J, Liu C, Hou T, Lei Z, Yuan T, Shimizu K, et al. Conversion of biomass waste to solid fuel via hydrothermal co-carbonization of distillers grains and sewage sludge. Bioresour Technol 2022;345:126545. https://doi.org/10.1016/j.biortech.2021.126545.

[39] Monells Martínez A. Green hydrogen to biogas: options for stormossen's plant in vaasa. Finland; 2023. http://www.theseus.fi/handle/10024/805129. [Accessed 17 November 2023].

[40] Merzari F, Langone M, Andreottola G, Fiori L. Methane production from process water of sewage sludge hydrothermal carbonization. A review. Valorising sludge through hydrothermal carbonization. Crit Rev Environ Sci Technol 2019;49:947–88. https://doi.org/10.1080/10643389.2018.1561104.

[41] Aragón-Briceño CI, Pozarlik AK, Bramer EA, Niedzwiecki L, Pawlak-Kruczek H, Brem G. Hydrothermal carbonization of wet biomass from nitrogen and phosphorus approach: a review. Renew Energy 2021;171:401–15. https://doi.org/10.1016/j.renene.2021.02.109.

[42] Liu T, Jiao H, Yang L, Zhang W, Hu Y, Guo Y, et al. Co-hydrothermal carbonization of cellulose, hemicellulose, and protein with aqueous phase recirculation: insight into the reaction mechanisms on hydrochar formation. Energy 2022;251:123965. https://doi.org/10.1016/j.energy.2022.123965.

[43] Langone M, Basso D. Process waters from hydrothermal carbonization of sludge: characteristics and possible valorization pathways. Int J Environ Res Publ Health 2020;17:6618. https://doi.org/10.3390/ijerph17186618.

[44] Stutzenstein P, Bacher M, Rosenau T, Pfeifer C. Optimization of nutrient and carbon recovery from anaerobic digestate via hydrothermal carbonization and investigation of the influence of the process parameters. Waste Biomass Valor 2018;9:1303–18. https://doi.org/10.1007/s12649-017-9902-4.

[45] Picone A, Volpe M, Messineo A. Process water recirculation during hydrothermal carbonization of waste biomass: current knowledge and challenges. Energies 2021; 14:2962. https://doi.org/10.3390/en14102962.

[46] Campbell BS, Thorpe RB, Peus D, Lee J. Anaerobic digestion of untreated and treated process water from the hydrothermal carbonisation of spent coffee grounds. Chemosphere 2022;293:133529. https://doi.org/10.1016/j.chemosphere.2022.133529.

[47] Codignole Luz F, Volpe M, Fiori L, Manni A, Cordiner S, Mulone V, et al. Spent coffee enhanced biomethane potential via an integrated hydrothermal carbonization-anaerobic digestion process. Bioresour Technol 2018;256:102–9. https://doi.org/10.1016/j.biortech.2018.02.021.

[48] Boutaieb M, Román S, Ledesma B, Sabio E, Guiza M, Ouederni A. Towards a more efficient Hydrothermal Carbonization: processing water recirculation under different conditions. Waste Manag 2021;132:115–23. https://doi.org/10.1016/j.wasman.2021.07.023.

[49] Kabadayi Catalkopru A, Kantarli IC, Yanik J. Effects of spent liquor recirculation in hydrothermal carbonization. Bioresour Technol 2017;226:89–93. https://doi.org/10.1016/j.biortech.2016.12.015.

[50] Uddin MH, Reza MT, Lynam JG, Coronella CJ. Effects of water recycling in hydrothermal carbonization of loblolly pine. Environ Prog Sustain Energy 2014;33: 1309–15. https://doi.org/10.1002/ep.11899.

[51] Kambo HS, Minaret J, Dutta A. Process water from the hydrothermal carbonization of biomass: a waste or a valuable product? Waste Biomass Valor 2018;9:1181–9. https://doi.org/10.1007/s12649-017-9914-0.

[52] Stemann J, Erlach B, Ziegler F. Hydrothermal carbonisation of empty palm oil fruit bunches: laboratory trials, plant simulation, carbon avoidance, and economic feasibility. Waste Biomass Valor 2013;4:441–54. https://doi.org/10.1007/s12649-012-9190-y.

[53] Ghavami N, Özdenkçi K, Chianese S, Musmarra D, De Blasio C. Process simulation of hydrothermal carbonization of digestate from energetic perspectives in Aspen Plus. Energy Convers Manag 2022;270:116215. https://doi.org/10.1016/j.enconman.2022.116215.

[54] Yu Y, Lei Z, Yuan T, Jiang Y, Chen N, Feng C, et al. Simultaneous phosphorus and nitrogen recovery from anaerobically digested sludge using a hybrid system coupling hydrothermal pretreatment with MAP precipitation. Bioresour Technol 2017;243:634–40. https://doi.org/10.1016/j.biortech.2017.06.178.

[55] Koskue V, Freguia S, Ledezma P, Kokko M. Efficient nitrogen removal and recovery from real digested sewage sludge reject water through electroconcentration. J Environ Chem Eng 2021;9:106286. https://doi.org/10.1016/j.jece.2021.106286.

[56] Kruse A, Dahmen N. Water – a magic solvent for biomass conversion. J Supercrit Fluids 2015;96:36–45. https://doi.org/10.1016/j.supflu.2014.09.038.

[57] Kang K, Azargohar R, Dalai AK, Wang H. Noncatalytic gasification of lignin in supercritical water using a batch reactor for hydrogen production: an experimental and modeling study. Energy Fuel 2015;29:1776–84. https://doi.org/10.1021/ef5027345.

[58] Sricharoenchaikul V. Assessment of black liquor gasification in supercritical water. Bioresour Technol 2009;100:638–43. https://doi.org/10.1016/j.biortech.2008.07.011.

[59] Guo Y, Wang SZ, Xu DH, Gong YM, Ma HH, Tang XY. Review of catalytic supercritical water gasification for hydrogen production from biomass. Renew Sustain Energy Rev 2010;14:334–43. https://doi.org/10.1016/j.rser.2009.08.012.

[60] Yakaboylu O, Harinck J, Smit KG, De Jong W. Supercritical water gasification of biomass: a literature and technology overview. Energies 2015;8:859–94. https://doi.org/10.3390/en8020859.

[61] Özdenkçi K, Prestipino M, Björklund-Sänkiaho M, Galvagno A, De Blasio C. Alternative energy valorization routes of black liquor by stepwise supercritical water gasification: effect of process parameters on hydrogen yield and energy efficiency. Renew Sustain Energy Rev 2020;134:110146. https://doi.org/10.1016/j.rser.2020.110146.

[62] Fang Z, Sato T, Smith RL, Inomata H, Arai K, Kozinski JA. Reaction chemistry and phase behavior of lignin in high-temperature and supercritical water. Bioresour Technol 2008;99:3424–30. https://doi.org/10.1016/j.biortech.2007.08.008.

[63] Ghavami N, Özdenkçi K, Salierno G, Björklund-Sänkiaho M, De Blasio C. Analysis of operational issues in hydrothermal liquefaction and supercritical water gasification processes: a review. Biomass Conv Bioref; 2021. https://doi.org/10.1007/s13399-021-02176-4.

[64] Chakinala AG, Kumar S, Kruse A, Kersten SRA, van Swaaij WPM, Wim, Brilman DWF. Supercritical water gasification of organic acids and alcohols: the effect of chain length. J Supercrit Fluids 2013;74:8–21. https://doi.org/10.1016/j.supflu.2012.11.013.

[65] Feng H, Cui J, Xu Z, Hantoko D, Zhong L, Xu D, et al. Sewage sludge treatment via hydrothermal carbonization combined with supercritical water gasification: fuel production and pollution degradation. Renew Energy 2023;210:822–31. https://doi.org/10.1016/j.renene.2023.04.071.

[66] Yan M, Liu J, Yoshikawa K, Jiang J, Zhang Y, Zhu G, et al. Cascading disposal for food waste by integration of hydrothermal carbonization and supercritical water gasification. Renew Energy 2022;186:914–26. https://doi.org/10.1016/j.renene.2022.01.049.

[67] Taufer NL, Benedetti V, Pecchi M, Matsumura Y, Baratieri M. Coupling hydrothermal carbonization of digestate and supercritical water gasification of liquid products. Renew Energy 2021;173:934–41. https://doi.org/10.1016/j.renene.2021.04.058.

[68] Aragón-Briceño CI, Grasham O, Ross AB, Dupont V, Camargo-Valero MA. Hydrothermal carbonization of sewage digestate at wastewater treatment works: influence of solid loading on characteristics of hydrochar, process water and plant energetics. Renew Energy 2020;157:959–73. https://doi.org/10.1016/j.renene.2020.05.021.

[69] Marin-Batista JD, Mohedano AF, Rodríguez JJ, de la Rubia MA. Energy and phosphorous recovery through hydrothermal carbonization of digested sewage sludge. Waste Manag 2020;105:566–74. https://doi.org/10.1016/j.wasman.2020.03.004.

[70] Lühmann T, Wirth B. Sewage sludge valorization via hydrothermal carbonization: optimizing dewaterability and phosphorus release. Energies 2020;13:4417. https://doi.org/10.3390/en13174417.

[71] Wilk M, Gajek M, Śliz M, Czerwińska K, Lombardi L. Hydrothermal carbonization process of digestate from sewage sludge: chemical and physical properties of hydrochar in terms of energy application. Energies 2022;15:6499. https://doi.org/10.3390/en15186499.

[72] Roy UK, Radu T, Wagner J. Hydrothermal carbonisation of anaerobic digestate for hydro-char production and nutrient recovery. J Environ Chem Eng 2022;10: 107027. https://doi.org/10.1016/j.jece.2021.107027.

[73] Aragón-Briceño C, Ross AB, Camargo-Valero MA. Evaluation and comparison of product yields and bio-methane potential in sewage digestate following hydrothermal treatment. Appl Energy 2017;208:1357–69. https://doi.org/10.1016/j.apenergy.2017.09.019.

[74] He M, Zhu X, Dutta S, Khanal SK, Lee KT, Masek O, et al. Catalytic co-hydrothermal carbonization of food waste digestate and yard waste for energy application and nutrient recovery. Bioresour Technol 2022;344:126395. https://doi.org/10.1016/j.biortech.2021.126395.

[75] Akarsu K, Duman G, Yilmazer A, Keskin T, Azbar N, Yanik J. Sustainable valorization of food wastes into solid fuel by hydrothermal carbonization. Bioresour Technol 2019;292:121959. https://doi.org/10.1016/j.biortech.2019.121959.

[76] Cao Z, Jung D, Olszewski MP, Arauzo PJ, Kruse A. Hydrothermal carbonization of biogas digestate: effect of digestate origin and process conditions. Waste Manag 2019;100:138–50. https://doi.org/10.1016/j.wasman.2019.09.009.

[77] Yan M, Chen F, Li T, Zhong L, Feng H, Xu Z, et al. Hydrothermal carbonization of food waste digestate solids: effect of temperature and time on products characteristic and environmental evaluation. Process Saf Environ Protect 2023; 178:296–308. https://doi.org/10.1016/j.psep.2023.08.010.

[78] Zheng C, Ma X, Yao Z, Chen X. The properties and combustion behaviors of hydrochars derived from co-hydrothermal carbonization of sewage sludge and food waste. Bioresour Technol 2019;285:121347. https://doi.org/10.1016/j.biortech.2019.121347.

[79] Aragon-Briceño C, Pożarlik A, Bramer E, Brem G, Wang S, Wen Y, et al. Integration of hydrothermal carbonization treatment for water and energy recovery from organic fraction of municipal solid waste digestate. Renew Energy 2022;184: 577–91. https://doi.org/10.1016/j.renene.2021.11.106.

[80] Zhao P, Shen Y, Ge S, Yoshikawa K. Energy recycling from sewage sludge by producing solid biofuel with hydrothermal carbonization. Energy Convers Manag 2014;78:815–21. https://doi.org/10.1016/j.enconman.2013.11.026.

[81] Basso D, Patuzzi F, Castello D, Baratieri M, Rada EC, Weiss-Hortala E, et al. Agro-industrial waste to solid biofuel through hydrothermal carbonization. Waste Manag 2016;47:114–21. https://doi.org/10.1016/j.wasman.2015.05.013.

[82] Wang X, Shen Y, Liu X, Ma T, Wu J, Qi G. Fly ash and H2O2 assisted hydrothermal carbonization for improving the nitrogen and sulfur removal from sewage sludge. Chemosphere 2022;290:133209. https://doi.org/10.1016/j.chemosphere.2021.133209.

[83] Jia J, Chen H, Wang R, Liu H, Zhao Z, Lei H, et al. Mass and energy equilibrium analysis on co-hydrothermal carbonization coupled with a combined flash-Organic Rankine Cycle system for low-energy upgrading organic wastes. Energy Convers Manag 2021;229:113750. https://doi.org/10.1016/j.enconman.2020.113750.

[84] Breeze P. Chapter 5 - steam turbine combined heat and power systems. In: Breeze P, editor. Combined heat and power. Academic Press; 2018. p. 41–9. https://doi.org/10.1016/B978-0-12-812908-1.00005-5.

[85] Wang Q, Wu S, Cui D, Zhou H, Wu D, Pan S, et al. Co-hydrothermal carbonization of organic solid wastes to hydrochar as potential fuel: a review. Sci Total Environ 2022;850:158034. https://doi.org/10.1016/j.scitotenv.2022.158034.

[86] De Blasio C, Lucca G, Özdenkci K, Mulas M, Lundqvist K, Koskinen J, et al. A study on supercritical water gasification of black liquor conducted in stainless steel and nickel-chromium-molybdenum reactors. J Chem Technol Biotechnol 2016;91: 2664–78. https://doi.org/10.1002/jctb.4871.

[87] Gong M, Wang L, Hu J, Feng A, Wang M, Fan Y. Influence of reaction parameters on the fate of nitrogen during the supercritical water gasification of dewatered sewage sludge. Waste Manag 2022;151:28–38. https://doi.org/10.1016/j.wasman.2022.07.034.

[88] Huang J, Wang Z, Qiao Y, Wang B, Yu Y, Xu M. Transformation of nitrogen during hydrothermal carbonization of sewage sludge: effects of temperature and Na/Ca acetates addition. Proc Combust Inst 2021;38:4335–44. https://doi.org/10.1016/j.proci.2020.06.075.

[89] Sharma HB, Dubey BK. Co-hydrothermal carbonization of food waste with yard waste for solid biofuel production: hydrochar characterization and its pelletization. Waste Manag 2020;118:521–33. https://doi.org/10.1016/j.wasman.2020.09.009.
[90] Pecchi M, Patuzzi F, Basso D, Baratieri M. Enthalpy change during hydrothermal carbonization of biomass: a critical review. J Therm Anal Calorim 2020;141:1251–62. https://doi.org/10.1007/s10973-019-09117-4.
[91] Berge ND, Ro KS, Mao J, Flora JRV, Chappell MA, Bae S. Hydrothermal carbonization of municipal waste streams. Environ Sci Technol 2011;45:5696–703. https://doi.org/10.1021/es2004528.
[92] Rebling T, von Frieling P, Buchholz J, Greve T. Hydrothermal carbonization: combination of heat of reaction measurements and theoretical estimations. J Therm Anal Calorim 2015;119:1941–53. https://doi.org/10.1007/s10973-014-4361-7.
[93] Eshtiaghi N, Markis F, Yap SD, Baudez J-C, Slatter P. Rheological characterisation of municipal sludge: a review. Water Res 2013;47:5493–510. https://doi.org/10.1016/j.watres.2013.07.001.
[94] Edifor SY, Nguyen QD, van Eyk P, Biller P, Lewis DM. Rheological studies of municipal sewage sludge slurries for hydrothermal liquefaction biorefinery applications. Chem Eng Res Des 2021;166:148–57. https://doi.org/10.1016/j.cherd.2020.12.004.
[95] Özdenkçi K, De Blasio C, Sarwar G, Melin K, Koskinen J, Alopaeus V. Techno-economic feasibility of supercritical water gasification of black liquor. Energy 2019;189:116284. https://doi.org/10.1016/j.energy.2019.116284.
[96] Özdenkçi K, De Blasio C, Muddassar HR, Melin K, Oinas P, Koskinen J, et al. A novel biorefinery integration concept for lignocellulosic biomass. Energy Convers Manag 2017;149:974–87. https://doi.org/10.1016/j.enconman.2017.04.034.
[97] Giwa T, Akbari M, Kumar A. Techno-economic assessment of an integrated biorefinery producing bio-oil, ethanol, and hydrogen. Fuel 2023;332:126022. https://doi.org/10.1016/j.fuel.2022.126022.
[98] Nguyen TAH, Bui TH, Guo WS, Ngo HH. Valorization of the aqueous phase from hydrothermal carbonization of different feedstocks: Challenges and perspectives. Chemical Engineering Journal 2023;472:144802. https://doi.org/10.1016/j.cej.2023.144802.
[99] Ghavami N, Özdenkçi K, Salierno G, Björklund-Sänkiaho M, De Blasio C. Analysis of operational issues in hydrothermal liquefaction and supercritical water gasification processes: a review. Biomass Conv Bioref; 2021. https://doi.org/10.1007/s13399-021-02176-4.

PROCEEDINGS OF THE 33rd European Symposium on Computer Aided Process Engineering (ESCAPE33), June 18-21, 2023, Athens, Greece

Novel biorefinery ideas for conversion of biomass to biofuel

Niloufar Ghavami,[a] Karhan Özdenkçi,[a] Simeone Chianese,[b] Dino Musmarra, [b] Cataldo De Blasio [a]

[a] *Faculty of Science and Engineering, Åbo Akademi University, Rantakatu 2, 65100 Vaasa, Finland*
[b] *Department of Engineering, University of Campania "Luigi Vanvitelli", Via Roma 29, 81031 Aversa, Italy*

Abstract

The current economic model produces large amounts of waste causing environmental problems. In contrast, circular economy focuses on the efficient utilization of resources, increasing materials' lifecycle, recycling, and decreasing environmental damage. Biorefineries are the foundation for accomplishing sustainable development goals and transitioning to the circular economy. Biomass wastes are sustainable feedstock for biorefineries and are increasing due to population growth and urbanization.
Thermochemical conversion technologies specifically supercritical water gasification, hydrothermal liquefaction, and hydrothermal carbonization are viable technologies for wet biomass feedstock. Therefore, the objective of this article is to investigate a possible biorefinery integration scenario with the mentioned processes and the feasibility of the integrated processes. A study on biorefinery processes could facilitate the transition to a circular economy and sustainability and provide a holistic view for decision-makers.

Keywords: Circular economy, Biomass waste, Biorefinery, Thermochemical conversion methods.

1. Introduction

Growing waste production due to urbanization and population growth results in several environmental risks. For instance, sewage sludge (SS) is one of the major waste streams. The generation of SS in the 27 European Union member countries, (EU-27), varies between 0.1 kg per population equivalent and year to 30.8 kg per population equivalent and year [1]. SS contains organic content, inorganic compounds, various microorganisms and pathogens, nitrogen and phosphorous and toxic pollutants [2]. Therefore, energy recovery and the disposal process of SS is quite challenging.
Different methods with various operating conditions are applied for processing SS including supercritical water gasification (SCWG) at temperatures higher than 400 °C, hydrothermal liquefaction (HTL) at 250–400 °C, and hydrothermal carbonization (HTC) at 180–280 °C [3]. The superiority of the mentioned processes is the removal of costly pre-treatment drying in biomass conversion to biofuels [4]. Water's physical characteristics have an important role in hydrothermal processes. The physical properties change significantly at the sub-critical and critical regions and consequently, water behaves like a non-polar organic solvent and a catalyst in hydrothermal processes [5]. In HTL, the organic matter is liquefied at moderate temperature to biocrude oil and other by-products such as aqueous phase (AP), bio-char, and gaseous products [6]. HTL

process consists of three main steps: depolymerization followed by decomposition and recombination [7]. HTC technology is a proper approach to converting wet biomass feedstock to a carbonized solid (hydrochar) with a moderately high heating value as a solid fuel and nutrient-rich aqueous phase [8,9]. The HTC process mechanisms include hydrolysis, dehydration, decarboxylation, aromatization, condensation, and polymerization [10]. It is worth mentioning that the aqueous phase from HTL and HTC contains a huge amount of organic and inorganic compounds that need further processing [11,12]. SCWG is one of the effective thermochemical technologies for converting organic matter to hydrogen-rich gas products which used by Modell for the first time in the 1970s [13,14]. As reviewed by Ghavami et al. [5], SCWG resulted in char formation being inevitable, especially with feedstocks involving unhydrolyzed large molecules, causing reactor plugging. Therefore, in order to reduce the risk of char formation and precipitation, the aqueous phase from HTL and HTC is considered as the SCWG feedstock because of involving lighter and dissolved organics [15].
Integration of mentioned processes as a biorefinery concept is considered a sustainable approach to move towards a circular bioeconomy, carbon neutrality, waste management, and biofuel production [16]. Biorefineries are integrations of various processes producing multiple value-added products, in contrast with the traditional approach with a single product. Moreover, multiple products increase the rate of return on investment and protect against market uncertainties and fluctuations [17]. Designing a biorefinery requires a comprehensive understanding of integrated processes. In our previous article, we studied the integration of the HTC process to a biogas plant [10]. Therefore, the objective of this study is to investigate the integration of hydrothermal processes with a biogas plant.

2. Process description and feedstock selection

Figure 1 depicts a complete view of the proposed biorefinery. SS feedstock is divided between anaerobic digestion (AD) and HTL unit operations, and the digestate from the AD process is directed to the HTC process. The aqueous phase of HTC and HTL processes enters the SCWG process for syngas production. The HTC process of SS digestate is at 200 °C and autogenous pressure with 30% solid load. The HTL process is simulated under the condition of 350 °C and autogenous pressure with 19% solid load. The aqueous phase from HTL and HTC gasified in 600 °C and 250 bar condition.

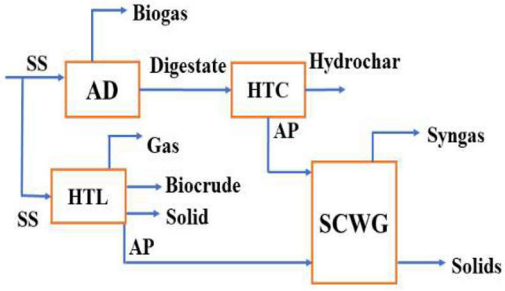

Figure 1. Flow diagram of the proposed biorefinery

Table 1 reports the dry basis elemental composition and the heating values (HHV) of the feedstocks and products based on the experimental results [18,19]. HTL, HTC, and SCWG processes are simulated in Aspen Plus V11.1 according to the following assumptions. The physical and chemical properties of non-conventional solids (NC solids) are estimated by 'HCOALGEN' and 'DCOALIGT'. Heating values for non-conventional components are calculated with a unified correlation valid for wide range of substances [20]. Gas phase in HTL contains 85.3 mol% CO_2, 0.9 mol% H_2, 6.4 mol%

CH_4, 4.4 mol% CO, and 2.9 mol% N_2. Gas phase in HTC contains 90 mol% CO_2, 1 mol% H_2, 3 mol% CH_4, 6 mol% CO.

Table 1. Dry basis elementary composition of feedstocks and products [18,19]

Sample	HHV (MJ/kg)	C	H	N	S	O	Ash	Yield
SS	14.1	33.1	5.5	5	0.7	25.9	29.8	-
SS digestate	14.9	28.7	3.1	3.4	1.5	16.4	46.9	-
Biocrude	28.3	53.3	6.01	3.9	1.1	29.9	4.7	37.1
Hydrochar	15.4	34.5	4.3	2.9	1.2	12.8	44.3	78

Prior to the simulation, it is needed to define components, thermodynamic method, and capacity. The component list is a combination of conventional and non-conventional substances including water, hydrogen, oxygen, carbon dioxide, carbon monoxide, methane, and nitrogen as conventional besides SS, digestate, hydrochar, biocrude oil, dissolved organics, and ash as nonconventional. The thermodynamic method selected PSRK for HTC and HTL sections while Peng-Robinson used for the SCWG section. In addition, mass balance is required to define yields on a non-inert basis for the RYIELD reactors in HTC and HTL processes. Yield reactors are used due to the presence of non-conventional substances in the HTL and HTC feedstocks. The yields of the HTC reactor are calculated as 0.15, 0.81, 0.04, 0.005, 2.64e-6, 4.22e-5, and 0.00015 for hydrochar, water, organics, CO_2, H_2, CH_4, and CO, respectively. Similarly, the HTL yields are 0.05, 0.02, 0.83, 0.02, 0.06, 3.14e-5, 0.0016, 0.0019, and 0.0013 for biocrude oil, solid, water, organics, CO_2, H_2, CH_4, CO, and N_2, respectively. For the SCWG process, a yield reactor is used to decompose the non-conventional components to the stable elemental components. Then, after separating ash, RGIBBS reactor is used as an equilibrium reactor based on minimizing Gibbs free energy. Figure 2 depicts the process simulation of the proposed biorefinery.

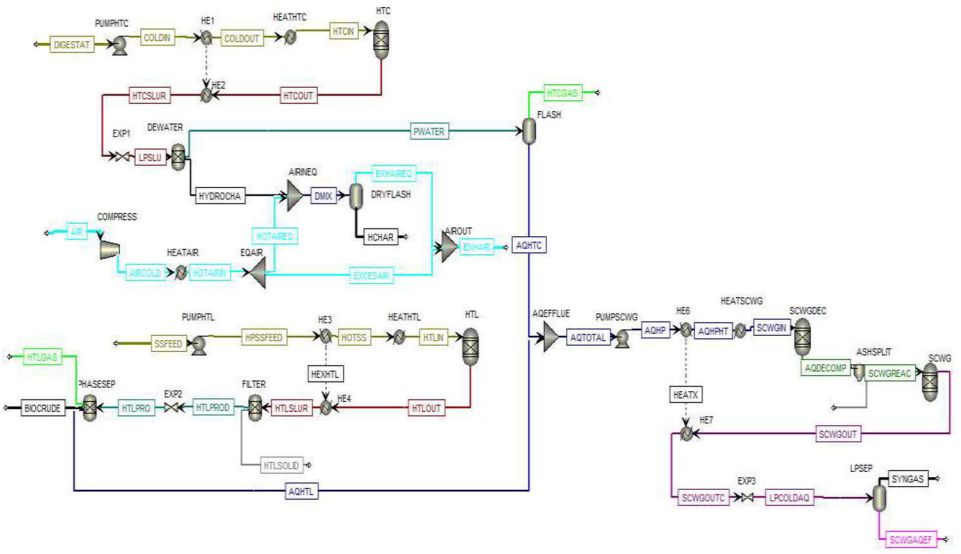

Figure 2. Process simulation of the proposed biorefinery

In the HTC section, the digestate feedstock (DIGESTAT) is pumped to 45 bars and is heated to 200 °C to reach the reaction condition in the HTC reactor. The stream exchange heat with the reactor downstream by units 'HE1' and 'HE2' up to 180 °C and then reach the temperature 196 °C by the external source in HEATHTC heater. The product mixture

goes through expansion and separation after heat exchange with the feedstock. Hydrochar is separated from the process water in the dewatering section and is dried down to 20% moisture by compressed air at 110 °C and 1.2 bars as described more in detail by Ghavami et al. [10]. The HTC process water is conducted to a flash separation for removing gas products and then mixed with the HTL process water. In the HTL part of the simulation, SS feedstock (SSFEED) is pumped to 170 bars and is heated to 350 °C to be prepared for the reaction condition and same as the HTC part the reactor product exchange heat with the feedstock by units 'HE3' and 'HE4', then it reaches reaction condition by HTATHTL. The product mixture is passed through a filter to remove the HTLSOLID after heat exchange with the SS feedstock. HTL products (gas, biocrude oil, and aqueous phase) are separated via a drum after expansion. The mixture of aqueous effluents (AQTOTAL) is pumped and heated with the same procedure as HTC and HTL to 250 bars and 720 °C. After the heat exchange with the aqueous mixture (units 'HE6' and 'HE7') and expansion, the syngas is separated in a flash unit.

3. Result and discussion

3.1. Mass balance

Different methodologies applied for mass balance calculations due to using various feedstock and data availability for each process. For the HTC and HTL sections, mass balance calculations were conducted by hydrochar, biocrude oil, liquid, and gas yields as well as proximate and ultimate analysis. Moreover, oxygen and hydrogen in organics calculated by experimental COD and BMP. Ash content in biocrude oil is assumed as 4.72% based on error bars of the dry-ash-free elemental composition. In SCWG section, mass balance calculations in the decomposition reactor were based on elemental compositions. Figure 3 depicts mass balances for HTC, HTL, and SCWG reactors.

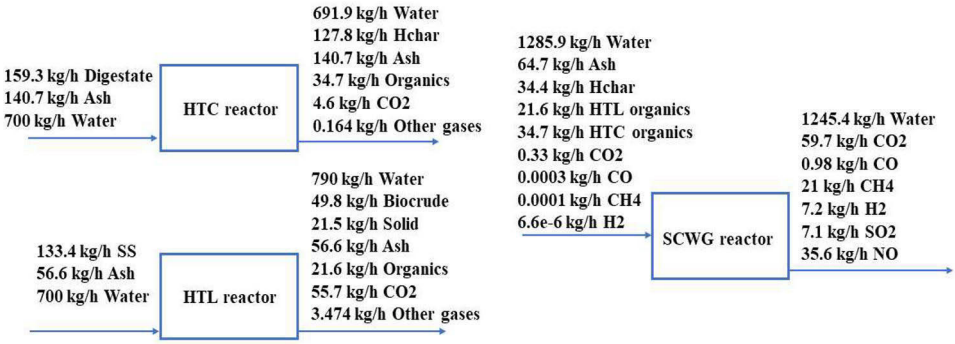

Figure 3. Mass balance in HTC, HTL, and SCWG reactors

3.2. Energy balance

Table 2 reports power and heat requirement for the proposed biorefinery as well as energy obtained from HTL solid and syngas. The electricity requirement results from the pumps and the compressor while heat requirement results from the external heat supplied to air and HTC and HTL reactor inlets. Since SCWG inlet is at high temperature, it is compromising the combined heat and power (CHP) production. Therefore, the duty of "HEATSCWG" unit is considered as 25 % electricity and 75 % heat requirement. Similarly, the CHP obtained from combustion of syngas and HTL solid is also assumed as 25 % electricity and 75 % heat. The biocrude oil can also be used as a fuel in the process or be upgraded to a transportation fuel. Meanwhile, the hydrochar can be used as a fertilizer, benefiting from the nutrients and minerals. In addition, the remaining fertilizer elements can be recovered from SCWG process as the solid outlet.

Table 2. Power and heat requirement for the biorefinery

Electricity requirement (kW)		Heat requirement (kW)	
PUMPHTC	1.7	HEATHTC	16.1
PUMPHTL	7.8	HEATHTL	50.2
PUMPSCWG	15.1	HEATAIR	162.1
COMPRESS	56.4	DEWATER	5.9
0.25 x HEATSCWG	41.9	0.75 x HEATSCWG	125.6
Total	122.9	Total	359.9
Electricity outcome (kW)		Heat outcome (kW)	
Syngas	152.8	Syngas	458.3
HTL solid	38.5	HTL solid	115.5
Total	191.3	Total	573.8

3.3. Feasibility and future aspects

The proposed biorefinery process is applicable to biogas plants with various feedstocks. Hydrothermal processes are suitable for converting the wet biomass. In addition, the nutrients and minerals can be recovered on the solid downstreams regarding the usage as a fertilizer. The total heat and power that required for the biorefinery is 482.8 kW and the total produced energy is 765.1 kW.

The proposed process has high potential in terms of feasibility since the combination improves the economic performance and overcome the operational issues of each conversion method. HTC is industrially applied for sewage sludge [21], and SCWG was stated to be potentially feasible for a more challenging feedstock (black liquor) [4]. HTL is stated to be feasible for large-scale [22]; meanwhile, it is possible to improve via co-HTC as well. SCWG of aqueous effluents produces syngas sufficient for net CHP production and addresses the discharge issue of HTL and HTC sections.

4. Conclusion

The scheme of a biorefinery is proposed in this article and integrated processes including HTC, HTL, and SCWG are simulated in Aspen Plus. Heat and electricity requirements are defined based on the simulation results. Moreover, the process is able to produce CHP especially via syngas after covering the energy requirements as well as the biocrude oil product and solids to be used as fertilizers.

5. References

[1] Havukainen J, Saud A, Astrup TF, Peltola P, Horttanainen M. Environmental performance of dewatered sewage sludge digestate utilization based on life cycle assessment. Waste Management 2022;137:210–21. https://doi.org/10.1016/j.wasman.2021.11.005.

[2] Tiwari N, Garua B, Bansal M, Sharma JG. 20 - Biorefinery and waste management by co-digestion of sewage sludge with organic wastes. In: Shah MP, Rodriguez-Couto S, Shah N, Banerjee R, editors. Development in Waste Water Treatment Research and Processes, Elsevier; 2022, p. 365–86. https://doi.org/10.1016/B978-0-323-85584-6.00021-2.

[3] Park M, Kim N, Lee S, Yeon S, Seo JH, Park D. A study of solubilization of sewage sludge by hydrothermal treatment. Journal of Environmental Management 2019;250:109490. https://doi.org/10.1016/j.jenvman.2019.109490.

[4] Özdenkçi K, De Blasio C, Sarwar G, Melin K, Koskinen J, Alopaeus V. Techno-economic feasibility of supercritical water gasification of black liquor. Energy 2019;189:116284. https://doi.org/10.1016/j.energy.2019.116284.

[5] Ghavami N, Özdenkçi K, Salierno G, Björklund-Sänkiaho M, De Blasio C. Analysis of operational issues in hydrothermal liquefaction and supercritical water gasification processes: a review. Biomass Conv Bioref 2021. https://doi.org/10.1007/s13399-021-02176-4.

[6] Nallasivam J, Prashanth PF, Vinu R. Chapter 4 - Hydrothermal liquefaction of biomass for the generation of value-added products. In: Varjani S, Pandey A, Taherzadeh MJ, Ngo HH, Tyagi RD, editors. Biomass, Biofuels, Biochemicals, Elsevier; 2022, p. 65–107. https://doi.org/10.1016/B978-0-323-88511-9.00018-5.
[7] Gollakota ARK, Kishore N, Gu S. A review on hydrothermal liquefaction of biomass. Renewable and Sustainable Energy Reviews 2018;81:1378–92. https://doi.org/10.1016/j.rser.2017.05.178.
[8] Son Le H, Chen W-H, Forruque Ahmed S, Said Z, Rafa N, Tuan Le A, et al. Hydrothermal carbonization of food waste as sustainable energy conversion path. Bioresource Technology 2022;363:127958. https://doi.org/10.1016/j.biortech.2022.127958.
[9] Xu Z-X, Ma X-Q, Zhou J, Duan P-G, Zhou W-Y, Ahmad A, et al. The influence of key reactions during hydrothermal carbonization of sewage sludge on aqueous phase properties: A review. Journal of Analytical and Applied Pyrolysis 2022;167:105678. https://doi.org/10.1016/j.jaap.2022.105678.
[10] Ghavami N, Özdenkçi K, Chianese S, Musmarra D, De Blasio C. Process simulation of hydrothermal carbonization of digestate from energetic perspectives in Aspen Plus. Energy Conversion and Management 2022;270:116215. https://doi.org/10.1016/j.enconman.2022.116215.
[11] Merzari F, Langone M, Andreottola G, Fiori L. Methane production from process water of sewage sludge hydrothermal carbonization. A review. Valorising sludge through hydrothermal carbonization. Critical Reviews in Environmental Science and Technology 2019;49:947–88. https://doi.org/10.1080/10643389.2018.1561104.
[12] Watson J, Wang T, Si B, Chen W-T, Aierzhati A, Zhang Y. Valorization of hydrothermal liquefaction aqueous phase: pathways towards commercial viability. Progress in Energy and Combustion Science 2020;77:100819. https://doi.org/10.1016/j.pecs.2019.100819.
[13] Wei N, Xu D, Hao B, Guo S, Guo Y, Wang S. Chemical reactions of organic compounds in supercritical water gasification and oxidation. Water Research 2021;190:116634. https://doi.org/10.1016/j.watres.2020.116634.
[14] Reddy SN, Nanda S, Dalai AK, Kozinski JA. Supercritical water gasification of biomass for hydrogen production. International Journal of Hydrogen Energy 2014;39:6912–26. https://doi.org/10.1016/j.ijhydene.2014.02.125.
[15] Ong BHY, Walmsley TG, Atkins MJ, Walmsley MRW. A Kraft Mill-Integrated Hydrothermal Liquefaction Process for Liquid Fuel Co-Production. Processes 2020;8:1216. https://doi.org/10.3390/pr8101216.
[16] Culaba AB, Mayol AP, San Juan JLG, Ubando AT, Bandala AA, Concepcion II RS, et al. Design of biorefineries towards carbon neutrality: A critical review. Bioresource Technology 2022:128256. https://doi.org/10.1016/j.biortech.2022.128256.
[17] Giwa T, Akbari M, Kumar A. Techno-economic assessment of an integrated biorefinery producing bio-oil, ethanol, and hydrogen. Fuel 2023;332:126022. https://doi.org/10.1016/j.fuel.2022.126022.
[18] Rahman T, Jahromi H, Roy P, Adhikari S, Hassani E, Oh T-S. Hydrothermal liquefaction of municipal sewage sludge: Effect of red mud catalyst in ethylene and inert ambiences. Energy Conversion and Management 2021;245:114615. https://doi.org/10.1016/j.enconman.2021.114615.
[19] Parmar KR, Ross AB. Integration of Hydrothermal Carbonisation with Anaerobic Digestion; Opportunities for Valorisation of Digestate. Energies 2019;12:1586. https://doi.org/10.3390/en12091586.
[20] Channiwala SA, Parikh PP. A unified correlation for estimating HHV of solid, liquid and gaseous fuels. Fuel 2002;81:1051–63. https://doi.org/10.1016/S0016-2361(01)00131-4.
[21] Buttmann M. Industrial scale plat for sewage sludge treatment by hydrothermal carbonization in Jinin/China and phosphate recovery by Terranova ultra HTC process, 2017.
[22] Seiple TE, Skaggs RL, Fillmore L, Coleman AM. Municipal wastewater sludge as a renewable, cost-effective feedstock for transportation biofuels using hydrothermal liquefaction. Journal of Environmental Management 2020;270:110852. https://doi.org/10.1016/j.jenvman.2020.110852.

ISBN 978-952-12-4374-5